N° d'ordre 2025ISAL0011

THESE de DOCTORAT DE L'INSA LYON,
membre de l'Université de Lyon

Ecole Doctorale **N° 206**
Ecole Doctorale de chimie de Lyon

Spécialité/ discipline de doctorat **: Génie des procédés**

Soutenue publiquement le 05/02/2025, par :
Daniella Gonçalves Portela

Treatment of combined sewer overflow by vertical flow treatment wetlands with new design to improve water quality

---

Devant le jury composé de :

Dittmer, Ulrich	Professor (PhD)	University of Kaiserslautern-Landau	Rapporteur
Gajewska, Magdalena	Professor (PhD)	Gdańsk University	Rapporteure
Morvannou, Ania	Chargée de recherche (PhD)	Ecobird	Examinatrice
Lipeme Kouyi, Gislain	Professor (PhD)	INSA - Lyon	Président
Molle, Pascal	Directeur de recherche (HDR)	INRAE	Directeur de thèse
Tondera, Katharina	Professor (PhD)	ENTPE	Co-directrice de thèse
Troesch, Stéphane	Chargé de recherche (PhD)	Ecobird	Invité

Thèse accessible à l'adresse : https://theses.insa-lyon.fr/publication/2025ISAL0011/these.pdf © [D. Gonçalves Portela], [2025], INSA Lyon, tous droits réservés

Département FEDORA – INSA Lyon - Ecoles Doctorales

SIGLE	ECOLE DOCTORALE	NOM ET COORDONNEES DU RESPONSABLE
ED 206 CHIMIE	CHIMIE DE LYON https://www.edchimie-lyon.fr Sec. : Renée EL MELHEM Bât. Blaise PASCAL, 3e étage secretariat@edchimie-lyon.fr	M. Stéphane DANIELE C2P2-CPE LYON-UMR 5265 Bâtiment F308, BP 2077 43 Boulevard du 11 novembre 1918 69616 Villeurbanne directeur@edchimie-lyon.fr
ED 341 E2M2	ÉVOLUTION, ÉCOSYSTÈME, MICROBIOLOGIE, MODÉLISATION http://e2m2.universite-lyon.fr Sec. : Bénédicte LANZA Bât. Atrium, UCB Lyon 1 Tél : 04.72.44.83.62 secretariat.e2m2@univ-lyon1.fr	Mme Sandrine CHARLES Université Claude Bernard Lyon 1 UFR Biosciences Bâtiment Mendel 43, boulevard du 11 Novembre 1918 69622 Villeurbanne CEDEX e2m2.codir@listes.univ-lyon1.fr
ED 205 EDISS	INTERDISCIPLINAIRE SCIENCES-SANTÉ http://ediss.universite-lyon.fr Sec. : Bénédicte LANZA Bât. Atrium, UCB Lyon 1 Tél : 04.72.44.83.62 secretariat.ediss@univ-lyon1.fr	Mme Sylvie RICARD-BLUM Laboratoire ICBMS - UMR 5246 CNRS - Université Lyon 1 Bâtiment Raulin - 2ème étage Nord 43 Boulevard du 11 novembre 1918 69622 Villeurbanne Cedex Tél : +33(0)4 72 44 82 32 sylvie.ricard-blum@univ-lyon1.fr
ED 34 EDML	MATÉRIAUX DE LYON http://ed34.universite-lyon.fr Sec. : Yann DE ORDENANA Tél : 04.72.18.62.44 yann.de-ordenana@ec-lyon.fr	M. Stéphane BENAYOUN Ecole Centrale de Lyon Laboratoire LTDS 36 avenue Guy de Collongue 69134 Ecully CEDEX Tél : 04.72.18.64.37 stephane.benayoun@ec-lyon.fr
ED 160 EEA	ÉLECTRONIQUE, ÉLECTROTECHNIQUE, AUTOMATIQUE https://edeea.universite-lyon.fr Sec. : Philomène TRECOURT Bâtiment Direction INSA Lyon Tél : 04.72.43.71.70 secretariat.edeea@insa-lyon.fr	M. Philippe DELACHARTRE INSA LYON Laboratoire CREATIS Bâtiment Blaise Pascal, 7 avenue Jean Capelle 69621 Villeurbanne CEDEX Tél : 04.72.43.88.63 philippe.delachartre@insa-lyon.fr
ED 512 INFOMATHS	INFORMATIQUE ET MATHÉMATIQUES http://edinfomaths.universite-lyon.fr Sec. : Renée EL MELHEM Bât. Blaise PASCAL, 3e étage Tél : 04.72.43.80.46 infomaths@univ-lyon1.fr	M. Hamamache KHEDDOUCI Université Claude Bernard Lyon 1 Bât. Nautibus 43, Boulevard du 11 novembre 1918 69 622 Villeurbanne Cedex France Tél : 04.72.44.83.69 direction.infomaths@listes.univ-lyon1.fr
ED 162 MEGA	MÉCANIQUE, ÉNERGÉTIQUE, GÉNIE CIVIL, ACOUSTIQUE http://edmega.universite-lyon.fr Sec. : Philomène TRECOURT Tél : 04.72.43.71.70 Bâtiment Direction INSA Lyon mega@insa-lyon.fr	M. Etienne PARIZET INSA Lyon Laboratoire LVA Bâtiment St. Exupéry 25 bis av. Jean Capelle 69621 Villeurbanne CEDEX etienne.parizet@insa-lyon.fr
ED 483 ScSo	ScSo[1] https://edsciencessociales.universite-lyon.fr Sec. : Mélina FAVETON Tél : 04.78.69.77.79 melina.faveton@univ-lyon2.fr	M. Bruno MILLY (INSA : J.Y. TOUSSAINT) Univ. Lyon 2 Campus Berges du Rhône 18, quai Claude Bernard 69365 LYON CEDEX 07 Bureau BEL 319 bruno.milly@univ-lyon2.fr

[1] ScSo : Histoire, Géographie, Aménagement, Urbanisme, Archéologie, Science politique, Sociologie, Anthropologie

Thèse accessible à l'adresse : https://theses.insa-lyon.fr/publication/2025ISAL0011/these.pdf © [D. Gonçalves Portela], [2025], INSA Lyon, tous droits réservés

Acknowledgements

I would like to express my deepest gratitude to my supervisors, Pascal Molle and Katharina Tondera, for their invaluable guidance throughout this scientific journey. Your patience and clarifying revisions have been essential to my learning and growth. It was inspiring to observe your active engagement in the TWs community and your dedication to research.

I am also grateful for the financial support provided by the NICE project, which made this work possible.

My thanks to the Reversaal team for their technical support and insightful advice. This study would not have been possible without the help of Olivier, Gaël, Jérémy, and Arnold with the equipment on the field.

I would like to express my gratitude to Anacleto Rizzo and Damien Tedoldi for their valuable contributions to my steering committee and for their assistance with classes and data discussions.

I express my gratitude to my husband and my family, who have always supported me in all my decisions and have always been at my side, even without being physically present. Amo vocês.

To my friend who has been with me these last three years, I am deeply grateful for the shared moments around the table, enjoying good food and wine, and for the adventures in France. These experiences and your encouragement gave me the strength to end this thesis. Thank you for being there.

Lastly, I am thankful to all my colleagues for the good moments we shared at work. Each person who stopped by the office just to ask, “Ça vas?” brought a meaningful difference to my day. A special thanks to Jean Marc Perret for his incredible support with a variety of tasks—whether administrative, finding materials for the field, discovering cultural activities, or even explaining politics. Your help has been truly invaluable.

Thèse accessible à l'adresse : https://theses.insa-lyon.fr/publication/2025ISAL0011/these.pdf © [D. Gonçalves Portela], [2025], INSA Lyon, tous droits réservés

Abstract

Combined sewer overflows (CSOs) are significant sources of aquatic pollution and have been efficiently treated in CSO Treatment Wetlands (CSO-TWs). In addition, CSO TWs are Nature-Based Solution (NBS) that provide ecosystem services. However, the system's performance in removing dissolved pollutants and micropollutants can be affected by the characteristics of rainfall. Hence, over one and a half years, trials were conducted to evaluate performance of two aerated CSO-TW pilots under different operational conditions. Both pilots (CSOA and CSOB) featured a new design with forced aeration and almost one meter saturated layer. CSOA used gravel as top filtering layer, while CSOB utilized sand and an additional transition layer. Samples were collected at the inlet and outlet of the filters, and within the filter sensor were installed to online monitoring. Tracer tests were performed in both pilots to evaluate their hydrodynamics. Aerations strategies were tested using intermittent and air blowers operation during the wet period. The optimal aeration strategy was then tested on both filters for comparison, and the effects of variable organic and hydraulic loads were also assessed. Global water quality parameters and micropollutants were measured at the inlet and outlet through laboratorial analysis, while redox potential and oxygen concentrations were monitored online. Ten and 5 samples of fecal indicator (FI) were taken for CSOA and CSOB, respectively. The results indicate that aeration increased the residence time and mixing degree. While the NTIS was 5.3 in CSOA and 8 in CSOB for the water retained above the surface, the use of forced aeration resulted in a reduction of these values to1.8 in CSOA and 2.7 in CSOB . For both filters, the hydraulic retention time remained between 6.5 and 10 hours. In highly aerated conditions, dissolved pollutants, such as dissolved COD and ammonium-nitrogen (NH_4-N), were efficiently removed in both filters. In CSOA, the aeration strategy with low oxygen transfer resulted in minimal NH_4-N removal. However, maintaining highly aerated conditions led to a notable increase in median removal efficiency, reaching 75%. The removal efficiencies were similar in CSOA and CSOB under the same aeration strategy, with the exception of a slight higher removal of TSS in CSOB. Observations of higher nitrification rates, when the air blowers were active for extended periods, were supported by redox potential > 300 mV and oxygen concentration > 5 mg/L. During the feeding event, NH_4-N was transformed into NO_3-N, with the possibility of partial or total transformation depending on the nitrogen inlet concentration fed into the filter. The limitation of direct nitrification during the feeding event was mostly due to the short HRT. Consequently, feeding events where NH_4-N was not completely transformed and accumulated in the saturated layer led to nitrate production during the subsequent dry period and feeding event. The main factor for occurrences of nitrate peaks in this aerated system was the transformation of accumulated nitrogen within the filter. The intensity of the nitrate peak was found to vary in response to the mass of accumulated nitrogen and the duration of the dry period. The micropollutants analyses included industrial chemicals frequently and pharmaceutical. The 6PPD-quinone was efficiently removed in the filter in both filters. Benzothiazoles were also efficiently removed, the removal efficiency was more variable. The pharmaceuticals showed moderate to low removal and for compounds such as carbamazepine there was no or negative removal. The fecal indicators analyzed showed negligible reduction and need further investigation. In general, aeration was not a key factor removing micropollutants and FI, as it was for dissolved pollutants removal. This thesis showed that aerated CSO TWs are suitable for removing particulate and dissolved pollutants, with some limitations for ammonium removal and absence of denitrification. For micropollutants and fecal indicator a polishing treatment is necessary to improve water quality. In future work, analysis of microbial community modelling tools could provide insights to the upscaling of the system.
Keyword: Biofilter; pollution control; intensified system; high hydraulic load.

Thèse accessible à l'adresse : https://theses.insa-lyon.fr/publication/2025ISAL0011/these.pdf © [D. Gonçalves Portela], [2025], INSA Lyon, tous droits réservés

Résumé

Les surverses de déversoir d'orage constituent des sources importantes de pollution aquatique et ont été efficacement traitées par les filtres plantés à écoulement vertical. Cependant, les performances du système en matière d'élimination des polluants dissous et des micropolluants peuvent être affectées par les caractéristiques des précipitations. C'est pourquoi deux filtres plantés à écoulement vertical (CSOA et CSOB), équipés d'un nouveau design avec aération forcée et d'une couche saturée d'environ un mètre ont été testés sur une période d'un an et demi. Le CSOA utilisait du gravier comme couche de filtration supérieure, tandis que le CSOB utilisait du sable et une couche de transition. Des traçages ont été effectués pour évaluer leur hydrodynamique. Les stratégies d'aération ont été testées dans le CSOA et la stratégie d'aération optimale a ensuite été testée sur les deux filtres pour comparaison, et les effets des charges organiques et hydrauliques variables ont également été évalués. Les paramètres globaux de qualité de l'eau et les micropolluants ont été mesurés à l'entrée et à la sortie, tandis que le potentiel redox et les concentrations en oxygène ont été surveillés en ligne. Dix échantillons d'indicateurs fécaux (IF) ont été prélevés pour le CSOA et cinq pour le CSOB. Les résultats indiquent que l'aération a augmenté le temps de séjour et le degré de mélange. Le NTIS était de 5,3 dans le CSOA et de 8 dans le CSOB pour l'eau retenue à la surface, l'utilisation d'une aération forcée a permis de réduire ces valeurs à 1,8 dans le CSOA et 2,7 dans le CSOB. Pour les deux filtres, le temps de séjour est resté compris entre 6,5 et 10 heures. Dans des conditions fortement aérées, les polluants dissous, tels que la DCO dissoute et NH_4-N, ont été efficacement éliminés dans les deux filtres. Dans le CSOA, une stratégie d'aération avec un faible transfert d'oxygène a conduit à une élimination minimale du NH_4-N. Cependant, le maintien de conditions hautement aérées a permis une augmentation notable de l'efficacité médiane d'élimination, atteignant 75 %. Les taux d'élimination étaient similaires dans le CSOA et le CSOB sous la même stratégie d'aération, à l'exception d'une élimination légèrement plus élevée des MES dans le CSOB. Des taux de nitrification plus élevés ont été observés lorsque les souffleurs d'air étaient actifs pendant de longues périodes, ce qui était confirmé par un potentiel redox > 300 mV et une concentration en oxygène > 5 mg/L. Lors des phases d'alimentation, le NH_4-N était transformé en NO_3-N, avec une transformation partielle ou totale possible selon la concentration en azote à l'entrée du filtre. La limitation de la nitrification directe pendant les phases d'alimentation était principalement due au court temps de rétention hydraulique. Par conséquent, lors des phases d'alimentation où le NH_4-N n'était pas complètement transformé et s'accumulait dans la couche saturée, une production de nitrates était observée pendant les périodes sèches suivantes et les phases d'alimentation ultérieures. Le principal facteur à l'origine des pics de nitrate dans ce système aéré était la transformation de l'azote accumulé dans le filtre. L'intensité des pics de nitrate variait en fonction de la masse d'azote accumulée et de la durée de la période sèche. Les analyses de micropolluants incluaient des produits chimiques industriels courants et des produits pharmaceutiques. Le 6PPD-quinone a été efficacement éliminé dans les deux filtres, de même que les benzothiazoles, qui ont montré une efficacité d'élimination plus variable mais également significative. Les produits pharmaceutiques ont présenté des taux d'élimination modérés à faibles, et pour des composés tels que la carbamazépine, aucune élimination ou même une élimination négative n'a été observée. Les indicateurs fécaux analysés ont montré une réduction négligeable, nécessitant des recherches supplémentaires. En général, l'aération n'a pas été un facteur clé pour l'élimination des micropolluants et des indicateurs fécaux, contrairement à son rôle dans l'élimination des polluants dissous. Cette thèse a montré que les systèmes de déversoir d'orage aérés sont adaptés pour éliminer les polluants particulaires et dissous, avec certaines limites pour l'élimination de l'ammonium et l'absence de dénitrification. Pour les micropolluants et les indicateurs fécaux, un traitement de finition est nécessaire pour améliorer la qualité de l'eau. Dans les travaux

Thèse accessible à l'adresse : https://theses.insa-lyon.fr/publication/2025ISAL0011/these.pdf © [D. Gonçalves Portela], [2025], INSA Lyon, tous droits réservés

futurs, l'analyse des communautés microbiennes et des outils de modélisation pourrait fournir des informations utiles pour le passage à une échelle supérieure du système.
Mots-clés : Biofiltre ; contrôle de la pollution ; système intensifié ; charge hydraulique élevée.

Thèse accessible à l'adresse : https://theses.insa-lyon.fr/publication/2025ISAL0011/these.pdf © [D. Gonçalves Portela], [2025], INSA Lyon, tous droits réservés

List of Tables

Table 1.1 - EMC of CSO pollutants from literature, along with the range of concentrations . 22
Table 1.2 - Mean removal efficiency of standard parameters in CSO-TWs of different scales. 32
Table 2.1 - Percentage of tracer mass recover, hydraulic indicators of theoretical and measured mean time. t_{10} and t_{90} are the time until 10% and 90% of the tracer mass leaves the filter, respectively, N, is the number of tanks in series. 53
Table 2.2 - TSS, CODt and CODs values of minimum, maximum and median concentration at the inlet and outlet of CSOa and CSOb. 55
Table 3.1– Classification of aeration strategies operated in the pilots. In each aeration strategy the air blowers were switched on and off during the feeding, drainage and dry period. 68
Table 3.2 – Median inlet concentration, in parenthesis, the minimum and maximum measurement for each filter according to their respective top layer material and aeration condition classification. 69
Table 4.1- Summary of the frequency and period during which samples were collected, and the operation of the filters during this period. The number of samples (n) collected in each filter, CSO A (A) and CSO B (B), are indicated, as well. 92
Table 4.2 - Removal efficiency in CSOA, for the compounds 6PPD-quinone (6PPD-Q), aminobenzothiazole (ABT), benzothiazoles (BT), N,N-Diethyl-3-methylbenzamide (DEET), Diclofenac (DFC), Gabapentin (GBP), Iomeprol (IOP), Irbesartan (IBT). The n represents the total number of samples used to calculate the removal efficiency. Tests with inlet and outlet < LOQ are not included in n. 97
Table 4.3 - Removal efficiency in CSOB, for the compounds 6PPD-quinone (6PPD-Q), aminobenzothiazole (ABT), benzothiazoles (BT), N,N-Diethyl-3-methylbenzamide (DEET), Carbamazepine (CBP), Diclofenac (DFC), Gabapentin (GBP), Iomeprol (IOP), Irbesartan (IBT). The n represents the total number of samples used to calculate the removal efficiency. Tests with inlet and outlet < LOQ are not included in n. 97
Table 5.1 - Removal efficiency in CSOA and CSOB for all aeration strategies tested in each pilot 110

Thèse accessible à l'adresse : https://theses.insa-lyon.fr/publication/2025ISAL0011/these.pdf © [D. Gonçalves Portela], [2025], INSA Lyon, tous droits réservés

List of Figures

Figure 1.1 - German, French and Italian design approaches of the CSO-TW. a) Top view of the systems with all their components. b) Cross section of the filter showing the depth of heir different layers. Figure adapted from Meyer et al. (2013). 27
Figure 2.1 –Photo on the top left (A): top view of CSOa; top right (B): top view of CSOb. Vertical profile of CSOa and CSOb on the bottom (C) 46
Figure 2.2 - A: Graphs of output mass curve in time for CSOa. B: Graphs of residence time distribution (RDT) in CSOa using Gamma distribution to fit experimental data. C: Graphs of output mass curve in time for CSOb. D: Graphs of residence time distribution (RDT) in CSOb using Gamma distribution to fit experimental data. 51
Figure 2.3 - Inlet and outlet concentrations of TSS and COD under each tested aeration condition in CSOa (F10, F10/40, 10/40 and 75/15). 54
Figure 2.4 – Tukey's boxplot of removal performance of TSS, COD and dissolved COD in the filters CSOa (n = 17 for COD and CODs and n = 15 for TSS) and CSOb (n = 19) under the aeration condition 75/15. 56
Figure 2.5 - Inlet and outlet concentrations of NH_4-N, NO_3-N and NO_2-N for each tested aeration conditions in CSOa (F10, F10/40, 10/40 and 75/15). 58
Figure 2.6 – Tukey's boxplot of inlet and outlet concentrations of NH_4-N and outlet concentration of NO_3^-N in the filters CSOa and CSOb. The number of tests performed (n) is indicated for each condition. 58
Figure 2.7 - Redox potential measured in two events in CSOa with a HL of 0.5 m. The first test under the aeration strategy F10 is indicated by the green line, and the second test under the 75/15 aeration strategy is indicated by the dashed blue line. Measurements were taken at 0.6 m depth from the bottom of the pilot. 60
Figure 2.8 - Correlation of loaded and removed COD per event, on the left, and NH_4-N, on the right. Events in CSOa are indicated with an "a" and with a "b" for CSOb. The colors yellow, blue and green indicate different hydraulic loads. 62
Figure 3.1– Cross section of the filters CSOa and CSOb. 67
Figure 3.2- Top view, on the right, and cross section, on the left, to represent the positions of the probes. Three probes (ORP, oxygen and N forms) are 0.6 m from the bottom and one probe of N forms is at the outlet. The distances are in meters. 70
Figure 3.3 - N transformation processes within a filter at different times. The first feeding event, Event I, is followed by a dry period, after which a subsequent feeding event, Event II, occurs. The yellow dot represents the intersection of paths where the compounds are added together. 72
Figure 3.4 - Oxygen uptake for the first, blue bar, and last, empty bar, day of event in a sequence of events alternating low and increasing concentration of ammonium. 73
Figure 3.5 - PCA results in the filter CSOA, analyzed regarding 7 different parameter that are related to the nitrogen transformation process. 75
Figure 3.6 – The measurements for ORP curves were standardized to the hydrogen reference and the duration of drainage time was normalized. The end of feeding and aeration are indicated. The graphs represent fluctuations in the ORP curves when air blowers are switched off. 76
Figure 3.7 – Estimated O_2 uptake and NH_4-N outlet concentration in filter CSOA. 79
Figure 3.8 – NO_3-N production and NH_4-N retention rates for the trials with > $15gO_2.h^{-1}.m^{-2}$ in CSOA. The line crossing the axis represent the NO_3-N production equal to the retained NH_4-N. 80

Thèse accessible à l'adresse : https://theses.insa-lyon.fr/publication/2025ISAL0011/these.pdf © [D. Gonçalves Portela], [2025], INSA Lyon, tous droits réservés

Figure 3.9 - Components of NO_3-N retained and discharged in each feeding event. This is a sequence of trials with HL of 1.5 $m^3.m^{-2}$ conducted in CSOA. 82
Figure 3.10 - Online measures of N forms and DO concentration in a piezometer 60 cm from the bottom. These are the dynamics after 80% of the inflow volume was recovered and aeration is switched off in trials of 1.5 $m^3.m^{-2}$. 84
Figure 4.1 – Cross section indicating filter' layers 91
Figure 4.2 - Inlet (IN) and outlet (OUT) concentrations. The limit of quantification, represented by the dashed red line, is 0.05 $\mu g.L^{-1}$ for ABT (aminobenzothiazole) and 0.1 $\mu g.L^{-1}$ for BT (benzothiazole) and OHBT(hydroxybenzothiazole). The number of samples analyzed for the compound is indicated by n. 96
Figure 4.3 - Inlet (IN) and outlet (OUT) concentrations. The limit of quantification, represented by the dashed red line, is 0.02 $\mu g.L^{-1}$ for gabapentin and 0.05 $\mu g.L^{-1}$ for iomeprol and irbesartan. The number of samples analyzed for the compound is indicated by n. 99
Figure 4.4 - The top graph (a) shows the inlet and outlet concentration of particulate (P) and dissolved (S) metals, as well as removal efficiencies for CSOA. The graphs on the right (b and c) highlight metals at CSOA in lower concentrations. CSOB is represented in graph (d), which provides an overview of inlet, outlet and removal efficiency. Graphs (e) and (f) detail the concentration of metals entering in CSOB in lower concentrations. 104
Figure 4.5 - Inlet, outlet and reduction of *E. coli* and total coliforms in CSOA and CSOB.. 106
Figure 5.1 - Loaded ammonium correlation with removed ammonium under continuous aeration strategy. 111
Figure 5.2 - Filtration speed and accumulated load in CSOB over with HL of 1.5 m^3/m^2 in each trial 113
Figure 5.3 – Accumulated volume at the outlet of the CSOB. The black line represents the trial of 1.0 m^3/m^2 of HL that occurred eight months before the clogged trial of 1.0 m^3/m^2 of HL. The orange line trial of 1.5 m^3/m^2 of HL was two months after the clogged trial. 113
Figure 5.4 - Accumulated TSS and HL in CSOA and CSOB filters. The curve off accumulated HL curve for CSOB is discontinued at 22 m^3/m^2, as the filter clogged. 114
Figure 5.5 - TKN inlet concentration and NH_4-N outlet concentrations in CSOA and CSOB for highly aerated conditions. 116
Figure 5.6 – NO_3-N and NH_4-N measurements at the outlet of CSOA and dynamics of NH_4-N transformation within the filter, measured with a sensor at 60 cm from the bottom. 118

Thèse accessible à l'adresse : https://theses.insa-lyon.fr/publication/2025ISAL0011/these.pdf © [D. Gonçalves Portela], [2025], INSA Lyon, tous droits réservés

Content

GENERAL INTRODUCTION 14
Research objectives and thesis outline 16
1 Literature Review 19
1.1 Management of combined sewer overflow 19
1.2 Pollutant concentrations in CSO discharge 21
1.3 Legal situation 23
1.4 Treatment Wetlands for combined sewer overflows 24
1.5 General design considerations for CSO-TW 25
1.6 Relevance of filter material and plants 27
1.7 Hydrodynamics 28
1.8 Removal mechanisms 30
1.9 Performance of pollutant removal 31
1.9.1 Standard pollutants 31
1.9.2 Micropollutants 33
1.9.3 Pathogens 35
1.10 Clogging 35
1.11 Aeration in TWs 36
1.11.1 Oxygen requirements in TWs 36
1.11.2 Intensified TW 38
2 Removal of standard pollutants in an Aerated CSO-TW 42
2.1 Introduction 43
2.2 Material and methods 45
2.2.1 Experimental Systems 45
2.2.2 Pilots' operation 46
2.2.3 Hydraulic characterization 48
2.2.3 Sampling procedure, water quality physicochemical and statistical analysis 49
2.3 Results and Discussion 50
2.3.1 Tracer test 50
2.3.2 Removal performances 53
2.3.3 Redox potential 59
2.3.4 Surface load and performances 61
2.4 Conclusions 62
3 Online monitoring of nitrogen transformations in an aerated CSO-TW 64
3.1 Introduction 65
3.2 Material and Methods 67
3.2.1 Operational conditions 67
3.2.2 Sampling and influent characteristics 68
3.2.3 Online measurements 70
3.2.4 Nitrogen balance 71
3.2.5 Data analyses 71
3.3 Result and discussion 72
3.3.1 N forms in feeding and dry periods 72
3.3.2 Components affecting N transformations 74
3.3.3 ORP curves 76
3.3.4 Transformation processes in the event 77
3.3.5 Dynamic of NO_3-N during successive events 81
3.3.6 Limitations on NO_3-N production and NH_4-N removal 83
3.4 Conclusions 85

Thèse accessible à l'adresse : https://theses.insa-lyon.fr/publication/2025ISAL0011/these.pdf © [D. Gonçalves Portela], [2025], INSA Lyon, tous droits réservés

4 Performance of aerated CSO TW in removing micropollutants 87
4.1 Introduction 88
4.2 Material and Methods 91
4.2.1 Operational conditions and sampling 91
4.2.2 Sampling 93
4.2.3 Analysis of micropollutants in the dissolved phase of water samples 93
4.2.4 Analysis of metals 94
4.2.5 Fecal indicators (FI) analysis 94
4.2.6 Dataset analysis 94
4.3 Results and Discussion 95
4.3.1 Selected micropollutants 95
4.3.2 Fecal Indicators 105
4.4 Conclusions 107
5 General discussion and perspectives 109
5.1 General discussion 109
5.1.1 Standard parameters 109
5.1.2 Filter aging and clogging issues 112
5.1.3 Nitrogen transformations 114
5.1.4 Micropollutants 119
5.2 Perspectives 119
GENERAL CONCLUSIONS 122
ANNEX 1 125
ANNEX 2 132
ANNEX 3 135
ANNEX 4 140
ANNEX 5 141
REFERENCES 142

Thèse accessible à l'adresse : https://theses.insa-lyon.fr/publication/2025ISAL0011/these.pdf © [D. Gonçalves Portela], [2025], INSA Lyon, tous droits réservés

GENERAL INTRODUCTION

Countries that use combined sewer systems (CSS) to manage stormwater (SW) runoff during rain events have a historical with polluted surface water (Ahmed et al., 2020; Passerat et al., 2011; Soriano and Rubió, 2019). These systems convey diluted wastewater mixed with SW to wastewater treatment plants (WWTPs) designed for a limited hydraulic capacity. When this capacity is exceeded during heavy rainfall, combined sewer overflow (CSO) is discharged directly into surface waters. Climate modeling studies predict that in long term rainfall increases could lead to up to 50% more CSO spills in a Mediterranean area of France (Gogien et al., 2023). Damage caused by CSO discharge are observed through solid resuspension (Sternbeck et al., 2002), eutrophication (Tang et al., 2009) and deterioration of bathing water (Ahmed et al., 2020). Options to address CSO include separating wastewater and stormwater systems, infiltrate locally the rain and runoff water or implementing onsite CSO treatment. Retrofitting sewer systems for separation is often costly (Rizzo et al., 2020), and locally infiltrating rain and SW with a nature-based solution can take years to show results in reducing CSO volumes. In this context, onsite CSO treatment can be a more efficient solution, allowing time to implement sustainable urban drainage systems (SUDs) over time.

Facilities with the purpose to retain CSO already exist, such as storage and retention basins (Gasperi et al., 2012a; Nickel and Fuchs, 2019). This type of concrete basin is used to store overflows of a certain volume, which is then returned to the sewer during dry periods for treatment by the treatment plant. They can be expensive in terms of both investment and operational costs. To better address current and future pollution control of urban SW, facilities equipped with systems that can both buffer and treat CSO locally are worth considering. Vertical flow treatment wetlands (VFTW) are particularly suitable for CSO treatment. VFTWs manage stochastic hydraulic loads and, alongside their detention capacity, effectively treat CSO during rainfall events with short duration and high peak flows (Rizzo et al., 2018). VFTW treating CSOs, also referred to as CSO-TWs (Cross et al., 2021), show efficient treatment, resulting in quality effluent that reduces annual pollutant loads into surface water (Masi et al., 2023; Pálfy et al., 2017b). Studies also demonstrated CSO-TWs' socioeconomic benefits, alleviating urban water management pressures and contributing to improved well-being (Bozovic et al., 2017; Masi et al., 2017).

VFTW design is based on a planted porous substrate with different layers that are effective in removing pollutant. A specific feature of CSO TWs is the throttle, which limits the outflow rate and maintains HRT when the filter is flooded. The system favors filtration and straining of

Thèse accessible à l'adresse : https://theses.insa-lyon.fr/publication/2025ISAL0011/these.pdf © [D. Gonçalves Portela], [2025], INSA Lyon, tous droits réservés

suspended solids (McDowell-Boyer et al., 1986; Yavuz Corapcioglu and Haridas, 1984). The designs of CSO TWs vary, including German, French, and Italian approaches. The differences are in the depth of filtration layers or the presence of a saturated layer and primary treatment (Meyer et al., 2013; Rizzo et al., 2020). The biofilm that grows on the media contributes to the biological degradation of organic pollutants and micropollutants. The dissolved fraction of COD and nitrogen retained by adsorption in the filter and can be further degraded by microorganisms (Dittmer, 2006).

The performance of CSO TWs is affected by a factors, such as hydraulic loads, inflow concentrations, and dry periods (Pálfy et al., 2017c; Ruppelt et al., 2019). Full-scale CSO TWs can reach removal efficiencies of up to 94% for TSS, 80% for COD, and 63% for NH_4-N, though the NH_4-N shows more variability (Masi et al., 2023; Tondera, 2019). Solids are generally effectively removed in CSO TWs, while ammonium removal is less consistent, as it relies on the availability of adsorption sites for NH_4-N. These sites are renewed after NH_4-N is nitrified, which is a three-step process involving initial adsorption during the wet period followed by nitrification, under aerobic conditions during the dry weather. Additionally, the mass nitrified during the dry period is released at the beginning of subsequent feeding event (Dittmer, 2006; Pálfy et al., 2017c). The nitrification efficiency of the VFTW system depends on a variety of factors, including the adsorption capacity of the material (sand or reactive material), biofilm growth, which is affected by the age of the system, temperature, the mass of adsorbed ammonia, and the length of the dry period between two events. It is challenging to design a system that consistently maintains stringent outflow ammonia concentrations. A dynamic design is essential to maintain low levels (Pálfy et al., 2017b), and the use of specific adsorbing materials can increase investment costs. Furthermore, the three-step process of nitrification in passive systems can result in nitrate flushes, which in some cases may result in high TN outflow concentrations. This could prove problematic when TN outflow concentrations are targeted by regulation.

CSO TWs can remove micropollutants and pathogens to a certain extent. Diclofenac and metoprolol removal varies widely, with efficiencies ranging from 20% to 80%, while carbamazepine often shows negative removal efficiency in CSO TWs (Ruppelt et al., 2020; Scheurer et al., 2015; Tondera et al., 2019), which can be due to remobilization, breakthrough, or metabolite recombination within the filter (Ruppelt et al., 2020; Tondera et al., 2019). For fecal indicators, such as *Escherichia coli* (*E. coli*) which are typically present in CSO at concentrations between 10^5 to 10^7 MPN/100 mL, CSO TWs have demonstrated up to a 2 log

Thèse accessible à l'adresse : https://theses.insa-lyon.fr/publication/2025ISAL0011/these.pdf © [D. Gonçalves Portela], [2025], INSA Lyon, tous droits réservés

reduction when using sand (Ruppelt et al., 2018; Scheurer et al., 2015). Such level of disinfection is often not sufficient when the discharge concerns bathing waterbodies or shellfish farming area.

Given the problematic of passive CSO-TW systems regarding nitrogen removal, micropollutants and pathogens, intensified aeration in CSO-TWs could be a solution. The impact of oxygen transfer in aerated VFTW for the treatment of domestic WW has been evaluated in various studies (Boog et al., 2018; Dong et al., 2012; John et al., 2020). Boog et al. (2018) and Khan et al. (2022) showed that high aeration rates in TWs led to nearly 99% removal of NH_4-N. Active aeration using an air blower also demonstrated to improve the performance of TWs considering all biodegradable dissolved pollutants, increasing their resilience to seasonal variations in temperature and robustness despite occurrence of air blowers failure (Boog et al., 2018; Murphy et al., 2016; Redmond et al., 2014). While hydraulic loads and influent quality differ between WW and CSO, the studies on aerated VFTWs were essential to formulate the hypothesis that active aeration could improve dissolved pollutants removal in CSO TWs. This study was conducted under the NICE European project with the main objective of evaluating how aeration can be applied in CSO TWs systems to improve the effluent quality. The specific objectives of the study are:

- Understand the main mechanisms of particulate and dissolved pollutants retention/degradation in aerated CSO TWs;
- Identifying the factor affecting dynamics of nitrogen in the system for different aeration strategies, to target nitrification during feeding events;
- Intensifying hydraulic load events and dry periods to assess design performance under stress conditions that affect filter function;
- Assessing the effect of intensified aeration on micropollutant and pathogen removal.

Research objectives and thesis outline

This thesis investigates two aerated CSO TW pilot systems to understand how aeration influences the transformation processes for pollutants and micropollutants. The research is structured into seven chapters:

GENERAL INTRODUCTION, briefly introduces the key point of TWs for water pollution control, framing the problematics of this study.

Chapter 1, Literature review, provides a comprehensive review on pollutants in CSO and current management practices is presented, emphasizing relevant European and French

Thèse accessible à l'adresse : https://theses.insa-lyon.fr/publication/2025ISAL0011/these.pdf © [D. Gonçalves Portela], [2025], INSA Lyon, tous droits réservés

legislation aimed at controlling CSO pollution. Key design and operational aspects of TWs, especially how they manage variable hydraulic and pollutant loads, are discussed. The literature review also covers the benefits of aerated systems for wastewater treatment, providing context for the study of potential advantages in aerated CSO TWs.

Chapter 2 addresses the gaps in research on aerated TWs for treating CSO. It investigates how aeration affects the hydrodynamic properties of the system and how different aeration strategies impact the global performance related to standard pollutants. By varying hydraulic loads and inflow concentrations, we also aim to identify the efficiency range for dissolved pollutant removal and evaluate system stability. The study focuses on TSS, DCO, DCOs, NH_4-N, NO_3-N pollutants. The variation of operational parameters allowed to understand the mechanisms of dissolved pollutant removal, resulting in low DCOs and NH_4-N effluent concentrations despite variable hydraulic loads.

Chapter 3 untitled nitrogen dynamics in aerated CSO TWs under varying aeration conditions, addresses gaps in knowledge about the factors influencing nitrogen transformations. The chapter aims to assess the limitations to direct nitrification by investigating aerobic processes during feeding events and dry periods. Experiments compared NO_3-N produced during event to NH_4-N removal rate independent of transformations during the dry period. Using optimized aeration for NO_3-N production during the event, sequences of high hydraulic loads and long dry periods effects on nitrification were analyzed. Sensors were used to identify nitrification limitations during feeding events and nitrification during dry periods. The online monitoring tracked nitrogen dynamics during feeding, drainage, and aeration in dry periods, showing trends in nitrogen transformation under aerated conditions.

Chapter 4 assesses the performance of aerated CSO TWs on micropollutants removal and fecal indicators reduction. The analysis included selected chemical compounds, such as pharmaceutical, rubber products and metal. Two different aerated CSO TW designs were evaluated to assess the how gravel and sand top layer impact on removal efficiencies. These findings contribute to understanding the role of aeration in CSO TW efficiency for micropollutant management and disinfection.

Chapter 5, Discussion and perspectives, section presents the findings of the study, outlining the overall processes of the aerated CSO TWs and integrating the chapter results to establish design guidelines for such systems. This chapter presents the results of the study on filter aging after receiving annual hydraulic loads close to those designed for conventional CSO TWs.

Thèse accessible à l'adresse : https://theses.insa-lyon.fr/publication/2025ISAL0011/these.pdf © [D. Gonçalves Portela], [2025], INSA Lyon, tous droits réservés

Furthermore, the chapter outlines potential avenues for future research, suggesting areas for testing in the filter to gain deeper insights into adsorption and microbiological processes.

In the GENERAL CONCLUSIONS, all the study is summarized to answer the main objectives of this study.

Thèse accessible à l'adresse : https://theses.insa-lyon.fr/publication/2025ISAL0011/these.pdf © [D. Gonçalves Portela], [2025], INSA Lyon, tous droits réservés

1 Literature Review

1.1 Management of combined sewer overflow

Stormwater management is an important issue for local authorities, as it directly impacts the quality and quantity of the receiving environment (surface water and groundwater) through pollution control, habitat conservation, supporting river flows, and groundwater recharge. Integrating stormwater management into urban planning helps to prevent flooding and reduces the malfunctioning of sanitation systems (sewers and wastewater treatment plants). Furthermore, there are additional benefits, including the promotion of biodiversity, an enhanced living environment, and a reduction in the urban heat island effect. It is crucial to restrict urban discharges during wet weather in order to safeguard the receiving environment. There are two main types of discharges: combined sewer overflows (CSOs) and runoff water from separate rainwater sewers. In the case of CSOs, the objective is to discharge volumes in excess of water when the capacity of the sewer system or wastewater treatment plants (WWTP) is exceeded.

Many agglomerations with a part of combined sewers, or due to ageing sewers or uncontrolled connections, tend to collect rainwater, which can affect the functioning of WWTPs. Indeed, WWTPs are designed to treat dry weather flows and an amount of stormwater (SW), but cannot cope with all flow variations - 2 to 7 times the dry weather flow in Germany, for example, is accepted at the WWTP (Uhl and Dittmer, 2005). Nevertheless, the level of pollution from urban SW discharges can be higher than or equal to that of wastewater in terms of concentrations of metals, suspended solids, and hydrocarbons. Furthermore, the mass flows of these pollutants are significantly higher (Ellis et al., 2005). SW discharges associated with separate or combined sewer systems have been identified as a source of physical, chemical and ecological degradation of the receiving environment (Passerat et al., 2011; Soriano and Rubió, 2019). This is a contributing factor to the failure to achieve good ecological status, as required by the European Water Framework Directive. It can also affect economic activities, especially in coastal areas with sensitive uses (shellfish and/or bathing areas).

To prevent overflows, the priority is to infiltrate rainwater at source, i.e., as close as possible to the point where it reaches the ground, in order to divert it as far as possible from combined or separate sewer systems. Nature-based solutions can play an important role in achieving this goal. However, the disconnection rate from the system takes time (several years) and the efficiency on CSO volume discharge requires a large development of rain infiltration

Thèse accessible à l'adresse : https://theses.insa-lyon.fr/publication/2025ISAL0011/these.pdf © [D. Gonçalves Portela], [2025], INSA Lyon, tous droits réservés

systems(Montoya-Coronado et al., 2024). The problem is exacerbated by climate change, which increases rainfall intensity and hence CSOs.

In addition to flowrate of SW runoff the concentration of pollutants is affected by climate, seasonality, catchment area characteristics and urbanization. Rainfall volume and stormflow peak vary based on duration, intensity and frequency of rainfall events (Davie, 2010). SW surface management based on storage strategies mainly focuses on attenuating hydraulic peak. In a CSS, the occurrence of overflow during a rain event is dependent on the hydraulic capacity of the sewer system or the WWTP, as well as the impervious area connected to the sewer and the condition of the sewer, which is often linked to its age. When overflow occurs, it is managed either by directing it to a receiving water body, storage tanks, or retention basin (Gasperi et al., 2012a; Nickel and Fuchs, 2019). These CSO facilities have a large storage capacity.

The implementation of treatment wetlands at the point of discharge can be a useful complementary approach to managing hydraulic and pollutant flows, as it can quickly reduce the impact on the water body and avoid high investment costs in sewers or WWTPs. A wide variety of treatment wetlands have been tested (stormwater ponds, surface flow wetlands, floating treatment wetlands, horizontal and vertical flow treatment wetlands), the main characteristics of which are described in detail in Tondera et al. (2018). Vertical flow treatment wetlands, which are more robust than horizontal flow systems in accepting high hydraulic load variations have been well studied. CSOs, which are a mixture of domestic wastewater (WW) and SW, are more concentrated than rainwater, making their treatment more challenging, especially when precise discharge limits have to be guaranteed by local authorities.

The extent of overflow due to urbanization depends on factors such as imperviousness, land use (e.g., residential, industrial, rural), and population density (Lee and Bang, 2000; Nickel and Fuchs, 2019). Urbanization reduces the space available for runoff water to infiltrate, increasing the volume of water conveyed to the CSS. This leads to more CSO volume and events and increases the risks of floods due to overload of drainage system. Additionally, urban runoff contributes to the wash off of pollutants from paved surface, carrying a variate of contaminates from human activities into the sewer system. Therefore, not only is the volume of CSO problematic, but also the accumulated load of organic matter, nutrients, pathogens and emerging contaminants it carries. These pollutants can cause eutrophication and resuspension of solids, along with disturbances to local microbial communities in river, resulting in a loss of river water quality (Noyer et al., 2020; Zhang et al., 2023).

Thèse accessible à l'adresse : https://theses.insa-lyon.fr/publication/2025ISAL0011/these.pdf © [D. Gonçalves Portela], [2025], INSA Lyon, tous droits réservés

1.2 Pollutant concentrations in CSO discharge

A wide range of CSO concentrations can be observed due to the climate and the catchment area. The data-driven model developed by Montoya-Coronado et al. (2024) identified the various income sources contributing to overflows in CSS. In addition to wastewater and runoff water connected to the sewer, the water from surrounding soil infiltration should be considered. As a result, it is challenging to accurately predict overflow volumes and pollutant concentrations across different contexts and even between two events in the same catchment area. While models can provide a reasonable estimate of the series of overflows to be treated, monitoring is essential to reduce uncertainties.

Rainfall dependence on the land use was observed by Lee and Bang (2000) to affect peaks of pollutants in runoff from areas that are small (< 100 ha) but highly occupied. These pollutant flushes in runoff result from the resuspension of solids and in CSSs can be influenced by the intensity of rain and runoff depth (Jensen et al., 2022; Perera et al., 2019). However, flush phenomena and its application in SW runoff management remain controversial (Jensen et al., 2022). Bertrand-Krajewski (1998) defined first flush occurrences as events where the majority of pollutant mass is carried at the very beginning of the rainfall event, although this was found to be rare based on the data analyzed in his study. Nevertheless, the first flush concept is incorporated into local legislation, requiring facilities intercepting overflow from CSSs in WWTP to address pollutants in the first flush, as seen in Carimate, Italy (Masi et al., 2023).

In the study of Madoux-Humery et al. (2015), the authors observed a high variability in the temporal variation of TSS concertations in a CSO event. In general, the primary source of TSS in CSO comes from WW but the increased flow rate intensifies the resuspension of solids, changing the proportion of carried solids. Then, the re-suspension of in-sewer sediment are affected by the intensity of rain events, causing variability in the pollutant concentrations in CSO from one event to another. The proportion of SW to wastewater in sewer overflow ranges from 4:1 to 100:1 (Tondera et al., 2021).

Since the quality of SW varies within a precipitation event, one representation of the total pollutants washed out is the Event Mean Concentration (EMC). They are typically used as an estimate of the overall scale of pollution on a rainfall event scale. The EMC is calculated by summing the pollutant mass throughout the rain event and dividing by the total volume (Barbosa et al., 2012), Equation 1, or by sampling proportional to flow.

$$EMC = \frac{\int_0^t QC\ dt}{\int_0^t Q\ dt} \quad 1$$

Thèse accessible à l'adresse : https://theses.insa-lyon.fr/publication/2025ISAL0011/these.pdf © [D. Gonçalves Portela], [2025], INSA Lyon, tous droits réservés

Where, Q is the flow volume in time and C is concentration of a pollutant, over a time interval.

Examples of EMC concentration ranges of pollutants in CSOs are shown in Table 1.1.

Table 1.1 - EMC of CSO pollutants from literature, along with the range of concentrations

References	TSS ($mg.L^{-1}$)	COD ($mgO_2.L^{-1}$)	TKN ($mgN.L^{-1}$)	NH_4 ($mgN.L^{-1}$)	PO_4^{3-} ($mgP.L^{-1}$)
Gasperi et al. (2012b)	-	136 – 446	7.2 - 27	3.3 - 9.3	0.5 – 1.4
Masi et al. (2023)	15 - 318	47 – 534	-	0 – 26	-
Gooré Bi et al. (2015)	19 - 730	41 - 830	3.6 - 31	-	-
Yin et al. (2017)	80 - 303	47 - 714	-	1.4 – 33.6[a]	-
Tondera et al. (2019)	1 - 110	15 - 170	-	-	-

a NH_3-N form

CSO effluent contains a variety of pollutants and contaminants from both SW and raw sewage. As a result of the dilution of sewage, there is considerable variation in the loads and occurrences of micropollutants (Madoux-Humery et al., 2015). The chemical classes of micropollutants include a variety of compounds with different origin and properties. In addition, the occurrence of these contaminants in CSOs varies depending on the event and catchment area (Mutzner et al., 2022).

These contaminants originate from various sources, including the human use of pharmaceuticals and personal care products in domestic sewage, wash-off from impervious surfaces, vehicle emissions, runoff from nearby industrial areas, and agricultural activities (Gasperi et al., 2012b; Lamprea and Ruban, 2011). Analysis of CSO from different studies has showed the presence of metals, polyaromatic hydrocarbons (PAHs), pesticides, pharmaceuticals and industrial chemicals (Madoux-Humery et al., 2013; Nickel and Fuchs, 2019; Phillips et al., 2012). However, occurrences of pharmaceuticals and pesticides were found predominant from various sites (Mutzner et al., 2022). For example, the pharmaceuticals carbamazepine and diclofenac were frequently observed, with the latter reaching mean concentration of 2.0 µg L^{-1} (Ryu et al., 2014; Tondera, 2019; Madoux-Humery et al., 2013; Del Río et al., 2013). While benzotriazoles, an industrial chemical, were observed by (Launay et al., 2016; Ryu et al., 2014; Scheurer et al., 2015; Tondera, 2019), with concentrations ranging from 7 to 19 µg L^{-1} in the study by Launay et al. (2016).

Escherichia coli (*E. coli*) and intestinal enterococci, which are fecal indicators, are frequently studied parameters for evaluating the water quality of CSOs. The presence of these indicators in CSO samples is considerable, in the order of 10^6 and 10^5 CFU per 100 mL of *E.*

Thèse accessible à l'adresse : https://theses.insa-lyon.fr/publication/2025ISAL0011/these.pdf © [D. Gonçalves Portela], [2025], INSA Lyon, tous droits réservés

coli and enterococci, respectively (Passerat et al., 2011; Scheurer et al., 2015). Passerat et al. (2011) showed that direct discharge of CSO during peak rainfall led to concentrations of $4x10^4$ *E. coli* and $8x10^3$ intestinal enterococci per 100 mL in the river. The deterioration of the natural environment caused by point source pollution from sewer systems through CSOs (Passerat et al., 2011; Zhang et al., 2023) has resulted in more stringent legislation regarding CSO discharge.

1.3 Legal situation

The European Union has established minimum requirements for best environmental practices for all member states through Council Directives. Council Directive 91/271/EEC outlines wastewater treatment standards based on factors such as population equivalents (p.e.) and the sensitivity of the area to pollution. According to this directive, the overflow of sewage into receiving waters due to storm events should be limited by measure such as dilution rate or number of discharge per years. However, it is up to the Member States to decide how to limit the overflow by defining an acceptable dilution rate or a number of overflows per year.

Findings from the study of Lamprea and Ruban (2011) showed potential risks of direct discharge of untreated SW into surface water, as suspended solids concentrations exceeded the 35 $mg.L^{-1}$, which is the limit set in 91/271/EEC for treated wastewater. These occurrences highlight the necessity for periodic revision of the directive, specially, on the discharge of CSO. Since 2019, the directive has been evaluated to address pollution sources from sewer overflow and small communities, introducing restrictions on emerging contaminants and adopting new approaches to energy and the circular economy.

In the ongoing proposal for a revised Directive, COM/2022/541, the collection of CSO and urban runoff in a leak-proof network should be managed for agglomerations with WWTP of a p.e. >100 000 and in sensitive areas, to reduce occurrences of pollution during wet weather. Additionally, CSO should not represent more than 1% of the volume collected in dry weather condition in a WWTP. For agglomerations of 10 000 p.e., the CSO quality should be monitored. The requirement for nutrient removal and polishing treatment to remove micropollutants might be implemented in all large facilities, WWTP of >100 000 p.e.. These new regulations will be progressively implemented until 2040.

In France, wastewater treatment is an important part of preserving the aquatic environment of the watershed outlined in the Water Management Scheme (Schéma Directeur d'Aménagement et de Gestion des Eaux - SDAGE). A fundamental guideline in SDAGE 2022-

Thèse accessible à l'adresse : https://theses.insa-lyon.fr/publication/2025ISAL0011/these.pdf © [D. Gonçalves Portela], [2025], INSA Lyon, tous droits réservés

2027 is to reduce source of pollution from untreated stormwater and limit overflow by increasing areas of infiltration. The criteria for CSO discharge are regulated by the administrative act of July 21, 2015 (Arrêté du 21 juillet 2015), which stipulates that CSO spills must not exceed 5% of the total volume discharged in WWTPs. However, this limit is not always respected. Montoya-Coronado et al. (2022) observed overflow volumes exceeding 11% in the catchment area of Ecully, part of the Greater Lyon Metropolitan area.

Each municipality is responsible for monitoring the implementation of the regulation. It is compulsory to verify occurrences of overflows for each CSO structure that collects more than 120 kg/d of BOD5, which corresponds to 2000 p.e.. For higher daily loads, continuous monitoring of overflow volume and concentration are required. When a treatment system is installed to treat online CSO, it is considered as a WWTP and has to comply with the outlet standards targeted by the municipal WWTP (Rizzo et al., 2020).

Climate change is affecting magnitude and frequency of rainfall (Gogien et al., 2023), aggravating the pollution caused by CSO spills (Cheng and AghaKouchak, 2015). Climate change concerns are addressed in both European and French regulations. Strategies such as replacing impervious areas with spaces for stormwater infiltration and implementing facilities to treat CSO are being emphasized.

1.4 Treatment Wetlands for combined sewer overflows

Treatment Wetlands (TWs) are increasingly utilized as a green solution to treat polluted water. The flow direction, whether horizontal or vertical, is a crucial characteristic that defines the hydraulic behavior throughout the TW. Furthermore, the main treatment occurring in free water or fixed media categorizes the system as either a surface flow (SFW) or subsurface flow (SSFW) wetland. The basic types of TW are distinguished by (Dotro et al., 2017) :

- Free water surface (FWS): the flow is predominantly horizontal, with dense vegetation anchored in dispersed media or floating vegetation, exhibiting robustness to variable flows. Large areas are required to accommodate this system.
- Horizontal subsurface flow (HSSF): water is retained beneath the media, where a biofilm adheres to the media, facilitating biological degradation of pollutants. Anoxic conditions prevail in the filter without mechanical aeration. This TW can be more suitable to constant inflow and pretreated water.
- Vertical subsurface flow (VF): a substantial portion of pollutants undergoes biodegradation beneath the surface, as in HSSF. The gravel layer and drainage pipes at the bottom of the

Thèse accessible à l'adresse : https://theses.insa-lyon.fr/publication/2025ISAL0011/these.pdf © [D. Gonçalves Portela], [2025], INSA Lyon, tous droits réservés

filter provide effective drainage, which promotes better oxygenation throughout the cross-section and establishes aerobic conditions. This system performs well under variable flows with intermittent feeding.

It is common to combine or modify these basic types to meet the specific requirements of effluent concentrations. Considering the characteristics of each TW, design approaches based on VF has proven to be most suitable to treat CSO, which will be referred by CSO-TW (Cross et al., 2021). This type was selected due to its capacity to maintain good performance and attenuate hydraulic peaks. Compared to HSSF and FWS, CSO-TWs offer the advantage of lower areal occupation, as they are capable of treating a greater volume of water in a shorter time. Furthermore, some CSO-TW designs offer additional benefits, such as compactness, resilience to a wide range of hydraulic loads, and the potential to provide ecosystem services (Rizzo et al., 2018).

1.5 General design considerations for CSO-TW

The design of CSO-TWs can vary based on inflow characteristics or target. Countries such as Italy, Germany, France, and US adapted CSO-TWs differently, considering space constraints, expertise and weather conditions (Meyer et al., 2013; Rizzo et al., 2020; Tao et al., 2014). What they have in common is at least one vertical-flow filter bed sealed to with a geomembrane to prevent infiltration. Drain pipes at the bottom of the filter bed convey water to the outlet, where a throttle regulates the outflow rate. Another common characteristic is the freeboard, designed to store water on top of the filter bed to treat a maximum of the CSO spill.

In the US, CSO-TWs may be the combination of one or more TWs. A FWS is employed for primary treatment and a VFTW for secondary treatment, as discussed by Tao et al. (2014). This system effectively handles inflow fluctuations, as the FWS provides ample space for flood storage. However, the footprint required for the FWS is larger compared to a SSFW, making land space a decisive factor for the TW type selection (Rizzo et al., 2020; Shutes et al., 1997).

In Germany, the VF, also known as the Retention Soil Filter, is preceded by a storage tank. Once the precipitation has ceased, the retained water that did not overflow to the filter is transferred to the WWTP. The TW comprises a filter bed with 1 to 2 m of freeboard on top of the filter surface, 0.75 to 1 m of filtration layer, and 0.25 m of drainage layer (Figure 1.1). The filtration layer consists of sand with at least 20% carbonate content to ensure pH buffer capacity (DWA-A178, 2019). A thin layer of crushed stone or fine gravel prevents erosion at the inlet point (Meyer et al., 2013).

Thèse accessible à l'adresse : https://theses.insa-lyon.fr/publication/2025ISAL0011/these.pdf © [D. Gonçalves Portela], [2025], INSA Lyon, tous droits réservés

In French CSO-TW systems, the flow enters in the filter after passing through a screening stage, which may or may not include a sand and grease trap. Sludge accumulates on the top of the filter layer, forming a deposit layer of compost and filters are alternated monthly. For small event, only one bed is used, while for intense events interconnections between filters allow using the whole surface by an overflow from one filter to the other one. The detention space for this filter can reach up to 2 m, (Figure 1.1). Coarse sand forms the initial media (d_{10} between 0.4 and 0.7 mm), with a depth of around 0.6 m. A transition layer of 0.1 m depth of fine gravel (2-8 mm) separates the filtration and drainage layers, with the latter being 0.3 m deep coarse gravel (10-25 mm) (Molle et al., 2013). The permanently saturated drainage layer provides resilience to plants and prevents biomass dehydration in dry weather. It allows as well decreasing the preferential pathway that can impact dissolved outflow concentrations (Pálfy et al., 2017c). Aeration pipes connected to the atmosphere are implemented above the permanent saturated layer to allow oxygenation at the bottom of the unsaturated layer (Meyer et al., 2013; Pálfy et al., 2017a).

In Italy, based on the concept of first flush, CSO sediment is collected in a tank and distributed to four VF TWs. The filter bed comprises three layers: 0.2 m of fine gravel at the top, followed by 0.4 m of siliceous coarse sand, and finally 0.2 m of coarse gravel. Similar to French CSO-TW, the bottom layer remains permanently saturated. Ponding in this filter is limited to 0.2 m, as after receiving the first flush, higher hydraulic load bypasses the filters and enters directly into the FWS (Figure 1.1).

The deposit layer on top of the filtration layer can occurs in all CSO-TWs. Tondera et al. (2019) observed a 0.1 m deposit layer in a Retention Soil Filter that had been in operation for 4 years. In the French approach, the deposit layer was observed at the star of the system, which benefited the filter performance (Molle et al., 2013). In colder seasons, during periods of low temperatures, the deposit may take longer to mineralize, slowing infiltration, but it does not adversely affect the filter. Even if heterogeneous, the accumulation rate has been measured at a rate of 3.5 $cm.y^{-1}$ on average (Pálfy et al., 2017a).

Thèse accessible à l'adresse : https://theses.insa-lyon.fr/publication/2025ISAL0011/these.pdf © [D. Gonçalves Portela], [2025], INSA Lyon, tous droits réservés

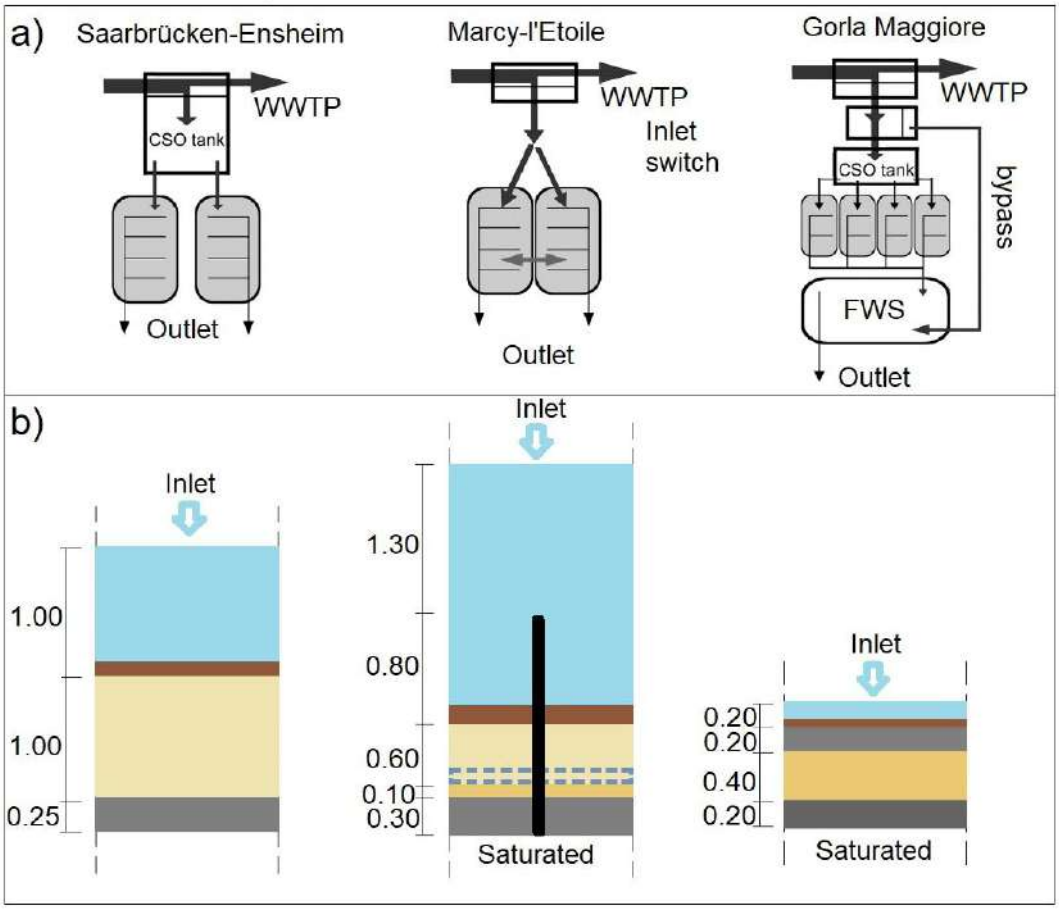

Figure 1.1 - German, French and Italian design approaches of the CSO-TW. a) Top view of the systems with all their components. b) Cross section of the filter showing the depth of heir different layers. Figure adapted from Meyer et al. (2013).

1.6 Relevance of filter material and plants

Vertical filter contains at least two different size substrates for drainage and filtration, but a transition layer can compose the filter design. The type of substrate suitable for composing the filter are classified in the Unified Soil texture Classification System (ASTM Standard D2487, 2011) as: medium and fine sand (0.075-2 mm), coarse sand (2-4.25 mm), which can be considered as fine gravel for TWs, gavel (4.75-20 mm) and coarse gravel (20-75 mm).

Careful selection of substrate is crucial, as inefficiencies in pollutant removal or solids filtration may be attributed to the filter materials (Langergraber et al., 2019; Shutes et al., 1997). Media containing crystalline aluminosilicates, such as zeolite, are used to enhance ammonium adsorption due to their cation exchange capacity (Bruch et al., 2011; Fachini and Vasconcelos, 2006). In Germany, less than 2% of silt and clay is recommended to prevent clogging (Bruch et al., 2011). Although silt, clay, and organic material present in suspended solids can form a deposit layer that, due to high microbial activity, favor degradation of pollutants (Uhl and

Thèse accessible à l'adresse : https://theses.insa-lyon.fr/publication/2025ISAL0011/these.pdf © [D. Gonçalves Portela], [2025], INSA Lyon, tous droits réservés

Dittmer, 2005). The recommendation for effective nitrification, in addition to the type of material, is a minimum depth of 0.5 m (Langergraber et al., 2019).

Each soil matrix has porosity characteristics that determine water content, hydraulic conductivity and space for bacterial growth within the filter. Porosity within a filter can range from 30% to 45%, according to material size, shape and compaction. Flow conditions within the filter depend on its hydraulic conductivity, that is dependent on the porosity and the small particle size (Kadlec and Wallace, 2008; Reed et al., 1995).

Phragmites australis, or common reeds, are the most commonly planted species in CSO-TW in Europe, typically at a density of 5 plants/m². This species is well-suited to flooded areas and is perennial. They mechanically disrupt deposit layers through stem movement with wind or during sprouting. Root systems, which may extend up to 0.6 m for common reeds, serve as microbial attachment substrates and regulate microbial communities, thus extending the operation time without clogging. Vegetation management in CSO-TWs, usually, maintain vegetation without harvesting. Plant litter, a seasonal trait process, provides insulate during winter and allows a faster deposit of organic matter that can help the adsorption of pollutants such as ammonia and metals. (Langergraber et al., 2019; Tondera et al., 2018). However, tree harvesting is necessary to prevent from preferential flows.

1.7 Hydrodynamics

In the preceding section, we discussed the characteristics of materials and vegetation, both of which influence the hydrodynamics of the filter (Shutes et al., 1997). Hydraulic conductivity (k_s) is an inherent property of the material conducting water flow and varies over time due to substrate compaction (Sanford et al. 1995), biomass and solids accumulation. The hydraulic conductivity can be maintained due to the movement of plants when a deposit layer is formed on the surface of the filter (Brix, 1997; Woods Ballard et al., 2016). On the one hand, the root systems in the gravel layer can occupy porous space and reduce the hydraulic conductivity. On the other hand, the hydraulic conductivity in systems with a sand layer may be influenced by root and rhizome growth, resulting in the creation of additional porous space or the formation of preferential pathways. It should be noted that substrate with high hydraulic conductivity may compromise pollutant removal efficiency (Dotro et al., 2017). In the SUDs manual, material with a saturated hydraulic conductivity of 10^{-5} m.s^{-1} is presented as example of a bioretention filter medium. The main layer of the filter using sand requires a material that does not contain

Thèse accessible à l'adresse : https://theses.insa-lyon.fr/publication/2025ISAL0011/these.pdf © [D. Gonçalves Portela], [2025], INSA Lyon, tous droits réservés

an of excessive fine particles to maintain a hydraulic conductivity of at least10^{-4} m.s^{-1} (Meyer et al., 2013). Otherwise, the permeability of the filter can be adversely affected.

On the one hand, reductions in permeability caused by vegetation and microorganisms decrease k_s. Decreasing permeability may contribute to increase residence time, influencing pollutants removal (Dotro et al., 2017; Shutes et al., 1997). In CSO-TW, the outlet throttle is usually the main driver of hydraulic retention time and infiltration rate (Dittmer, 2006). Hence, the filtration speed of CSO-TW is designed to range between 0.01 and 0.05 $L \cdot s^{-1} \cdot m^{-2}$ (Rizzo et al., 2020). By controlling the discharge flow rate during CSO peak flow in a rainfall event, it is possible to reduce the hydraulic pressure on the receiving surface water body (Rizzo et al., 2018). Filter design provides basic information on filter hydraulic properties, but tracer tests are widely used to characterize filter hydrodynamics (Headley and Kadlec, 2007). These tests identify HRT and preferential flow paths, indicating the duration and homogeneity of contact between biomass and effluent. The theoretical HRT is calculated by dividing TW volume by outflow rate, but dead zones or preferential paths can reduce active volume and HRT.

In tracer tests conducted by Pálfy et al. (2017c), the authors observed hydraulic shortcuts when the event began, resulting in outflow concentration peaks of dissolved pollutants. Increasing filter saturation over the event duration favor treatment by promoting more even flow distribution and minimizing preferential flow paths. The tracer test performed in Pálfy et al. (2017c) demonstrated that in the initial unsaturated phase, HRT was at 1 h, with water infiltration only near to the feeding point. After the filter reached complete saturation, HRT increased to 16 h. Therefore, at the beginning of an event, saturation and hydraulic conductivity play a significant role in the flow distribution within the filter, which consequently affects HRT. At the highest water level, due to the throttle, the infiltration rate is maintained stable, leading to the maximum HRT designed for the filter when working in ideal conditions, without clogging or preferential paths.

Hydrodynamic will impact effluent quality. Firstly, heterogeneous flows will impact microbial population distribution. Secondly, the shorter the HRT, the lower the biological degradation of biodegradable pollutants due to kinetic rate limitations. Additionally, microbial communities may have less advantage in oxygen exploitation when the CSO TW is fully saturated. Overall, hydraulics are closely linked to the efficiency of pollutants treatment.

Thèse accessible à l'adresse : https://theses.insa-lyon.fr/publication/2025ISAL0011/these.pdf © [D. Gonçalves Portela], [2025], INSA Lyon, tous droits réservés

1.8 Removal mechanisms

In TWs, pollutant removal processes involve physical, chemical, and biological mechanisms. Sedimentation and filtration, classified as physical mechanisms, primarily retain suspended solids in CSO-TWs. Unsettled influent with high loads of suspended solids may lead to more significant sedimentation/filtration, particularly in systems such as French TWs. The trapping of suspended solids primarily occurs in the upper layers through filtration, with additional aid from straining that occurs when suspended solids remain blocked on the pore spaces within the filter (McDowell-Boyer et al., 1986; Yavuz Corapcioglu and Haridas, 1984). The biofilm growth sustained by the media surface has the effect of decreasing pore space and improving solid filtration. In general, the submerged plant tissue provides improve sedimentation of suspended solids (Brix, 1997). On average, particles retained through filtration are above 5 µm in size (Tondera et al., 2018). Physical filtration effectively removes total suspended solids (TSS) and pathogenic organisms attached to the solid particles at high removal rates, relatively independent of hydraulic loading rates (HLR) and HRT compared to other parameters.

Dissolved pollutants and micropollutants with hydrophobic characteristics, such as ammonium and metals, are retained through sorption processes, where adhesion onto the material is variable depending on the affinity between the compound and the adsorbent material. Changes in filter physico-chemical characteristics (e.g., dissolved oxygen, pH, temperature) and the concentration of dissolved compound in the liquid phase can result in a new equilibrium. This can result in the transformation or release of adsorbed substances, with the potential for substances adsorbed onto the substrate to be exchanged for particles with a stronger affinity to the substrate under the given conditions. A stabilization period for sorption processes occurs during the initial stages of filter operation (Malaviya and Singh, 2012). Available sorption sites vary according to substrate characteristics, biofilm development, and the presence of a deposit layer on top. Certain materials, such as zeolite and pozzolana, can be added to the filtration bed to enhance adsorption capacity of ammonium (Pálfy et al., 2017c). Runoff in combined sewers often brings substances such as hydrocarbons (PAHs) and heavy metals, which are removed through filtration or adsorption (Malaviya and Singh, 2012).

The process of biofilm formation is also important for the microbial processes, as the microorganisms responsible for biodegradation are present. The biofilm and deposit layer serve as biologically active zones where organic dissolved pollutants are adsorbed then degraded (Ruppelt et al., 2020). Microbes within the biofilm incorporate adsorbed substances into their bulk. Oxidation-reduction potential (ORP) reactions result from microbial metabolism and

Thèse accessible à l'adresse : https://theses.insa-lyon.fr/publication/2025ISAL0011/these.pdf © [D. Gonçalves Portela], [2025], INSA Lyon, tous droits réservés

reflect their development. The most common microbial processes in TWs are aerobic oxidation and anaerobic reduction. Aerobic conditions favor the kinetics of organic matter removal and nitrogen oxidation (Kadlec and Wallace, 2008). Efficient removal of organic matter and nitrogen is essential to prevent water surface pollution. In the classical path of nitrification-denitrification for nitrogen removal, ammonia is transformed into nitrate in aerobic zones and into a gaseous form in anoxic zones. Based on stoichiometric reactions, the oxygen concentration required for nitrification is approximately 4.6 times the loaded ammoniacal nitrogen (Vymazal, 2007). However, the absence of anaerobic zones in the current design of the CSO-TW makes denitrification less likely.

Additionally, biological mechanisms for microbiological purification include microorganism predation, parasitism, and starvation or dehydration (Waldhoff, 2008). Oxidation of microbes and predation by protozoa in the biofilm depend on biological conditions and microbial communities. Therefore, filtration and adsorption may be the primary mechanisms for eliminating microorganisms (Ruppelt et al., 2018). The removal process in TWs can also involve one or more mechanisms acting to degrade a substance. For example, some micropollutans, are removed by biodegradation or plant uptake (Matamoros et al., 2012).

1.9 Performance of pollutant removal

1.9.1 Standard pollutants

The TSS, COD, DBO_5, NH_4-N and NO_3-N are pollutants widely used as parameters to assess water quality and filter performance in the treatment of CSOs (Meyer et al., 2013; Pálfy et al., 2017a; Rizzo et al., 2020) . Studies (Dittmer et al., 2016; Frechen et al., 2006; Masi et al., 2023; Tondera et al., 2019) have demonstrated the robustness of full-scale CSO-TWs and their effective performance over three or more years of operation. Passing throughout filtration layer, the outlet concentration of suspended solids (SS) is significantly reduced, often reaching levels below 10 $mg.L^{-1}$ (Pálfy et al., 2017a; Uhl and Dittmer, 2005). Removal of TSS and chemical oxygen demand (COD) is consistently high and stable, with low variations of TSS outlet concentration and removal efficiencies of up to more than 95% (Table 1.2). For the typical mean inlet concentrations of COD showed in Table 1.1, studies with CSO TWs reported mean outlet concentrations around 30 $mg.L^{-1}$ and 62 $mg.L^{-1}$ (Tondera, 2019; Masi et al., 2023).

Degradation of soluble COD (CODs) and ammonium-nitrogen (NH_4-N) is more sensitive to bacterial activity and microbial processes. Temperature plays a critical role in regulating microbial metabolic rates, with higher temperatures enhancing removal efficiency.

Thèse accessible à l'adresse : https://theses.insa-lyon.fr/publication/2025ISAL0011/these.pdf © [D. Gonçalves Portela], [2025], INSA Lyon, tous droits réservés

Ammonium nitrification is generally limited by a lack of oxygen during feeding events due to the saturation of the filter. Adsorption onto organic matter or specific adsorbing material plays a major role in ammonia removal. Ammonia breakthrough occurs when nitrogen loads exceed the filter's adsorption capacity (Woźniak et al., 2007). Therefore, ammonium removal rate can be higher at the beginning of an event when there are more sites for adsorption, and these rates decrease as these sites become filled. The introduction of oxygen into the unsaturated layer results in the transformation of adsorbed ammonium into nitrate, and the adsorption sites on the substrate are renewed, ready to be refilled in subsequent cycles. The adsorption of NH_4-N is higher in filters with a sand layer, achieving removal rates of up to more than 90% (Table 1.2). Oxygenation within the filter, essential for aerobic bacteria, may be hindered during prolonged ponding or short dry periods, reducing removal rates. Short dry periods can prevent complete transformation of ammonium into nitrate, and extreme dry periods in unsaturated filters may weaken bacteria and reduce their performance in removing CODs and nitrification (Uhl and Dittmer, 2005).

Table 1.2 - Mean removal efficiency of standard parameters in CSO-TWs of different scales.

		Removal efficiency (%)				
	Scale	TSS	COD	CODs	NH_4-N	PO_4^3-P
Uhl and Dittmer (2005)	Full	-	84	-	96	-
Ruppelt et al. (2019)	Pilot	-	80	-	83 - 98	54 - 80
Pálfy et al (2017a)	Full	96	79	37	72	8
Fournel (2012)	Pilot	78	60	20 - 60	33 - 95	-
Tondera et al. (2019)	Full	76 - 94	63 - 80	-	-	-
Masi et al. (2023)	Full	-	83	-	63	-

Ruppelt et al. (2019) conducted a study correlating ORP with NH_4-N outlet concentrations in pilot-scale CSO-TWs. With CSO inflow concentrations within the range of those in Table 1.1 - EMC of CSO pollutants from literature, along with the range of concentrations and predominance of oxidative states within the filters, the outlet concentration of ammonium-nitrogen was found to be below 1 $mg.L^{-1}$. However, when conditions within the filter shifted

Thèse accessible à l'adresse : https://theses.insa-lyon.fr/publication/2025ISAL0011/these.pdf © [D. Gonçalves Portela], [2025], INSA Lyon, tous droits réservés

towards a more reductive state (ORP between -250 mV and 0 mV), indicative of an anoxic zone, the outlet concentration of ammonium increased to over 8 $mg.L^{-1}$ (Wießner et al., 2005). Some authors consider soils with a redox potential below 300 mV as reductive environments, conducive to denitrification processes as long as carbon source is available (Kadlec and Wallace, 2008).

The C/N ratio additionally limits denitrification processes, as heterotrophic bacteria utilize carbon as a source of electrons to reduce nitrate. Denitrification under anoxic conditions in the saturated layer requires ideally twice as much carbon as NO_3-N and 18 h of HRT (Morvannou et al., 2017). However, distribution of denitrifying bacteria throughout the filter may be irregular, resulting in varying rates of nitrogen removal (Shirdashtzadeh et al., 2022). Masi et al. (2023) and Ávila et al. (2013) observed total nitrogen (TN) removal rates in VF during feeding events of approx. 47% and 20%, respectively. During a feeding event, TN removal relies on ammonium retention, which can be variable depending on the sorption capacity of the filter, and denitrification where nitrogen is completely removed.

The phosphate load in the inflow to CSO-TWs is typically low (Table 1.2), as observed in Pálfy et al. (2017a) . Ruppelt et al (2019) achieved better removal of phosphate (PO_4^3-P) with a serial connection of two filters, resulting in an outlet concentration of 0.18 $mg.L^{-1}$. However, in single filters, some leaching of PO_4^3-P may occur when adsorption capacity is exceeded (Pálfy et al., 2017c; Ruppelt et al., 2019). Contrary to nitrogen, phosphate is mostly accumulated sorbed in the filter with part of it is taken by plants. Then, phosphorous removal depends on the adsorption capacity of the media, which is not renewable and is limited to the total load over time (Dotro et al., 2017; Tondera, 2019). However, phosphates contribute to the eutrophication of sensitive surface waters, leading to strict regulations on the release of phosphates.

The aging of the filter is characterized by reduced removal in TSS and COD compared to removal after filters' maturation (Tondera, 2019; Tondera et al., 2019). While less biodegradable substances showed a trend on lost their removal efficiencies over time. Therefore, media saturation should be considered in filter management strategies.

1.9.2 Micropollutants

Micropollutants carried by rainwater often coalesce with organic matter and within SS particles, as is the case of most toxic metals and PAHs. For these particle-bound substances, the removal by sedimentation and filtration is effective of up to more than 80% removal efficiency in CSO-TWs (Masi et al., 2023; Pálfy et al., 2017c). Scheurer et al. (2015) observed high removal rates

Thèse accessible à l'adresse : https://theses.insa-lyon.fr/publication/2025ISAL0011/these.pdf © [D. Gonçalves Portela], [2025], INSA Lyon, tous droits réservés

(>90%) for readily biodegradable pharmaceuticals in CSO-TWs. In a simulated event with SW, Janzen et al. (2009) demonstrated removal rates of 79–96% for a VF TW treating micropollutants used in UV filters, antioxidants, or plasticizers. These results indicates that the system has the potential to effectively control the spread of micropollutants. However, many persistent and slow biodegradable micropollutants are not easily removed or show variable removal rates in COS TWs. Examples of such micropollutants include diclofenac, sulfamethoxazole, and carbamazepine (Ruppelt et al., 2020; Scheurer et al., 2015). Additionally, the adsorption capacity of the filter's substrate is limited for these compounds, which may require the replacement of the media to maintain performance removing micropollutants (Tondera et al., 2019).

Operation parameters are crucial for maintaining filter performance and maximizing the removal of the wide range of contaminants entering the filter. Operational parameters such as organic loading rate (OLR) and HLR show strong correlations with micropollutants removal (Ilyas et al., 2021; Ruppelt et al., 2020). Matamorros et al. (2007) observed that efficiently removed pharmaceuticals are less affected by flooding, which is a normal condition in CSO TWs. Temperature and filter age, as well, can play a role in micropollutant removal (Tondera et al., 2019).

Micropollutants with variable removal rates may demonstrate enhanced stability under certain conditions. A comparison of layer thicknesses of CSO-TWs pilots by Ruppelt et al. (2020) found that metoprolol showed reduction of up to 70% in thicker layer. Diclofenac showed better removal efficiency under higher ORP, which are indicative of aerobic conditions (Ruppelt 2019). Additionally, removal rates of approximately 75% for diclofenac were observed in studies by Scheurer et al. (2015) and Tondera et al. 2013 (2013). Likewise, the biodegradation of sulfamethoxazole was high under aerobic conditions (Ilyas et al., 2020). For pharmaceuticals that are recalcitrant and persistent, such as carbamazepine, the operational conditions do not necessarily lead to improved removal performance of TW (Ilyas et al., 2021).

It is noteworthy to consider that the filter's performance in retaining micropollutants may result in the formation of byproducts and risks of washout during rainfall events (Scheurer et al., 2015). The removal efficiency of micropollutants is dependent on the characteristics of the filter design, particularly the thickness of the filtration layer, and the removal pathways (Ruppelt et al., 2020). Therefore, predicting removal efficiency for some parameters can be challenging. There are few studies on the removal of micropollutants in CSO TWs. The

Thèse accessible à l'adresse : https://theses.insa-lyon.fr/publication/2025ISAL0011/these.pdf © [D. Gonçalves Portela], [2025], INSA Lyon, tous droits réservés

availability of further results on this topic would contribute to a better understanding of the removal pathway of micropollutants.

1.9.3 Pathogens

Microbial contaminants and their retention in CSO-TW are commonly measured using analyses of *E. coli*, intestinal enterococcus, and coliforms, which are fecal indicator (FI) bacteria. The inlet of FI fluctuates according to rainfall events, justifying the high variability at the filter outlet. Despite fluctuations in loading rates, SSF-CWs have shown resilience in microbial removal performance (Tondera et al., 2018). The retention of *E. Coli*, somatic coliphages and *Giardia* occurs mainly in the top layer and connection of two filters can improve FI reduction (Ruppelt et al., 2018).

The retention of SS considerably contributes to the removal of *E.coli* and intestinal enterococcus in pilot scale CSO-TW, reaching up to 2 $\log_{10}$ reduction (Ruppelt et al., 2018). Similarly, in Ávila et al. (2013) found that CSO treatment resulted in the removal of 1.4 $\log_{10}$ of *E.coli* in the VFTW pilot but the authors reached 4 $\log_{10}$ including HSSF after VFTW. Full-scale CSO-TW have reported removal rates for *E. coli* that are similar to those reported in other studies, averaging 1.2 $\log_{10}$ (Waldhoff, 2008). In the filter studied by (Scheurer et al., 2015), the median removal were slightly higher, at 2.7 and 2.2 $\log_{10}$ for *E.coli* and enterococcus, respectively. The authors suggest that removal of FI differs depending on the retention time, layer material and organic inlet concentration.

The reduction FI remained relatively constant over 3 years, with reductions of 1.1 ± 1.5 $\log_{10}$ of *E. coli*, 1.3 ± 1.7 $\log_{10}$ of intestinal enterococci and 0.6 ± 1.5 $\log_{10}$ of intestinal enterococci reported in Tondera (2019). Zacharias et al. (2020) observed a preferential sanitation effect in the first 0.3 meters of the surface layer in a large-scale CSO-TW cross-section. Additionally, Ruppelt et al. (2018) found that exposing microbes to a wider adsorptive surface, either by coupling two filters or increasing the depth of the filtrating surface, improved FI removal.

1.10 Clogging

Clogging in TW results from the accumulation of solids in the filter pores, primarily due to the filtration process. Factors contributing to clogging include particulate deposition, biomass production from biological activity, chemical precipitation, and the presence of roots (Kadlec

Thèse accessible à l'adresse : https://theses.insa-lyon.fr/publication/2025ISAL0011/these.pdf © [D. Gonçalves Portela], [2025], INSA Lyon, tous droits réservés

and Wallace, 2008). Residual solids and biomass trapped in the pores reduce the active volume of the filter, thereby affecting wastewater treatment efficiency.

Seasonality plays a role in plant development, with increased reed density during certain seasons leading to more challenging conditions for filter oxygenation and altering hydraulics. The combination of high organic loads and increased frequency of events during the winter months can result in a reduction in infiltration speed. The top layer of sand is susceptible to accumulating surface organic deposits. However, this clogging may be reversible if the solids can be mineralized during the resting period. In the French approach, the absence of primary decantation is compensated for by rotating parallel filters. One filter is in use while the other is mineralizing the organic matter that has been loaded previously. In the event of heavy rainfall, both filters can be utilized.

In cases where clogging is caused by the media properties, such as low hydraulic conductivity, it is possible to implement a pretreatment process to settle solids before they reach the filter (Laber, 2000). However, filters without primary treatment and non-uniform grain size distribution of gravel tend to suffer irreversible internal clogging. For CSO TWs using gravel media with uniform granulometry, high HLRs of up to 95 $m^3m^{-2}y^{-1}$ can be achieved without clogging (Masi et al., 2023). Modelling the filter operation aid on the prediction of clogging (Tondera et al., 2018).

1.11 Aeration in TWs

1.11.1 Oxygen requirements in TWs

The decomposition of organic matter and nitrification in TWs are limited by the availability of oxygen. Therefore, the oxygen supply in TWs must meet the demand for maintaining active microorganisms and processing new inputs of carbon and nitrogen. Respiration and decomposition are redox reactions that release energy, facilitating the creation of new cells. Autotrophic and heterotrophic microbes, which use nitrogen and carbon as energy sources, require different proportions of oxygen for growth. Based on stoichiometry, autotrophic microbes consume ten times more oxygen than heterotrophic microbes, explaining the predominance of heterotrophs in aerobic zones (Wynn and Liehr, 2001). Nitrification is a part of autotrophic respiration. As with activated sludge systems, in aerated TWs, estimation of oxygen consumption can be based on empirical values and the stoichiometry of reactions (Cooper, 1999). Cooper (1999) determined the Oxygen Consumption Rate (OCR) that can be used to estimate the mass of oxygen consumed, as defined the Equation 2.

Thèse accessible à l'adresse : https://theses.insa-lyon.fr/publication/2025ISAL0011/these.pdf © [D. Gonçalves Portela], [2025], INSA Lyon, tous droits réservés

$$OC = V[(BOD_{in} - BOD_{out}) + 4.3(NH_4\text{-}N_{in} - NH_4\text{-}N_{out})] \quad 2$$

Where V is the volume of water send in a period in m^3, e.g. $m^3.d^{-1}$; BOD_{in} and BOD_{out} are, respectively, BOD concentrations at the inlet and outlet; and $NH4N_{in}$ and $NH4N_{out}$ are, respectively, ammonium nitrogen concentrations at the inlet and outlet.

Depending on the available data, C and N can be estimated using COD or BOD_5 and TKN or NH_4-N. However, when possible, TKN is the better parameter for estimating O_2 requirements (Nivala et al., 2013). This estimation needs to be used carefully, as it assumes that oxidation is the only removal mechanism This excludes other potential processes, such as ammonification of the filtered organic N, adsorption of ammonium, which can be nitrified, and alternative nitrification pathways (e.g., partial nitrification/denitrification, Anammox, and Canon). Still, knowing typical inlet concentrations and expected outlets provides helpful guidance for designing VFTW, as C and N compounds are the main source for oxidative reactions (Nivala et al., 2013).

Photosynthesis, respiration, oxygen mass transfer from plants, and decomposition represent a minority contribution to TWs oxygen demand. These processes do not have the same impact on the oxygen mass balance since some reactions occur locally in root zones while others affect more comprehensive areas (Kadlec and Wallace, 2008; Nivala et al., 2013). Oxygen contributions through photosynthesis and plant convective transport up to the roots tend to be localized in VFTWs (Kadlec and Wallace, 2008).

DO tends to fluctuate with biological activity, temperature and salinity. Wynn and Liehr (2001) demonstrated in their model that seasonal trends of microbial dynamic and DO concentration can sometimes overestimate or underestimate oxygen consumption based on stoichiometric. For example, lower DO concentrations in water may be related to warmer temperatures or higher electrical conductivity. Kadlec and Wallace (2008) and Vera-Puerto et al. (2022) also highlighted the importance of considering altitude effects when designing TWs. At sea level, the partial pressure of oxygen is 21.11 kPa (1 atm), and represents 21% of air by volume, or 23% by mass of atmospheric pressure. However, at higher altitudes, absolute pressure decreases, consequently reducing the partial pressure of oxygen and its availability in TWs. Additionally, the mass transfer of oxygen in the biofilm is affected by the degree of water mixing, increasing in turbulent flow conditions (Kugaprasatham et al., 1992). Therefore, oxygen saturation depends on temperature, altitude, and how it is incorporated into the water.

Thèse accessible à l'adresse : https://theses.insa-lyon.fr/publication/2025ISAL0011/these.pdf © [D. Gonçalves Portela], [2025], INSA Lyon, tous droits réservés

Oxygen enters the filter's empty spaces through convection, driven by the downward flow of water, or diffusion, from the atmosphere at the surface layer. The amount of oxygen transfer to the biofilm can increase with longer resting periods when the media are unsaturated, and the pores are exposed to oxygen diffusion. Loading can also contribute to oxygen supply by incorporating atmospheric oxygen from fresh influent. Filters with intermittent flow may utilize drainage pipes, as in the French style presented in Figure 1.1, to dissipate air bubbles compressed under water in the filter during feeding.

TWs exhibit a stratified oxygen gradient characteristic of their flow direction and feeding operation. In CSO-TWs, the non-steady-state flow and flooded operation lead to a vertical oxygen profile with anaerobic zones at the bottom of the filter by the end of a loading event. In a filter column loaded with diluted WW, Woźniak et al. (2007) observed that re-oxygenation of the water in the lower parts of the filter occurred due to oxygen entrapped in the sand pores. However, high loading rates can result in oxygen levels dropping to 0 mg/L across all filter depths, with the oxygen from the pores consumed entirely. Similarly, the study by Ruppelt (2019) showed oxidizing conditions in the upper layer due to the availability of oxygen, which gradually shifted to reducing conditions at the end of loading.

1.11.2 Intensified TW

Aerated filter features at least 0.90 m of a saturated drainage layer of coarse gravel, where air bubbles can move upward. Langergraber et al. (2020) and Nivala et al. (2020) recommend maintaining a permanently saturated layer (saturation layer height > 0.80 m) to create anoxic zones for denitrification. Additionally, in the intensified TW configuration allows for the creation of aerobic zones when air is evenly distributed through air diffusers placed at the bottom. The aerobic zones increase the removal rates of organic matter and ammonium nitrogen (Dotro et al., 2017; Wallace et al., 2020).

Despite the higher availability of oxygen due to mechanical aeration, only a percentage of the gaseous oxygen is transferred to the liquid phase. Tests to obtain the Standard Oxygen Transfer Efficiency (SOTE) for aerated systems express the SOTE percentage per meter, typically ranging between 5 to 7%, depending on water quality, media, and bubble diameter (Nivala et al., 2020). The SOTE is used to calculate Actual Oxygen Transfer Rate (AOTR). According to Boog et al. 2014 the AOTR is represented by the equation 3

$$\mathrm{AOTR} = Q_{air,in} * \rho_{air} * 0.23 * \mathrm{SOTE} \quad (3)$$

Thèse accessible à l'adresse : https://theses.insa-lyon.fr/publication/2025ISAL0011/these.pdf © [D. Gonçalves Portela], [2025], INSA Lyon, tous droits réservés

Where $Q_{air,in}$ is the air flowrate programmed in the air diffuser, $m^3.h^{-1}$; ρ_{air} is the density of air, $kg.m^{-3}$; 0.23 is the 23% of total mass of air.

Several studies (Freeman et al., 2018; Nivala et al., 2020; Vera-Puerto et al., 2022) agree that better oxygen transfer is achieved with smaller bubble diameters, as the surface area in contact with water increases. Mass transfer shows a positive effect on bubble residence time, while airflow has a negative impact on this parameter. Consequently, increased airflow reduces bubble residence time, which in turn reduces the SOTE (Vera-Puerto et al., 2022).

Controlling aeration can increase the activity of aerobic microorganisms, resulting in stable background concentrations of soluble and particulate matter (Wallace et al., 2008). Dong et al. (2012) quantified that DO in the water in the upper layer increased up to 2.5 $mg.L^{-1}$ with continuous aeration in the VFTW. The use of intensified aeration in TWs, regardless of flow type or surface loads, commonly stimulates autotrophic bacteria respiration, thereby increasing transformation rates of NH_4-N into NO_3-N, as observed in studies by Boog et al. (2014), Dunqiu et al. (2012), John et al. (2020), and Murphy et al. (2016). For example, aerated VFTW establishes a homogeneous vertical gradient, as observed in hydrodynamic tests (Boog et al., 2014). Simulations by John et al. (2020) showed that higher air ratios in water result in almost constant bacterial distribution throughout the vertical cross-section of an aerated VFTW. Maintaining controlled aeration allows pollutant load fluctuations and HLR variations to be managed without stressing bacteria (Dong et al., 2012).

Control of aeration is an important factor on carbon and nitrogen removal processes. Continuous aeration achieves the highest nitrification rates, but intermittent aeration favors total nitrogen removal due to the formation of aerobic and anoxic zones (Ilyas and Masih, 2017). This is possible due to controlled distribution and growth of bacterial inside a filter when using forced aeration (John et al., 2020). In the study of Tao et al. (2010), intermittent aeration increased the layer depth with aerobic activity, which, coupled with the accumulation of suspended solids, enhanced nitrogen removal. Boog et al. (2014) and Dong et al. (2012) obtained similar results, showing improved total nitrogen removal with intermittent aeration. Boog et al. (2014) noted that intermittent aeration reduces costs and diversifies the microbial community. Additionally, compared with continuous aeration, intermittent aeration may reduce evaporation and evapotranspiration losses, as TW with mechanical aeration affects energy flows (Nivala et al., 2022).

Wallace et al. (2008) compared non-aerated and aerated HSSF and free surface water wetlands, finding that overall TSS removal was improved. The authors hypothesized that the

Thèse accessible à l'adresse : https://theses.insa-lyon.fr/publication/2025ISAL0011/these.pdf © [D. Gonçalves Portela], [2025], INSA Lyon, tous droits réservés

aerobic environment promoted protozoa development, which reduced turbidity. Other studies using aerated systems (including HSSF, VF and surface TWs) to treat domestic or high-strength wastewater and for polishing treatment have shown improved removal efficiency of COD and NH_4-N (Boog et al., 2018; Dong et al., 2012; Dunqiu et al., 2012; Khan et al., 2022). A study Boog et al. (2018) on aerated VF for domestic wastewater treatment showed organic matter removal efficiency higher than 90% for BOD and TOC, with almost complete nitrification (99% removal of NH_4-N).

The potential of aeration for removing microbial contaminants is not entirely clear (Nivala et al., 2020). Wallace (2008) and Stefanakis et al. (2019) observed a reduction of fecal coliforms by around 2 log in the effluent of aerated TWs. Stefanakis et al. (2019) noted that when combined with other treatment technologies, aerated TWs achieve the sanitation levels required by legislation for wastewater reuse. In the study conducted by Headley et al. (2013) an aerated VFTW was observed to drastically reduce *E. coli* in the first 10 cm of the filter, maintaining a stable level across the remainder of the filter. The authors attribute this to the rapid mixing of water in the filter. Furthermore, additional studies are required on the removal of micropollutants by aerated TWs. Nivala et al (2019) concluded that emerging contaminants with high to moderate biodegradability are effectively removed in aerated SSF TWs. Auvinen et al. (2017) found that in full-scale aerated HSSF, the target pharmaceuticals were effectively removed, although only a few of them were affected by aeration. The authors attributed the good performance to long HRT.

The aerated filter demonstrated resilience despite seasonal variations of temperature and interruptions in aeration (Boog et al., 2018; Redmond et al., 2014). SSF wetland took 3 to 8 d to recover from 6 d of air blowers failure (Boog et al., 2018). Additionally, well established nitrifying bacteria demonstrated resistance to mechanical failures, recovering nitrification rates within a few days after aeration was restored (Murphy et al., 2016). It should be noted that intensified aeration has no effect on compounds that are primarily removed through adsorption, such as phosphorus (Wallace et al., 2008). However, it can lead to a delay in the exhaustion of the adsorptive material, as nitrogen adsorption, for example, may decrease. One area of concern is biological fouling, which can impact the SOTE and air blower functionality, but it has not been frequently recorded in TWs. Wallace et al. (2020) suggest effective cleaning of the air distribution network with acid (HCl) in case of fouling. Aeration strategy and maintenance in TW are not fully understood, as many factors affect oxygen transfer (Vera-Puerto et al., 2022).

Thèse accessible à l'adresse : https://theses.insa-lyon.fr/publication/2025ISAL0011/these.pdf © [D. Gonçalves Portela], [2025], INSA Lyon, tous droits réservés

Further studies on aerated TWs could help to address some of the knowledge gaps identified by Nivala et al. (2020). Furthermore, there is a lack of available data on aerated TWs for CSO.

Thèse accessible à l'adresse : https://theses.insa-lyon.fr/publication/2025ISAL0011/these.pdf © [D. Gonçalves Portela], [2025], INSA Lyon, tous droits réservés

2 Removal of standard pollutants in an Aerated CSO-TW

This paper was published in Ecological Engineering, a complete list of publications is presented in ANNEX 5

Impact of Forced Aeration on Vertical Flow Treatment Wetland Performances for Combined Sewer Overflow

Daniella Portela[1], Katharina Tondera[2], Stéphane Troesch[3], Pascal Molle[1]
[1] INRAE, REVERSAAL, F-69625, Villeurbanne, France
[2] Université Claude Bernard Lyon 1, LEHNA UMR 5023, CNRS, ENTPE, F-69518, Vaulx-en-Velin, France
[3] Ecobird, 69630 Chaponost, France
* daniella.goncalves-portela@inrae.fr

Highlights

- Aeration increased mixing capacity and avoided short circuits in CSO wetland pilots;
- Appropriate aeration strategy enhances nitrification of NH_4-N in flooded filter;
- The system has maintained low outlet concentrations of dissolved pollutants.

Abstract

Combined Sewer Overflow Treatment Wetlands (CSO wetlands) are designed to remove pollutants under stochastic events with variable hydraulic loads. Upgrading them with forced aeration promises to increase the effectiveness and resilience of the treatment. We have tested two vertical CSO wetlands with forced aeration (CSOa and CSOb) to understand the effects of aeration on CSO treatment. Both filter beds have 0.95 and 0.80 m of saturated layer. CSOa uses gravel as top filtering layer, while CSOb utilizes sand and an additional transition layer. Tracer tests were conducted in both filters with and without aeration to assess the impact of aeration on hydraulic performance. CSOa operated with four different aeration conditions, with the optimal condition tested on both filters for comparison. Samples were taken for analysis of global parameters and the redox potential was monitored online. In the tracer test, CSOa allowed to observe the mixing impact of aeration, which avoids any preferential path when influent entered the filter. The addition of a sand layer at the surface (CSOb) allows for a more even distribution of water on the top, which limits preferential flows when aeration is off. In both filters, the results showed that aeration increased the residence time and mixing degree (NTIS < 3). Testing different aeration strategies revealed the dependence of dissolved pollutant removal on oxygen supply. In CSOa, the median outlet concentration varied from 23 to 6.4 $mg.L^{-1}$ in TSS, 153 to 32 $mg.L^{-1}$ total COD (CODt), 124 to 20 $mg.L^{-1}$ soluble COD (CODs) and 5 to 2.5 $mg.L^{-1}$ NH_4-N according to aeration strategy. The lower outlet concentrations were always under the highest aeration condition. Under the optimal condition (75 min on/15 min off), median removal of CSOa was 97% TSS, 85% CODt, 78% CODs and 75% NH_4-N. Besides COD and TSS, outlet concentration and removal efficiency did not significantly differ between CSOa and CSOb. Pollutant removal demonstrated a linear correlation with organic surface load. Overall, forced aeration in CSO-TW distinctly affected filter dynamics and improved its performance.

Keywords: Forced Aeration Strategy; Hydraulic Loads; Nitrification; Bioretention Filters; CSO-TW.

Thèse accessible à l'adresse : https://theses.insa-lyon.fr/publication/2025ISAL0011/these.pdf © [D. Gonçalves Portela], [2025], INSA Lyon, tous droits réservés

2.1 Introduction

As rainfalls have a stochastic feature, infrastructure managing stormwater needs to be adapted to receive inflows with a high level of variability in terms of volume, pollutant loads, frequency and intensity (Gioia et al., 2021; Seidl et al., 1998). Unlike steady inflow in domestic wastewater treatment systems, facilities treating overflows from combined sewers operate under specific conditions that influence effluent concentrations (Kadlec and Wallace, 2008). The proportions of stormwater (SW) and domestic wastewater (WW) in combined sewer systems (CSS) are between 4:1 to 100:1 during rain events (Tondera et al., 2021). Madoux-Humery et al. (2015) and Phillips et al. (2012) observed a large number of contaminants in the frequently occurring combined sewer overflows (CSOs), resulting from the re-suspension of sewer deposits and suspended solids from runoff. Episodes of heavy rain events are likely to intensify due to global warming (IPCC, 2023), increasing concerns of greater spill frequency, volume and impact of CSO pollution on receiving waters. Urban expansion, marked by increased construction and reduced infiltration areas, further increase SW flow in combined sewer systems (Salerno et al., 2018). Implementing facilities to treat CSO emerges as a viable technical solution to protect surface water and water pollution control (Oral et al., 2020).

French regulation requires that CSO treatment wetlands, regardless of discharge location, guarantee at least the same outlet concentrations as required at wastewater treatment plants of the same catchment area. This necessitates the use of a treatment technology that is able to maintain performance when operating under extremely varying conditions. Treatment wetlands (TWs) intended for CSO treatment are Nature Based Solutions (NBSs) adaptable to the local context. They work by retaining water to attenuate peak flows and removing pollutants (Dou et al., 2017; Stefanakis, 2019). Different variations of CSO wetlands have been implemented according to national regulation approaches (Germany, France, and Italy (Dotro et al., 2017; Rizzo et al., 2020)). Nevertheless, it is essential to undertake a meticulous design process and, in certain instances, to implement optimization measures in order to comply with the most rigorous regulatory standards.

In classical vertical CSO wetlands, the top layer has a depth of more than 0.45 m and up to 1 m, followed by a drainage layer, which can be saturated or not, and it can have a transient layer between the two layers. The indicated media for the filtration layer is sand (0 – 2 mm) with at least 10^{-4} m/s of hydraulic conductivity (Dotro et al., 2017). In Germany, there is a recommendation to add 20% of limestone to the filtration substrate to keep the pH buffering capacity (DWA-A178, 2019). The drainage layer at the bottom is 0.20 – 0.30 m in depth and

Thèse accessible à l'adresse : https://theses.insa-lyon.fr/publication/2025ISAL0011/these.pdf © [D. Gonçalves Portela], [2025], INSA Lyon, tous droits réservés

consists of 16 – 22 mm coarse gravel. Some vertical CSO wetlands maintain a saturated zone to prevent the loss of plants during dry weather periods, dilute high inflow concentrations and avoid hydraulic short cuts (Pálfy et al., 2017c).

Pollutant removal in vertical CSO wetlands mainly occurs in the upper layer through filtration, adsorption and biological degradation. An aerobic environment favors organic matter removal and nitrogen oxidation (Ruppelt et al., 2018; Uhl and Dittmer, 2005). Design guidelines for vertical CSO wetlands (ANR, 2013; DWA-A178, 2019) include a throttle to control the outflow and a freeboard for water retention, ensuring hydraulic peak attenuation and that a minimum hydraulic retention time is maintained during peak hydraulic loading events.

Every vertical CSO wetland system has a pollutant removal capacity that depends on internal or external factors. For example, filter design and operation favor certain groups of bacteria (aerobic/anaerobic). Presence, abundance and therefore performance of these bacteria depend on factors such as hydraulic and organic loads, as well as influent quality. In the CSO wetland, COD removal rates of approx. 80% and total suspended solids (TSS) removal of 50 to 90% have been observed (Ruppelt et al., 2019; Tondera et al., 2013). Masi et al. (2017) observed a mass reduction of 93% of the ammonium-nitrogen (NH_4-N) inflow load. Additionally, for events occurring in summer, the outlet concentration was close to zero at the end of an event. To be efficient and consistent in particulate organic matter removal and nitrification, CSO wetland design has to be robust and perform effectively across in a wide range of rainfall events (Pálfy et al., 2017b).

Despite vertical CSO wetlands' efficient removal capacity of organic matter, there is a need to enhance the removal of dissolved pollutants and to create conditions to promote effective denitrification (Rizzo et al., 2020). It is essential to ensure aerobic conditions when the surface of the filter is covered with water since anaerobic conditions can inhibit or slow down the degradation of major pollutants such as COD and NH_4-N (Uhl and Dittmer, 2005). Furthermore, traditional vertical CSO wetlands undergo a two-step process of ammonia transformation. First, adsorption occurs during feeding phases, when the filter is submerged. Then, in between events during dry weather, nitrification occurs in the unsaturated filtration layer converting NH_4-N to nitrogen-nitrate (NO_3-N). Denitrification is unlikely to occur in this second step due to the aerobic predominance. During the subsequent event, NO_3-N is flushed out in significant quantities at the outset (Pálfy et al., 2017c). Consequently, total nitrogen outlet concentrations are highly fluctuating. Additionally, long-lasting events or those with high concentrations of dissolved COD can push the system functioning to a limit since biological degradation

Thèse accessible à l'adresse : https://theses.insa-lyon.fr/publication/2025ISAL0011/these.pdf © [D. Gonçalves Portela], [2025], INSA Lyon, tous droits réservés

processes depend on oxygen conditions and hydraulic residence time (HRT) (Rizzo et al., 2020).

The incorporation of forced aeration into TWs for the treatment of domestic and industrial wastewaters has demonstrated promising results in achieving enhanced treated effluent quality beyond that achieved in classical TWs (Boog et al., 2014; Murphy et al., 2016; Nivala et al., 2019). Enhancing internal mixing, optimizing hydraulic retention time, and controlling oxygen conditions improve both pollutant removal and system resilience (Boog et al., 2018; Headley et al., 2013; Miyazaki et al., 2023). However, to our best knowledge, studies on TWs with forced aeration treating CSO have not been published.

In this context, this study aims to investigate the impact of aeration on the removal efficiency of specific dissolved pollutants and the system's resilience under high hydraulic loads. The research includes (i) analysis of system hydrodynamics in event-driven vertical flow wetlands under forced aeration, (ii) determining optimal aeration condition to nitrify ammonium-nitrogen and remove dissolved organic matter, and (iii) assessing aeration effects in different hydraulic loads.

2.2 Material and methods

2.2.1 Experimental Systems

On the REFLET INRAE research Platform, France, Craponne, 45°44'11.5"N 4°43'06.0"E, two aerated vertical CSO wetlands pilots (CSOa and CSOb) are installed, each having a surface area of 20 m². The pilots were planted with 2.5 stems per m² of common reed (*Phragmites australis*) in the middle of September 2022. Influent (12 $m^3.h^{-1}$) is distributed by a single feeding point in the middle from a suspended pipe that was positioned one meter above the surface. An outlet adjustable standpipe controls the saturated layer height, and a throttle controls the outflow rate. At the bottom of the filter are drainage pipes (diam. 125 mm) and aeration driplines of 16 mm internal diameter connected to an air blower (1.1 kW) that promotes forced aeration. Airflow, pressure and temperature can be measured by a vortex flowmeter EH Prowirl F200, a pressure transmitter BDSensors 18.601G for low pressure, and a platinum resistance thermometer EH iTHERM CompactLine.

The pilots operate in saturated conditions in the coarse gravel layer, with varying levels of saturation between pilots (Figure 2.1). From bottom to top, the media within CSOa consists of a 0.95 m of coarse gravel (10/20 mm) covered with a layer of 0.20 m of gravel (2/4 mm), and those of within CSOb consists of 0.80 m of coarse gravel (10/20 mm) and is followed by a

Thèse accessible à l'adresse : https://theses.insa-lyon.fr/publication/2025ISAL0011/these.pdf © [D. Gonçalves Portela], [2025], INSA Lyon, tous droits réservés

transient layer of 0.15 m of gravel (2/4 mm) and a filtrating layer of 0.20 m of sand (0/4 mm). The permanent saturation level is of 0.95 m and 0.80 m for CSOa and CSOb, respectively.

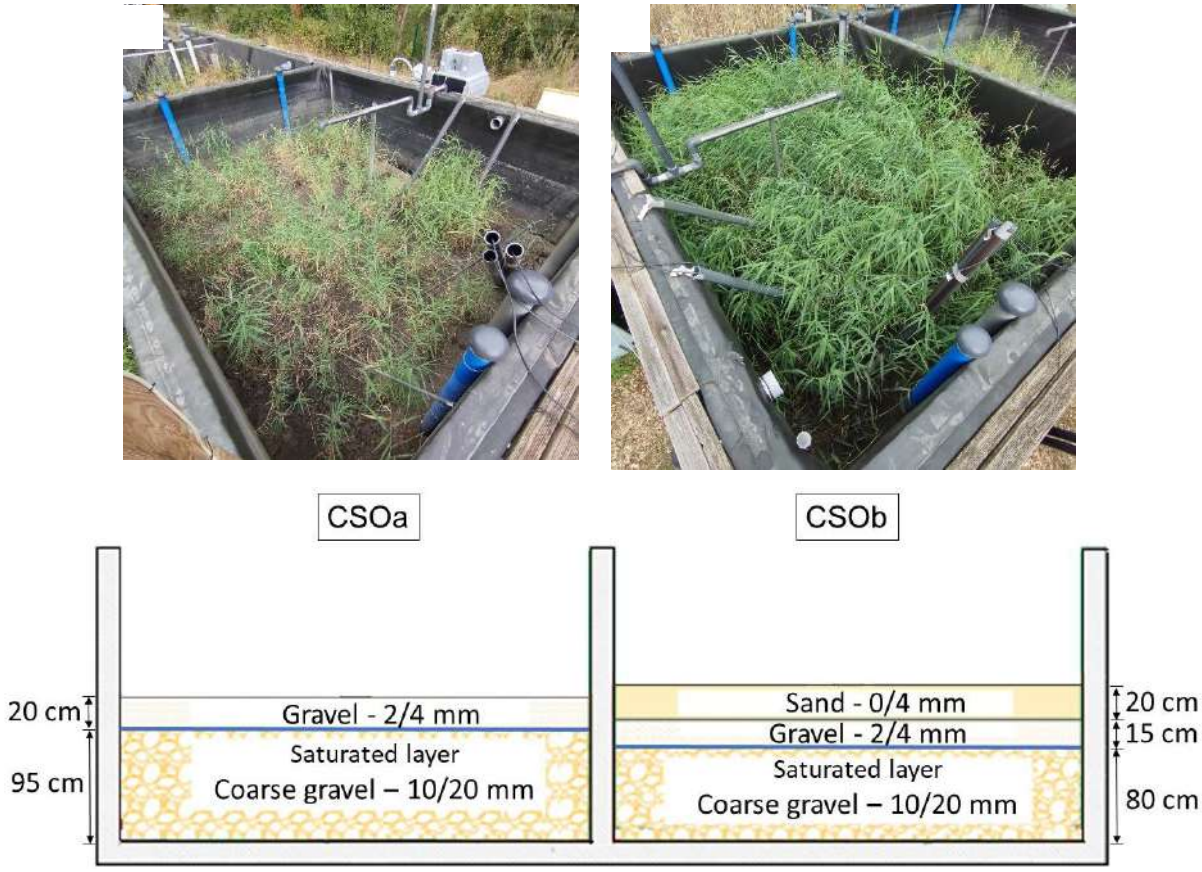

Figure 2.1 –Photo on the top left (A): top view of CSOa; top right (B): top view of CSOb. Vertical profile of CSOa and CSOb on the bottom (C)

2.2.2 Pilots' operation

The pilots were fed with pre-conditioned combined sewage (CS) to simulate CSOs. The CSO pilot feed is reproduced using real domestic WW from a combined sewer (city of Craponne) mixed with real storm water from a separate SW sewer that was stored in a 200 m^3 retention basin. Fresh domestic WW and stored SW were mixed during feeding in a unitary pipe in a way that typical ranges of physicochemical CSO characteristics were reached (Andrés-Doménech et al., 2018; Cross et al., 2021; Gasperi et al., 2012b; Masi et al., 2017). This was done by mixing 1 part of wastewater with 4 to 11 parts of stormwater. To simulate the impact of different rainfall events, hydraulic loads (HL) of 0.5, 1.0 and 1.5 $m^3.m^{-2}$ per event were selected. Once the feeding process was complete, drainage commenced until the permanent

Thèse accessible à l'adresse : https://theses.insa-lyon.fr/publication/2025ISAL0011/these.pdf © [D. Gonçalves Portela], [2025], INSA Lyon, tous droits réservés

saturated water level was reached, which was controlled by the standpipe. Dry periods from 2 to 18 days were established in between each loading event.

Outflow throttling was adjusted to reach 0.04 $L.s^{-1}.m^{-2}$ at the highest water level (1.1 m on the filter surface). During an inflow event, the average airflow rate was maintained at 1.15 $m^3.m^{-2}.h^{-1}$.

The oxygen consumption (OC) needed for pollutant degradation and mass oxygen transfer (OT), in each event were estimated using the equations 1 and 2:

$$OC = Q * (\Delta COD + 4.5 * \Delta TKN) \quad 1$$

$$OT = t_{aeration} * Q_{air} * \rho_{air} * m_{O_2/air} * SOTE \quad 2$$

where: Q is the inflow ($L.d^{-1}$); ΔCOD is the chemical oxygen demand consumed ($mg.L^{-1}$ – non biodegradable COD is neglected); ΔTKN is the Total Kjeldahl Nitrogen consumed ($mg.L^{-1}$); t is aeration time (h); Q_{air} is the delivered air flow from the blower ($m^3.h^{-1}$); ρ_{air} is the air density ($kg.m^{-3}$), mO_2/air is the mass of oxygen in the air equal to 21% (in number of mols) and a Standard Oxygen Transfer Efficiency (SOTE) of 0.09. The SOTE was obtained from water column aeration tests (1 m in height) filled with gravel 10/20 mm (Séranne et al., 2021).

Different aeration strategies were applied in four phases on CSOa, increasing progressively the aeration time:

- F10: air blower switched on for 10 min when feeding started then remained switched off during the rest of the event, including the drainage phase;
- F10/40: only during the feeding phase, the air blower followed a cycle of 10 min on and 40 min off, and the drainage phase was carried out without aeration;
- 10/40: during the feeding and drainage phase, the air blower followed a cycle of 10 min on and 40 min off;
- 75/15: during the feeding and drainage phase, the air blower followed a cycle of 75 min on and 15 min off.

The simulated rainfall events on CSOb worked only under the aeration condition 75/15. Feeding (1 to 3 h), drainage (10 to 23 h) and air blowers' operation time (0.3 to 12. 7h) varied according to the hydraulic load. Consequently, higher hydraulic loads had longer total aeration time. During dry periods, the air blower was turned on for 10 min every 10 h to facilitate oxygen transfer in the deeper zones of the saturated layer.

Thèse accessible à l'adresse : https://theses.insa-lyon.fr/publication/2025ISAL0011/these.pdf © [D. Gonçalves Portela], [2025], INSA Lyon, tous droits réservés

2.2.3 Hydraulic characterization

To understand the hydrodynamics of the filter during the pollutant removal process, we conducted two tracer test campaigns, one with and one without aeration. Combining two different tracers in one campaign allowed the evaluation of hydraulics (residence time, degree of mixing and presence of preferential path) before the ponding phase (at the beginning of an event) and once surface ponding (0.2 m) is present. This allows the impact of the ponding zone on tracer distribution at the surface, to be identified. Each campaign consisted of a pulse injection of fluorescein solution (0.14 $g.L^{-1}$ and 0.5 $g.L^{-1}$ in CSOa and CSOb, respectively) into the inlet point when feeding started, then an Amino G acid solution (1.26 $g.L^{-1}$ and 1.5 $g.L^{-1}$, respectively) at the same point were injected when the ponding occurred. The tracer solutions were prepared with products from Thermo Scientific Chemicals. The outflow rate increased continuously until the second tracer was injected, and then the flow rate was maintained with the throttle at a consistent flow at the inlet and outlet.

A fluorimeter (TRMC-Fluo of Tetraedre) was positioned at the outlet of each pilot to measure tracer fluorescence in mV, and the values were converted to $mg.L^{-1}$ with the help of calibration curves created in advance with the outlet water (data not shown).

The main hydraulic indicators, mean retention time (t_{mean}) and number of tanks in series (TIS-N), were estimated using Equations 4 and 5. Residence Time Distribution E(t) (Equation 3) is the normalization of output concentration measurement on time, wherein Q in m^3/h is the outflow and C in g/m^3 is the outlet concentration of the tracer

$$E(t) = \frac{Q(t)*C(t)}{\int_0^\infty Q(t)*C(t)dt} \qquad 3$$

The gamma distribution determined N through error minimization of resultant E(t), which was calculated with measured data. In this study, the used gamma distribution function is:

$$E(t)_{gamma} = \frac{N}{t_{mean}*\Gamma(N)}\left(\frac{N*t}{t_{mean}}\right)^{N-1} exp\left(-\frac{N*t}{t_{mean}}\right) \qquad 4$$

wherein N is the number of complete stirred tanks in series; t (h) is time; t_{mean} (h) is the experimental HRT, and Γ(N) (h-1) is the gamma distribution, calculated with the SOLVER tool in ExcelTM. The experimental HRT t_{mean} is the integral over time and E(t) (Tchobanoglous et al., 2003):

$$t_{mean} = \int_0^\infty t * E(t)dt \qquad 5$$

The theoretical hydraulic residence time (t_t) represents the ideal duration for the fluid spend in the filter and, ideally, it is equal to t_{mean}. However, dead zones or preferential paths reduces

Thèse accessible à l'adresse : https://theses.insa-lyon.fr/publication/2025ISAL0011/these.pdf © [D. Gonçalves Portela], [2025], INSA Lyon, tous droits réservés

the time of the fluid in the filter, therefore, deviating t_{mean} from t_t. Plug flows and completely mixed tanks are ideal models, which do not occur undisturbed in practice. The calculated TIS-N is a hydraulic indicator showing if the hydraulics in the tested TW are closer to a plug flow (N=∞) or to a continuous stirred tank reactor (CSRT, N=1) reactor.

2.2.3 Sampling procedure, water quality physicochemical and statistical analysis

After finishing the tracer tests on the pilot, continuous monitoring began with online sensors and sampling campaigns for laboratory analyses. The monitoring campaign lasted from March to October 2023 in CSOa and July to October 2023 in CSOb. Composite samples were taken by a programmed autosampler (ISCO 5800) throughout the feeding and drainage phases at the inlet and outlet of each pilot. At the inlet, 150 mL was sampled every 2 min (constant inflow), while at the outlet, 100 mL was sampled for every 200 L of effluent that passed through and discharged from each pilot. The samples were analyzed for the global parameters CODt, CODs, total suspended solids (TSS), ammonium-nitrogen (NH_4^+-N), nitrite-nitrogen (NO_2^--N), and nitrate-nitrogen (NO_3^--N). With the total and soluble COD, particulate COD (CODp) was calculated. The laboratory analyses were conducted in accordance with the standards NF EN 872 and NF T 90-101 for TSS and COD as well as NF EN ISO 14911 and EN ISO 10304-1 for the ionic chromatography of NH_4^+, NO_2^-, NO_3^-. Analyses of TKN (standard EN 25663) were also conducted to identify any non-dissolved forms of nitrogen and to allow calculation of total nitrogen removal and OC. Additionally, probes were placed inside the pilots at 60 cm from the bottom and at the outlet to monitor redox potential. This was found to be an indicator of biochemical reactions and microbial activity in CSO wetland pilots (Ruppelt et al., 2019).

Statistical analysis was done using MS Excel 2016 to obtain at the inlet and outlet minimum, maximum and median concentrations. The dataset distribution and the assessment of its normality was checked with plots in RStudio. In parallel, Fisher's F-test was performed to assess variance between the filters' dataset. If observed that data did not meet normal distribution or equal variance, the Mann-Whitney U test was used to compare CSOa and CSOb. Fisher's F-test and Mann-Whitney U test were calculated with RStudio for differences with a significance level of $p < 0.05$.

Thèse accessible à l'adresse : https://theses.insa-lyon.fr/publication/2025ISAL0011/these.pdf © [D. Gonçalves Portela], [2025], INSA Lyon, tous droits réservés

2.3 Results and Discussion

2.3.1 Tracer test

Each campaign lasted approx. 40 h, and the recovered mass of the tracer was between 77% and 97% (Table 2.1). Headley and Kadlec (2007) suggest that to validate a tracer test a minimum of 80% of the injected mass needs to be recovered at the outlet, hence, the results were considered representatives for evaluating the TWs' hydrodynamics.

The theoretical residence time in the saturated zone was estimated by dividing the water volume in the saturated layer per mean outflow rate in the steady state. The transient flow rate until the establishment of ponding was not considered in this study to simplify HRT calculation. Figure 2.2A shows the curve of outflow tracer mass over time for the tested conditions on CSOa.

At the start of feeding, an early peak with t_{mean}=2.5 h, appeared when aeration was off (Figure 2.2A). While using aeration, the residence time in the saturated zone is longer. Once ponding occurs, inlet water is better distributed at the filter's surface, and the HRT of the two tested conditions was closer to t_t=9.1 h. Therefore, aeration appears to better mix the tracer in the whole volume and avoid short-circuiting at the beginning of an event.

Figure 2.2B shows the bell shape in the dimensionless curves of residence time distribution (RTD). The RTD curve, representing the conditions without aeration, has different shapes from the beginning of the event to ponding. Ponding allows a better water distribution on the top and decreases preferential flows. In contrast, the event with aeration showed characteristics close to Continuous Stirred Tank Reactors (CSTR) from the beginning to the ponding.

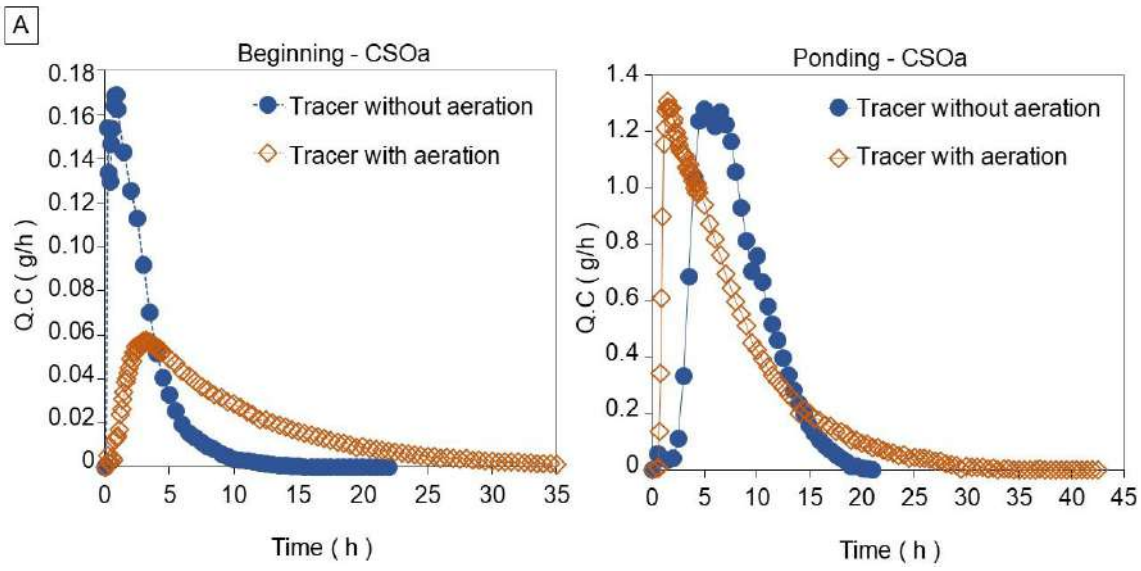

Thèse accessible à l'adresse : https://theses.insa-lyon.fr/publication/2025ISAL0011/these.pdf © [D. Gonçalves Portela], [2025], INSA Lyon, tous droits réservés

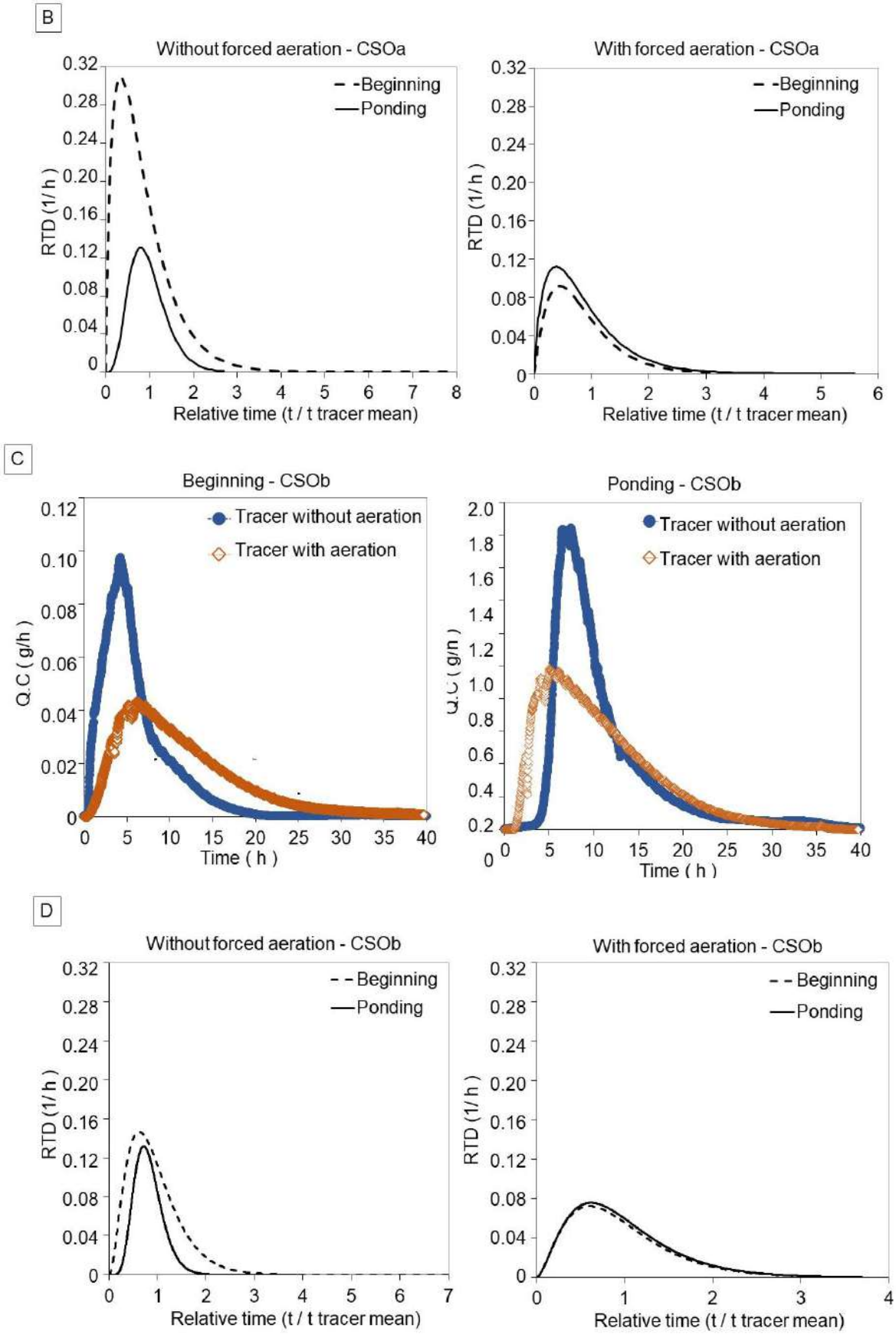

Figure 2.2 - A: Graphs of output mass curve in time for CSOa. B: Graphs of residence time distribution (RDT) in CSOa using Gamma distribution to fit experimental data. C: Graphs of

Thèse accessible à l'adresse : https://theses.insa-lyon.fr/publication/2025ISAL0011/these.pdf © [D. Gonçalves Portela], [2025], INSA Lyon, tous droits réservés

output mass curve in time for CSOb. D: Graphs of residence time distribution (RDT) in CSOb using Gamma distribution to fit experimental data.

In the CSOb filter, the lower permeability of the sand at the surface allows a better surface distribution of water at the beginning of an event. Consequently, preferential pathways were considerably reduced compared to CSOa. Figure 2.2C shows the results of the outflow mass over time at the beginning and at the ponding phase of CSOb. The t_{mean} at the beginning of feeding was 5.6 h and in contrary to CSOa, there was no early peak. The t_{mean} of the ponding phase in CSOb without and with aeration were 9.1 h and 10.5 h, respectively, meaning that during the ponding the mean and theoretical HRT were almost equivalent regardless of aeration. Improvements due to forced aeration on CSOb were observed in the degree of mixing (Figure 2.2D), which was similar to observations from CSOa. In the campaign with aeration, the RDT curves overlapped, indicating uniform mixing of the liquids in the filter.

The t_{mean}, t_{10}, and t_{90}, were obtained using gamma distribution and are presented in Table 2.1, as well as the number of tanks in series and tracer mass recovery. The presence of tracer indicated by t_{10}=0.5 h in the test without aeration of CSOa leads to the conclusion that water percolates only in a small part of the saturated zone before leaving. Consequently, without aeration a large part of the filter (49%) acts as a dead zone in the beginning phase. Fournel (2012) and Palfy et al.(2017c) observed preferential paths studying non-aerated vertical CSO wetlands; they explained the presence of short-circuiting when feeding starts with infiltration mainly limited to the area around the feeding point. Eventually, extended periods of low inflow may compromise the CSO wetlands treatment, although it remains negligible in events where ponding is rapidly established. In our study, we assume that air bubbles ascending through the filter media force tangential movements of particles moving downwards from the moment feeding starts, which increases the retention time and creates a stronger mixing pattern. Studies on wastewater treatment with TW have confirmed that dead zones and/or short-circuiting, which compromise the effluent treatment, can be attenuated with forced aeration (Boog et al., 2014; Dotro et al., 2017).

Table 2.1 presents the impact of aeration on NTIS. The presence of aeration in both filters leads to NTIS around 2 for the saturated and ponding phases due to the improved of mixing degree. In a study by Boog et al. (2014) with an aerated vertical flow wetland treating domestic sewage, the authors observed similar hydraulic characteristics of the liquid within the filter since NTIS was close to 1 due to forced aeration. On the one hand, switching off aeration in the filter without sand results in a small NTIS of 1.7 at the beginning, but a significant dead zone

Thèse accessible à l'adresse : https://theses.insa-lyon.fr/publication/2025ISAL0011/these.pdf © [D. Gonçalves Portela], [2025], INSA Lyon, tous droits réservés

and reduced HRT due to sub-optimal mixing. On the other hand, despite aeration, the presence of sand improves surface distribution and reduces the dead zone, but during the ponding phase, NTIS increases, indicating a flow pattern closer to a plug flow reactor.

Table 2.1 - Percentage of tracer mass recover, hydraulic indicators of theoretical and measured mean time. t_{10} and t_{90} are the time until 10% and 90% of the tracer mass leaves the filter, respectively, N, is the number of tanks in series.

	Without aeration				With aeration			
	Beginning		Ponding		Beginning		Ponding	
	CSOa	CSOb	CSOa	CSOb	CSOa	CSOb	CSOa	CSOb
Mass recover (%)	77	97.5	78	87.1	87	92.5	83	80.9
t_t (h)	5	7	8	13.8	5	9	8	13.5
t_{mean} (h)	2.3	5.6	7.6	9.1	8.1	10.9	6.5	10.5
t_{10} (h)	0.5	2.1	3.9	5.3	2.3	3.7	1.6	3.9
t_{90} (h)	4.7	9.9	12.1	13.3	15.5	19.8	12.9	18.9
NTIS	1.7	3	5.3	8	2.2	2.7	1.8	2.7

2.3.2 Removal performances

2.3.2.1 TSS and COD removal

Figure 2.3 presents the inlet and outlet concentrations of the different aeration strategies for TSS and COD as measured in CSOa. Inlet concentrations were obtained by mixing WW and SW using ratios of 1:4 to 1:11 (as described in Section 2.2). Filtration is very efficient independently of aeration strategies. Outlet concentrations were always lower than 30 $mg.L^{-1}$ for TSS and in most cases, except during the F10 aeration strategy, they were below 12 $mg.L^{-1}$ (Table 2.2). The TSS concentrations at the outlet of CSOa and CSOb (Figure 2.3 and Table 2.2) were comparable to conventional vertical CSO wetlands (Tondera, 2019) and TWs receiving SW with TSS concentrations similar to the ones in CSO (Schmitt et al., 2015).

Thèse accessible à l'adresse : https://theses.insa-lyon.fr/publication/2025ISAL0011/these.pdf © [D. Gonçalves Portela], [2025], INSA Lyon, tous droits réservés

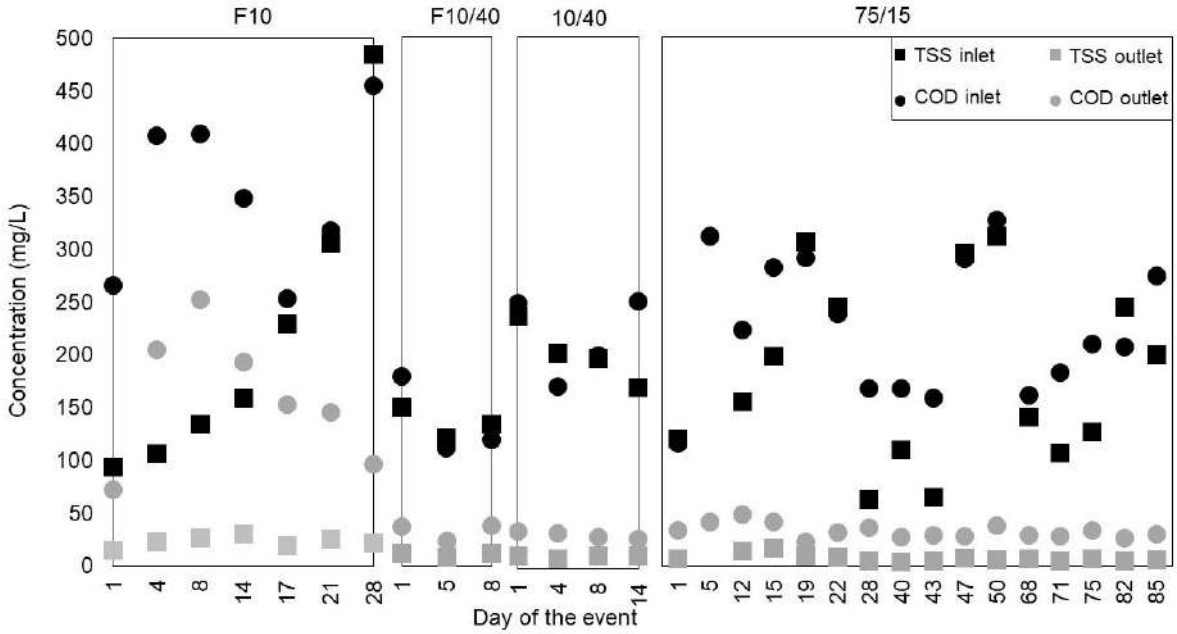

Figure 2.3 - Inlet and outlet concentrations of TSS and COD under each tested aeration condition in CSOa (F10, F10/40, 10/40 and 75/15).

For COD, the condition F10 in CSOa did not adequately degrade the CODs, leading to high outlet COD concentrations. During the F10 condition, the oxygen transferred to the water only meets 1 to 5% of the average oxygen demand of the influent, adversely affecting COD degradation. However, in other phases, COD degradation appears more efficient, consistently maintaining CODt outlet concentrations below 50 $mg.L^{-1}$ regardless of the aeration strategy. Oxygen transferred to the water ranged from 6 - 9%, 20 - 44%, and 50 - 100% of the average oxygen demand for the F10/40, 10/40, and 75/15 aeration strategies, respectively. The increase of oxygen diffusion in the filter creates zones for the growth of aerobic heterotroph bacteria (Vymazal, 1999). Due to the increased aeration times, certain aeration strategies resulted in lower COD_t concentrations at the outlet, as shown in the results of Figure 2.3 and Table 2.2. By changing the aeration strategy to the interval F10/40, the outlet stayed around 30 $mg.L^{-1}$ instead of 250 $mg.L^{-1}$ observed in the F10 aeration strategy. The performance was comparable to, or even better than in other studied CSO wetlands without primary settlement that showed COD concentrations around 40 $mg.L^{-1}$ in the outlet (Masi et al., 2023; Pálfy et al., 2017a). Despite variations on hydraulic and pollutant loads, the outlet concentrations remained stable. It shows the resiliency of the aerated system, maintaining high retention of solids and COD degradation, in accordance with other CSO wetland systems (Rizzo et al., 2020).

The median outlet concentrations and removal efficiencies resultant from tests in CSOa and CSOb are presented in Table 2.2 and Figure 2.4.

Thèse accessible à l'adresse : https://theses.insa-lyon.fr/publication/2025ISAL0011/these.pdf © [D. Gonçalves Portela], [2025], INSA Lyon, tous droits réservés

Table 2.2 - TSS, CODt and CODs values of minimum, maximum and median concentration at the inlet and outlet of CSOa and CSOb.

		Inlet concentration ($mg.L^{-1}$)			Outlet concentration ($mg.L^{-1}$)		
		TSS	CODt	CODs	TSS	CODt	CODs
CSOa	MIN	94	253	110	15	72	58
F10	MAX	485	455	315	30	252	226
(n= 7)	MEDIAN	159	348	183	23	153	124
CSOa	MIN	121	111	20	8	24	20
F10/40	MAX	149	179	62	12	38	28
(n= 3)	MEDIAN	133	119	34	12	37	24
CSOa	MIN	170	171	26	9	28	17
10/40	MAX	237	251	42	12	35	31
(n= 4)	MEDIAN	200	225	34	12	32	20
CSOa	MIN	120	116	55	6	23	10
75/15a	MAX	312	416	155	16	49	37
(n= 17*)	MEDIAN	155	223	112	6	32	25
CSOb	MIN	52	93	56	1	10	10
75/15b	MAX	315	308	200	11	35	30
(n= 19)	MEDIAN	133	207	90	4	27	18

*For TSS n =15

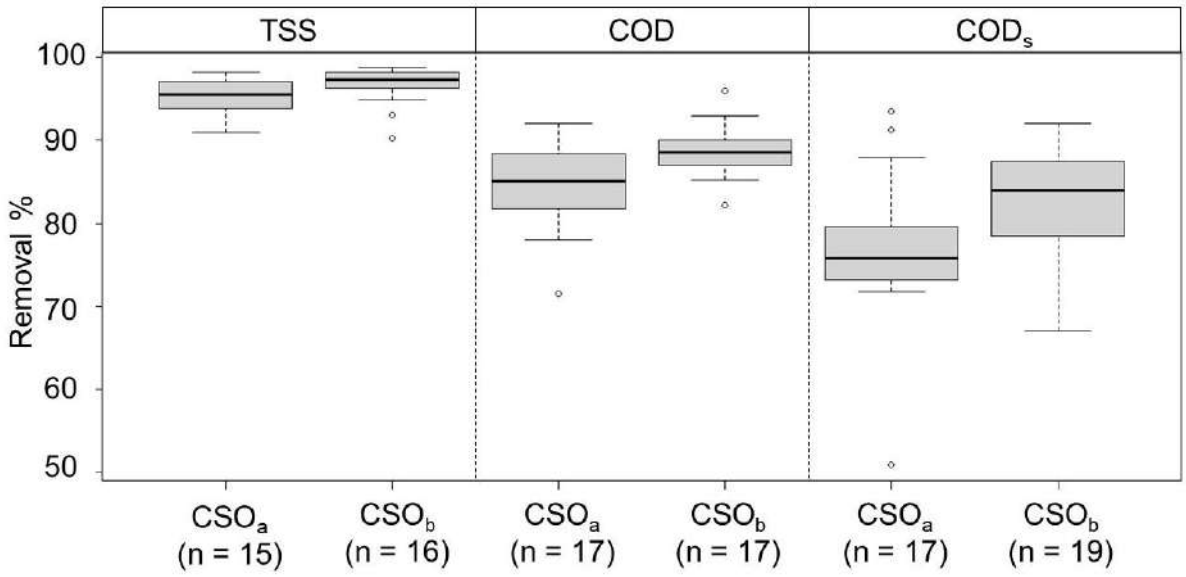

Thèse accessible à l'adresse : https://theses.insa-lyon.fr/publication/2025ISAL0011/these.pdf © [D. Gonçalves Portela], [2025], INSA Lyon, tous droits réservés

Figure 2.4 – Tukey's boxplot of removal performance of TSS, COD and dissolved COD in the filters CSOa (n = 17 for COD and CODs and n = 15 for TSS) and CSOb (n = 19) under the aeration condition 75/15.

When comparing CSOa and COSb under condition 75/15, the addition of a sand layer resulted in an improvement of TSS removal (p= 0.045). However, both filters consistently demonstrated TSS removal rates of >90% (Figure 2.4). There was a significant difference in the removal of CODt between CSOa and CSOb (p = 0.002), as well as a significant difference in the CODt outlet concentrations between the filters (p = 0.008). The CODs removal efficiency did not show significant differences between the performances of the two filters (p = 0.162). The median concentrations of effluent CODt were 32 $mg.L^{-1}$ in CSOa and 27 $mg.L^{-1}$ in CSOb, which is in accordance with studies of Palfy et al. (2017a) and Dittmer (2006). In some events, the effluent concentration was 10 $mg.L^{-1}$. These results are below the concentrations observed in the studies of Palfy et al. (2017a) and Dittmer (2006). It is likely that the higher CODt removal on CSOb is due to the lower concentration of TSS at the CSOb outlet (p = 0.009), as the sand layer can retain more solids. The 83% median removal of TSS in CSOa is not far from 89% removal in CSOb but CSOb had less variation than CSOa.

Independently of inlet variations, the removal efficiencies of CODt and CODs for both CSOa and CSOb were high. For example, removal efficiency of both filters under the 75/15 aeration strategy, showed a COD removal of consistently above 70% in all events (Figure 2.4).

In the above-mentioned studies on none-aerated vertical CSO wetlands by Dittmer (2006) and Pálfy et al., (2017a), less than 50% of CODs removal were found. Depending on the system design, the treatment process has low CODs removal due to the absence of aeration during feeding (saturated conditions) (Meyer et al., 2013). Generally, the adsorption characteristics of the filter material together with the characteristics of localized bacterial communities in the filter play an important role in CODs removal (Pálfy et al., 2017a). A dry period of longer than 10 days leads to the susceptibility of microorganism dehydration. When the next event begins, the transfer of electrons in water and adsorption processes are hindered as microorganisms strive to reach their saturation levels, thereby limiting the degradation of dissolved pollutants (Uhl and Dittmer, 2005). The studied systems minimized the dehydration issue with a permanently saturated layer of almost 1 m depth. While studies using passive aeration have generally shown low removal efficiency of CODs, under the specific condition created by aeration strategy of 75/15, the median CODs removal efficiency reached 75% in CSOa and

Thèse accessible à l'adresse : https://theses.insa-lyon.fr/publication/2025ISAL0011/these.pdf © [D. Gonçalves Portela], [2025], INSA Lyon, tous droits réservés

82% in CSOb. This shows that forced aeration in CSO wetlands can maintain high oxidizing conditions and thus degrade dissolved organic compounds.

2.3.2.2 Removal of nitrogen forms

The resulting inlet and outlet concentrations of nitrogen forms from 31 events loaded into CSOa (Figure 2.5) showed NO_2-N concentration remaining below 1.60 $mg.L^{-1}$ in all conditions, irrespective of the aeration strategy. As expected the concentrations of NO_2-N are low due to its unstable oxidative form in TWs (Kadlec and Wallace, 2008). However, the effects of aeration on NH_4-N and NO_3-N forms were noticeable. The median NH_4-N outlet concentrations from all strategies tested on CSOa ranged from 3 to 6 $mg.L^{-1}$. However, the 75/15 aeration strategy demonstrated the lowest variation in NH_4-N outlet concentrations, even at the highest inlet concentrations (Figure 2.6).

The calculation of oxygen transfer considered the oxygen consumed in the process of organic matter degradation and nitrogen transformation. The lack of oxygen in the condition F10 compromised both organic matter and NH_4-N removal. However, covering at least 20% of the oxygen demand in the condition created by the 10/40 aeration strategy tests improved NH_4-N removal. For a larger range of inlet concentration, the 75/15 aeration strategy demonstrated greater resilience to outlet variation of NH_4-N, even when the oxygen transferred was lower than the oxygen demand (calculated by Equations 1 and 2). Although these calculations are approximate, they nevertheless enable us to estimate the aeration times required to maintain efficient nitrification.

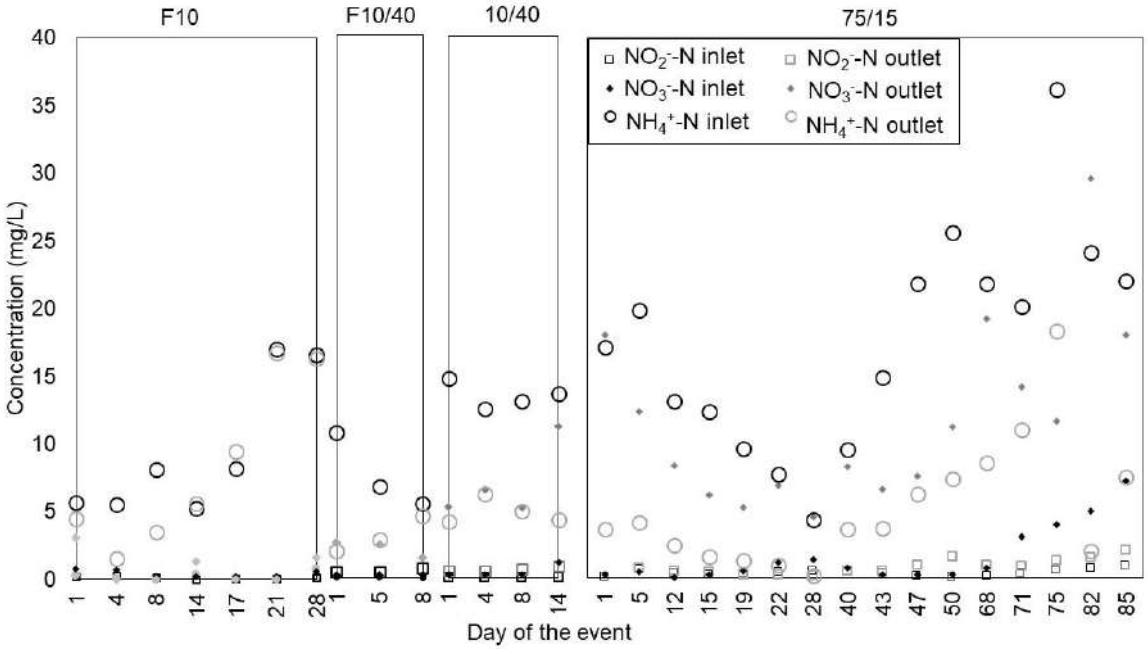

Thèse accessible à l'adresse : https://theses.insa-lyon.fr/publication/2025ISAL0011/these.pdf © [D. Gonçalves Portela], [2025], INSA Lyon, tous droits réservés

Figure 2.5 - Inlet and outlet concentrations of NH_4-N, NO_3-N and NO_2-N for each tested aeration conditions in CSOa (F10, F10/40, 10/40 and 75/15).

Under the 75/15 aeration strategy and until day 43, NH_4-N was <6 $mg.L^{-1}$ at the outlet when inlet concentrations were <20 $mgN.L^{-1}$. In addition, on days 1, 40, 68, 71 and 82 of the 75/15 aeration strategy operation, the sum of inorganic nitrogen concentrations at the outlet showed 5 to 2 $mgN.L^{-1}$ more than the concentrations measured at the inlet. Besides possible analytical uncertainties, mineralized compounds from plants and microorganisms lead to the release of nitrogen and an imbalance of inorganic nitrogen concentration at the inlet and outlet, as observed in the study of Collin et al (2010). Thus, this factor can cause an elevation of inorganic nitrogen in the outlet compared to concentrations measured at the inlet.

In filters with passive aeration, dry periods shorter than 5 days have a negative impact on NH_4-N removal by reducing the filter's adsorption capacity (Dittmer, 2006; Uhl and Dittmer, 2005). Seasonality is another factor influencing the nitrification process as temperature affect nitrification. For example, Pálfy et al (2017c) simulated in a passive CSO wetland NH_4-N adsorption in different seasons. They showed that in winter, 25% of the loaded nitrogen was nitrified over two dry days, while 60% was nitrified over 12 dry days. However, in this study, under the condition created in the 75/15 aeration strategy, after a short dry period of two days, the outlet concentrations remained stable due to a direct nitrification process that did not compromise the adsorption capacity of the media.

The median concentrations of NH_4-N and NO_3-N are shown in Figure 2.6.

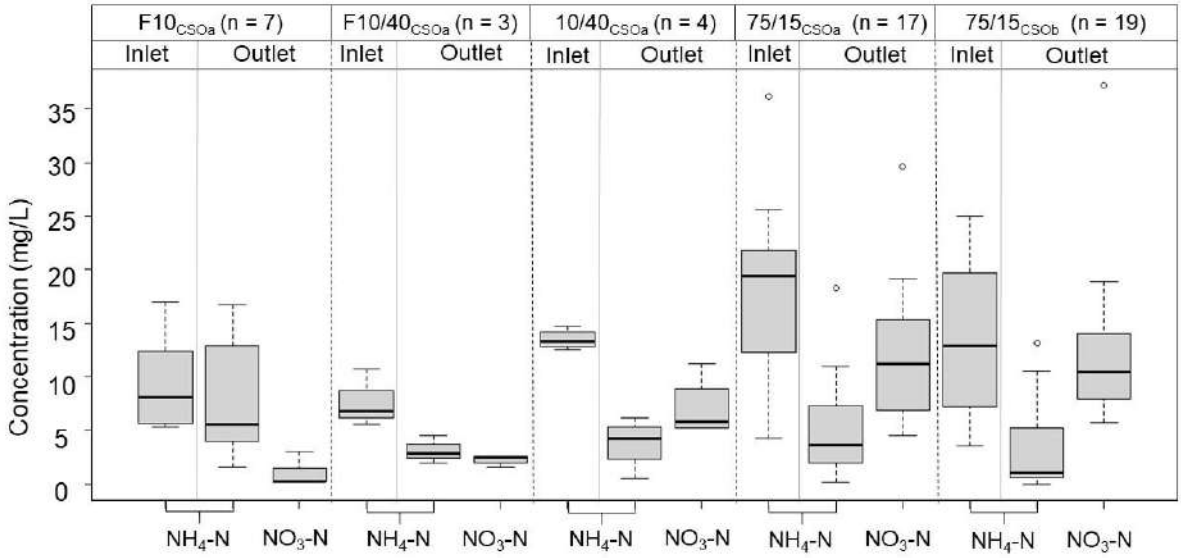

Figure 2.6 – Tukey's boxplot of inlet and outlet concentrations of NH_4-N and outlet concentration of NO_3^-N in the filters CSOa and CSOb. The number of tests performed (n) is indicated for each condition.

Thèse accessible à l'adresse : https://theses.insa-lyon.fr/publication/2025ISAL0011/these.pdf © [D. Gonçalves Portela], [2025], INSA Lyon, tous droits réservés

Conventional vertical CSO wetlands with passive aeration can achieve a high rate of nitrification. For example, NH_4-N removal in the range of 72% to 93% was reported by Pálfy et al. (2017a) and Ruppelt et al., (2018). However, the drawback of conventional vertical CSO wetlands is the requirement of a two-step process to achieve nitrification. The first step is ammonium adsorption during the feeding, and then during dry weather, when oxygen passes through the filter, nitrification occurs. Then, it is not always possible to guarantee either the amount of nitrified ammonium or the slow release of NO_3-N during the draining phase in this two-steps process (Tondera et al., 2018; Uhl and Dittmer, 2005).

Mechanical aeration may have induced nitrification zones in the filter, resulting in the transformation of NH_4-N to NO_3-N during the event. Much literature has reported consistent results regarding ammonium oxidation in TWs containing forced aeration (Boog et al., 2014; Dunqiu et al., 2012; John et al., 2020; Murphy et al., 2016), agreeing with the observed NO_3-N production in this study. However, the absence of anoxic zones makes the occurrence of denitrification less probable. In our study, total nitrogen within CSOa and CSOb was mostly removed through nitrogen assimilation into the biomass and direct nitrification, but denitrification did not occur due to a shortage of carbon source as outlet CODs is very low. Palfy et al (2017a) and Uhl and Dittmer (2005) noted in their CSO wetland similar results.

NH_4-N and NO_3-N results of CSOa and CSOb were very similar. The NH_4-N removal rate reached up to 90%, and the median removal was 75% (CSOa) and 83% (CSOb) in the highly aerated condition (75/15). In terms of the NH_4^+-N removal, no significant differences were observed between CSOa and CSOb ($p = 0.143$), despite the material surface area of sand potentially providing a higher adsorption capacity than gravel. Aeration may have favored direct nitrification during events, but it does not make adsorption a preponderant mechanism.

2.3.3 Redox potential

In the events in which redox potential was measured, there were consistent patterns related to aerobic and anoxic/anaerobic activity that were reproduced in more than one event. A general potential profile was observed at the outlet and inside the filter, 60 cm from the bottom. Whenever nitrification rates were high, redox potential generally was >300 mV, indicating aerobic conditions. According to Murphy et al. (2016), redox potential >300 mV hinders the process of denitrification, which is more effective under anaerobic conditions that promote facultative anaerobic denitrifying bacteria.

Thèse accessible à l'adresse : https://theses.insa-lyon.fr/publication/2025ISAL0011/these.pdf © [D. Gonçalves Portela], [2025], INSA Lyon, tous droits réservés

Figure 2.7 shows measurements taken at 0.6 m from the bottom of the filter throughout the event, highlighting the contrast between the lowest and highest aeration conditions.

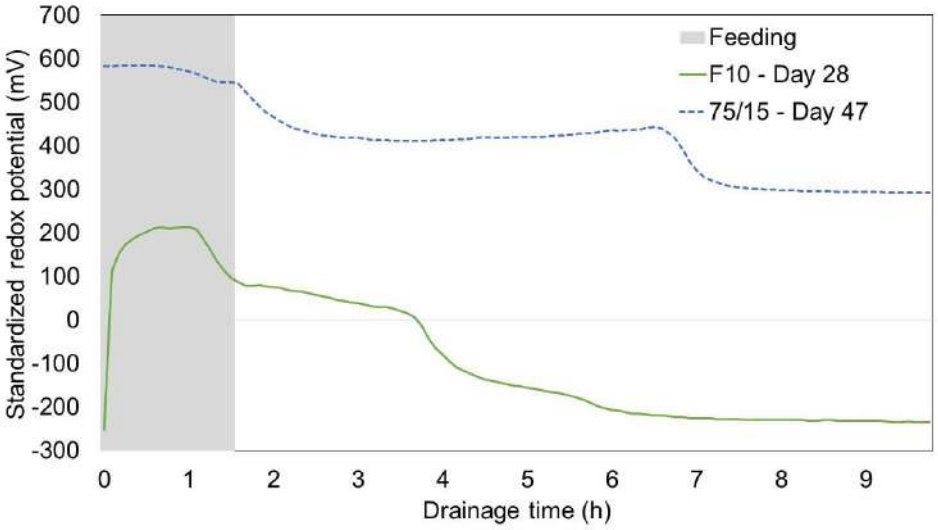

Figure 2.7 - Redox potential measured in two events in CSOa with a HL of 0.5 m. The first test under the aeration strategy F10 is indicated by the green line, and the second test under the 75/15 aeration strategy is indicated by the dashed blue line. Measurements were taken at 0.6 m depth from the bottom of the pilot.

The response to aeration was immediate, and in conditions with higher aeration (75/15), the redox potential was never <300 mV. Redox potential increased from - 250 mV to 100 mV within the 10 min aeration period (F10 aeration strategy). In addition, after the feeding, values went from 130 mV to negative values in 2 hours once the aeration operation had ceased (Figure 2.7). The redox measurements under aeration strategy F10 suggests that an anaerobic state predominated during the majority of the drainage period.

After feeding, each aeration strategy commonly exhibited a characteristic pattern in their redox potential curves at outlet of the filter. In aeration strategy F10, the redox curves were descended, while F10/40 and 10/40 showed plateaus before descending. Therefore, during F10/40 and 10/40, it was possible to achieve a steady state before oxygen depletion occurred. In aeration strategy 75/15, a transition point marked the curve's ascent and the redox potential of condition 75/15 ranged from 350 up to 700 mV at measurement points inside and outside of the filter. Measurements inside the filter (Figure 2.7), showed the redox dropping from 590 to 540 mV, and from 210 to 90 mV with aeration strategies 75/15 and F10, respectively. Ruppelt et al. (2019) explained that the consumption of COD leads to a drop of the redox potential, with values around 700 mV being their maximum potential, as measured in aeration strategy 75/15.

Thèse accessible à l'adresse : https://theses.insa-lyon.fr/publication/2025ISAL0011/these.pdf © [D. Gonçalves Portela], [2025], INSA Lyon, tous droits réservés

After the feeding period in the 75/15 aeration strategy, the redox potential remained constant at approx. 300 mV during the drainage period.

2.3.4 Surface load and performances

After all trials, the cumulative hydraulic load onto filter CSOa reached 40 $m^3.m^{-2}$ over 8 months and received more than 5 $kg_{TSS}.m^{-2}$. No hydraulic issues or signs of clogging were observed, as expected given gravel media. Other filters with similar media have operated without any signs of clogging for a longer time reaching 10 kg_{TSS} $m^{-2}.y^{-1}$ (Masi et al., 2023). The removal of solids was linearly correlated with solid loads independent of operational factors such as hydraulic loads or aeration conditions, whereas the organic loads removal were more dependent on the availability of oxygen in the pilot system. The result of aeration strategies F10/40 and 10/40 followed a pattern between loaded and removed COD mass, unlike F10, confirming that the oxygen supply is much lower than the oxygen demand. In the F10 aeration strategy, the correlation curve was shifted downward as the removal of CODs containing in CODt was inefficient and more dependent on other processes than aerobic oxidation.

Events under 75/15 aeration strategy in CSOa and CSOb showed strong correlations between the mass load applied and the load removed with close linearity curve. As observed in Figure 2.8, events with an HL of 0.5 m tend to load a lower mass of COD and NH_4-N. Increasing the HL leads to higher organic loads, consistently following the same removal pattern. Additionally, increasing NH_4-N mass loads shows more dispersion in results of NH_4-N removal. However, a moderate correlation (R^2) was still observed. Figure 2.8 shows the correlation between the loaded and removed mass of COD and NH_4-N.

Thèse accessible à l'adresse : https://theses.insa-lyon.fr/publication/2025ISAL0011/these.pdf © [D. Gonçalves Portela], [2025], INSA Lyon, tous droits réservés

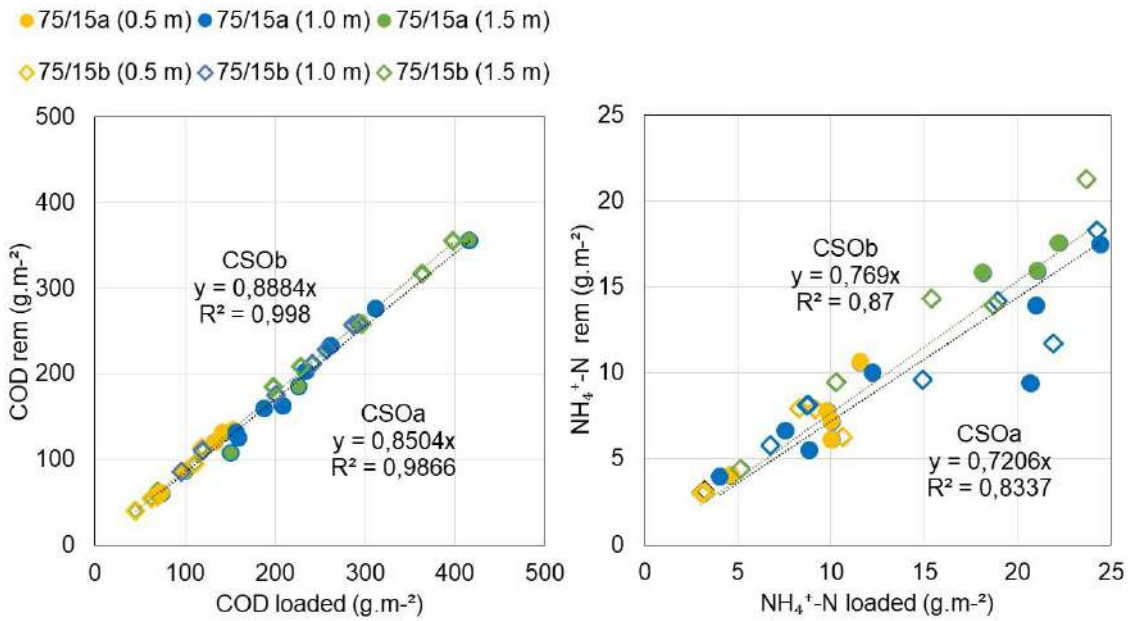

Figure 2.8 - Correlation of loaded and removed COD per event, on the left, and NH_4-N, on the right. Events in CSOa are indicated with an "a" and with a "b" for CSOb. The colors yellow, blue and green indicate different hydraulic loads.

With aeration intervals of 75/15, a stable and linear relationship between applied and removed loads shows that performances stay stable for both COD and NH_4-N irrespective of the hydraulic and organic loads applied to the pilot systems during this study. Consequently, the dependence of the outlet concentration on the inlet concentration was greater. This appears logical as long as hydraulic retention time is stable throughout feeding and drainage phases and there is no lack of oxygen.

2.4 Conclusions

This study aimed to assess the impact of forced aeration on the performance and hydraulics of two pilot-scale CSO wetlands (CSOa and CSOb). Tests were conducted to compare the filter's hydrodynamics with and without aeration in two phases including the beginning of feeding and ponding phase were conducted. Performance was evaluated under a range of aeration strategies and loading conditions. The optimal aeration strategy, as determined within CSOa, was reproduced within a second pilot scale system (CSOb) to gain insight into the impact on filter performance when designing it with a filtrating sand layer and gravel transient layer.

Tracer tests confirmed that in CSOa (without a sand layer), there are short-circuiting and reduced HRT at the beginning of an event when operating without aeration. It is evident that aeration has a significant impact on mixing and consequently HRT, ensuring a uniform flow

Thèse accessible à l'adresse : https://theses.insa-lyon.fr/publication/2025ISAL0011/these.pdf © [D. Gonçalves Portela], [2025], INSA Lyon, tous droits réservés

distribution in both filters, particularly in CSOa. Once ponding conditions occur following loading, stopping the aeration will result in a more plug-flow condition.

Regarding pollutant removal, extended aeration intervals effectively degraded dissolved pollutants. Under the 75/15 aeration strategy, CSOa showed a median removal of 78% in CODs and 75% in NH_4-N, while CSOb exhibited removals of 83% in CODs and 92% in NH_4-N. The filters performed similarly, removal of TSS and COD were close to 95% and 85%, respectively, with a slight better removal efficiency in CSOb. The sand layer potentially trapped organic matter attached to solids, which improved TSS and COD removal in CSOb.

A well-balanced oxygen transfer to oxygen demand ratio was found to be a key factor in the aerobic degradation of dissolved COD and ammonia nitrification. In contrast to passive aeration filters, mechanical aeration maintained low concentrations of NH_4-N at the outlet due to the direct nitrification that occurs during the feeding and drainage phase. The system is not reliant on passive re-oxygenation after drainage to proceed with nitrification, which means that nitrate does not tend to accumulate and be washed out in subsequent events.

The correlation between mass loaded and removal rates remained consistent regardless of hydraulic loads. The filters demonstrated stability against varying surface loads, performing well for the most aerated aeration strategy (75/15).

The obtained results confirm the advantages of aerated vertical CSO wetlands treatment. Future work could contribute to understanding how long dry periods without loading might affect performances. Additionally, studies on the dynamics of nitrogen over time will contribute to understanding the influences of dry periods on nitrification rates and optimizing the aeration strategy and blower settings, thereby reducing energy costs.

ACKNOWLEDGEMENTS

The authors would like to thank the financial support provided by the H2020 NICE project and extend appreciation to Olivier Garcia for the valuable technical support on the field.

Thèse accessible à l'adresse : https://theses.insa-lyon.fr/publication/2025ISAL0011/these.pdf © [D. Gonçalves Portela], [2025], INSA Lyon, tous droits réservés

3 Online monitoring of nitrogen transformations in an aerated CSO-TW

Abstract

This study focused on the removal of pollutants from combined sewer overflow (CSO) using aerated vertical flow wetlands (VFW). Over the course of one year, the systems were fed with mixed stormwater and wastewater, showing typical CSO inlet characteristics, with NH_4-N concentrations ranging from <0.1 to 25 $mg \cdot L^{-1}$. The hydraulic loading rates of 0.5, 1.0, and 1.5 $m^3.m^{-2}$ per event, and different aeration strategies were tested. These strategies ranged from moderate to poor aeration (between 0.2 to 6.5 $gO_2.h^{-1}.m^{-2}$) to highly aerated (> 15 $gO_2.h^{-1}.m^{-2}$). Online measurement of ORP, DO and NH_4-N and NO_3-N were used in monitoring nitrogen oxidation processes during feeding events and in the calculation of nitrogen mass balance. The results of the ORP and DO measurements indicated that aerobic reactions were maintained stable under highly aerated conditions. The period using only highly aerated conditions favored NH_4-N nitrification to NO_3-N during a feeding event. Although variations in ORP and a decrease in DO when inflow ammonium concentrations were high limiting the system's nitrification were observed. In the tested conditions (aeration rate and average HRT of 7.3 h), the maximum nitrification of 10 $mg \cdot L^{-1}$ of nitrogen was reached during a feeding event (direct nitrification). For inflow TKN concentrations above this value, ammonia storage as NH_4-N in interstitial pores or adsorption onto biofilm occurred. This stored ammonium is then transformed during prolonged dry periods. The nitrate flushes and peaks during subsequent events were correlated with the nitrogen accumulated in the filter at the end of drainage and the duration of the dry period. These results highlight the potential of aeration to improve direct nitrification in VFWs, with performance depending mainly on inlet TKN concentrations.

Key-words: Sensor, nitrification; dry period; event-driven; CSO.

Thèse accessible à l'adresse : https://theses.insa-lyon.fr/publication/2025ISAL0011/these.pdf © [D. Gonçalves Portela], [2025], INSA Lyon, tous droits réservés

3.1 Introduction

Effluent containing nutrients, such as nitrogen, are of high concern due to their association with eutrophication in aquatic environment (Tang et al., 2009). Consequently, directives, such as the Council Directive 91/271/EEC, have regulated the discharge levels of nitrogen in its different forms. Biological nitrogen transformation in treatment wetlands (TWs) occurs through different pathways, including conventional nitrification and denitrification as well as alternative pathways, such as partial nitrification/denitrification, Anammox, and Canon processes (Saeed, 2012). However, main processes in the majority of TWs are based on the conventional nitrogen removal through nitrification and denitrification (Saeed, 2012). Nitrogen removal in subsurface TWs include as well NH_4-N adsorption onto organic matter, a process that is typically faster than nitrification itself (McBride and Tanner, 1999). While adsorption rapidly immobilizes NH_4-N, nitrification can occur during longer period as long as aerobic conditions are present as observed in a vertical flow treatment wetland (VFTW) treating domestic wastewater (WW) (Morvannou et al., 2014). In addition to adsorption, nitrogen compounds are retained through filtration, plant uptake, and biomass assimilation (Maltais-Landry et al., 2009; Saeed, 2012). However, these immobilized forms of nitrogen remain in the system unless they are mineralized.

Nitrogen removal requirements are more challenging in TWs that operate under variable hydraulic and organic loads, such as CSO. In that context, the design of VFTW must be sized to avoid significant bypass of untreated polluted water or preferential flows resulting from oversizing, as in both cases outflow concentrations is impacted. Particularly in the case of combined sewer overflow (CSO) treatment, the filter must handle large ranges of nitrogen concentrations and loads (0 to 26 $mg.L^{-1}$ of NH_4-N as observed by Masi et al. (2023). Passive TWs treating CSO, or CSO TWs, are limited to the main process of nitrogen adsorption during feeding events, and nitrification during the dry periods (DP) when oxygen is present. Consequently, NO_3-N accumulation in the filter often occurs during DP, resulting in discharge peaks of NO_3-N during the subsequent wet period (Dittmer, 2006; Pálfy et al., 2017c; Woźniak et al., 2007).

Passive aeration relies on oxygen molecules entering the water through diffusion and convection of atmospheric oxygen, as well as through plant roots although this last one is negligible (Kadlec and Wallace, 2008). Therefore, it is difficult to control oxygen supply throughout the entire event when relying only on passive aeration, which limits aerobic reactions (Woźniak et al., 2007). In contrast, intensified TWs improve the oxygen transfer from

Thèse accessible à l'adresse : https://theses.insa-lyon.fr/publication/2025ISAL0011/these.pdf © [D. Gonçalves Portela], [2025], INSA Lyon, tous droits réservés

water to the biofilm by mechanical aeration (Nivala et al., 2013) and can achieve optimal performance when evenly distributed (Nivala et al., 2020).

Overall, forced aeration increases the resilience of the system to hydraulic and organic load variations. In a study conducted by Gilmore et al. (1999), an aerated filter column was observed to completely remove a limited load of NH_4-N, regardless of hydraulic load (HL), when heterotrophic and nitrifying bacteria did not compete for oxygen. Uggetti et al. (2016) and Butterworth et al. (2013) conducted studies on aerated TWs with NH_4-N inlet concentrations up to 30mg.L^{-1} , resulting in complete nitrification and a notable increase in nitrate at the filter effluent. Both studies used a control filter without mechanical aeration, proving the effectiveness of nitrification in the filter with mechanical aeration. The increase in DO concentration improved nitrification. However, optimized aeration strategies can be targeted to reduce excessive aeration and operational costs.

In systems using mechanical aeration, such as activated sludge, maintaining DO levels at 3 -4 mg.L^{-1} is recommended to promote nitrification (Metcalf et al., 2014). In addition to oxygen, an adequate HRT is also necessary. A short HRT can reduce nitrification efficiency if limited by kinetic rate (Zheng et al., 2020). In a study of an aerated surface flow wetland (SFW) treating livestock WW, Jamieson et al. (2003) observed that while aeration increased nitrification, residence time remained a critical design parameter for achieving consistent nitrogen removal.

During nitrification reactions inorganic nitrogen is assimilated into the production of new cells (Vymazal, 2007). According to Platzer (1999), the nitrification process is influenced by factors such as maximum growth of bacteria, yield coefficient, filter design, temperature and oxygen supply, which can vary between systems. Hence, the acclimation of biomass can be an important step to increase the nitrification capacity of TWs (Villaverde, 2000). In aerated systems with constant ammonium loads, conditions are favorable for maintaining a stable community of nitrifying bacteria. These systems tend to support a well-established nitrifying bacterial community, which is more resilient to changes in environmental conditions or system operations. The robustness of nitrification in aerated TWs has been demonstrated even under air blower failure. Murphy et al. (2016) observed a rapid restart of nitrifying bacterial activity in a VFTW after a two-week period without aeration. However, the potential impact on the nitrification process under intermittent operation with highly and poorly aerated conditions in aerated CSO TWs remains a gap in our knowledge.

Thèse accessible à l'adresse : https://theses.insa-lyon.fr/publication/2025ISAL0011/these.pdf © [D. Gonçalves Portela], [2025], INSA Lyon, tous droits réservés

Aerated CSO TWs have demonstrated improved performance in removing particulate and dissolved pollutants (Chapter 2). Therefore, increasing oxygen availability during the feeding events creates favorable conditions for nitrification. The nitrogen dynamics within aerated CSO TWs and the operational parameters limiting nitrification efficiency remain unclear. Thus, the main goal of this study is to assess how nitrification is driven in aerated CSO TWs and its limitations. Therefore, the specific objectives are to (i) identify the surface load effects on oxidative processes during feeding and dry period; (ii) evaluate NH_4-N removal rate and NO_3-N production rate; (iii) analyze NH_4-N removal mechanisms for the state of maximum aeration capacity; (iv) estimate the limitation of direct nitrification process during feeding events.

3.2 Material and Methods

3.2.1 Operational conditions

The data was collected from two aerated CSO TWs, each with a composition that differed from the other, as showed in Figure 3.1. One filter consisted of two different sizes of gravel, CSOA, from the bottom to the top the first layer was 95 cm of coarse gravel (10/20) and 20 cm of gravel (2/4). The other filter, CSOB, consisted at 80 cm of coarse gravel (10/20) at the bottom, 15 cm gravel (2/4) in the transition layer, and 20 cm of coarse sand (0/4) on the top. For both filters, the bottom layer was permanently saturated with water.

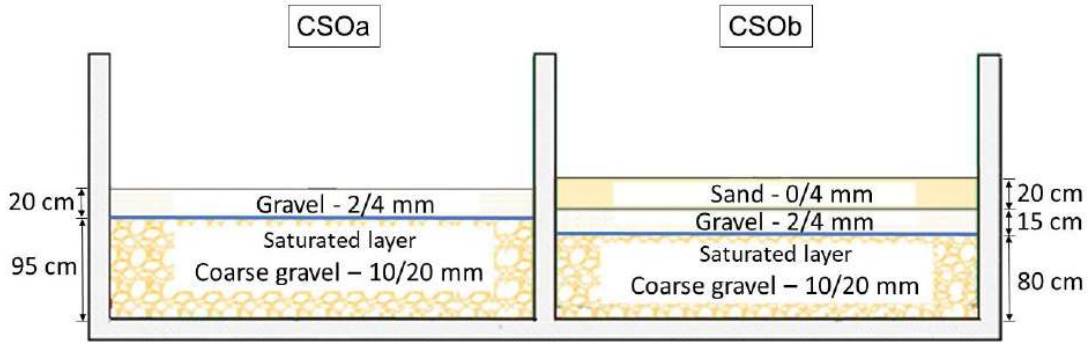

Figure 3.1– Cross section of the filters CSOa and CSOb.

To promote aeration, driplines (6 diffusers per m²) were distributed at the bottom and connected to air blowers. The air blowers were intermittently switched on and off at different time according to feeding and dry periods (see Table 3.1). All trials were operated at a maximum blast air rate of 50 Hz, with average air flow of 1.15 $m^3.m^{-2}.h^{-1}$. In CSOA filter different aeration strategies were tested creating different conditions within the filter. During a period of trials with low aeration, air blowers were completely deactivated during DP. In CSOB

Thèse accessible à l'adresse : https://theses.insa-lyon.fr/publication/2025ISAL0011/these.pdf © [D. Gonçalves Portela], [2025], INSA Lyon, tous droits réservés

filter, only highly aerated conditions were tested. The tested aeration conditions were categorized into low to moderated aeration and highly aerated. This classification was based on their respective estimated oxygen transfer (OT), calculated using the equation from Chapter 2, and the total volume of air blown into the filter per surface area during the feeding events.

Table 3.1– Classification of aeration strategies operated in the pilots. In each aeration strategy the air blowers were switched on and off during the feeding, drainage and dry period.

Aeration condition, estimated OT, volume of air blown per surface area	Feeding		Drainage starts from 80% of inlet volume was recovered		Dry period
Low to moderated aeration, 0.2 to 6.5 $gO_2.h^{-1}.m^{-2}$, 0.3 to 3.4 $m^3.m^{-2}$	10 min ON	OFF	OFF		10 min ON 600 min OFF
	10 min ON	40 min OFF	OFF		
	10 min ON	40 min OFF	10 min ON	40 min OFF	
Highly aerated, over 15 $gO_2.h^{-1}.m^{-2}$, over 6.0 $m^3.m^{-2}$	75 min ON	15 min OFF	75 min ON	15 min OFF	
	Continuous aeration		Continuous aeration		

Three types of hydraulic loads (HL) were tested 0.5, 1.0 and 1.5 $m^3.m^{-2}$per event, for both filters. The feeding event includes feeding and drainage phases while during dry period (DP) the filter rested without receiving any load. The length of DP varied from ~ 2 to 6 d for trials under low to moderate aeration, and from 2 to 17 d for trials under highly aeration.

The filters started operating on March 2023 for CSOA filter and on August 2023 for CSOB filter, and both filters operated until June 2024. In the last six months of trials, the gravel filter operated only under highly aerated condition and maximum HL of 1.5 $m^3.m^{-2}$ while CSOB filter showed signs of clogging and was discontinued. The total accumulated HL in CSOA and CSOB was 93 and 55 $m^3.m^{-2}$, respectively. In the last six month of operation CSOA received 37 $m^3.m^{-2}$.

In the phase of highly aerated conditions (Table 3.1) the maximum nitrification capacity during event was tested in the CSOA filter. A detailed description of these experimental systems is provided in Chapter 2 with results of the global performance of the filters.

3.2.2 Sampling and influent characteristics

Inflow and outflow samples were collected using refrigerated automatic samplers proportional to flow. As inflows were stable, during feeding events, 100 mL of inlet samples were collected every 2 min and 150 mL of the outlet was sampled every 200 L intervals. All

Thèse accessible à l'adresse : https://theses.insa-lyon.fr/publication/2025ISAL0011/these.pdf © [D. Gonçalves Portela], [2025], INSA Lyon, tous droits réservés

samples were analyzed for global parameters (TSS, COD, NH_4-N, and NO_3-N) within 24 h. Other parameters, such as anions, ions and conductivity were also measured but are not presented in this study. Additionally, BOD_5 and total Kjeldahl nitrogen (TKN) were measured monthly or more frequently. Domestic wastewater (WW) and stormwater (SW) were combined to reproduce the CSO influent. SW was pumped from a stirred storage basin and WW from a lifting station. The two were mixed in the pipe that conveyed both waters. The inflow characteristics for the tests performed under the two aeration conditions, are presented in Table 3.2.

Table 3.2 – Median inlet concentration, in parenthesis, the minimum and maximum measurement for each filter according to their respective top layer material and aeration condition classification.

Parameter	CSOA				CSOB	
($mg.L^{-1}$)	n	Low to moderate	n	Highly	n	Highly
TSS	14	164 (94 – 485)	36	65 (30 – 338)	13	125 (52 - 227)
BOD_5	2	94 (77 -112)	4	100 (65 – 117)	2	91 (78 -104)
COD	14	252 (111 - 455)	38	117 (38 – 509)	16	180.5 (93 - 294)
TKN	2	18.7 (15.6 - 22)	8	8.3 (2.3 – 19.1)	2	26.4 (26.4 – 32.5)
NH_4-N	14	9.4 (5.2 - 17)	38	6.9 (<0.1 – 25.5)	16	14.7 (6.3 - 25)
NO_3-N	14	<0.2 (<0.2-1.2)	38	1.9 (<0.2 – 17.7)	16	1.0 (<0.2 – 7.4)

The system maintained a stable pH, due to an adequate carbonate concentration to buffer nitrification acidification. An increasing NO_3-N concentration was observed for highly aerated condition in the CSOA due to recirculation of outlet water to the storage basin in case of long period without any rain. TKN was calculated for the trials where it was not directly measure. Since TKN includes both organic nitrogen and ammonium nitrogen (NH_4-N), the organic nitrogen was calculate based on its presence in the solids fraction of the inflow and outflow.

$$Coef N_{org} = \frac{TKN - NH_4 - N}{TSS} \quad (1)$$

$$TKN_{calc} = Coef N_{org} * TSS + NH_4 - N \quad (2)$$

where TKN, NH_4-N and TSS were measured according to the respective methods standard EN 25663, EN ISO 10304-1 and NF EN 872. Then the fraction of $CoefN_{org}$ in the SS is used to estimate N_{org} in the trials where TKN was not measure to calculate TKN_{calc}.

Thèse accessible à l'adresse : https://theses.insa-lyon.fr/publication/2025ISAL0011/these.pdf © [D. Gonçalves Portela], [2025], INSA Lyon, tous droits réservés

3.2.3 Online measurements

Probes to measure DO, oxi-reduction potential (ORP), NH_4-N and NO_3-N were installed inside the filters, with measurements recorded every 5 min. Figure 3.2 shows a cross-section schematic of the piezometer positions.

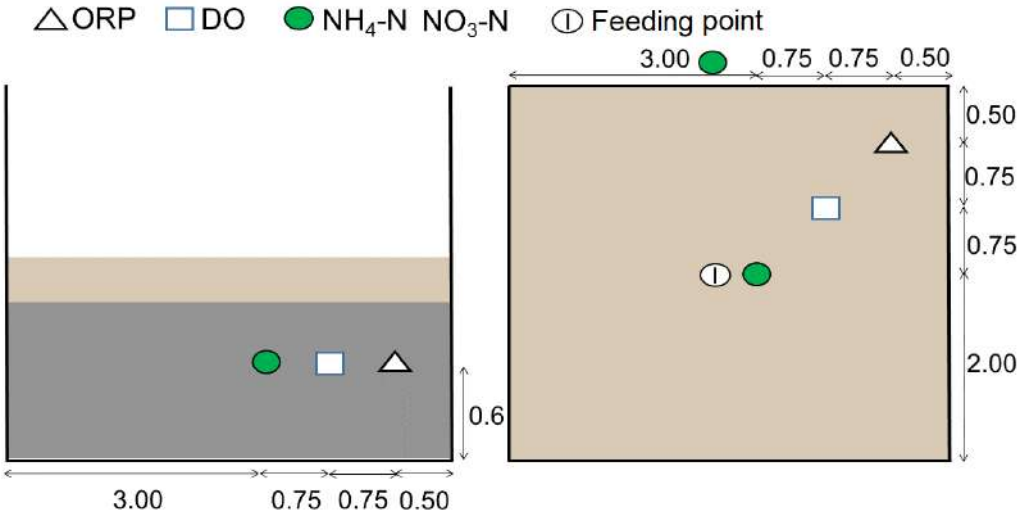

Figure 3.2- Top view, on the right, and cross section, on the left, to represent the positions of the probes. Three probes (ORP, oxygen and N forms) are 0.6 m from the bottom and one probe of N forms is at the outlet. The distances are in meters.

ORP measurements, with precision of ± 100 mV, captured instantaneous variations during the feeding event and when aeration was switched on during DP inside the filter. In the phase of highly aeration, oxygen probes were installed at the same depth as ORP probes to compare instantaneous measurements of DO and ORP. Additionally, DO measurement were used to calculate the O_2 uptake. The measurement accuracy and repeatability of oxygen probes were ± 0.1 $mg.L^{-1}$ and ± 0.05 $mg.L^{-1}$, respectively.

The oxygen uptake ratio was determined after air blowers were switched off, at the end of the drainage phase. The rate of decrease is defined by a zero order equation ($dC/dt = k$). Each DO profile was analyzed individually to calculate O_2 uptake (data not shown). The first measurement was taken after the air blowers were switched off and began the last measurement was taken until it reached 0.2 $mg.L^{-1}$ or before the end of drainage.

The NH_4-N and NO_3-N probes were placed within the same piezometer. The measurement error was ± 1 $mg.L^{-1}$, and calibration was continuously validated by comparing values measured with the probe to results from the laboratory. When necessary, a new calibration or the change of reference electrode were done, and a new calibration curve was plotted.

Thèse accessible à l'adresse : https://theses.insa-lyon.fr/publication/2025ISAL0011/these.pdf © [D. Gonçalves Portela], [2025], INSA Lyon, tous droits réservés

3.2.4 Nitrogen balance

Nitrogen mass balance aimed at defining the portion of ammonia that is directly nitrified at each feeding event, stored inside the filter or nitrified during rest periods, assuming that denitrification can be neglected due to a lack of carbon (observed in outlet concentration in Chapter 2). With the following equations, it was calculated nitrate production during each feeding events.

The mass of NO_3-N stored in the filter before a feeding event (Eq 3) and the NO_3-N remaining in the filter after a feeding event (Eq 4) were estimated by the equations:

$$NO_3\text{-}N_{stored} = NO_3\text{-}N_{mean0} * A * H * \varepsilon \quad \text{(Equation 3)}$$

$$NO_3\text{-}N_{remained} = NO_3\text{-}N_{last} * A * H * \varepsilon \quad \text{(Equation 4)}$$

where NO_3-N_{mean0}, is the mean concentration of NO_3-N measured at the outflow when the event begins until the volume of water in the saturated layer is entirely recovered at the outlet. The volume of water in the saturated layer was calculated with: A = 20 m², for surface area; H = 0.95, for height of saturated layer; and ε = 0.36, for the porosity of gravel (6.84 m^3). The NO_3-N_{last} is the last recorded concentration of NO_3-N with the outlet probe at the end of the drainage. It is assumed that the remaining NO_3-N in the saturated layer at the end of an event has the same concentration.

The nitrified mass of NH_4-N during the event was estimated using Eq 5.

$$NO_3\text{-}N_{produced} = NO_3\text{-}N_{out} - NO_3\text{-}N_{in} - NO_3\text{-}N_{stored} + NO_3\text{-}N_{remaining} \quad (5)$$

where NO_3-N_{in} and NO_3-N_{out} are the masses measured in laboratory through composite samples.

Nitrates stored in the filter before a feeding event can result from nitrification of adsorbed ammonium or produced by decomposition of organic material during DP. Then, NO_3-N produced during DP is measured by the NO_3-N that remained in the filter after a feeding event minus NO_3-N stored in the filter at the end of subsequent dry period.

3.2.5 Data analyses

Data on the mean, maximum and minimum concentration of DO, redox potential and nitrogen forms from online probes were analyzed using Rstudio. This data, along with physicochemical and operational parameters, was compiled in Excel for the other calculations. Statistical analyses were also conducted in Rstudio. The multivariate statistic method of

Thèse accessible à l'adresse : https://theses.insa-lyon.fr/publication/2025ISAL0011/these.pdf © [D. Gonçalves Portela], [2025], INSA Lyon, tous droits réservés

principal component analysis was used to study the components influencing variations in nitrogen dynamics.

3.3 Result and discussion

3.3.1 N forms in feeding and dry periods

The cycle of nitrogen forms between feeding events and dry periods is not independent. Adsorption and storage in the water volume between events can lead to transformations and impacts on the subsequent event. Figure 3.3 presents the main pathways impacting nitrogen dynamic inside the filter. The ammonium loaded into the filter can be entirely or partially nitrified. In the event that the ammonium is partially nitrified, nitrification will occur during the aeration phase in DPs. However, it is possible that the transformation of remaining nitrogen extends to followings feeding events and DPs.

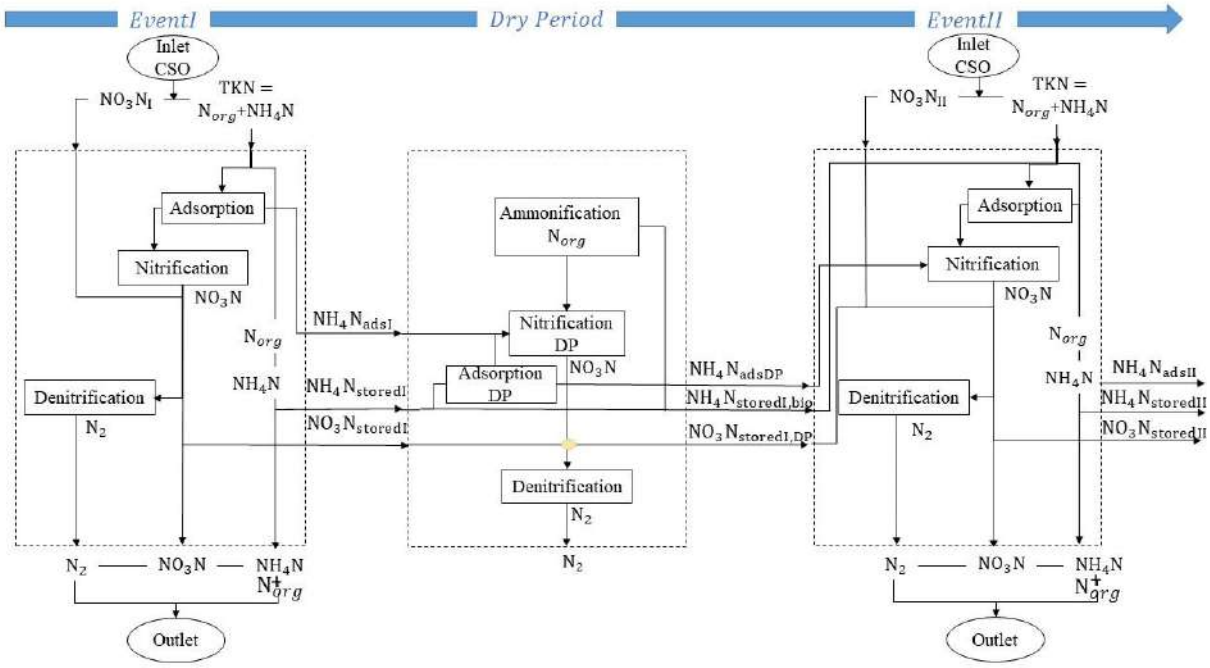

Figure 3.3 - N transformation processes within a filter at different times. The first feeding event, Event I, is followed by a dry period, after which a subsequent feeding event, Event II, occurs. The yellow dot represents the intersection of paths where the compounds are added together.

Nitrogen can be released as NH_4-N, NO_3-N or N_2 or stored as NH_4-N and NO_3-N in interstitial water, or adsorbed NH_4-N or N_{org} onto organic matter or mineral substrate. In the studied filters, as denitrification is negligible due to a lack of carbon, NO_3-N retained in Event I is released in Event II while water from saturated layer is renewed. During the DP, stored

Thèse accessible à l'adresse : https://theses.insa-lyon.fr/publication/2025ISAL0011/these.pdf © [D. Gonçalves Portela], [2025], INSA Lyon, tous droits réservés

NH_4-N along with mineralized N_{org}, can be converted into nitrate by nitrification. Based on the OT calculation from Chapter 2, the total mass of oxygen transferred for the different lengths of DP ranged from 0.5 to 3 kgO_2. The nitrification reaction requires 4.57 times the mass of oxygen to nitrify a given mass of NH_4-N. This corresponds to a possible nitrification of 0.11 to 0.65 kg of NH_4-N. However, this estimation is based on the assumption that the bacteria are ready to quickly consume all the oxygen transferred during the 10 min aeration period, which may not be realistic. The impact of DP on the nitrifying bacteria population is not yet fully understood, as there is a possibility that bacteria may die or decrease performance during this period. Therefore, despite the system has the potential to nitrify a considerable amount of ammonium in a short DP period, the possibility of NH_4-N being carried from one feeding event to the next must be considered.

The mineralization and nitrification of storage ammonium occurred during feeding events when SW (with less than 2 $mg.L^{-1}$ of TKN) was fed to the filter. Despite the low ammonium inlet concentration, these events resulted in the flushing of up to 8 $mg.L^{-1}$ of NO_3-N. During this phase, the O_2 uptake was variable reaching a minimum of 0.09 $mgO_2.L^{-1}.h^{-1}$ on the last day of DP showing low oxygen consumption, event 3 from Figure 3.4. The nitrifying bacterial community in the studied filter appears to be influenced by the availability of ammonium in the system.

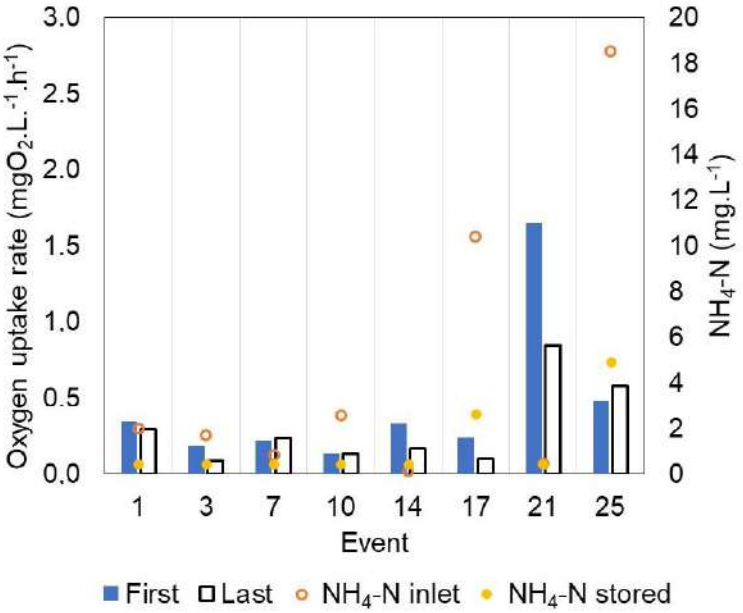

Figure 3.4 - Oxygen uptake for the first, blue bar, and last, empty bar, day of event in a sequence of events with increasing concentration of ammonium.

Thèse accessible à l'adresse : https://theses.insa-lyon.fr/publication/2025ISAL0011/these.pdf © [D. Gonçalves Portela], [2025], INSA Lyon, tous droits réservés

A comparison of the O_2 uptake on the first and last days of the dry period in the events of Figure 3.4 shows that the pattern of oxygen consumption is not always consistent. In some cases, it is maintained at a constant level, while in others it decreases. This can be attributed to the amount of ammonia loaded and accumulated in the saturated layer. The O_2 uptake fluctuations is likely due to the nitrification of stored ammonia as well as oxygen consumption for respiration. In the absence of nutrients, microbial community can die.

The remaining ammonium may be advantageous for bacteria acclimation in the filter, maintaining a minimum level of bacterial activity during DPs, avoiding mineralization of organic nitrogen. In a study by Murphy et al. (2015), an event-driven aerated TW loaded with highly variable influent required nutrient dosing to prevent loss of bacterial mass between events. This may explain the feeding events in which ammonium removal performance decreased.

The variations in O_2 uptake during the feeding event will be discussed in the section 3.3.4.

3.3.2 Components affecting N transformations

In Figure 3.5, PCA shows the correlations between the analyzed variables for trials performed under highly aerated conditions to promote as many aerobic reactions as possible. The selected variables are used to evaluate the correlation between variables during the nitrification process, including both feeding events and the dry period. Additionally, these variables can be correlated to the flush of nitrate. In the PCA were summarized results from 30 trials, where the parameters explain 71% of the variance. The variables include NH_4-N concentrations at the inlet and outlet of the previous event (V1 and V2), which indicate the impact of stored ammonium on the next event. The length of DP (V3), as it can affect the nitrate amount flushed at the beginning of a feeding event, represented by nitrate peaks (V4). The oxygen uptake when air blower are off (V5), indicating of microbial activity during the event. The proportion of nitrogen released, in relation to the loaded nitrogen (V6) and TKN at the outlet (V7), are representing the influences of nitrification during the event.

Thèse accessible à l'adresse : https://theses.insa-lyon.fr/publication/2025ISAL0011/these.pdf © [D. Gonçalves Portela], [2025], INSA Lyon, tous droits réservés

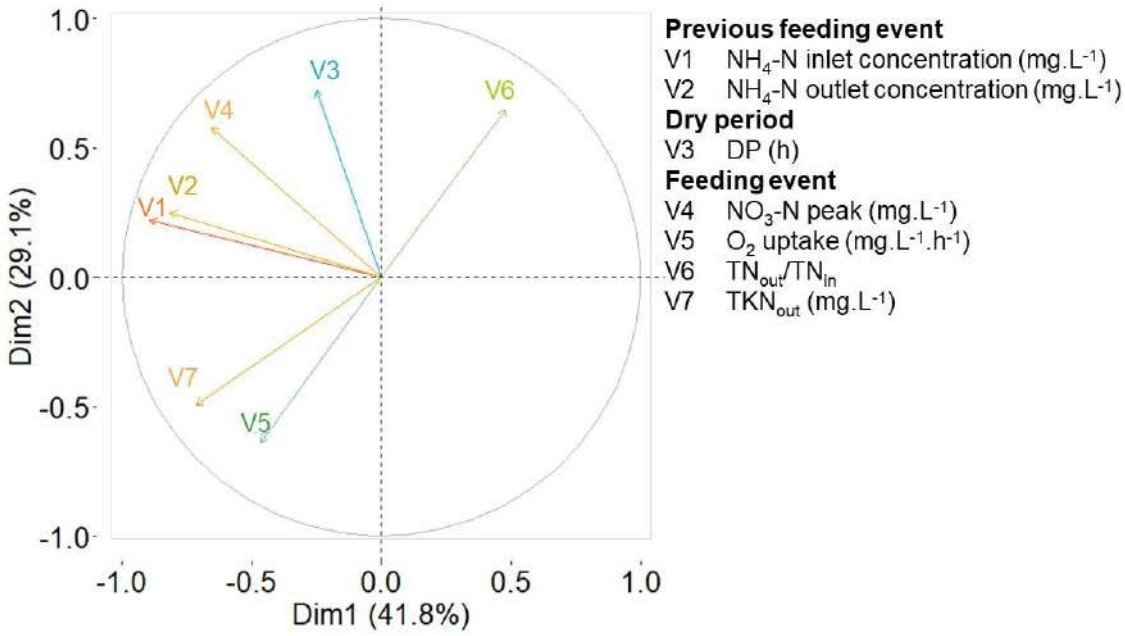

Figure 3.5 - PCA results in the filter CSOA, analyzed regarding 7 different parameter that are related to the nitrogen transformation process.

The parameter V4 represents the nitrate peak flush at the beginning of an event and indicates the peak intensity by taking into account the maximum concentration of nitrate measured at the outlet in the first hours of feeding. Accumulation of NO_3-N during the dry period will result in NO_3-N peak flush at the beginning of the subsequent event. This parameter appears to be affected by dry period and the NH_4-N outlet concentration from the previous event. In addition, there is a strong dependency between the inlet and outlet concentrations of NH_4-N (V1 and V2).

The duration of the dry period (V3) only affects the nitrate peak if NH_4-N is stored in the filter. The concentration of NH_4-N retained during the DP is represented by the NH_4-N concentration at the outlet of the previous event (V2). The higher outlet concentrations of NH_4-N suggested that nitrification during the event was insufficient and NH_4-N was being released untreated. A longer DP allows more time for NH_4-N retained from the prior feeding event to transform into NO_3-N, increasing the chances and intensity of nitrate peak. Other studies have also indicated that peaks are associated with DP (Dittmer, 2006; Pálfy et al., 2017c). Most of NO_3-N produced in DP originate from NH_4-N retained in the interstitial water and adsorbed. The part coming from organic N in TSS (< 6% of nitrogen in TSS - (Molle et al., 2005)) is negligible regarding outflow TSS concentrations.

Thèse accessible à l'adresse : https://theses.insa-lyon.fr/publication/2025ISAL0011/these.pdf © [D. Gonçalves Portela], [2025], INSA Lyon, tous droits réservés

The parameters, O_2 uptake at the end of an event (V5) and TKN at the outlet (V7) were positively related, as high outlet TKN concentrations require more oxygen for nitrification. The nitrification rate is correlated on both TKN concentration at the inlet and O_2 uptake. Consequently, parameters V5 and V7 are closer from each other due to their positive correlation. While O_2 uptake shows negative correlation on TN removal due to the possible predominance of NH_4-N storage as denitrification is negligible.

TN removal was observed in over half of the trials, the mean TN removal of these trials was 28 (±18)%, which can be mainly attributed the NH_4-N retained in interstitial water and possibly adsorption. In all trials, the TN at the outlet (TN_{out}) was mainly composed of NO_3-N. When TN_{out} was equal or higher than the TN_{in}, the NO_3-N was the predominant form of nitrogen at the outlet. This result was observed for both filters, with the mean percentage of NO_3-N in TN_{out} being 81% in CSOA and 92% in CSOB. Therefore, PCA analyses supports the hypothesis that TN removal depends on NH_4-N remaining in the saturated layer (with denitrification being negligible), as TN_{out}/TN_{in} ratio (V6) is negatively correlated by the parameters that positively influence nitrification (V5 and V7). If nitrification is not total, NH_4-N remains in the filter or is discharged.

Temperature, which ranged from 5 to 21°C, was considered for analysis with other parameters but it was removed due to its low correlation on these principal components.

3.3.3 ORP curves

ORP and DO forms measurements trough probes were used to identify the aerobic and anaerobic conditions in the filter. Figure 3.6 shows the evolution of ORP measurements along a feeding event under highly aerated conditions in CSOA.

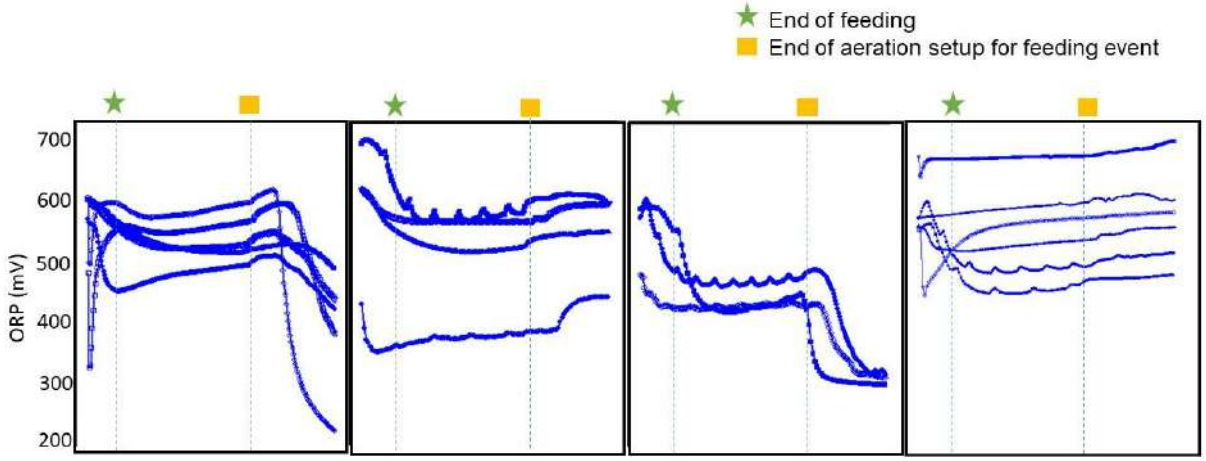

Figure 3.6 – The measurements for ORP curves were standardized to the hydrogen reference and the duration of drainage time was normalized. The end of feeding and aeration are

Thèse accessible à l'adresse : https://theses.insa-lyon.fr/publication/2025ISAL0011/these.pdf © [D. Gonçalves Portela], [2025], INSA Lyon, tous droits réservés

indicated. The ORP variations in events of CSOA were grouped in by their similarity when air blowers are switched off.

During the event, highly aerated conditions resulted in ORP values ranging between 300 and 700 mV. NH_4-N at the inlet and stored in the filter affected the ORP during the, resulting in four different ORP profiles (Figure 3.6), grouped by their pattern when the blowers are active without feed and one when the blowers are off. In all feeding events, the activation of air blowers immediately during the feeding increased the ORP. At the end of feeding, marked by the star, a plateau is established and extend into the drainage period. During the plateau, the ORP and DO concentrations remain stable due to high OT, which maximized aerobic reactions and maintained ORP above 450 mV. This plateau was also observed by Ruppelt et al. (2019), however, with a typical plateau that did not extend to drainage after feeding ended due to the limitation of CSO TW with passive aeration. The ORP values exceeding 300 mV indicate aerobic conditions (Kadlec and Wallace, 2008).

While both O_2 and ORP indicated the predominance of aerobic activity, their decline following the cessation of mechanical aeration occurred at different rates (Figure 3.6). Once aeration stopped, ORP stability could be disrupted, with measurements decreasing but remaining in aerobic conditions. By the end of the drainage phase, the ORP and DO concentration reached values around 300 mV and 0.2 $mg.L^{-1}$, respectively, indicating a state between aerobic and anoxic conditions. The exchange of ions result in simultaneous oxidation-reduction reactions, i.e. redox couples, and remaining organic matter and ammonium without sufficient oxygen can create instabilities on ORP values.

In this study, fluctuations in ORP during drainage influenced ORP variations during DP. When drainage ended with ORP >500 mV, a steady-state of approx. 600 mV was observed throughout the DP. This indicates that when nitrification is complete during the feeding event, bacterial respiration remains stable during DP without impacting ORP. When drainage ended and the ORP was around 200 mV the aeration during DP affected more the ORP. The ORP and DO measurements indicated that as long as DO and NH_4-N were available, nitrification continued, leading to an accumulation of NO_3-N within the filter.

3.3.4 Transformation processes in the event

In the studied aerated CSO TW, low aeration conditions resulted in oxygen limitation and minimal production of NO_3-N. Under this condition, a total of 56.4 $gNH_4\text{-}N.m^{-2}$ was loaded into the filter, and 47.0 $g.m^{-2}$ of NH_4-N and 0.5 $g.m^{-2}$ of NO_3-N were recovered at the outlet, due to

Thèse accessible à l'adresse : https://theses.insa-lyon.fr/publication/2025ISAL0011/these.pdf © [D. Gonçalves Portela], [2025], INSA Lyon, tous droits réservés

limited transformation of NH_4-N within the filter. Increasing OT to highly aerated conditions improved the nitrification rates, and consequently NH_4-N removal. From 113 $g.m^{-2}$ of NH_4-N loaded into the filter, a total of 34 $g.m^{-2}$ of NH_4-N and 57 $g.m^{-2}$ of NO_3-N were recovered at the outlet of the filter. Most of the loaded mass of NH_4-N was directly transformed to NO_3-N during the event without depending on the duration of the DP.

Palfy et al. (2017c) studied the capacity of a passive CSO TW to adsorb NH_4-N in the filtering media, indicating an adsorption capacity of 46 $gNH_4\text{-}N.m^{-2}$ using reactive media in the filtrating layer. In CSO TWs relying on nitrification during DPs, the adsorption capacity of the filtration material plays a critical role in avoiding NH_4-N release during feeding events. During DPs, when aerobic conditions dominate, adsorption capacity is renewed through nitrification. In mechanically aerated TWs treating WW, aerobic processes are further accelerated, enhancing NO_3-N production (Boog et al., 2014; Dong et al., 2012).

To estimate the maximum nitrification capacity of the studied filter, trials were analyzed by correlating the O_2 uptake rate with ammonium release after air blower were switched off (Figure 3.7). Denitrification was considered negligible, as most of the trials were dominated by aerobic reactions. In addition, the short HRT and lack of carbon turn denitrification unviable as observed in other studies of aerated systems that accumulate NO_3-N (Jamieson et al., 2003; Khan et al., 2022).

The increase in nitrate production during the event demonstrated that direct nitrification occurred in the filter, albeit to a limited extent. The aeration conditions and HRT were maintained at fixed levels while the NH_4-N concentration was variable. This resulted in a tendency for higher NH_4-N storage in the saturated layer of filter by the end of drainage phase, as the NH_4-N inlet concentration increased. This NH_4-N remaining in the filter affected the rate of oxygen consumption. Consequently, the removal of NH_4-N by nitrification during the event was constrained by the nitrogen inlet concentration. The duration of feeding events, aside to the availability of NH_4-N and oxygen, may have an impact on the dynamic of population growth.

Figure 3.7 shows NH_4-N outlet concentration in events where nitrification occurred and oxygen consumption measurements after air blowers were switched off. In the first six months of operation and for short drainage phase, less than 15 h, O_2 uptake was low despite the high availability of ammonium. When the filter reached a more mature stage, and after drainage phases lasting more than 20 h there was a tendency for O_2 uptake to increase due to higher NH_4-N concentrations at the outlet. The rapid uptake of oxygen in the presence of remaining NH_4-N reflected a high activity of nitrifying bacteria.

Thèse accessible à l'adresse : https://theses.insa-lyon.fr/publication/2025ISAL0011/these.pdf © [D. Gonçalves Portela], [2025], INSA Lyon, tous droits réservés

At this stage, the measurement of maximum O_2 uptake of 7.3 mg.L^{-1}.h^{-1} (Figure 3.7) can give some direction on the maximum rate at which nitrifying bacteria degrade NH_4-N in optimal conditions. Using the oxygen demand for nitrification (4.5 g of O_2 per g of NO_3-N produced), along with the average HRT of 7.3 h in the beginning and ponding phases measured in tracer tests (Chapter 2), the maximum NO_3-N production was estimated. To better estimate the direct nitrification, an average O_2 uptake of 0.3 mg.L^{-1}.h^{-1} of aerobic respiration was accounted for, which was estimated when the air blowers were switched off at the end of a dry periods and NH_4-N concentrations were minimal (below 0.1 mg.L^{-1} in the interstitial pores). Based on these estimations, the maximum NO_3-N production during the drainage was approximately 10 mg.L^{-1} over the HRT.

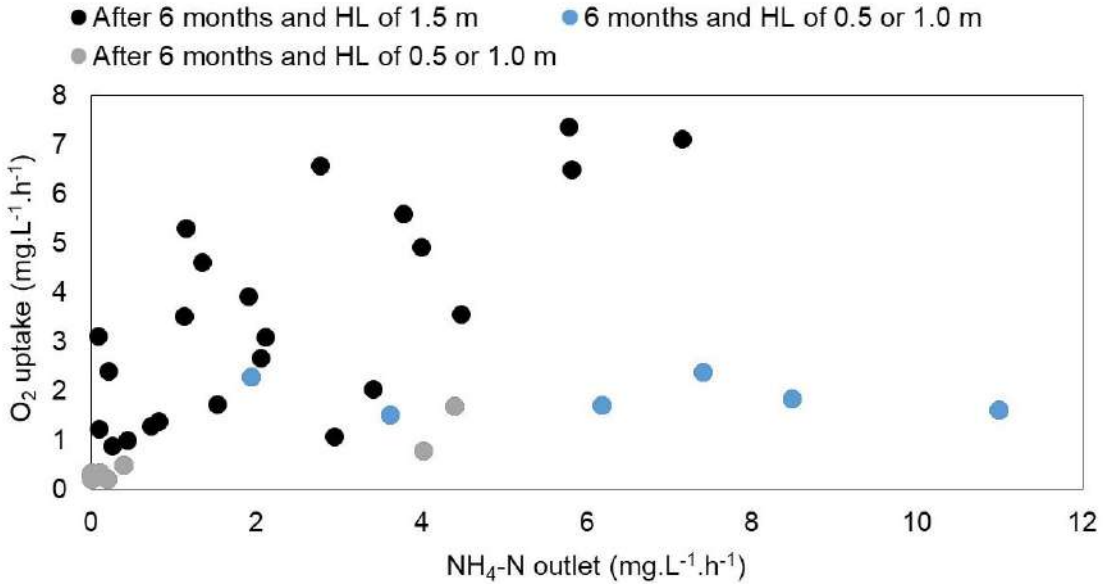

Figure 3.7 – Estimated O_2 uptake and NH_4-N outlet concentration in filter CSOA.

In most trials with influent TKN concentrations below the maximum nitrification threshold of 10 mg.L^{-1}, low NH_4-N concentrations were maintained at the outlet. In these trials, less than 30% of the total loaded NH_4-N mass was discharged. While plant uptake are possible pathways for ammonium removal, it was not considered in the calculations. According to Tanner (1996), the mean plant uptake is 0.7 g N.m^{-2}.d^{-1}. In this study, the mean loaded mass was 14.4 g NH_4-N.m^{-2} per event, except for events with SW, exceeding the mean plant uptake capacity. In trials where influent TKN $\leq$ 10 mg.L^{-1} commonly showed the following characteristics: complete removal of loaded NH_4-N, with low NH_4-N outlet concentration; and negligible production of NO_3-N during the subsequent DP.

Thèse accessible à l'adresse : https://theses.insa-lyon.fr/publication/2025ISAL0011/these.pdf © [D. Gonçalves Portela], [2025], INSA Lyon, tous droits réservés

The Eq.5 was used to estimate the direct NO_3-N production compared to NH_4-N removal. The trials were categorized into two groups, inlet TKN ≤ 10 mg.L^{-1} and inlet TKN > 10 mg.L^{-1}, as showed in Figure 3.8. Trends on retention of NH_4-N and overproduction of NO_3-N in each feeding event were observed.

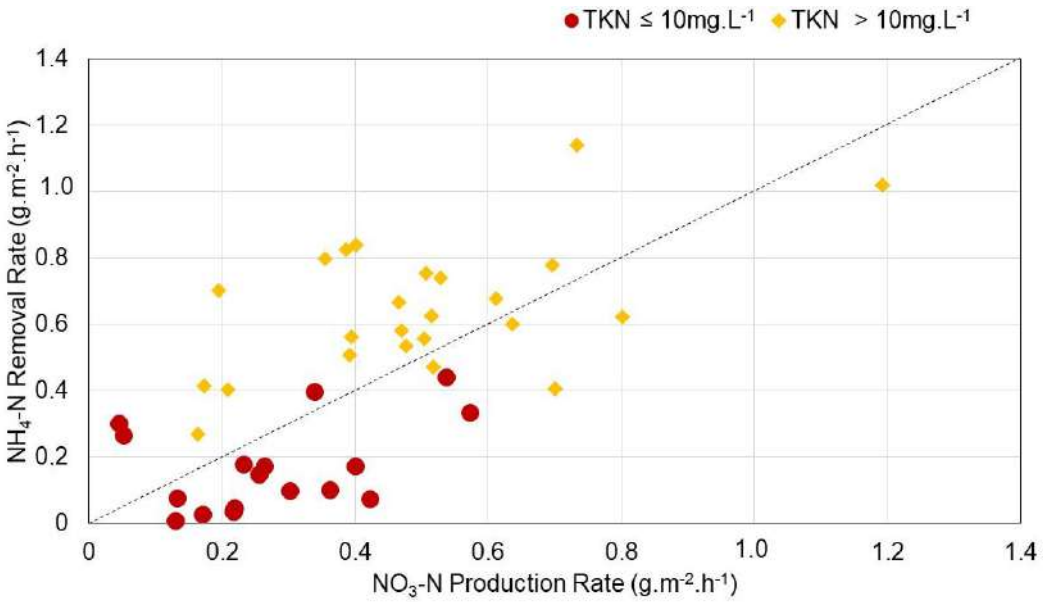

Figure 3.8 – NO_3-N production and NH_4-N retention rates for the trials with > 15gO_2.h^{-1}.m^{-2} in CSOA. The line crossing the axis represent the NO_3-N production equal to the retained NH_4-N.

Trials with inlet TKN concentration above 10 mg.L^{-1} present a nitrate production globally lower than NH_4-N reduction, as shown in Figure 3.8. This lower nitrate production indicates that direct nitrification was insufficient to transform all NH_4-N into NO_3-N. At high NH_4-N inlet concentrations, NH_4-N retention in interstitial water and possible adsorption were considerable. For these trials with high nitrogen load, NH_4-N was partially nitrified while some of it was retained in the saturated layer, leading to the discharge of untreated NH_4-N. The stored NH_4-N could accumulate in small amounts by adsorption.

Inlet TKN concentration ≤ 10 mg.L^{-1} appears to be a threshold for complete direct nitrification under highly aerated conditions. NH_4-N removal in feeding events closer the dashed line, Figure 3.8, was mainly due to direct nitrification with minimal NH_4-N storage in the filter. While events below the line showed higher NO_3-N production than NH_4-N removal during the drainage event. The NO_3-N production may exceed the NH_4-N removal rates due to the nitrification of stored NH_4-N from previous trials in the presence of excess oxygen. Therefore, the excess NO_3-N is the result of the degradation of NH_4-N adsorbed or retained in the interstitial water.

Thèse accessible à l'adresse : https://theses.insa-lyon.fr/publication/2025ISAL0011/these.pdf © [D. Gonçalves Portela], [2025], INSA Lyon, tous droits réservés

The filter CSOB, operated under the same highly aerated conditions as CSOA, consistently maintained low NH_4-N outlet concentration when inlet TKN was below 10 $mg.L^{-1}$. However, sensor data from CSOB to confirm direct nitrification were unavailable. As showed in Figure 3.3, nitrogen transformations involve complex processes that vary between systems, and further sensor data would be necessary to validate the maximum direct nitrification in CSOB. Feeding events where NO_3-N rates were not equal or higher than NH_4-N removal despite TKN loads below 10 $mg.L^{-1}$, dots above the line in Figure 3.8, might occurred due to reduced activity of nitrifying bacteria. For low ammonia stored and/or long dry periods, it is likely that nitrifying bacteria might be affected which may be specifically the case when filters are fed with SW only. The lack of ammonium in the influent may have caused nitrifying bacteria to be starved, reducing their activity. However, additional studies are needed to explain it.

3.3.5 Dynamic of NO_3-N during successive events

NO_3-N distribution for successive events is shown in Figure 3.9. It represents the distribution of NO_3-N - produced, released, and retained within the filter for each event using Eq 3 to 5. Nitrate present in the influent is the *NO_3-Nin (E)*. NO_3-N produced during the feeding and drainage period from direct nitrification of loaded NH_4-N is the *Transformed NO_3-N released (E)*. NO_3-N not recovered at the outlet by the end of the event, which was nitrified during the drainage, is referred to as *NO_3-N retained (E)*.

Additionally, stored nitrate produced during a previous feeding event before is the *NO_3-N retained (B)*. While nitrate generated during the DP through nitrification of stored NH_4-N is the *Transformed NO_3-N (DP)*.

Thèse accessible à l'adresse : https://theses.insa-lyon.fr/publication/2025ISAL0011/these.pdf © [D. Gonçalves Portela], [2025], INSA Lyon, tous droits réservés

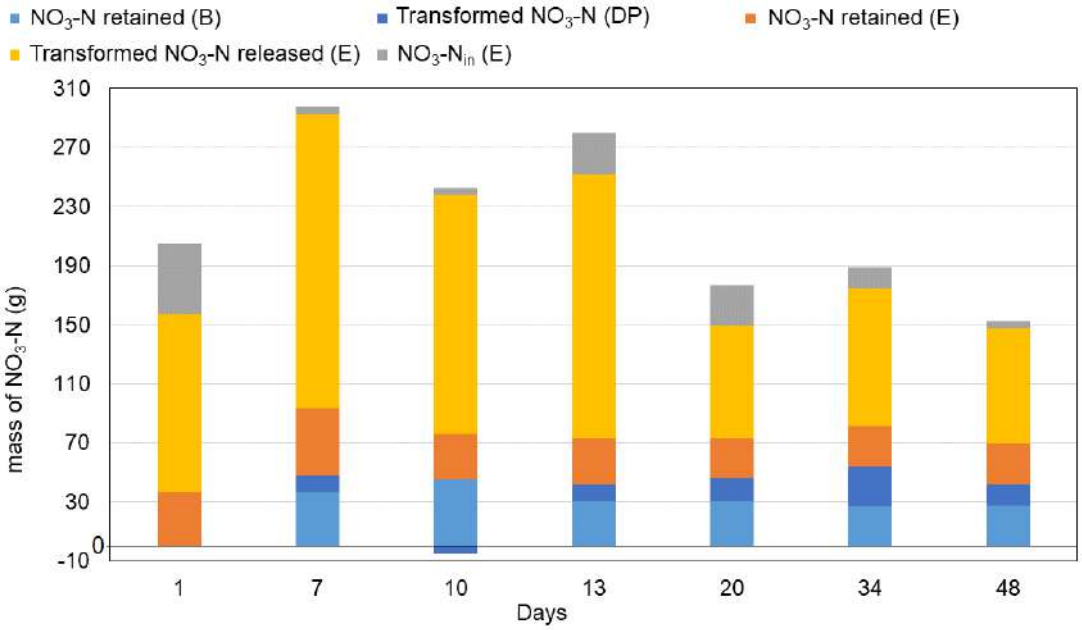

Figure 3.9 - Components of NO_3-N retained and discharged in each feeding event. This is a sequence of trials with HL of 1.5 $m^3.m^{-2}$ conducted in CSOA.

In day 1, Figure 3.9, the effects of the previous event and the DP were not considered. For subsequent trials, the *NO_3-N retained (E)* from one feeding event corresponds to the *NO_3-N retained (B)* in the following event. The NO_3-N stored from the previous event and the nitrified NH_4-N that was transformed into NO_3-N was flushed at the beginning of the feeding event. Therefore, the total NO_3-N accumulated within the filter is released in the next trial and if denitrification occurs part of the NO_3-N is deduced from the total. A comparison of the mass of nitrate retained at the end of a drainage phase indicated that, during a DP, up to 25 g (or 2.8 $mg.L^{-1}$) of nitrate could be removed. While the most favorable conditions for denitrification are during the dry period, given the potential for anoxic conditions and longer retention times, it is important to consider the limitations of carbon availability and the uncertainty to calculate the mass of nitrate produced during DP.

Between day 7 to day 10, Figure 3.9, the *Transformed NO_3-N (DP)* was negative, as approx. 5g of *NO_3-N retained (E)* was removed during DP. While this might suggest denitrification, the removed mass is minimal and could be attributed to uncertainties. In this analysis, it is assumed that removal of NO_3-N indicate no production of NO_3-N during DP. Additionally, when no NH_4-N is stored in the saturated layer, there is no or little production of nitrate.

From day 7 to day 13, Figure 3.9, high nitrogen loads and short dry period were observed. The low nitrate production during these short dry periods resulted in the accumulation of NH_4-N. Then, the accumulated NH_4-N in the presence of sufficient oxygen resulted in the

Thèse accessible à l'adresse : https://theses.insa-lyon.fr/publication/2025ISAL0011/these.pdf © [D. Gonçalves Portela], [2025], INSA Lyon, tous droits réservés

overproduction of nitrate from day 20 to 48. In this case, increasing the aeration time during the DP can prevent NH_4-N accumulation.

After day 20, Figure 3.9, longer DPs and increased nitrate production during the DP resulted in nitrate peaks. The accumulated untransformed NH_4-N, combined with long DP durations in the later trials, slightly increased the mass of NO_3-N at the outlet of the filter of up to 15 g. Despite the predominance of direct nitrification during the events, high inlet TKN concentrations and long dry periods can result in nitrates flushes at the subsequent events. During the period of high aerated conditions, an extreme case of flush with an NO_3-N outlet concentration reaching 45 $mg.L^{-1}$ was measured in CSOA. The event was preceded by 18 d DP and a previous NH_4-N inlet concentration of 30 $mg.L^{-1}$. This nitrate flush can induces some issues in respecting outlet requirements of TN outflow concentration when stringent.

3.3.6 Limitations on NO_3-N production and NH_4-N removal

The occurrence of overloads and short DP (< 3 days) leads to a reduction in the filter's capacity to remove NH_4-N. Chapter 2 demonstrated consistent removal in CSOA and CSOB regardless the HL, which varied from 0.5 to 1.5 m, as HRT is maintained until drainage phase ends. A linear correlation was observed between the TKN influent concentration and the TKN removal rate when the system was highly aerated. Consequently, it can lead to partial nitrification for high inflow concentrations.

When aeration switched is on, nitrification can produce up to 1.2 $g.m^{-2}$ NO_3-$N.h^{-1}$ (Figure 3.8) and NH_4-N concentrations are maintained stable at the outlet. However, once aeration is switched off, an increase of NH_4-N concentration is observed after 4 to 5 h of drainage. The curves of DO and N forms after air blower are switched off during drainage are showed in Figure 3.10.

Thèse accessible à l'adresse : https://theses.insa-lyon.fr/publication/2025ISAL0011/these.pdf © [D. Gonçalves Portela], [2025], INSA Lyon, tous droits réservés

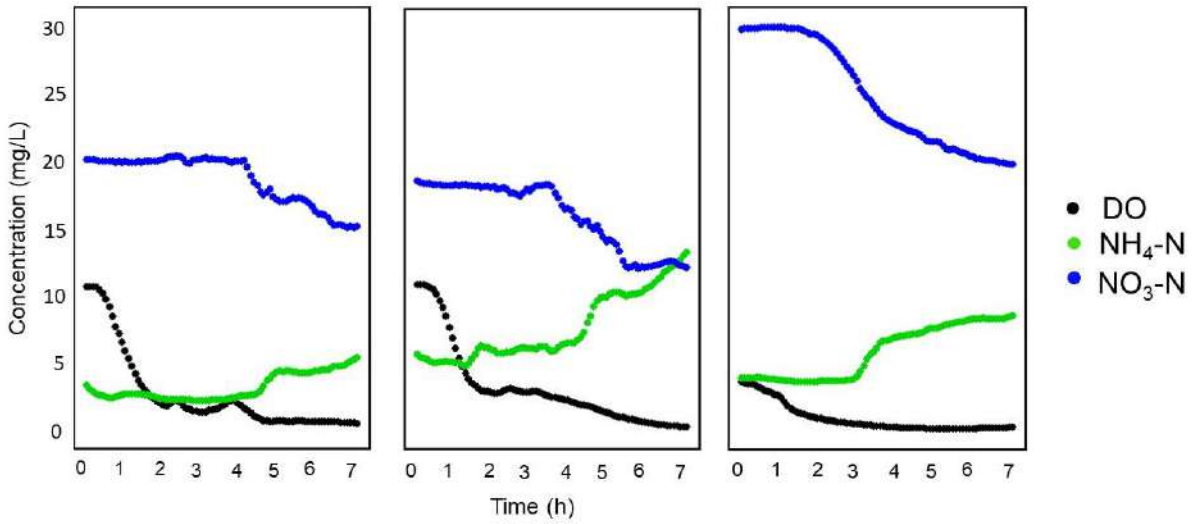

Figure 3.10 - Online measures of N forms and DO concentration in a piezometer 60 cm from the bottom. These are the dynamics after 80% of the inflow volume was recovered and aeration is switched off in trials of 1.5 $m^3.m^{-2}$.

When the aeration is switched on, the NH_4-N is homogenously distributed throughout the filter, due to the mixing effect and aerobic condition can ensure a stable nitrification. Outflow NH_4-N concentration stays stable at a level that depends on inlet concentrations and nitrification rate. Conversely, when the air blowers are switched off, the system behaved more as a plug flow reactor (see Chapter 2). During this drainage phase without aeration (Figure 3.10), the concentration of NO_3-N decreases as the depletion of oxygen impacts nitrification. In addition, the plug flow hydraulic brings less nitrified nitrogen to the outlet around 4 h after the air blowers were switched off. To maintain a low ammonia concentration at the outlet, it could be relevant to increase the aeration period so that drainage phase without aeration does not exceed 4 h.

The ammonia concentration in the filter depends on inlet concentration and the rate at which dissolved oxygen concentration is consumed. Higher inlet concentrations lead to higher oxygen consumption, reducing the dissolved oxygen content during the aeration phase and accelerating oxygen depletion during the non-aeration phase. Consequently final outlet ammonia concentration will be higher.

In this study, the system retained 50% of a NH_4-N of 1035 g, coming after a sequence of trials with load rates > 20 $mg.L^{-1}$ of NH_4-N. Typically, in CSO inlet concentration NH_4-N < 34 $mg.L^{-1}$ (Gasperi et al., 2012b; Gooré Bi et al., 2015; Yin et al., 2017), which is lower than the maximum conditions tested here. In the maximum load test the filter received a shock load, which resulted in a removal efficiency lower than the median 70% NH_4-N removal. However,

Thèse accessible à l'adresse : https://theses.insa-lyon.fr/publication/2025ISAL0011/these.pdf © [D. Gonçalves Portela], [2025], INSA Lyon, tous droits réservés

the system was still able to retain half of the load that is higher than the 23% retention observed by Pálfy et al (2017c) in a test with shock loads.

3.4 Conclusions

The pilot-scale study on the dynamics of nitrogen transformation and nitrification allows the drawing of some relevant conclusions. While oxygen consumption is maintained constant during active mechanical aeration, switching off the air blowers results in immediate effects on DO concentrations and aerobic degradation rates. The rate at which DO levels decline depends on the concentration of ammonia within the filter. It is possible to reduce the ammonium concentration to lower levels during aeration, although this will depend on the inlet concentration. This removal is linked to the direct nitrification potential of the system. Based on measurements of DO and ammonium concentration, in the tested condition, it was estimated that a maximum of 10 $mg.L^{-1}$ of TKN in inlet concentration can be directly nitrified during the event. For higher concentrations, the ammonium removal will be variable and might affect the treatment objectives.

When aeration is switched off at the end of a feeding event, the ammonium concentrations at the outlet of the filter can reach the same concentrations as at the inlet. However, this only occurs if a high concentration of ammonium has been accumulated in the filter from previous events. The oxygen consumed during the nitrification process results in a rapid decline in DO levels when high ammonia concentrations are present within the filter, which can suppress further nitrification. In addition, switching off aeration result in a plug flow condition and the decreased in nitrification. Consequently, the ammonia concentration increases at the end of the drainage phase. The time lapse between switching off aeration and the increase in ammonium concentration was approximately around 4 hours. This information is useful in defining the optimal time to stop aeration to prevent an increase in ammonium concentration.

Another parameter that can impact outlet concentrations of nitrogen is linked to the possible flushing of nitrate at the beginning of an event. The amount of ammonia stored at the end of the previous event and the length of the dry period are determinate on the nitrate flushing. The adsorbed ammonia onto the media and organic matter, which are in minor concentrations, and the mass of ammonia in the interstitial water can be nitrified during dry periods according to its length and the number of aeration cycle. It result in an increase of nitrate during the dry period that will be release at the subsequent feeding event. Peaks generally appear after at least

Thèse accessible à l'adresse : https://theses.insa-lyon.fr/publication/2025ISAL0011/these.pdf © [D. Gonçalves Portela], [2025], INSA Lyon, tous droits réservés

3 d of DP and for long DP of 18 d with high concentration of ammonium accumulated in saturated layer, nitrate peaks with a concentration of 45 $mg.L^{-1}$ can be produced.

The release of ammonium and nitrate is strongly influenced by the initial conditions established within the filter (e.g., transformed NO_3-N in dry period and stored NH_4-N) and the inflow ammonia concentration. However, in most of the event direct nitrification was the main mechanism removing ammonium. Analysis of kinetics of nitrification and a modelling study to predict direct nitrification of NH_4-N can assist in the design of new aerated CSO TWs.

Thèse accessible à l'adresse : https://theses.insa-lyon.fr/publication/2025ISAL0011/these.pdf © [D. Gonçalves Portela], [2025], INSA Lyon, tous droits réservés

4 Performance of aerated CSO TW in removing micropollutants

Abstract

Treatment wetlands (TWs) have been proposed as a reliable method for removing pollutants from combined sewer overflow (CSO). However, to our best knowledge, this is the first study evaluating the performance of aerated TWs in removing micropollutants from CSO. In two pilot-scale TWs fed with domestic wastewater mixed with stormwater, the role of filter design under different operational conditions was assessed. Samples were collected for more than one year and analyzed for 92 micropollutants using suspect screening, but not all could be quantified in every sample. Hence, a selection of compounds was made for further analysis based on their occurrence or chemical class. Metals were analyzed in the dissolved and particulate fractions of the samples every 3 months. Fecal indicator (FI) analyses were conducted after the filters had been in operation for over one year. In general, the filters showed positive removal efficiencies with considerable variability for both rubber products and pharmaceuticals. Compounds such as DEET, gabapentin and iomeprol, had moderate to low removal efficiencies for both filters, with median removal rates below 48%. Conversely, compounds such as irbesartan had mostly negative removal efficiencies, suggesting desorption. The filters effectively removed particulate metals, although dissolved metals generally passed through without being retained. The FI analysis indicated that disinfection was negligible, with an *E. coli* reduction < 1 $\log_{10}$. The results showed moderate retention of micropollutants in aerated CSO TWs, with no considerable enhancement in removal due to aeration.

Keywords: nature-based solutions (NBS); biofilter; emerging contaminants; intensified TW; industrial chemicals.

Thèse accessible à l'adresse : https://theses.insa-lyon.fr/publication/2025ISAL0011/these.pdf © [D. Gonçalves Portela], [2025], INSA Lyon, tous droits réservés

4.1 Introduction

Combined sewer overflow (CSO) discharge is a major source of pollution for surface water quality. Alongside organic matter and nutrients, it carries a variety of micropollutants and microbes, which have an adverse impact on the aquatic ecosystem and pose risks to human health (Gasperi et al., 2012b; Gooré Bi et al., 2015; Launay et al., 2016; Nickel and Fuchs, 2019; Noyer et al., 2020; Perry et al., 2024). The various groups of micropollutants include, among others, metals, polycyclic aromatic hydrocarbons (PAH), pharmaceuticals, and industrial compounds. They can be categorized by their source and form. Metals and PAHs that are commonly found in higher concentrations in particulate form than in dissolved form. These substances originate from natural sources or resultant from human activities, such as road runoff, roofs and faced painting (Samrani et al., 2004; Sorme and Lagerkvist, 2002). Lamprea and Ruban (2011) showed an elevated concentration of Zn, Pb and Cu during wet weather due to contribution of stormwater (SW) to wastewater (WW).

The presence of biocides and specific industrial chemicals in SW runoff, which is mixed with sewage during rain events in combined sewer systems, is a common occurrence. Pharmaceuticals and other industrial chemicals in CSO often stem from WW dilution (Becouze-Lareure et al., 2019; Launay et al., 2016). These micropollutants vary with events and are dependent on the characteristics of the catchment area. For example, pharmaceuticals such as carbamazepine and diclofenac are frequently detected in CSO generated in urban catchments (Nickel and Fuchs, 2019).

CSOs often contain elevated concentrations of microorganisms and micropollutants, which includes bacterial pathogens and persistent chemical, such as PFAS, analgesic drugs and iodinated contrast agents (Heberer, 2002; Perry et al., 2024). Furthermore, these persistent micropollutants, present in WW and SW, can be even found in drinking water (Heberer, 2002). Aiming to preserve the aquatic environment, the European Union (EU) is amending its legislation to set new goals for the regulation of substances of priority substances in water policy. For instance, under the Directive (2013)/39/UE a later on updated watch list for Environmental Water Quality Standards (EQS) was established in (2015) to add compounds of "emerging concern" to the ones defined in Directive 2008/105/EC. A variety of micropollutants form different classes of industrial chemicals and pharmaceuticals are commonly found in WW and CSO across Europe (Becouze-Lareure et al., 2019; Kisielius et al., 2024; Launay et al., 2016; Tondera et al., 2019), corroborating the findings in this study. However, the concentrations and frequency of occurrences vary between country and over time (Kisielius et

Thèse accessible à l'adresse : https://theses.insa-lyon.fr/publication/2025ISAL0011/these.pdf © [D. Gonçalves Portela], [2025], INSA Lyon, tous droits réservés

al., 2024). Pharmaceuticals, such as betablocker, antibiotics and radiocontrast agents, in high concentration in WW during dry weather has predominant occurrence in CSOs (Madoux-Humery et al., 2015; Mutzner et al., 2022). Studies reported diclofenac concentrations in combined sewage exceeding 0.1 $\mu g.L^{-1}$ during wet weather condition (Del Río et al., 2013; Launay et al., 2016; Scheurer et al., 2015; Tondera et al., 2019), while the revised EQS recommends annual average limits of 0.04 $\mu g.L^{-1}$ in surface water. The concentration of carbamazepine was frequently reported to be in the range of 0.02 to 0.27 $\mu g.\ L^{-1}$ (Tondera et al., 2019; Del Río et al., 2013; Madoux-Humery et al., 2013; Ryu et al., 2014) in CSO. The new Directive UWWD (2022)/0345 requires a minimum removal of 80% from 6 substances from the 12 listed in areas sensitive to micropollutants (e.g., areas for shellfish production and bathing water), with carbamazepine being one of the compounds. Pharmaceutical peak concentrations of up to 19 $\mu g.L^{-1}$ of benzotriazoles have been found (Launay et al., 2016).

In addition to micropollutants, the presence of fecal indicators (FI), such as *Escherichia coli* (*E. coli)*, is of concern for water quality. The concentration of *E. coli* in CSOs was found to be around 10^6 CFU /100 mL (Passerat et al., 2011; Scheurer et al., 2015; Tondera et al., 2013). This can affect the microbial balance in receiving water bodies (Noyer et al., 2020) and also pose a risk to human health associated with water bathing quality. The Bathing Water Directive (2006) sets a limit of 500 CFU /100 mL for *E. coli* sufficient quality of bathing water in coastal areas. However, heavy rainfall events following CSO discharge have exceeded these limits (Manini et al., 2022).

The impacts of climate change on precipitation (IPCC, 2023) and overexploitation of local water resources have increased the demand for solutions for reclaimed water, which must meet high water quality standards (Shoushtarian and Negahban-Azar, 2020). This includes the removal of both organic and inorganic micropollutants and the need for effective disinfection to prevent risks. The Regulation (EU) (2020)/741 require a quality level depending on the irrigation method and crop category. For the highest quality standard, weekly monitoring is required to ensure *E. coli* $\leq$ 10 MNP/100mL, BOD_5 and TSS $\leq$ 10 $mg.L^{-1}$ and turbidity $\leq$ 5 $mg.L^{-1}$. For applications that may emit aerosols or for irrigation of pastures and forage, additional controls are required for Legionella spp., which must be < 1000 CFU/L, and for helminth eggs, which must not exceed 1 egg/L.

Vertical flow treatment wetlands have proven reliable for addressing CSO pollution, with the advantage of removing micropollutants and indicator bacteria and viruses at the same time (Ruppelt et al., 2020, 2018; Scheurer et al., 2015; Tondera et al., 2019; Zacharias et al., 2020).

Thèse accessible à l'adresse : https://theses.insa-lyon.fr/publication/2025ISAL0011/these.pdf © [D. Gonçalves Portela], [2025], INSA Lyon, tous droits réservés

However, the efficiency of micropollutant removal in TWs is affected by the physicochemical properties of the micropollutant (e.g., molecular weight, water solubility and hydrophobicity), and their biodegradability. Individual evaluation of these properties is necessary to achieve a better correlation with their removal efficiency in TWs (Ilyas et al., 2020). For a number of micropollutants, sorption is the primary mechanism for retaining them within the system. Hydrophobic compounds are adsorbed onto organic matter, while hydrophilic compounds remain dissolved in water (García et al., 2010). A standard measure of hydrophobicity is the octanol–water coefficient (log k_{ow}), where sorption is considered as low, moderate or strong: Strong hydrophobicity is attributed when log k_{ow} > 5.5, while hydrophilic compounds are commonly found to have log k_{ow} <2.5 (Botturi et al., 2021; Rogers, 1996).

The filtration capacity of CSO TWs is an advantage when removing total metals and PAHs (Pálfy et al., 2017a; Masi et al., 2023), as their are mainly bound to particulate matter. These systems also facilitate the removal of easily biodegradable compounds, comparable to activated sludge treatment (Scheurer et al., 2015). For instance, paracetamol, diclofenac, and metoprolol were effectively removed from CSO in TWs (Scheurer et al., 2015; Tondera et al., 2013) depending on the operational conditions (Tondera et al., 2019; Ruppelt et al., 2020, 2019). The aging of filtration material has been found to have a negative correlation with the removal of partially biodegradable or slowly biodegradable compounds (Tondera et al., 2019). In addition, the recombination of metabolites to carbamazepine was suggested within CSO TWs resulting in negative removal (Ruppelt et al., 2020).

Studies have been conducted to enhance the removal of biodegradable micropollutants in TWs by increasing oxygen availability. While CSO TWs are effective at removing micropollutants to some extent, enhancements to their treatment capacity could facilitate the production of reclaimed water that meets safety standards. Nivala et al. (2019) observed that under aerobic conditions, caffeine, ibuprofen and naproxen were consistently removed over time, as it is for most aerobic bioprocesses (Choubert et al., 2011). Similarly, Kahl (2017) found that high redox potential, was also associated with the removal of emerging contaminants.

It is therefore evident that filter design and operational conditions are crucial for optimizing performance in terms of both micropollutant removal and disinfection, which in turn expands possibilities for water reuse. To the best of our knowledge, this is the first study to assess the performance of aerated CSO TWs in removing micropollutants, and the study presents compounds that have not been previously studied in CSO TWs. Additionally, are present compounds that have not been study in CSO TWs. In this sense, we assessed the effectiveness

Thèse accessible à l'adresse : https://theses.insa-lyon.fr/publication/2025ISAL0011/these.pdf © [D. Gonçalves Portela], [2025], INSA Lyon, tous droits réservés

of aerated CSO TWs in removing micropollutants, evaluating the impact of aeration on micropollutant levels in effluent and disinfection potential of the process. We also compared the performance of two distinct CSO TW designs in removing micropollutants, providing insights into the water quality achieved by the filters.

4.2 Material and Methods

4.2.1 Operational conditions and sampling

Two aerated CSO TW pilots, CSOA and CSOB, each with a surface area of 20 m², were fed for more than one year at the REFLET platform in the Metropolitan area of Lyon, France. The land use in this catchment area is primarily residential. The pilots were fed with a mixture of stored runoff stormwater (SW) and raw wastewater (WW), with WW:SW ratios ranging from 1:4 to 1:13 and highly diluted WW to reach typical concentrations of CSO.

Detailed information on pilot characteristics and experimental site operation were described in Chapter 2. In short, the top layer consisted of 0.2 m of gravel (2/4 mm) in CSOA, and in CSOB 0.2 m of sand (0/4 mm) followed by 0.15 m gravel (2/4 mm). Both filters had a bottom layer of coarse gravel (10/20 mm), which was permanently saturated. The saturated layer was 0.95 m deep in CSOA and 0.8 m in CSOB, as in Figure 4.1. Each filter was connected to two airblowers by 4 mm High Density Polyethylene pipes. The airblowers, model Becker DT 4.16, operated at the maximum frequency of 50Hz with average airflow rate at 1.15 $m^3.m^{-2}.h^{-1}$ and total air flow volume was variable.

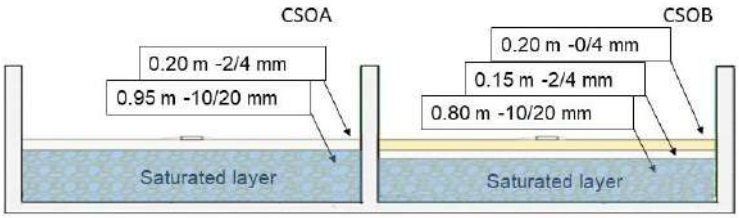

Figure 4.1 – Cross section indicating filter' layers

Samples of water for analyses of micropollutants and metals were collected throughout the whole period of filters operation, while samples for determination of fecal indicator (FI) were collected at the end of operation (Table 4.1). The feeding frequency was alternated with minimum dry periods of 50 h (~2 days) and a maximum of 416 h (~17 days). Table 4.1 shows the period and condition for samples collection.

Thèse accessible à l'adresse : https://theses.insa-lyon.fr/publication/2025ISAL0011/these.pdf © [D. Gonçalves Portela], [2025], INSA Lyon, tous droits réservés

Table 4.1- Summary of the frequency and period during which samples were collected, and the operation of the filters during this period. The number of samples (n) collected in each filter, CSO A (A) and CSO B (B), are indicated, as well.

Analysis	Frequency	Sampling	Estimated OT ($kgO_2.h^{-1}$)	HL ($m^3.m^{-2}$)	n
Ind. Chemical and pharmaceuticals	Every two events	May – Nov. 2023	0.01-0.13 or > 0.30	0.5, 1.0, 1.5	A = 19 B = 7
Pharmaceuticals	Every two events	Dec. 2023 – March 2024	> 0.30*	1.5	A = 7 B = 6
Heavy metals	Every 3 months	May 2023 - July 2024	0.01-0.13 or > 0.30	0.5, 1.0, 1.5	A = 5 B = 4
FI	Sequence of events	March-July 2024	> 0.30	1.5	A = 10 B = 5

*In each filter, there were 2 samples with OT around 0.13 $kgO_2.h^{-1}$ as the air blowers were operating at a reduced frequency.

During feeding events, the drainage time varied depending on the hydraulic load (HL) and the pilot. For CSOA, draining lasted between 9 and 20.5 h, while for CSOB it ranged from 11 to 24.3 h. Samples for the analysis of organic micropollutants and total metals were collected during periods with varying aeration conditions, ranging from poor to moderate or high aeration. These periods were operated with an estimated oxygen transfer (OT) of 0.01-0.13 $kgO_2.h^{-1}$ (for poor to moderate aeration) and > 0.30 $kgO_2.h^{-1}$ (for high aeration). In CSOB, most of the sampling occurred for high aeration conditions. During the first months of operation, dissolved micropollutants including industrial chemicals and pharmaceuticals were analyzed in 19 and 7 samples from CSOA and CSOB, respectively. From the 19 events analyzed for micropollutants, 5 were SW loaded with low or no percentage of WW. In a second phase, when the filters were operating exclusively at high hydraulic loads, 7 (in CSOA) and 6 (in CSOB) additional samples were analyzed for pharmaceuticals. Influent and effluent was sampled for the analyses of the metals, in particulate and dissolved phases, throughout the study.

The fecal indicators (FI) *E. coli* and total coliforms were monitored in the pilots over a period of three months during events with a HL of 1.5 $m^3.m^{-2}$ after 1.5 years of operation for CSOA and one year for CSOB, when the filters were mature. The drainage time for these trials was 22 h for CSOA and ranged from 23 to 39 h for CSOB. Additionally, the dry period varied

Thèse accessible à l'adresse : https://theses.insa-lyon.fr/publication/2025ISAL0011/these.pdf © [D. Gonçalves Portela], [2025], INSA Lyon, tous droits réservés

from a minimum of 50 h to a maximum of 316 h, with pilots operating under aerated conditions during this phase of monitoring.

4.2.2 Sampling

CSO samples were collected using an automatic sampler. Inlet time-proportional samples were collected with 100 mL collected every 2 min and stored in a single glass bottle. While outlet flow-proportional composite samples were carried out with samples pumped every 200 L. Each samples of 150 mL was stored in a separate glass bottle. All samples were maintained at 3°C in the autosampler throughout the drainage phase and transported in a refrigerated box to the lab. Both the inlet and outlet autosamplers were equipped with Teflon-coated hoses. Before each feeding event, the glass bottles were cleaned with an alkaline detergent, acetic acid solution and deionized water. The Teflon hoses were cleaned with the same products before the trials started and were periodically cleaned with detergent, diluted acetic acid and deionized water.

4.2.3 Analysis of micropollutants in the dissolved phase of water samples

Organic micropollutants were quantified using direct injection into a high-performance liquid chromatography system coupled with mass spectrometry (HPLC-MS), thereby bypassing conventional sample preparation steps such as compound extraction. This methodology builds upon and enhances Silva Thomsen et al. (2020), having been further optimized to detect a wider array of compounds, including 14 antibiotics and 53 other household-related organic micropollutants. Specifically, samples were first centrifuged in HPLC vials at 4000 g for 7 min using a Hermle Labortechnik GmbH Z 206 A centrifuge to precipitate particulates. After centrifugation, 900 µL of the resulting supernatant was transferred to a new HPLC vial and mixed with 100 µL of a methanolic internal standard solution. These mixtures underwent analysis by duplicate injections of 20 µL into an Agilent 1290 HPLC system (Waldbronn, Germany) coupled with a Sciex QTRAP 5500 mass spectrometer (Framingham, MA, USA).

Chromatographic separation was conducted on a Synergi Polar-RP column, 150 × 2 mm, 4 µm particle size (Phenomenex, Torrance, CA, USA), maintained at a temperature of 20°C. The flow rate of the solvent was set at 250 µL/min. The mobile phase consisted of water (eluent A) and methanol (eluent B), each containing 0.2% v/v formic acid. A multi-step linear gradient program was employed for the separation: from 0 to 1 min, 0% B; from 1 to 2.5 min, a gradient from 0% to 50% B; from 2.5 to 8.5 min, 50% to 80% B; from 8.5 to 9 min, 80% to 100% B;

Thèse accessible à l'adresse : https://theses.insa-lyon.fr/publication/2025ISAL0011/these.pdf © [D. Gonçalves Portela], [2025], INSA Lyon, tous droits réservés

held at 100% B from 9 to 14 min; from 14 to 14.5 min, a rapid return to 0% B; and maintained at 0% B from 14.5 to 19.5 min.

The mass spectrometer was operated using electrospray ionization in positive mode (ESI+) with a capillary voltage set at 4500 V and temperature of 400°C. The concentration of each compound was quantified based on a 9-point calibration curve, using certified analytical standards.

Each sample of influent and effluent was collected in duplicate and average value of duplicates were taken. In total, 92 compounds were analyzed. Twenty samples were analyzed in CSOA, and 8 in CSOB. A total of 28 compounds in CSOA and 31 in CSOB were identified at least once above the limit of quantification (LOQ), at the inlet and/or outlet. The selected compounds that appeared in both filters were benzothiazoles derivate, 6PPD-quinone, iomeprol, gabapentin and irbesartan.

4.2.4 Analysis of metals

Samples were filtered through 0.45 µm filters (Millipore) to separate particulate and dissolved phases. The filters were mineralized by aqua-regia digestion in a microwave oven. The filtrate was analyzed using inductively coupled plasma mass spectrometry (ICP-TQ-MS), following the standard procedure NF EN ISO 17294-2. All analyses were performed in duplicate and average was reported. The LOQ and a complete list of the analyzed metals are in the Annex 1. The analytical error varied between 10 and 25%, depending on the metal and whether it was the in particulate or dissolved phase.

4.2.5 Fecal indicators (FI) analysis

The samples were prepared for *E. coli* and total coliforms analysis using a dilution factor from 1 to 1/10000. Dilutions were prepared with a mix of a phosphate buffer solution and an $MgCl_2$ solution. The analyses were conducted using the Colilert® Quanti-Tray™ (MPN) enumeration method, with incubation at 37°C for 18 h (IDEXX Laboratories, Inc., Westbrook, Maine, USA).

4.2.6 Dataset analysis

For each feeding event, the removal efficiency was calculated for all selected micropollutants, a complete list with number of analyzed samples and frequency of occurrence is in the ANNEX 2. For the selected micropollutants, the values that were below the limit of quantification (LOQ) were replaced with the LOQ in the removal efficiency calculation. As

Thèse accessible à l'adresse : https://theses.insa-lyon.fr/publication/2025ISAL0011/these.pdf © [D. Gonçalves Portela], [2025], INSA Lyon, tous droits réservés

well, the mean and median inlet and outlet concentrations were determined by replacing < LOQ with the LOQ. These replacements were marked alongside the average value. If one or more values were < LOQ, the removal was considered to be the minimum removal efficiency. In addition, a conservative criterion for uncertainties on the measurements of industrial chemicals and pharmaceuticals was established. Measurements below ten times the LOQ were considered to have high uncertainty for comparison (Choubert et al., 2017). Thus, the removal rates of the filter were only compared for inlet or outlet concentrations exceeding the LOQ in ten times.

In order to determine the stability of the metal concentration at inlet and outlet, the coefficient of variation (CV= standard deviation/mean) was calculated for the small number of samples collected around 3 months apart. The results for metal measurements were analyzed using the mean and standard deviation. The statistical analyses were conducted using Excel 2016, and box and whisker plots were created for the selected micropollutants and FI using RStudio. As the data distribution was non-normal and the population was small, the median was taken as the reference value for evaluating the inlet and outlet concentrations and removal efficiencies. The median better represents the data distribution at the 50% reliability level, as extreme measurement results skew the distribution. The observed population was either skewed or tailored, making the median a more appropriate representation of the center of the population (von Sperling et al., 2020).

4.3 Results and Discussion

4.3.1 Selected micropollutants

4.3.1.1 Industrial chemicals

The complete list of micropollutants detected in the filter, along with their respective frequency of occurrences above the LOQ, is provided in the ANNEX 2. Many of the pharmaceutical substances quantified in this study has also been reported in previous studies on micropollutants in CSO (Becouze-Lareure et al., 2019; Launay et al., 2016; Madoux-Humery et al., 2015; Mutzner et al., 2022; Tondera et al., 2019). However, 2-anilino-5-(4-methylpentan-2-ylamino)cyclohexa-2,5-diene-1,4-dione (6PPD-quinone), a substance of emerging concern, has not been included the target list of previous studies, although it was quantified in this study. Similarly, while benzothiazoles are rarely mention in CSO studies, they were frequently detected in this study, appearing in at least 70% of the samples in which they were included in the targeted screening.

Thèse accessible à l'adresse : https://theses.insa-lyon.fr/publication/2025ISAL0011/these.pdf © [D. Gonçalves Portela], [2025], INSA Lyon, tous droits réservés

Benzothiazole (BT), its derivate aminobenzothiazole (ABT) and hydroxybenzothiazole (OHBT) originate from rubber products and industrial processes (Reddy and Quinn, 1997). 6PPD-quinone, a transformation product from tire wear, is associated with road washoff (Seiwert et al., 2022). It is a nonpolar hydrophobic compound (K_{ow} 5.6) and in all samples, it showed outlet concentrations consistently below the LOQ (< 0.02 μgL^{-1}). With a median removal efficiency of ≥ 70%, this was the compound with the highest removal rate in CSOA (Table 4.2). Rodgers et al. (2023) observed similar retention performance for 6PPD-quinone in SW bioretention systems.

Figure 4.2 shows a boxplot with inlet and outlet concentration of aminobenzothiazole (ABT), benzothiazole (BT) and hydroxybenzothiazole (OHBT), which were detected in all samples.

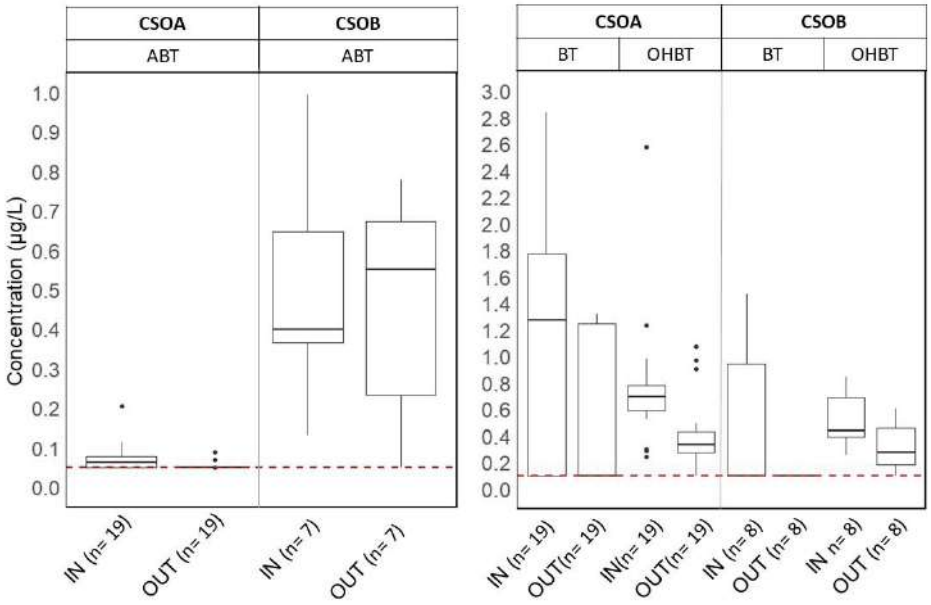

Figure 4.2 - Inlet (IN) and outlet (OUT) concentrations. The limit of quantification, represented by the dashed red line, is 0.05 $\mu g.L^{-1}$ for ABT (aminobenzothiazole) and 0.1 $\mu g.L^{-1}$ for BT (benzothiazole) and OHBT(hydroxybenzothiazole). The number of samples analyzed for the compound is indicated by n.

In CSOA, the inlet and outlet concentrations of ABT remained stable and close to the LOQ at 0.05 μgL^{-1}. In contrast, CSOB received higher ABT inlet concentrations than CSOA and had more events where outlet concentrations exceeded inlet concentration. The removal of ABT was variable in both filters. In some feeding events, ABT was almost completely removed, with an outlet concentration below the LOQ, whereas in others, no removal was observed. The median removal efficiency of ABT was approx. 26% (Table 4.2 and Table 4.3). However, inlet

Thèse accessible à l'adresse : https://theses.insa-lyon.fr/publication/2025ISAL0011/these.pdf © [D. Gonçalves Portela], [2025], INSA Lyon, tous droits réservés

or outlet concentrations were below the threshold of ten times the LOQ (0.05 μgL^{-1}), decreasing the confidence level of the calculated removal efficiency (Choubert et al., 2017).

Table 4.2 and Table 4.3 show the removal efficiency of all selected compounds (industrial chemicals and pharmaceutical), indicating those with high uncertainties and where <LOQ was substituted by LOQ to calculate removal efficiency, resulting in a potential underestimation of the presented value.

Table 4.2 - Removal efficiency in CSOA, for the compounds 6PPD-quinone (6PPD-Q), aminobenzothiazole (ABT), benzothiazoles (BT), N,N-Diethyl-3-methylbenzamide (DEET), Diclofenac (DFC), Gabapentin (GBP), Iomeprol (IOP), Irbesartan (IBT). The n represents the total number of samples used to calculate the removal efficiency. Tests with inlet and outlet < LOQ are not included in n.

CSOA	6PPD-Q** (n=7)	ABT* (n=19)	BT** (n=12)	OHBT* (n=19)	DEET* (n=10)	DFC* (n=6)	GBP* (n=10)	IOP* (n=10)	IBT (n=4)
Mean	69%	16%	51%	29%	27%	53%	30%	36%	-83%
SD	6%	37%	36%	38%	20%	11%	32%	30%	133%
Median	70%	28%	43%	42%	35%	58%	45%	48%	-69%

* high uncertainty
** minimum removal efficiency

Table 4.3 - Removal efficiency in CSOB, for the compounds 6PPD-quinone (6PPD-Q), aminobenzothiazole (ABT), benzothiazoles (BT), N,N-Diethyl-3-methylbenzamide (DEET), Carbamazepine (CBP), Diclofenac (DFC), Gabapentin (GBP), Iomeprol (IOP), Irbesartan (IBT). The n represents the total number of samples used to calculate the removal efficiency. Tests with inlet and outlet < LOQ are not included in n.

CSOB	6PPD-Q** (n=5)	ABT* (n=7)	BT** (n=3)	OHBT* (n=7)	DEET (n=10)	CBP (n=6)	DFC* (n=7)	GBP (n=10)	IOP* (n=9)	IBT (n=4)
Mean	97%	-21%	95%	30%	12%	-15%	-13%	6%	8%	-12%
SD	0.4%	92%	3%	50%	41%	8%	154%	37%	40%	21%
Median	97%	26%	93%	59%	32%	-15%	45%	23%	14%	-13%

* high uncertainty
** minimum removal efficiency

Removal efficiency was always positive for BT and OHBT (Figure 4.2). The median removal efficiency for BT was 43% in CSOA and 93% in CSOB, while for OHBT, it was 42% in CSOA and 59% in CSOB. Although CSOB showed high removal efficiency of BT, the results were inconclusive in attributing this performance to the sand layer, as the removal efficiency was calculated from three samples. In CSOA, the removal efficiency for both BT and OHBT was moderate. Laboratory tests showed that certain bacterial groups can adapt to

Thèse accessible à l'adresse : https://theses.insa-lyon.fr/publication/2025ISAL0011/these.pdf © [D. Gonçalves Portela], [2025], INSA Lyon, tous droits réservés

BT and biodegrade them in aerobic systems (Kowalska et al., 2019; Reddy and Quinn, 1997; Reemtsma et al., 1995). Asimakopoulos et al. (2013) found that BT was more effectively removed than OHBT when studying benzothiazoles derivate removal in activated sludge.

The log K_{ow} for ABT, BT and OHBT are 1.89, 2.01 and 1.76, respectively (Van Leerdam et al., 2009). Given their polar characteristics, it is unlikely that these compounds will bioaccumulate or adsorb to particles (Kowalska et al., 2019; Reddy and Quinn, 1997). Forced aeration may create favorable conditions for certain groups of bacteria that degrade organic micropollutants. However, aerobic conditions were not a key factor for removal of those micropollutants. For a period of reduced aeration in CSOA, lasting one month, the filter showed a similar performance removing benzothiazoles. Matamoros et al. (2016) studied a HSSF TW, which anaerobic zones predominate, and observed a stable removal of benzothiazoles around 63%, with low variability due to seasonality. This suggests that other factors not considered in this study may be responsible for removing those compounds under non-strict aerobic conditions. These results can be verified through analysis of the solids.

4.3.1.2 Pharmaceuticals

Analysis of the collected samples showed that iomeprol, gabapentin and irbesartan were the most frequently detected pharmaceutical compounds. They were monitored throughout the entire period of the experiments and belong to different therapeutic classes. Gabapentin is an analgesic, iomeprol is an x-ray contrast, and irbesartan is an antihypertensive. Figure 4.3 shows the ranges of inlet and outlet concentrations for these compounds.

Thèse accessible à l'adresse : https://theses.insa-lyon.fr/publication/2025ISAL0011/these.pdf © [D. Gonçalves Portela], [2025], INSA Lyon, tous droits réservés

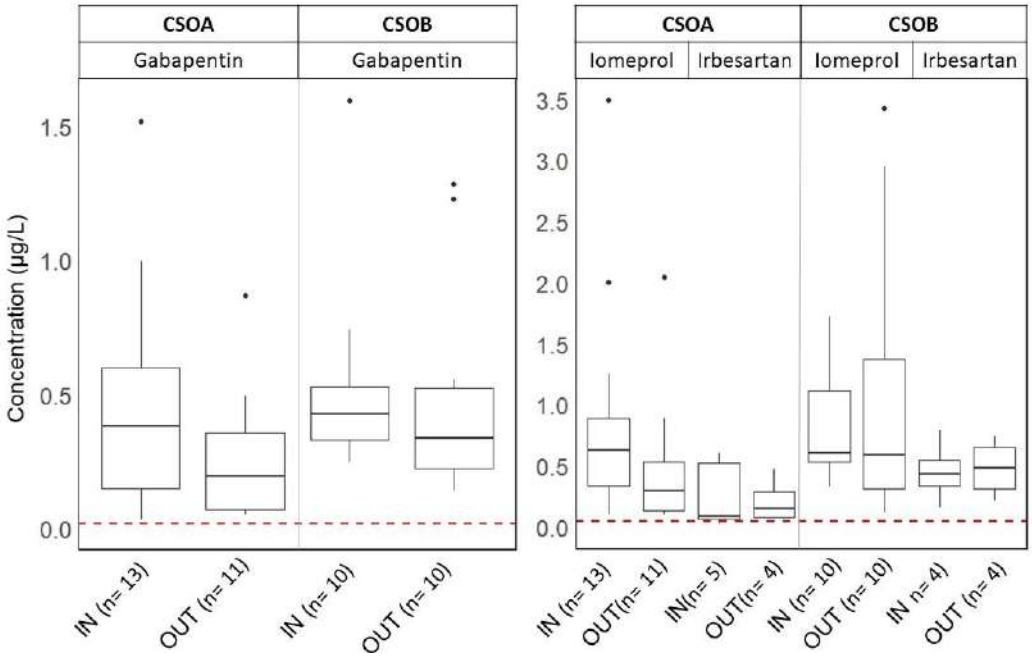

Figure 4.3 - Inlet (IN) and outlet (OUT) concentrations. The limit of quantification, represented by the dashed red line, is 0.02 µg.L^{-1} for gabapentin and 0.05 µg.L^{-1} for iomeprol and irbesartan. The number of samples analyzed for the compound is indicated by n.

Gabapentin and iomeprol showed variability at inlet concentrations of CSOA, but the outlet concentrations remained consistently low, at 0.25 µg.L^{-1} (Figure 4.3). The comparison of inlet concentrations in CSOA and CSOB showed similar median for all compounds, with outlet concentrations of gabapentin and iomeprol slightly lower for CSOA than for CSOB (Figure 4.3). The median removal efficiency of gabapentin in CSOA was 45% (Table 4.2), or 50% for eight measurements ten times above the LOQ, and 23% for CSOB (Table 4.3). For iomeprol, it was 47% for CSOA and 14% for CSOB (Table 4.2 and Table 4.3). The difference in removal of gabapentin and iomeprol may be related to the hydrodynamics of the filters, since on later trials CSOB clogged contrary to CSOA. It is probable that the hydrodynamics within the filter changed during the clogging process, which may have affected the time or contact area of the contaminant with the microorganisms, thereby reducing possible degradation and adsorption of pharmaceuticals.

With their low tendency to sorption, gabapentin (K_{ow} = -1.1) and iomeprol (K_{ow} = -1.45) have proven to be difficult to remove even with advanced post treatment at wastewater treatment plants, such as UV and powdered activated carbon (Kovalova et al., 2013; Mailler et al., 2016; Margot et al., 2011). Additionally, high concentrations of organic matter may negatively impact the removal of gabapentin (Auvinen et al., 2017). However, combining aerobic conditions and reactive media in a retention soil filter (RSF) has shown > 80% removal

Thèse accessible à l'adresse : https://theses.insa-lyon.fr/publication/2025ISAL0011/these.pdf © [D. Gonçalves Portela], [2025], INSA Lyon, tous droits réservés

for gabapentin in WW post-treatment when using RSF with granular activated carbon (Brunsch et al., 2018). The removal of pharmaceuticals in general in TWs, as for other micropollutants, has shown to be additionally highly variable. Zhang et al. (2014) emphasize that pharmaceuticals removal can be influenced by several mechanisms, including photolytic degradation, sorption, plant uptake, phytodegradation, and microbial degradation. The design and operational conditions of the TWs affect these mechanisms and therefore the removal efficiency differently. Brunsch et al. (2020) studied RSFs for sewage post-treatment periodically alternating with CSO influent, reaching 90% of gabapentin removal for CSO treatment. The 50% removal rate observed in CSOA is lower than the 90% median removal rate reported by Brunsch et al. (2020), where inlet concentrations were considerably higher, at 6.3 $\mu g.L^{-1}$. Auvinen et al. (2017) observed high removal of gabapentin, reaching almost complete removal of the compound, in aerated HSSF treating WW. Therefore, aerobic systems that are constantly fed may have a positive effect on the biodegradation of gabapentin. While in event-driven aerated TWs may help to manage organic matter and micropollutants such as gabapentin, within a short HRT.

The results demonstrated variable removal of irbesartan in both filters, with alternating positive and negative removal efficiency. The removal efficiencies of CSOA and CSOB were -69% and -13% (Table 4.2 and Table 4.3), respectively, based on four inlet and outlet samples per filter. In both filters, some feeding event resulted in slightly higher concentrations in the outlet than in the inlet, at under 30%, indicating no removal and potential remobilization or recombination of metabolites. Transformation products of irbesartan, such as valsartan acid and irbesartan related compound A, were found in the influent of a VF TW used as a tertiary treatment for domestic sewage (Tadić et al., 2024). The authors observed mean removal efficiencies of 13% for irbesartan, 75% for valsartan acid, and -150% for irbesartan-related compound A at peak concentrations. Process such as release through desorption and deconjugation reactions (hydrolyses step) can be related to the negative removal efficiency.

There are few studies on irbesartan removal in TWs. Lei et al. (2022) reported 45% removal in a sand based VF TW with irbesartan concentrations between 0.5 and 3 $\mu g.L^{-1}$, and removal improved by adding bark biochar in the filter. With a K_{ow} of 5.4, irbesartan is highly adsorbable, benefiting from materials that promote sorption (Lei et al., 2022). Studies on WWTPs with assisted chemical treatment or activated sludge with ozonation, where influent concentrations of irbesartan were higher than in our study, showed less than 50% removal (Botero-Coy et al.,

Thèse accessible à l'adresse : https://theses.insa-lyon.fr/publication/2025ISAL0011/these.pdf © [D. Gonçalves Portela], [2025], INSA Lyon, tous droits réservés

2018; Margot et al., 2013). Thus, in the feeding events tested for irbesartan, a combination of factor, including desorption or deconjugation, may have contributed to negative removal rates.

Diclofenac was detected above LOQ in 6 of the 13 samples analyzed in CSOA and 7 of the 10 samples analyzed in CSOB (ANNEX 2). The inlet concentration ranged from 0.02 to 0.25 $\mu g.L^{-1}$ and < LOQ in some cases, the removal efficiency was not calculated if inlet and outlet concentrations < LOQ. CSOA demonstrated more stable removal efficiency than CSOB, with positive averages and low standard deviation. In CSOB, the removal efficiency was highly variable with diclofenac either being removed below LOQ (< 0.05 $\mu g.L^{-1}$ or 0.02 $\mu g.L^{-1}$) or release at a concentration of 0.23 $\mu g.L^{-1}$. The median removal was 58% in CSOA and 47% in CSOB (Table 4.3).

Diclofenac has a log K_{ow} of 4.5 and negative charges, which in combination hinder sorption by plants (Brunsch et al., 2018; Garcia-Rodríguez et al., 2014). Therefore, it is probable that its removal is achieved through two main processes: biodegradation, which is favored but yet limited under high redox potential (Ruppelt et al., 2019), and photodegradation (Matamoros et al., 2012). In CSO TWs, degradation of diclofenac tends to improve after long dry periods and in filters with higher filtration layer depth (Ruppelt et al., 2020). Ruppelt et al. (2020) reported moderate removal rates of 30 to 40% in pilot scale filters with HL of 1.0 m^3m^{-2}, and Tondera et al. (2019) found a median removal rate of 47% in a mature full scale filter with annual outflow of 32 m^3m^{-2}. Scheurer et al. (2015) reported almost complete removal of diclofenac, with outlet concentration < LOQ, for inlet concentrations comparable to this study, though with a limited number of samples and maximum HL of 1.0 m^3m^{-2}. Nivala et al. (2019) found annual mean removal efficiencies of 74% in aerated vertical flow (VF) TW treating domestic WW at HLs of 0.095 m^3 per day. The removal efficiency of certain compounds is influenced by the contact time between the water and the biofilm. Auvinen et al. (2017) observed that longer HRT improved diclofenac removal in an aerated microcosm scale batch. The shorter HRT in CSO TWs may be a contributing factor to their moderate efficiency in removing diclofenac. The HRT of the studies' filters was between 6.5 and 10 h (Chapter 2), and longer HRT could have led to improved performance in retaining certain micropollutants. In addition, diclofenac is a persistent compound (Heberer, 2002), which, when it is nonbioavailable, accumulates over time (Alexander, 2000; Zhang et al., 2014).

Carbamazepine was measured in 11 and 10 feeding events of CSOA and CSOB, respectively. However, it was more frequently measured above the LOQ at the inlet of CSOB, with 6 samples showing a median removal efficiency of -15% (Table 4.3). The median inlet of

Thèse accessible à l'adresse : https://theses.insa-lyon.fr/publication/2025ISAL0011/these.pdf © [D. Gonçalves Portela], [2025], INSA Lyon, tous droits réservés

and outlet concentration were < 0.30 and 0.37 µg.L^{-1}, respectively. Similar results of negative removal were observed in other studies of CSO TW at pilots and large scale (Ruppelt et al., 2020; Scheurer et al., 2015; Tondera et al., 2019, 2013), where low or no removal, and remobilization of carbamazepine, occurred during certain events. The biodegradability of carbamazepine is limited, particularly under aerobic conditions (Hai et al., 2011). Studies suggest the recombination of carbamazepine transformation products (König et al., 2016). Although this process must be carefully evaluated as an increase in carbamazepine concentration could be attributed to a chemical analysis and sampling problem, or variation in influent concentrations (Trognon et al., 2024). As diclofenac, carbamazepine are known for its recalcitrance (Heberer, 2002), and filter aging can lead to desorption or breakthrough as suggested by (Tondera et al., 2019).

The insect repellent N,N-Diethyl-3-methylbenzamide (DEET) was monitored in all samples, with a median inlet concentration of 0.17 µg.L^{-1} for both filters. The median removal efficiency was approx. 35%, as showed in Table 4.2 and Table 4.3. In a WWTP, this compound demonstrated positive removal rates in secondary treatments (Sui et al., 2010). Sui et al. (2010) compared different secondary treatments of pharmaceuticals in WWTP treating domestic WW and sand filtration, reaching up to 50% removal efficiency for higher inlet concentrations (1.0 µg.L^{-1}) than this study.

4.3.1.3 Metals

The micropollutant analysis included an assessment of particulate and dissolved metals for some feeding events. Metal loads in CSO effluent exhibit wide variability, covering a large range of concentrations (Gasperi et al., 2014). Al and Fe are commonly present in high concentrations in WW and CSO flows (Carletti et al., 2008; J.-M. Choubert et al., 2011; Masi et al., 2023; Palli et al., 2021). The influent concentrations of the filters for Al and Fe were approx. 1500 and 2700 µg.L^{-1}, respectively, with most of it in particulate form (>0.45 µm) (Figure 4.4). Similarly, Zn, Ti, Mn, Pb, Cr and Co, had a high particulate fraction in the inlet. In contrast, Sr, Ba, B and Li were primarily found in dissolved form.

Metals bound to particles, such as Fe, Al and Zn were efficiently removed during the filtration process. The removal efficiency of Fe, Al, and Zn remained consistently high regardless of the filter design, with a mean removal rate of between > 98% and 85% and a low standard deviation (Figure 4.4). Similarly high removal efficiencies for Al, Fe, and Zn were reported in studies by Pálfy et al (2017a) and Masi et al. (2023) for CSO TWs with passive aeration in French and Italian design, respectively. As expected, forced aeration did not result

Thèse accessible à l'adresse : https://theses.insa-lyon.fr/publication/2025ISAL0011/these.pdf © [D. Gonçalves Portela], [2025], INSA Lyon, tous droits réservés

in improved metal removal, as it does not directly influence filtration efficiency. Total Zn removal in CSOB was higher, > 95%, and less variable than in Pálfy et al (2017a) or CSOA, which was due to the higher filtration capacity of CSOB. Blecken et al. (2009) reported similar removal performance in a SW biofilter, where the main retention occurred in the sandy loam top layer. In aerated systems, the straining of suspended solids may increase the collision of solid particles with the media favoring the removal of these metals, particularly in CSOB, which tended to better retain the solids.

The removal efficiencies of Pb and Cr were > 90% with coefficient of variation below 10% for both filters, which was expected to be effective given their high affinity for particle-bound (Baum et al., 2021). The mean removal efficiency of Cu was 66% in CSOA and 75% in CSOB, when considering the measured range is similar to the 84% found by Masi et al. (2023). For Ni, the removal efficiencies of 55% in CSOA and 67% in CSOB are coherent to the 31% in Masi et al. (2023). However, the coefficients of variation for Ni removal efficiency were high for both CSOA and CSOB (approx. 50%).

In both filters, particulate metals at the outlet were closer to or below the LOQ, due to the low concentration of TSS at the outlet. The coefficients of variation for the removal efficiency of particulate metals showed slight differences, with CSOA showing a coefficient of variation around 14%, whereas CSOB showed almost no variation. This stability in CSOB can be attributed to the sand layer, which tend to perform better removing TSS.

Dissolved metals were predominant in the filters' effluents Baum et al. (2021) observed that for SW treatment facilities, the removal efficiency decreased for smaller particle sizes. The mean concentration of dissolved Sr were high at the inlet and outlet of both filters, > 118 $\mu g.L^{-1}$ in CSOA and > 155 $\mu g.L^{-1}$ and CSOB (Figure 4.4), showing that the efficiency of the dissolved fraction removal was low. In addition, the high concentrations of also demonstrate the characteristics of the catchment area. High concentrations of Fe, Mg, Al, Sr and Ti were identified in road deposits (Lough et al., 2005; Sanders et al., 2003; Thorpe and Harrison, 2008). Ba, B and Li, which are mainly soluble, were barely removed, leaving the filter at concentrations between 18 and 32 $\mu g.L^{-1}$. Figure 4.4 shows that the concentrations of the dissolved fractions of these three metals remained within the same range at both inlet and outlet.

Thèse accessible à l'adresse : https://theses.insa-lyon.fr/publication/2025ISAL0011/these.pdf © [D. Gonçalves Portela], [2025], INSA Lyon, tous droits réservés

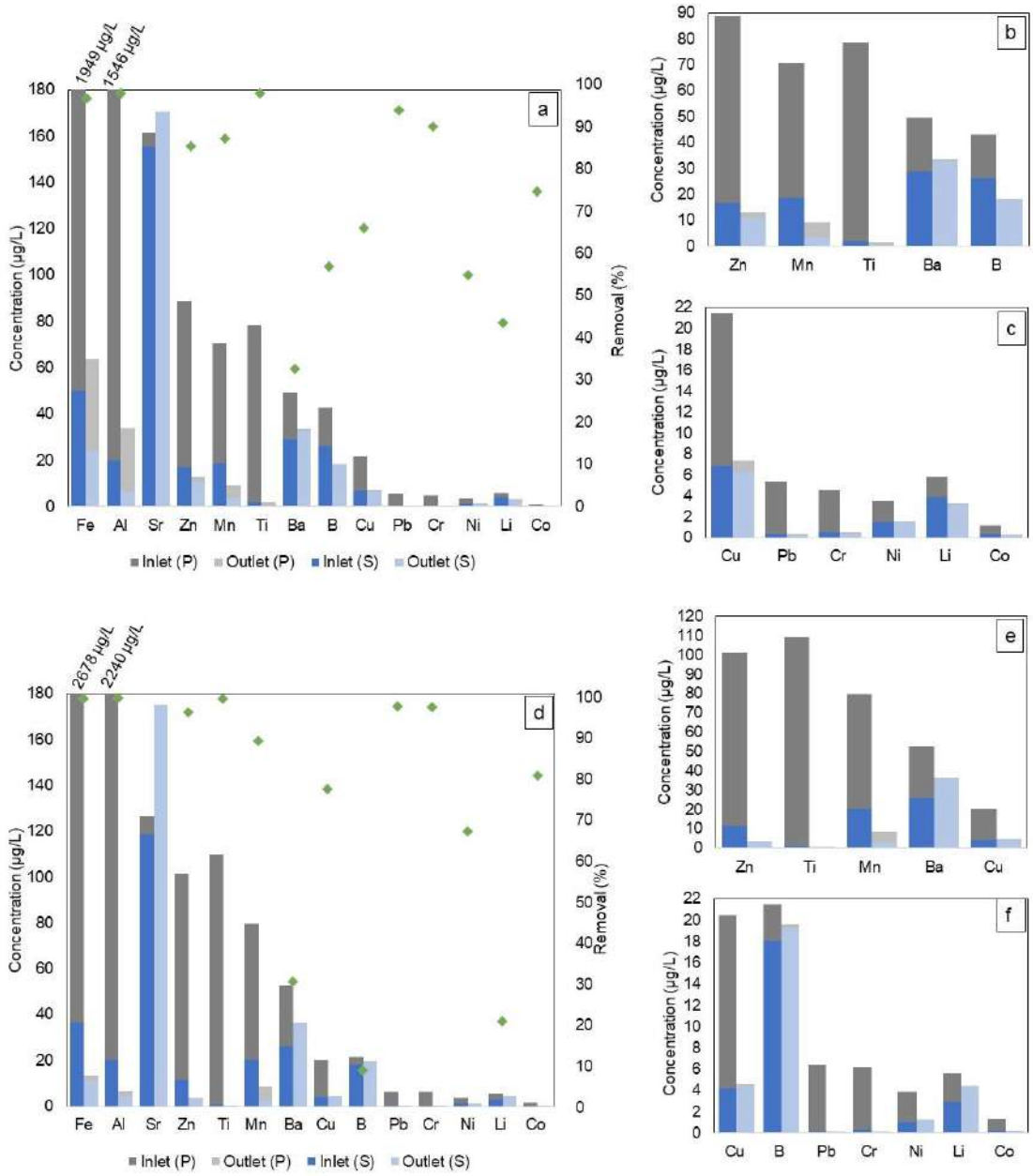

Figure 4.4 - The top graph (a) shows the inlet and outlet concentration of particulate (P) and dissolved (S) metals, as well as removal efficiencies for CSOA. The graphs on the right (b and c) highlight metals at CSOA in lower concentrations. CSOB is represented in graph (d), which provides an overview of inlet, outlet and removal efficiency. Graphs (e) and (f) detail the concentration of metals entering in CSOB in lower concentrations.

Regarding the dissolved metals, some of them such as Sr, Ba, B, Cu, Ni, Li, and Co showed the high variability in removal efficiency for both filters. The dissolved fraction of these metals were barely retained during the drainage event, with Sr even showing negative removal. As in this study, Pálfy et al (2017a) observed release of Sr in some events. In contrast, dissolved Fe, Mn, and Zn were more effectively removed, although the performance of the filters differed for

Thèse accessible à l'adresse : https://theses.insa-lyon.fr/publication/2025ISAL0011/these.pdf © [D. Gonçalves Portela], [2025], INSA Lyon, tous droits réservés

these metals. CSOB removed at least 20% more of the dissolved fraction of Fe and Zn than CSOA. In addition, the removal of dissolved Fe, Al and Mn in CSOB was more consistent, showing a coefficient of variation below 15%.

The forced aeration altered the hydrodynamics of the filter, the cohesion of the porous media, and maintained aerobic conditions, which did not considerably improved the removal efficiency of metals. However, the filter demonstrated an effective suspended solids removal by filtration, removing over 95% of total Ni and 55% of total Pb. The dissolved concentrations of Ni and Pb at the outlet were around 1.5 and 0.3 $\mu g.L^{-1}$, respectively, remaining the same as the inlet. With dilution in the surface water this values are likely the meet limits set in the guidelines. In the (2013)/39/EU EQS guideline, Ni and Pb are priority substances, with recommended limits of 2 $\mu g.L^{-1}$ and 1.2 $\mu g.L^{-1}$, respectively, in inland surface water. Other toxic metals, such as Cd and Br, which are also priority substances, were detected below the LOQ at both the inlet and outlet. The complete list with inlet and outlet mean concentrations of analyzed metals is in ANNEX 1.

4.3.2 Fecal Indicators

By the end of the trials there were analyses of FI based on ten samples in CSOA and five samples in CSOB. In both filters, *E. coli* median inlet concentration was 10^5 MNP/100 ml, or 5.5 $\log_{10}$ (Figure 4.5), consistent with CSO inlet concentrations reported in studies by Passerat et al. (2011) and Scheurer et al. (2015). The median outlet concentration remained similarly stable at 10^5 MNP/100 ml (Figure 4.5), for CSOA and CSOB. The median reduction observed were less than 1 $\log_{10}$. The difference between inlet and outlet concentrations of *E. coli*, as well for total coliforms, indicates a slight or no reduction in microbial levels. This reduction below 1 $\log_{10}$ is difficult to evaluate since high uncertainties related to analysis and sampling error.

E. coli retention in the studied aerated CSO TWs was less effective than other studies. In the filters studied by Ruppelt et al. (2018), median *E. coli* reduction varied from 0.9 to 3.2 $\log_{10}$. The author explained that increasing the thickness of filtration layers only resulted in slight improvements in *E. coli* retention, since most of the retention occurs in the upper part of the filtrating layer. The better results resulted from the filters in series, as the upper filter layer doubled. Tondera et al. (2019) and Scheurer et al. (2015) observed reductions around 2 $\log_{10}$ in *E. coli* in mature filters.

Thèse accessible à l'adresse : https://theses.insa-lyon.fr/publication/2025ISAL0011/these.pdf © [D. Gonçalves Portela], [2025], INSA Lyon, tous droits réservés

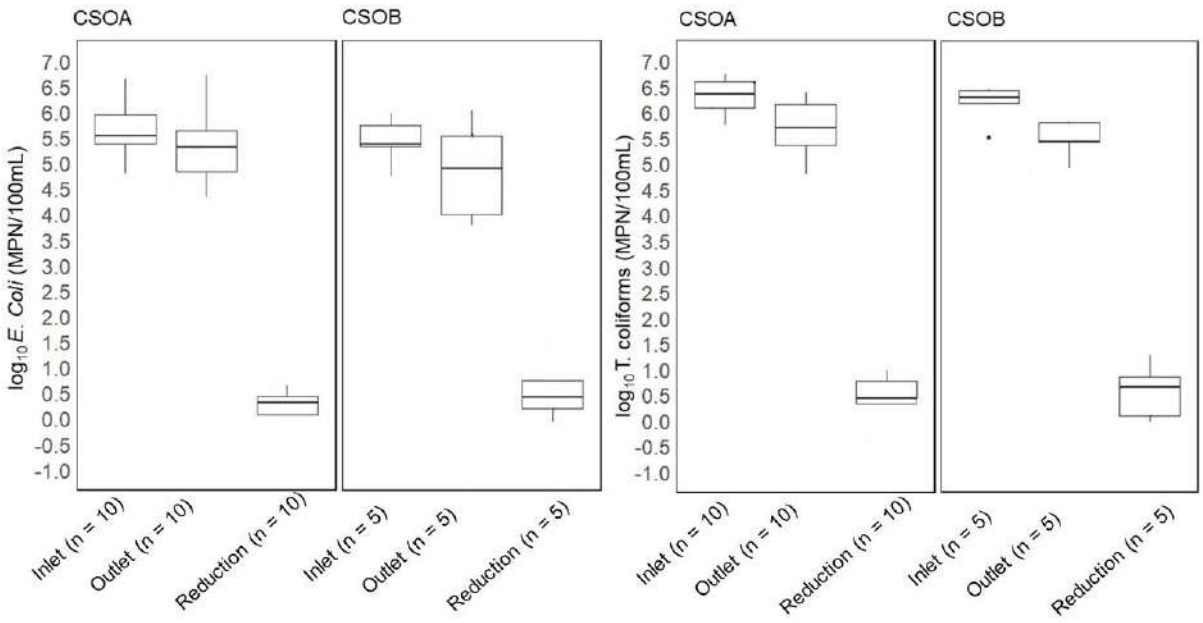

Figure 4.5 - Inlet, outlet and reduction of *E. coli* and total coliforms in CSOA and CSOB.

Several studies have linked FI to suspended solids in SW (Characklis et al., 2005), and CSOs (Passerat et al., 2011). In this study, we found that *E. coli* inlet and outlet concentration were correlate. This indicates that the increased reduction from one sample to another can be explained by the dilution effect, whereby less solids with attached microbes are carried into the filter. Despite both filters receiving similar solids loads, CSOB showed tendency to retain more *E. coli*. The specific surface area of the sand and the thicker deposit layer of CSOB may have contributed to more effective filtration and adsorption. This has the potential to positively affect *E. coli* retention, which can be further validated through additional analysis.

Stott et al. (2023) studied a surface TW treating agricultural drainage and observed persistent bacteria accumulating within the filter. The author also points out that not all *E. coli* are pathogenic, so increased counts do not necessarily indicate heightened health risks. The absence of *E. coli* reduction in this study could be related to the favorable conditions for *E. coli* microbes to resist in the saturated layer. Consequently, the microbes retained could be released during the drainage. However, further analysis is required to determine the accumulation of persistent bacteria. Furthermore, an investigation into retention time can help to explain factors affecting *E. coli*, and total coliform, reduction, as longer retention times typically improve filter performance for pollutants and microbes (Li et al., 2012). However, the relatively short HRTs in both filters likely contributed to lower disinfection performance. The saturated layer can help preserve biofilm moisture and improve filtration, preventing loss of biomass and increased porosity (Li et al., 2012), its effectiveness likely depends on adequate retention time.

Thèse accessible à l'adresse : https://theses.insa-lyon.fr/publication/2025ISAL0011/these.pdf © [D. Gonçalves Portela], [2025], INSA Lyon, tous droits réservés

Additionally, dry periods impact in the effectiveness of event-driven systems in reducing FIs have been studied (Ruppelt et al., 2018; Stott et al., 2018). The results demonstrated that there were no notable differences in *E. coli* reduction for the tested dry periods of approx. 3, 4, 7, 14 and 25 d. The study by Ruppelt et al (2018) also demonstrated that the prior dry period did not affect the overall reduction.

4.4 Conclusions

This study analyzed micropollutants at inlet and outlet of two aerated CSO TWs. The filters were designed differently, with a gravel top layer in CSOA and a sand top layer in CSOB. The influent was prepared by mixing runoff SW with domestic WW, which represents the micropollutants that could occur in real CSO events. In order to assess filters' capacity for disinfection and metals removal, parameters such as *E. coli*, total coliforms and particulate and dissolved metals were analyzed.

Removal of micropollutants (measured in the dissolved fraction) varied depending on inlet concentrations and compound characteristics. Benzothiazoles (ABT, OHBT and BT) were frequently detected and showed medium to good removal efficiencies. Occasionally, these compounds were released at rates higher than what was loaded onto the filter. 6PPD-quinone was highly removed in both filters, consistently reaching removal efficiencies > 70% with stable low outlet concentrations. 6PPD-quinone and OHBT were measured in the CSOA during periods of high and low aeration and maintained low outlet concentrations regardless of aeration conditions.

The filters showed positive removal efficiencies for the insect repellent DEET and the pharmaceuticals gabapentin and iomeprol. However, results of removal efficiency contain uncertainties due to concentrations close to the LOQ. The performance of CSOB in removing iomeprol and gabapentin may have been compromised during a period when the filter was clogged. In both filters, the removal efficiency of irbesartan was either close to zero or negative, suggesting that desorption may have occurred during some events. Similarly, carbamazepine was either not removed at all or even showed negative removal efficiency. Diclofenac showed variable removal rates in CSOB with a median removal efficiency of 45%, while its removal in CSOA was more consistent at 58%.

Overall, rubber products and pharmaceuticals had median removal rates at approx. 50%. Despite this moderate removal rate, both filters contributed to reducing the discharge of a variety of micropollutants to the aquatic environment. The performance of both aerated CSO

Thèse accessible à l'adresse : https://theses.insa-lyon.fr/publication/2025ISAL0011/these.pdf © [D. Gonçalves Portela], [2025], INSA Lyon, tous droits réservés

TWs pilots showed that forced aeration did not considerably enhance chemical pollutant or fecal indicator removal under the tested conditions. The trends for removal were similar between the filters, but direct comparisons were difficult due to measurement and sampling uncertainties.

Metals were analyzed in both particulate and dissolved phases. The particulate metals were effectively removed, as they are attached to the suspended solids. Despite the limited number of samples, differences in the filter design removing particulate metals were related to the performance of the filters removing TSS. The removal of dissolved metals was similar for both filters, with the sand layer having a minimal effect on reducing outlet concentrations' dispersion in CSOB. For the analyzed metals, the results of both filters indicate that the effects of aeration and filter design had minimal impact on the removal efficiency.

The reduction for FI was negligible, likely due to short hydraulic retention time. In the aerated CSO TWs, both aeration and throttling helped maintaining a homogeneous minimum retention time. However, the HRT ranging from 7 to 10 h was short to retain certain compounds and FI. Therefore, no effect of mechanical aeration on FI reduction could be shown.

To improve water quality in terms of micropollutants and/or bacteria, it is therefore necessary to further optimize operation (e.g. longer hydraulic retention times) or installation of post-treatment steps (e.g. sorptive media amendments, or UV disinfection should be explored. Future studies should assess these modifications under real CSO conditions to improve treatment efficiency.

Thèse accessible à l'adresse : https://theses.insa-lyon.fr/publication/2025ISAL0011/these.pdf © [D. Gonçalves Portela], [2025], INSA Lyon, tous droits réservés

5 General discussion and perspectives

5.1 General discussion

Local legislation may require the guarantee of discharge levels that are sometimes restrictive and complicated to meet with regard to the treatment of combined sewer overflows. While vertical treatment wetlands for CSO, when operated with passive aeration, provide effective particulate pollution retention, they have some limitations in treating the dissolved fraction. These limitations are linked to potential hydraulic short-circuits at the outlet of an event due to low medium saturation. As the filter becomes progressively saturated, the issues of hydraulics are mitigated, but oxygen transfer is restricted, and, for nitrification, the filtration material used and the alternation of feeding and resting periods are the main means. Indeed, nitrification occurs in three steps: the adsorption of ammoniacal nitrogen on the filtering material during the rain event, nitrification during the rest period, and the release of nitrates during the following rain event. In addition to the need for dynamic sizing to account for alternating feed (and corresponding load) and rest periods, this can result in nitrate flushes that may lead to high total nitrogen concentrations at the outlet.

In this context, Treatment Wetlands with forced aeration appear to be an interesting alternative for increasing performance reliability, avoiding the use of reactive materials, and possibly encouraging the reuse of treated water. However, there is currently limited feedback on how these systems perform for CSO treatment, and further investigation was required to better understand how to design and operate them. Key areas for investigation include the optimal settings for aeration during feeding events and rest periods, how to avoid hydraulic shortcuts, the evaluation of performance for different pollutants, as well as the definition of limited loads to guarantee specific outflow levels and the avoidance of clogging issues.

5.1.1 Standard parameters

The performance of two aerated CSO TW pilots for pollutant removal was evaluated under varying inlet concentrations, hydraulic loads, and aeration strategies. Both filters demonstrated consistent pollutant removal across different hydraulic loads. They showed resilience to variations in inlet concentrations, maintaining effective filtration and biological degradation of carbon under moderate or highly aerated conditions. However, biological processes were directly influenced by the aeration strategies employed.

Thèse accessible à l'adresse : https://theses.insa-lyon.fr/publication/2025ISAL0011/these.pdf © [D. Gonçalves Portela], [2025], INSA Lyon, tous droits réservés

The standard pollutants monitored included TSS, total and dissolved COD, anions and cations as well as additional parameters on a lower frequency (BOD, P, TKN, metals, emerging contaminants and pathogens). ANNEX 3 shows inlet and outlet concentrations in the filters for each aeration strategy tested. Trials with varying airflow (Qair_var) were initiated but discontinued due to difficulties in controlling airflow with precision. The volume of air transferred during Qair_var trials was not calculated due to unstable airflow; however, average values were obtained for each trial. Airflow in CSOA ranged from 0.5 and 9.3 m^3/h and from 1.0 and 18.6 m^3/h in CSOB. Aeration strategy has been tested as well at constant air flow but different aeration time. Table 5.1 shows performances of global parameters for the different aeration strategies, with CSOA operating under low to moderate aeration (F10, F10/40, and 10/40) and highly aerated conditions (75/15 and continuous (C)). While CSOB operated only operated under highly aeration conditions.

Table 5.1 - Removal efficiency in CSOA and CSOB for all aeration strategies tested in each pilot.

	Removal (±SD) % CSOA					Removal (±SD) % CSOB				
AS	n	TSS	COD	CODs	NH_4-N	n	TSS	COD	CODs	NH_4-N
F10	7	86 (±6)	54 (±16)	27 (±30)	19 (±33)					
F10/40	3	92 (±1)	75 (±6)	26 (±31)	52 (±32)					
10/40	4	94 (±1)	85 (±3)	34 (±16)	63 (±9)					
75/15	15	95 (±2)	85 (±4)	78 (±7)	73 (±14)	16	96 (±2)	89 (±3)	81 (±4)	82 (±16)
C	30	89 (±8)	82 (±10)	67 (±30)	79 (±12)	7	92 (±13)	90 (±4)	70 (±34)	93 (±5)
Qair_var	5	97 (±1)	87 (±7)	75 (±15)	40 (±32)	12	97 (±2)	90 (±3)	79 (±12)	81 (±14)

In CSOA, TSS removal was consistently effective, regardless of aeration strategy. However, COD removal was negatively impacted under the 10 min aeration strategy, achieving up to 50% removal. Approximately 80% of COD was removed using an aeration strategy that provided at least 30% of OT to cover the oxygen requirements[2] for removing COD. It should be noted that the dissolved fraction of COD is better degraded with longer aeration times. Aeration times 75/15 and C give performances of around 70%, and produce outlet concentrations close to non-biodegradable COD. Similarly, to dissolved COD, nitrification shows variation in performance due to aeration strategy, which varied from 19 to 79%. The period for trials under continuous aeration strategy in CSOA were longer than to the other

[2] Oxygen required (OR) = COD_{inlet} + 4.57*TKN_{inlet}

Thèse accessible à l'adresse : https://theses.insa-lyon.fr/publication/2025ISAL0011/these.pdf © [D. Gonçalves Portela], [2025], INSA Lyon, tous droits réservés

conditions, with larger range of inlet concentration, which explain higher measurements deviations. As showed in Chapter 2, under the aeration strategy 75/15, both filters were stable removing near to 70% of loaded ammonium. This performance was maintained under the continuous aeration strategy in CSOA.

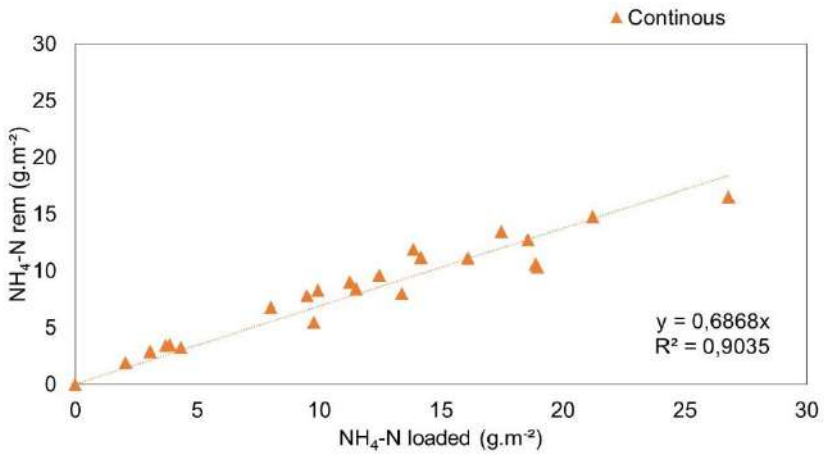

Figure 5.1 - Loaded ammonium correlation with removed ammonium under continuous aeration strategy.

In contrast to passive systems (Pálfy et al., 2017c; Uhl and Dittmer, 2005), the results demonstrate that under stable HRT and continuous aeration, direct nitrification remains stable regardless of the hydraulic load applied in the tested conditions. Consequently, the concentration of ammonium at the outlet will be largely dependent on inlet concentrations. One potential way to enhance the nitrification rate could be to reduce the outflow regulation rate, thereby increasing the HRT. However, this approach may necessitate an increase in the ponding/storage volume and the drainage time to accommodate high hydraulic loads.

Regarding the filtering material and the incorporation of a sand layer at the top, both filters demonstrated consistent performance in the removal of particulate and dissolved pollutants under highly aerated conditions. CSOB (with a sand layer), which was only tested under highly aerated strategies, consistently achieved removal efficiencies exceeding 70% for all parameters. However, under continuous aeration, the filter became clogged in winter, resulting in up to 15% of the inlet volume being bypassed untreated at HL of 1.5 m. The clogging issue will be discussed later. For the calculation of removal efficiency, only the treated volume sampled at the filter outlet was considered. It would have been beneficial to sample the bypass in order to assess the filter performance on sedimentation of solids when clogged.

Thèse accessible à l'adresse : https://theses.insa-lyon.fr/publication/2025ISAL0011/these.pdf © [D. Gonçalves Portela], [2025], INSA Lyon, tous droits réservés

5.1.2 Filter aging and clogging issues

In addition to performance comparisons, it is crucial to assess the aging and potential clogging issues associated with different material types used in the filter layers. This is an essential aspect in ensuring the long-term sustainability of the system. Despite the limited operational time of the experiment (1.5 years), the data already provides valuable insights into the varying behaviors in terms of solids retention and clogging issues.

Both filter showed high performances on removing TSS, but the sand layer appeared to affect the pathway of solids. CSOB, which uses sand, showed a higher increase of the organic deposit on the top. Further studies would be beneficial to confirm this, but it is likely that a thinner layer on the top would favor filtration at the surface, while a coarser material implies filtration in depth. The filtration at the surface had a significant impact on CSOB, resulting in clogging during the first winter when the reeds were dead and underdeveloped. Their mechanical role was unable to effectively compensate for the reduction in hydraulic conductivity of the deposit layer, and mineralization of the deposit was poor due to low temperatures. The clogging of CSOB was observed to occur only after a cumulative TSS load of about 3.2 kgTSS/m², which resulted in a decrease in outflow rate (Figure 5.2). The accumulated 3.2 kgTSS/m² is approximate, as some exceptional trials were not sampled. Therefore, the actual accumulated TSS may have been higher. In this condition, the surface organic deposit was identified as the factor controlling the hydraulic process, rather than the outlet throttle. However, at the beginning of the event, when the organic deposit is dry and shrinkage cracks allow for a higher infiltration rate, the outlet throttle does control the hydraulic process. Once the deposit becomes moist and more solids are trapped at the surface, the organic deposit becomes the limiting factor in the hydraulic process.

Thèse accessible à l'adresse : https://theses.insa-lyon.fr/publication/2025ISAL0011/these.pdf © [D. Gonçalves Portela], [2025], INSA Lyon, tous droits réservés

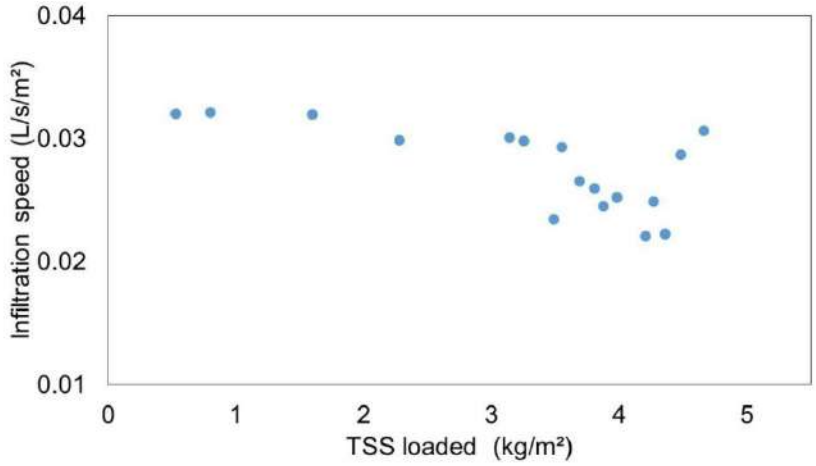

Figure 5.2 - Filtration speed and accumulated load in CSOB over with HL of 1.5 m^3/m^2 in each trial

As a result, surface clogging leads to a faster and higher ponding of the influent at the top, bypassing a portion of it. This has a significant impact on the recovered volume at the outlet, as illustrated in Figure 5.3. Following the development of reeds in spring, the mechanical role of the system returned to normal, with the infiltration rate returning to its usual level. The clogging caused by the sand layer was simply a seasonal process. Further studies would be required to ascertain whether, with higher plant development, clogging issues would be more limited or whether, with the increasing accumulation of the deposit layer, they would worsen over time.

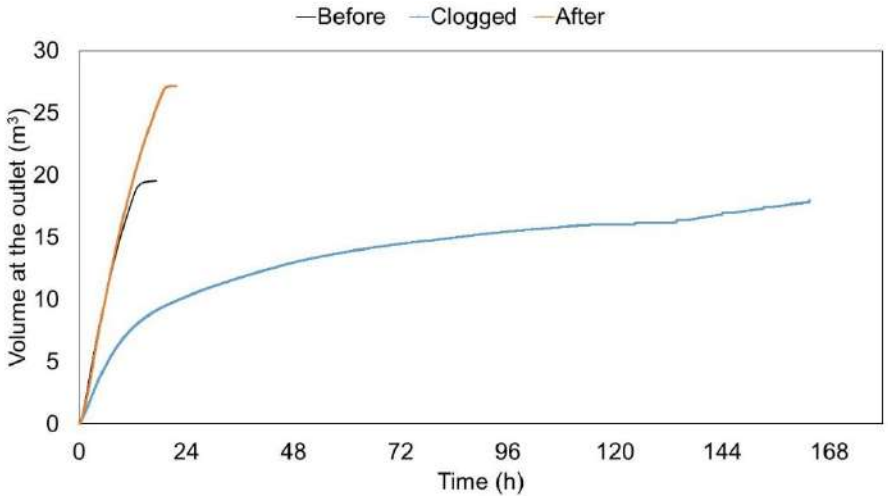

Figure 5.3 – Accumulated volume at the outlet of the CSOB. The black line represents the trial of 1.0 m^3/m^2 of HL that occurred eight months before the clogged trial of 1.0 m^3/m^2 of HL. The orange line trial of 1.5 m^3/m^2 of HL was two months after the clogged trial.

Thèse accessible à l'adresse : https://theses.insa-lyon.fr/publication/2025ISAL0011/these.pdf © [D. Gonçalves Portela], [2025], INSA Lyon, tous droits réservés

Another consequence of clogging, due to high ponding water, is related to the air pathway. The air supplied by the blowers to the filter was unable to compensate for the water level pressure, resulting in air accumulation inside the filter that escaped through piezometers. Consequently, a portion of the filter was not saturated due to air accumulation, and air distribution was not homogeneous.

In the absence of a sand layer (CSOA), no clogging was observed, even with a longer experimental time and a higher TSS cumulated load (Figure 5.4

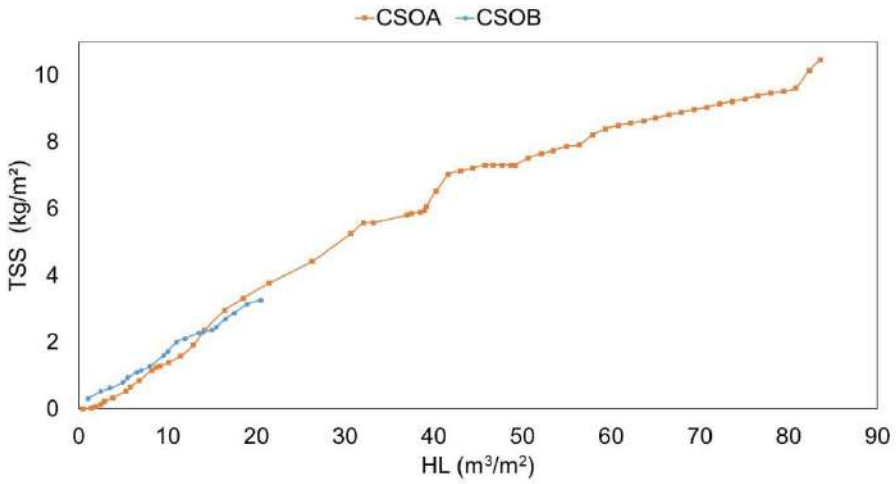

Figure 5.4 - Accumulated TSS and HL in CSOA and CSOB filters. The curve off accumulated HL curve for CSOB is discontinued at 22 m^3/m^2, as the filter clogged.

Therefore, despite comparable hydraulic loading rates (annual HL was 66 $m^3/m^2/y$ in CSOA and 55 $m^3/m^2/y$ in CSOB), the incorporation of a sand layer has a notable impact on the system's functionality. The absence of a sand layer does not prevent long-term clogging, but increases the system sensitivity during the winter months when the reed mechanical role is not present. Therefore, it can be concluded that the retention of solids is more distributed within the system when using coarser material. This may result in in-depth clogging over time if the solids cannot be mineralized and/or the TSS load is too high. It would be beneficial to consider a mineral solid annual load limit when designing the system to ensure its functionality over decades.

5.1.3 Nitrogen transformations

Maintaining low TN outlet concentrations is challenging due to the unpredictable frequency, intensity and concentrations of nitrogen at the inlet of the system. Denitrification is not a viable option in this system due to the limited carbon availability, particularly when

Thèse accessible à l'adresse : https://theses.insa-lyon.fr/publication/2025ISAL0011/these.pdf © [D. Gonçalves Portela], [2025], INSA Lyon, tous droits réservés

nitrification has already occurred. When nitrification is the primary objective, the TN outlet concentration is dependent on the storage and release dynamics of the various nitrogen forms during feeding events and ammonium transformations during dry periods. To achieve low ammonium concentrations at the outlet, it is essential to prioritize direct nitrification during feeding events. Maintaining efficient direct nitrification ensures that TN outlet levels will be close to the inlet concentrations. Consequently, if the inlet concentration levels are high, the outlet levels will also increase, and the nitrogen dynamic during dry periods will be more variable. The first limitation in guarantying specific outlet levels is related to the dilution ratio during rain events.

We have been able to conduct a mass balance and estimate the proportion of different processes affecting the outlet nitrogen form concentrations through online monitoring of events and sampling inlet and outlet waters. The observed processes included direct nitrification, storage, nitrification during rest periods, and release.

The initial factor influencing nitrification efficiency is the selected aeration strategy. Tracer experiments demonstrated that aeration is a crucial factor in preventing short-circuiting, which can impact outlet concentration, by mixing the interstitial water inside the filter. This approach proved effective in minimizing the uneven distribution on the top surface at the beginning of an event. Once ponding occurs, stopping the aeration does not result in short-circuiting, but the hydraulic conditions approach a plug flow state. The additional effect of the aeration strategy is related to the amount of oxygen transferred to the water for aerobic biological reactions. It is logical that a lack of oxygen will first impact nitrification. The 75 min. on/15 min. off aeration strategy, or a continuous aeration strategy, both occurring until 80% of the loaded volume is recovered at the outflow, will maintain high oxidative conditions and ensure nitrification.

It should be noted that the limiting factor for nitrification is not solely dependent on oxygen concentrations within the system. It is evident that the nitrification kinetics and the quantity of nitrifies influence the system's capacity to oxidize ammonia during the hydraulic retention time tested in our experiments. In terms of kinetics, we measured oxygen uptake at the end of a feeding event when aeration was stopped and estimated oxygen uptake for bacterial respiration. This allowed us to estimate the maximal TKN concentration that can be nitrified. Our findings suggest that all inlet concentrations above 10 mg TKN/L cannot be totally nitrified in the filters. We observed a tendency for outlet concentrations to correlate with inlet concentrations, which allowed us to estimate the outlet ammonia concentration that can be reached (Figure 5.5). The results show that for inlet TKN concentrations above 10 mg/L, there is a notable decline in

Thèse accessible à l'adresse : https://theses.insa-lyon.fr/publication/2025ISAL0011/these.pdf © [D. Gonçalves Portela], [2025], INSA Lyon, tous droits réservés

nitrification efficiency. To illustrate, if the objective is to maintain an outlet NH_4-N concentration below 5 mg/L, the filters will face challenges in maintaining this level for inlet concentrations above 18 mg TKN/L.

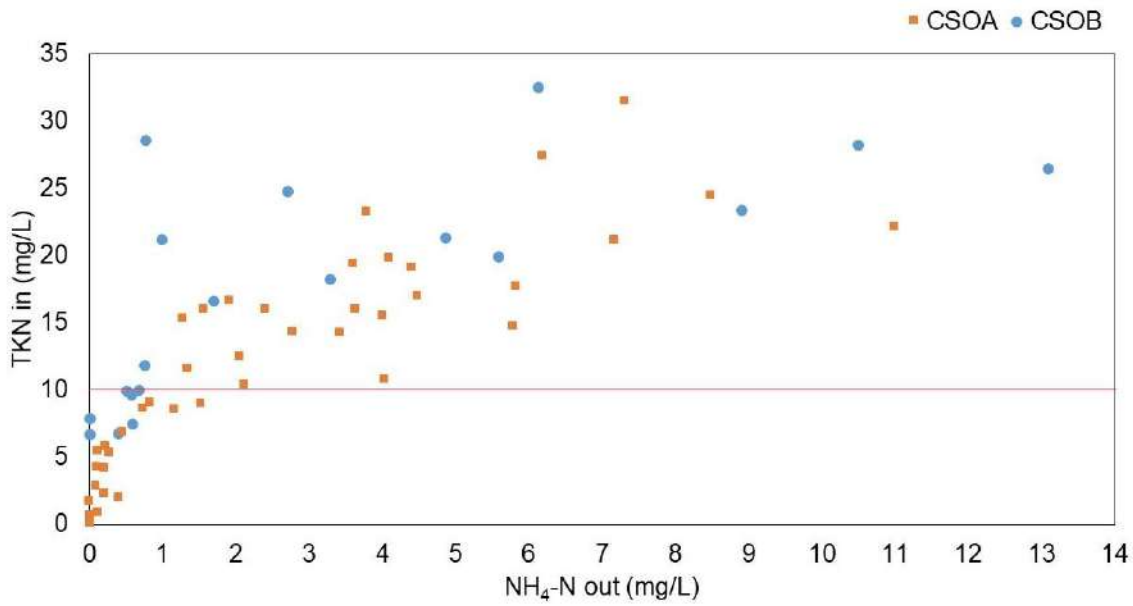

Figure 5.5 - TKN inlet concentration and NH_4-N outlet concentrations in CSOA and CSOB for highly aerated conditions.

The dispersion in the correlation between inlet and outlet concentration is due to other factors that affect the nitrification efficiency. In the absence of an observed temperature effect, the length of the dry period, for example, can impact the bacterial community and thus its ability to nitrify in the subsequent feeding event. The nitrifying bacteria die is not solely dependent on the duration of the dry period. It is also influenced by the residual ammonium concentration in the interstitial water at the end of a feeding event. Indeed, during the event the biomass maintenance/growth will depend on the loaded ammonium and the residual ammonium will enable biomass to withstand rest periods. During feeding events with a residual ammonium concentration, the NO_3-N sensor indicated an increase in NO_3-N concentration of approximately 2 mg/L every time that air blowers were switched.

Ammonium dynamics during dry periods are more stable with no or low concentrations of ammonium (<2 mg/L) in the interstitial water. This is because, in the absence of specific adsorbing material, nitrification occurs to a lesser extent. However, accumulation of NO_3-N during dry period can be considerable in events that up to 10 mg/L of ammonium remained in the saturated layer. The small aeration periods during the resting phase, partially or totally

Thèse accessible à l'adresse : https://theses.insa-lyon.fr/publication/2025ISAL0011/these.pdf © [D. Gonçalves Portela], [2025], INSA Lyon, tous droits réservés

nitrified. Consequently, longer rest period comprise a greater number of aeration phases, resulting in the release of nitrates at the beginning of the next feeding event. The amount of ammonia that will be retained in the interstitial water depends as well on the choice on the aeration stop during the feeding period. In this study, aeration were stopped at 80 % of the inlet volume recovered at the outlet. This correspond to 8, 16 or 24 m^3 recovered for events of 0.5, 1 and 1.5 m^3/m^2 respectively. Consequently, the higher the HL, the higher the volume infiltrating in the filter in the final unaerated period.

It was observed that in events starting with high interstitial ammonia concentrations, a reduction in oxygen levels can lead to an increase in ammonia after a period of 3-4 hours without aeration. To prevent excessive ammonia accumulation in the interstitial and adjust aeration according to event intensity, it is recommended that aeration be switched off when there is no ponding water and ammonium can be effectively removed within the filter. This approach involves stopping aeration based on a water level measurement rather than a recovered volume.

While this strategy aims to reduce ammonia concentration in interstitial water at the end of an event, it also increases the sensitivity of nitrifying bacteria to long rest periods. This presents a trade-off unless wastewater from the sewer is regularly introduced during rest periods to maintain ammonia levels.

In the event that direct nitrification is not optimized, nitrogen storage within the filter can result in elevated nitrate flushes at the outflow of the subsequent event. An example of nitrate flushing was observed during an event with a HL of 1.5 m, as showed in Figure 5.6. Before the event, 17.7 mg/L of NO_3-N remained in the saturated layer and was flushed along side the loaded nitrogen.

Thèse accessible à l'adresse : https://theses.insa-lyon.fr/publication/2025ISAL0011/these.pdf © [D. Gonçalves Portela], [2025], INSA Lyon, tous droits réservés

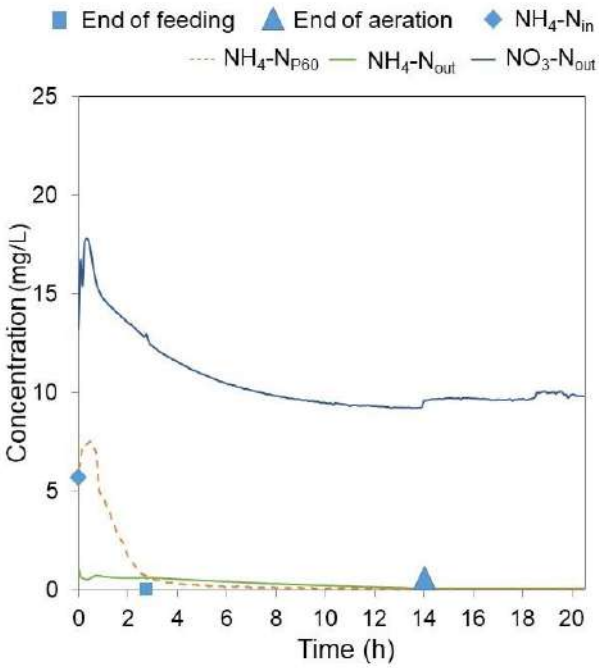

Figure 5.6 – NO_3-N and NH_4-N measurements at the outlet of CSOA and dynamics of NH_4-N transformation within the filter, measured with a sensor at 60 cm from the bottom.

During this event, 5.3 mg/L of NH_4-N was fed into the filter. At 60 cm from the bottom, NH_4-N concentration initially increased during the first hour, then decreased, reaching a minimum by the end of the feeding phase, Figure 5.6. After 6 h of drainage, NH_4-N concentration was 0.2 mg/L, while NH_4-N at the outlet remained below 0.1 mg/L. NO_3-N discharge rate were highest at the beginning of the event and progressively decreased stabilizing by the end of drainage phase. At the end of the event, NO_3-N outlet concentration were high as NO_3-N inlet concentration was 7.3 mg/L. This was atypical for CSO effluent but occurred due to pilot effluent recirculation mixed with WW when SW was unavailable.

The characteristics of nitrate peaks in aerated CSO TW are similar to those in classical systems, with a rapid discharge of high nitrate mass over a short period. If NH_4-N remains in the saturated layer at the end of drainage phase extending mechanical aeration can support continued nitrification. Nevertheless, nitrates flush peaks are lower thanks to direct nitrification than in passive system. This reinforces the importance of promoting direct nitrification and the need for effective aeration control during feeding and drainage phases.

Thèse accessible à l'adresse : https://theses.insa-lyon.fr/publication/2025ISAL0011/these.pdf © [D. Gonçalves Portela], [2025], INSA Lyon, tous droits réservés

5.1.4 Micropollutants

Organic and inorganic compounds micropollutants were monitored at both the inlet and outlet of the filters. The dissolved fraction of organic micropollutants included 93 compounds from various chemical classes. PAHs were analyzed in two inlet samples, where naphthalene, phenanthrene and fluoranthen were detected at the inlet concentrations below 30 ng/L. Due to the low concentration, these compounds were not analyzed in other samples. Compounds originating from rubber products ABT, OHBT, BT and 6PPD-quinone, were frequently detected above the LOQ at the inlet. These compounds showed moderate to high removal efficiency, and the different aeration strategies used in CSOA did not appear to influence their removal performance.

Pharmaceutical compounds, such as gabapentin, iomeprol, irbesartan, carbamazepine, and diclofenac, removal rates varied inconsistently and occasionally included negative removal. However, low inlet concentrations of these compounds in both filters led to uncertainty in the removal efficiency calculations. The occurrence of irbesatan and carbamazepine in the inflow was less frequent, and the filters were unable to remove them. In regard to the removal of different metals, the particulate form of metals was effectively removed, while the efficiency of dissolved metals was found to be poor. Both filters demonstrated good filtration efficiency, and as they operated over a period of one year, the system may have a reduced adsorption potential onto organic matter.

In the last trials, the filters' potential for disinfection was evaluated by measuring the fecal indicators (FI) *E. coli* and total coliforms. The reduction in FI was negligible, with less than a 1 log unit reduction This indicates that the filtration systems provided only limited disinfection capabilities. Therefore, aerated CSO TW improved removal of dissolved pollutants and certain micropollutants but was not efficient for hygienic purposes. Accordingly, additional treatment (disinfection, micropollutant) will be required for the objective of reusing the treated water, in line with the planned use.

5.2 Perspectives

This study provides a comprehensive analysis of nitrogen transformations and pollutant removal in aerated CSO treatment wetlands. However, the study showed some limitations where the topic could use more analyses to reach a deeper understanding of the processes and viability for scaling up.

Thèse accessible à l'adresse : https://theses.insa-lyon.fr/publication/2025ISAL0011/these.pdf © [D. Gonçalves Portela], [2025], INSA Lyon, tous droits réservés

Estimative of costs with installations, operation and maintenance of air blower can be an important aspect on the choice for the implementation of this system. The study of different aeration strategies showed that intermittent aeration, with 75 min of air blower switched on, 15 min switched off, was as effective as continuous aeration for pollutant removal, which can be advantageous to reduce energy consumption. The air blower was selected based on its ability to operate with an air flow capacity that can oxygenate the ponded water up to water column depth of 2.3 m. Tests conducted at a maximum frequency of 50 Hz demonstrated that the blower can effectively oxygenate the ponded water, as evidenced by the rise of air bubbles to the surface. By decreasing the air blower frequency it might be possible to deliver oxygen up to the ponded water without negative effects on the performance of the filter. However, to verify this hypothesis, further tests with reduced air flow are required. The number of tests conducted with varying air flow was limited to those performed when air blower frequencies were manually adjusted. Therefore, future experiments should test different air flows, as the technical specifications of an air blower can impact costs of installation and operation.

The intermittent aeration mode may offers not only economic advantages but also operational benefits. When CSOB was clogged, the intermittent aeration process created a mechanical effect of opening new paths with the bubbles and facilitating the movement of water above the top layer through the deposit layer each time the air blowers were activated. Despite continuous aeration was used during the clogging period in attempt to increase the potential biodegration of the deposited layer, the results was not successful. It is also not possible to ascertain whether the clogging was limited to the surface or occurred internally as well. To understand the limitations of the sand used in CSOB samples of the deposit layer could have being collected to analyze the biodegradability of this material and the depth of clogging.

Repeating the tracer tests in both filters would also help to understand the process of clogging and other hydrodynamic effects. The tracer tests were performed in the filter under continuous aeration when no organic matter was accumulated in it. For the intermittent aeration, we considered that while aerating the filter, the conditions were close to a continuous stirred tank reactor, and without aeration the conditions could shift to plug flow. Regarding the clogging, we observed that the distribution of solids appeared to differ in each filter. This indicate that a change in the hydrodynamics of the filter may have occurred, as well. Therefore, it would be interesting to have tracer test results for intermittent aeration and after one year of operation.

Thèse accessible à l'adresse : https://theses.insa-lyon.fr/publication/2025ISAL0011/these.pdf © [D. Gonçalves Portela], [2025], INSA Lyon, tous droits réservés

As demonstrated in the analyses of nitrogen dynamics analyses, nitrification was constrained by the TKN inlet concentrations. Further investigation into the impact of longer HRTs on nitrification can be helpful in acquiring knowledge on factor affecting nitrogen process. The short HRT may also have limited the removal of micropollutants and the reduction of FI. By controlling the filtration speed with the throttle increases HRT, with the drawback of reducing the volumetric capacity of the filter. Therefore, for a given inflow volume, a higher space is required, and the system footprint may also be affected. An additional option would be to enhance water quality through post-treatment. One possible solution is to treat part of the aerated CSO TW in a horizontal flow treatment wetland containing reactive media, such as biochar. This post treatment would favor denitrification, removal of micropollutants and disinfection. Post-treatment with UV is also an effective method, particularly for disinfection.

During the transformation process, there were fluctuations in oxygen consumption, which impacted the dynamics of nitrogen. These results could be linked into microbial genes to quantify bacterial activity, as it is currently unclear whether in the absence of ammonium, nitrifying bacteria enter in a dormant state or if they die. The impact of bacterial growth during feeding events on the kinetics of nitrification is also an important area of interest within the context of the nitrification process.

Thèse accessible à l'adresse : https://theses.insa-lyon.fr/publication/2025ISAL0011/these.pdf © [D. Gonçalves Portela], [2025], INSA Lyon, tous droits réservés

GENERAL CONCLUSIONS

In this study, experimental trials were conducted over a period of more than one year on two pilot-scale aerated CSO TWs. These filters were assessed regarding the influence of different top layer materials and aeration strategies on their performances. Both filters, CSOA and CSOB, operated under variable inlet concentrations and HLs 0.5, 1.0 and 1.5 m^3/m^2. By the end of the study, the filters were operating only with HLs of 1.5 m^3/m^2.

Before start feeding the filters with CSO, tracer tests, conducted both with and without aeration, showed considerable effects of aeration on mixing and HRT. When aeration was active, both filters demonstrated a more uniform inflow distribution. The hydrodynamic of the filters under continuous aeration were close to a continuous stirred tank reactor, while switching off the air blowers led to plug-flow hydrodynamic. However, the accumulation of solids in CSOB and the cold season affected the filter's hydraulic performance, which temporary clogged after an accumulated hydraulic load of 22 m^3/m^2.

The CSOA filter was the only one tested for low aeration conditions. Under this condition, the inadequate removal of dissolved pollutants was evidenced by the median NH_4-N removal rates of 2%. The highly aerated conditions showed notable improvements in the degradation of NH_4-N, with a median removal rate exceeding 75% in CSOA and 83% in CSOB. Overall, the results demonstrated that under highly aerated conditions, oxygen transfer was improved, which in turn enhanced the removal of pollutants, such as TSS, DCO, and dissolved COD, NH_4-N. By maintaining highly aerated conditions, the removal of all standard pollutants reached the highest rates, with consistent removal of particulate and dissolved pollutants. The performance of the filters was compared under the aeration strategy 75/15 (a highly aerated condition). The removal performance of both filter was similar, with CSOB showing a tendency to retain more TSS and COD, potentially attributable to the sand layer.

In comparison to passive aeration systems, aerated systems enhance the availability of dissolved oxygen in water, which improve the oxygen balance and increases nitrification rates. The results showed that forced aeration changed the nitrification process in the CSO TW, which became less reliant on the dry period. This led to the analysis of nitrogen dynamics during feeding events and dry periods. Online monitoring of ORP and DO was conducted to assess the stability and transitions in aerobic/anoxic conditions and oxygen consumption. The results demonstrated that stability was maintained when air blowers were switched on and fluctuations in these parameters occurred when aeration was switched off, particularly under high nitrogen loads.

Thèse accessible à l'adresse : https://theses.insa-lyon.fr/publication/2025ISAL0011/these.pdf © [D. Gonçalves Portela], [2025], INSA Lyon, tous droits réservés

The results demonstrated a tendency between oxygen consumption and NH_4-N concentration within the filter, which supported the estimation of the maximum nitrification capacity of 10 $mg.L^{-1}$ of TKN. The ammonium loaded into the filter that was not directly nitrified was retained in the interstitial pores or adsorbed onto organic matter at the end of the drainage period. The storage NH_4-N will depend on the inflow concentrations and could result in increased rate of TN removal. Due to direct nitrification, events with TKN concentrations up to the maximum nitrification capacity could result in the removal of the loaded NH_4-N during the event. In the case of high TKN loads, where DO concentration decreased rapidly after ceasing mechanical aeration, lead to the storage of NH_4-N in the saturated layer. This positively affect TN removal by temporarily retaining nitrogen within the filter. The stored NH_4-N can be transformed to NO_3-N either during the dry period or feeding events where oxygen transfer is higher than the demand for the nitrification of loaded ammonium.

The temporary retention of NH_4-N will affect the nitrate flush, depending on the amount of NH_4-N storage. Flush of nitrate was not observed to occur during a dry period of less than 3 d. Therefore, in addition to the NH_4-Nstorage longer dry periods will characterize the NO_3-N peaks intensity. Although NO_3-N production can occur during dry periods, direct nitrification during the event is the main transformation pathway of ammonium. In feeding events, with high TKN loads and short dry periods, direct nitrification could not prevent high NH_4-N release at the outlet after switching off the air blower. Due to the high concentration of NH_4-N within the filter, the rates of oxygen consumption increased, resulting in a lack of oxygen availability 4 h after the air blowers were switched off. Once the ponding water was in contact with the biofilm, there was no longer any available oxygen, which resulted in the effects of plug flow hydraulics becoming apparent.

The positive effects of aeration on the removal of dissolved pollutants have prompted an investigation into the filter's performance in removing micropollutants. The performance of both filters was evaluated for the removal of micropollutants from different chemical classes, including metals. The filters demonstrated effective removal of benzothiazoles (ABT, OHBT, BT), the subproduct 6PPD-quinone, and particulate metals. The removal efficiency of these compounds was not affected despite tested conditions with low aeration. For pharmaceutical micropollutants, such as gabapentin, iomeprol, irbesartan, carbamazepine, and diclofenac, removal rates were inconsistent and included negative removal. Gabapentin, iomeprol, and diclofenac, were detected at low concentrations in both filters, which contributed to uncertainty when calculating the removal efficiency. Irbesartan and carbamazepine occurred less frequently

Thèse accessible à l'adresse : https://theses.insa-lyon.fr/publication/2025ISAL0011/these.pdf © [D. Gonçalves Portela], [2025], INSA Lyon, tous droits réservés

in the inflow, and the filters could not remove them. Regarding the metals, particulate metals were efficiently removed, while dissolved metals showed poor removal.

In the last trials, the potential for disinfection was evaluated by measuring the fecal indicators (FI) *E. coli* and total coliforms. The reduction in FI was negligible, with less than a 1 log unit reduction, suggesting that the filters provided limited disinfection capabilities. Therefore, while aeration improved pollutant removal for certain micropollutants and FI it did not enhance.

Thèse accessible à l'adresse : https://theses.insa-lyon.fr/publication/2025ISAL0011/these.pdf © [D. Gonçalves Portela], [2025], INSA Lyon, tous droits réservés

ANNEX 1

The measurement < LOQ were replaced by LOQ and measurements under the limit of detection were replaced by LOQ/10. Inlet and outlet concentration in CSOA and CSOB are in Table 0.1 and Table 0.2.

Table 0.1 - The concentration of metals at the inlet and outlet of the CSOA was measured. The mean, standard deviation (SD), and median were calculated for each metal.

		Inlet			Outlet		
		Mean	SD	Median	Mean	SD	Median
Ag	Dissolved (µg/L)	< LOQ	-	< LOQ	< LOQ	-	< LOQ
Ag	Particulate (µg/L)	< LOQ	-	< LOQ	< LOQ	-	< LOQ
Ag	Particulate (mg/kg)	< LOQ	-	< LOQ	< LOQ	-	< LOQ
Al	Dissolved (µg/L)	19.86	3.35	18.87	6.44	2.60	5.77
Al	Particulate (µg/L)	1526.80	584.53	1782.00	27.38	43.81	12.95
Al	Particulate (mg/kg)	14679.40	6475.39	12351.00	1723.50	2489.40	1092.00
As	Dissolved (µg/L)	2.08	0.99	1.65	3.33	1.34	3.21
As	Particulate (µg/L)	1.30	0.53	1.30	0.04*	0.06	0.02*
As	Particulate (mg/kg)	12.38	4.92	10.80	2.76*	3.23	2.13*
B	Dissolved (µg/L)	26.15	18.35	21.40	18.16	12.41	16.75
B	Particulate (µg/L)	5.41	7.17	0.85	0.56*	0.31	0.55*
B	Particulate (mg/kg)	80.92	76.25	50.00	29.70*	20.17	25.00*
Ba	Dissolved (µg/L)	28.87	6.00	27.30	32.67	10.78	29.20
Ba	Particulate (µg/L)	20.58	8.23	24.90	0.71	0.82	0.58*
Ba	Particulate (mg/kg)	192.80	67.77	191.00	49.84	49.44	61.30
Cd	Dissolved (µg/L)	< LOQ	-	< LOQ	< LOQ	-	< LOQ
Cd	Particulate (µg/L)	< LOQ	-	< LOQ	< LOQ	-	< LOQ
Cd	Particulate (mg/kg)	< LOQ	-	< LOQ	< LOQ	-	< LOQ
Co	Dissolved (µg/L)	0.35	0.28	0.20	0.25	0.16	0.18

Thèse accessible à l'adresse : https://theses.insa-lyon.fr/publication/2025ISAL0011/these.pdf © [D. Gonçalves Portela], [2025], INSA Lyon, tous droits réservés

Co	Particulate (µg/L)	0.78	0.30	0.90	0.03*	0.05	0.02*
Co	Particulate (mg/kg)	7.45	2.95	6.62	2.03*	2.67	1.57*
Cr	Dissolved (µg/L)	0.50	0.29	0.43	0.31	0.21	0.26
Cr	Particulate (µg/L)	4.10	1.63	4.05	0.15*	0.19	0.06*
Cr	Particulate (mg/kg)	39.46	17.24	39.50	9.93*	11.41	6.33*
Cu	Dissolved (µg/L)	6.86	4.68	5.35	6.31	2.88	6.47
Cu	Particulate (µg/L)	14.64	7.25	13.70	1.02	0.95	1.01
Cu	Particulate (mg/kg)	131.40	34.94	147.30	73.20	65.27	107.50
Fe	Dissolved (µg/L)	50.05	41.86	30.80	23.72	20.32	19.14
Fe	Particulate (µg/L)	1898.80	805.03	2093.00	39.83	69.44	16.80
Fe	Particulate (mg/kg)	17967.40	7197.22	15528.00	2530.10	3938.98	1433.00
Li	Dissolved (µg/L)	3.86	2.36	2.83	3.23	1.53	2.85
Li	Particulate (µg/L)	1.92	0.74	2.16	0.04*	0.06	0.01*
Li	Particulate (mg/kg)	18.39	7.62	15.70	2.23*	3.71	1.00*
Mn	Dissolved (µg/L)	18.74	17.21	15.90	3.51	4.23	2.05
Mn	Particulate (µg/L)	51.86	26.42	43.15	5.54*	7.88	3.32*
Mn	Particulate (mg/kg)	521.40	240.30	560.00	370.65*	449.75	353.00*
Mo	Dissolved (µg/L)	0.66	0.19	0.60	0.72	0.25	0.85
Mo	Particulate (µg/L)	0.29	0.16	0.29	0.02*	0.01	0.02*
Mo	Particulate (mg/kg)	2.54	0.62	2.60	1.12*	0.97	1.60*
Ni	Dissolved (µg/L)	1.46	1.16	0.98	1.54	0.90	1.13
Ni	Particulate (µg/L)	2.17	0.76	2.34	0.25*	0.42	0.09*
Ni	Particulate (mg/kg)	30.49	18.81	22.56	16.67*	26.09	9.91*
Pb	Dissolved (µg/L)	0.31	0.23	0.16	0.18	0.15	0.08
Pb	Particulate (µg/L)	5.05	2.49	5.17	0.15*	0.18	0.07*

Thèse accessible à l'adresse : https://theses.insa-lyon.fr/publication/2025ISAL0011/these.pdf © [D. Gonçalves Portela], [2025], INSA Lyon, tous droits réservés

Pb	Particulate (mg/kg)	45.88	16.26	43.50	9.53*	10.74	7.90*
Rb	Dissolved (µg/L)	4.93	3.70	3.41	4.02	2.39	4.20
Rb	Particulate (µg/L)	3.28	1.42	3.49	0.06*	0.09	0.03*
Rb	Particulate (mg/kg)	30.81	11.42	27.08	3.63*	4.85	2.91*
Sb	Dissolved (µg/L)	0.47	0.19	0.40	0.68	0.26	0.59
Sb	Particulate (µg/L)	0.42	0.22	0.45	0.03*	0.04	0.02*
Sb	Particulate (mg/kg)	4.78	1.19	5.06	1.75*	2.56	1.00*
Se	Dissolved (µg/L)	0.09	0.04	0.09	0.07	0.02	0.08
Se	Particulate (µg/L)	0.05*	0.03	0.05*	0.01*	0.01	0.01*
Se	Particulate (mg/kg)	0.69*	0.24	0.58*	0.60*	0.51	0.88*
Sn	Dissolved (µg/L)	0.18	0.17	0.09	0.08*	0.07	0.05*
Sn	Particulate (µg/L)	1.85	1.02	2.15	0.08*	0.07	0.03*
Sn	Particulate (mg/kg)	16.25	4.90	17.50	4.32*	4.38	2.50*
Sr	Dissolved (µg/L)	155.27	59.38	129.00	169.95	23.58	163.00
Sr	Particulate (µg/L)	5.92	3.93	3.39	0.56*	0.49	0.70*
Sr	Particulate (mg/kg)	51.96	20.33	57.50	42.20*	39.17	52.15*
Ti	Dissolved (µg/L)	1.82	1.56	1.39	0.44	0.35	0.35
Ti	Particulate (µg/L)	76.72	35.36	82.99	1.21	2.02	0.48
Ti	Particulate (mg/kg)	723.50	310.73	609.00	78.29	115.03	36.00
Tl	Dissolved (µg/L)	< LOQ	-	< LOQ	< LOQ	-	< LOQ
Tl	Particulate (µg/L)	< LOQ	-	< LOQ	< LOQ	-	< LOQ
Tl	Particulate (mg/kg)	< LOQ	-	< LOQ	< LOQ	-	< LOQ
U	Dissolved (µg/L)	0.93	0.57	0.71	0.58	0.25	0.57
U	Particulate (µg/L)	0.15	0.06	0.16	0.01	0.01	0.01
U	Particulate (mg/kg)	1.37	0.39	1.38	0.38	0.42	0.25

Thèse accessible à l'adresse : https://theses.insa-lyon.fr/publication/2025ISAL0011/these.pdf © [D. Gonçalves Portela], [2025], INSA Lyon, tous droits réservés

V	Dissolved (µg/L)	0.95	0.52	0.89	1.67	0.74	1.35
V	Particulate (µg/L)	3.50	1.71	3.78	0.09*	0.06	0.06*
V	Particulate (mg/kg)	32.66	15.89	34.10	4.95*	4.48	3.99*
Zn	Dissolved (µg/L)	16.79	7.43	15.45	10.63	6.81	14.76
Zn	Particulate (µg/L)	71.99	28.48	77.40	2.30	2.54	2.19
Zn	Particulate (mg/kg)	679.80	237.71	644.00	163.87	157.74	225.00

* below the indicated values

Table 0.2 - The concentration of metals at the inlet and outlet of the CSOB was measured. The mean, standard deviation (SD), and median were calculated for each metal.

		Inlet			Outlet		
		Mean	SD	Median	Mean	SD	Median
Ag	Dissolved (µg/L)	< LOQ	-	< LOQ	< LOQ	-	< LOQ
Ag	Particulate (µg/L)	< LOQ	-	< LOQ	< LOQ	-	< LOQ
Ag	Particulate (mg/kg)	< LOQ	-	< LOQ	< LOQ	-	< LOQ
Al	Dissolved (µg/L)	20.32	3.72	19.24	4.20	2.24	3.49
Al	Particulate (µg/L)	2220.00	1285.22	2560.50	2.44	1.79	2.72
Al	Particulate (mg/kg)	16838.75	8128.67	17656.00	193.63	240.69	112.50
As	Dissolved (µg/L)	2.14	1.06	1.71	3.32	1.75	3.32
As	Particulate (µg/L)	1.79	1.00	1.91	0.01*	0.01	0.00*
As	Particulate (mg/kg)	13.85	5.35	14.20	0.79*	1.42	0.10*
B	Dissolved (µg/L)	18.09	11.57	17.35	19.22	12.53	13.74
B	Particulate (µg/L)	5.41	4.14	6.08	0.39*	0.38	0.34*
B	Particulate (mg/kg)	79.02	81.63	45.55	19.00*	22.17	11.75*
Ba	Dissolved (µg/L)	26.07	3.77	27.41	36.46	26.12	24.90
Ba	Particulate (µg/L)	26.63	13.45	30.15	0.11	0.22	0.00
Ba	Particulate (mg/kg)	209.00	73.31	207.00	17.56	34.87	0.16

Thèse accessible à l'adresse : https://theses.insa-lyon.fr/publication/2025ISAL0011/these.pdf © [D. Gonçalves Portela], [2025], INSA Lyon, tous droits réservés

Cd	Dissolved (µg/L)	< LOQ	-	< LOQ	< LOQ	-	< LOQ
Cd	Particulate (µg/L)	< LOQ	-	< LOQ	< LOQ	-	< LOQ
Cd	Particulate (mg/kg)	< LOQ	-	< LOQ	< LOQ	-	< LOQ
Co	Dissolved (µg/L)	0.25	0.22	0.17	0.24	0.22	0.16
Co	Particulate (µg/L)	1.08	0.58	1.25	0.00	0.00	0.00
Co	Particulate (mg/kg)	8.29	3.36	8.49	0.40	0.70	0.06
Cr	Dissolved (µg/L)	0.34	0.05	0.35	0.18	0.05	0.16
Cr	Particulate (µg/L)	5.84	2.91	6.82	0.02	0.03	0.00
Cr	Particulate (mg/kg)	46.15	18.06	44.03	2.44	4.61	0.18
Cu	Dissolved (µg/L)	4.19	0.82	4.21	4.42	1.33	4.20
Cu	Particulate (µg/L)	16.24	8.40	17.70	0.17*	0.22	0.09*
Cu	Particulate (mg/kg)	126.92	40.37	130.85	20.56	37.72	2.25
Fe	Dissolved (µg/L)	36.48	25.71	28.78	11.11	5.33	10.95
Fe	Particulate (µg/L)	2642.00	1549.12	2906.50	2.16*	4.17	0.09*
Fe	Particulate (mg/kg)	20058.25	8920.06	21334.00	336.19*	665.88	4.13*
Li	Dissolved (µg/L)	2.89	1.87	2.20	4.45	3.56	2.89
Li	Particulate (µg/L)	2.73	1.55	3.12	0.01*	0.00	0.01*
Li	Particulate (mg/kg)	20.82	9.21	21.96	0.39*	0.41	0.23*
Mn	Dissolved (µg/L)	16.77	22.46	7.63	2.86	2.79	2.34
Mn	Particulate (µg/L)	59.40	40.16	59.86	5.90*	11.80	0.01*
Mn	Particulate (mg/kg)	550.13	324.81	671.00	935.87*	1871.42	0.23*
Mo	Dissolved (µg/L)	0.59	0.14	0.56	0.70	0.28	0.61
Mo	Particulate (µg/L)	0.26	0.11	0.27	0.00*	0.00	0.00*
Mo	Particulate (mg/kg)	2.11	0.28	2.09	0.48*	0.83	0.08*
Ni	Dissolved (µg/L)	1.06	0.78	0.76	1.21	1.04	0.78

Thèse accessible à l'adresse : https://theses.insa-lyon.fr/publication/2025ISAL0011/these.pdf © [D. Gonçalves Portela], [2025], INSA Lyon, tous droits réservés

Ni	Particulate (µg/L)	3.05	1.42	3.46	0.05*	0.05	0.05*
Ni	Particulate (mg/kg)	35.73	18.57	29.50	5.27*	6.63	3.30*
Pb	Dissolved (µg/L)	0.16	0.07	0.16	0.13	0.13	0.08
Pb	Particulate (µg/L)	6.23	3.36	7.36	0.03*	0.03	0.03*
Pb	Particulate (mg/kg)	47.81	19.80	49.90	2.33*	4.32	0.23*
Rb	Dissolved (µg/L)	2.98	1.71	2.47	3.79	2.56	3.19
Rb	Particulate (µg/L)	4.71	2.93	4.90	0.00*	0.01	0.00*
Rb	Particulate (mg/kg)	35.40	15.65	38.89	0.62*	1.14	0.06*
Sb	Dissolved (µg/L)	0.50	0.24	0.39	0.61	0.27	0.59
Sb	Particulate (µg/L)	0.54	0.35	0.55	0.01*	0.01	0.01*
Sb	Particulate (mg/kg)	5.13	1.07	5.24	0.47*	0.42	0.41*
Se	Dissolved (µg/L)	0.07	0.02	0.07	0.06	0.03	0.06
Se	Particulate (µg/L)	0.06	0.02	0.07	0.00*	0.00	0.00*
Se	Particulate (mg/kg)	1.57	2.24	0.49	0.30*	0.51	0.06*
Sn	Dissolved (µg/L)	0.06*	0.03	0.07*	0.02*	0.01	0.02*
Sn	Particulate (µg/L)	2.02*	1.15	2.25*	0.02*	0.01	0.02*
Sn	Particulate (mg/kg)	15.25*	4.48	17.05*	1.07*	0.96	0.64*
Sr	Dissolved (µg/L)	118.79	19.96	120.50	174.76	34.53	161.96
Sr	Particulate (µg/L)	7.44	5.07	6.08	0.20	0.29	0.09
Sr	Particulate (mg/kg)	58.61	23.31	53.98	27.23	48.98	4.13
Ti	Dissolved (µg/L)	0.93	0.31	0.94	0.45	0.53	0.24
Ti	Particulate (µg/L)	108.75	71.51	109.50	0.05	0.05	0.03
Ti	Particulate (mg/kg)	807.23	365.75	867.50	5.10	8.48	1.13
Tl	Dissolved (µg/L)	< LOQ	-	< LOQ	< LOQ	-	< LOQ
Tl	Particulate (µg/L)	< LOQ	-	< LOQ	< LOQ	-	< LOQ

Thèse accessible à l'adresse : https://theses.insa-lyon.fr/publication/2025ISAL0011/these.pdf © [D. Gonçalves Portela], [2025], INSA Lyon, tous droits réservés

Tl	Particulate (mg/kg)	< LOQ	-	< LOQ	< LOQ	-	< LOQ
U	Dissolved (µg/L)	0.54	0.13	0.57	0.89	0.91	0.48
U	Particulate (µg/L)	0.20	0.10	0.23	0.00*	0.00	0.00*
U	Particulate (mg/kg)	1.55	0.47	1.58	0.20*	0.31	0.06*
V	Dissolved (µg/L)	1.24	0.68	0.95	1.49	0.68	1.62
V	Particulate (µg/L)	4.74	3.10	5.24	0.05*	0.03	0.05*
V	Particulate (mg/kg)	34.89	19.80	39.20	2.38*	1.79	1.63*
Zn	Dissolved (µg/L)	11.76	6.96	11.87	4.24	0.90	4.26
Zn	Particulate (µg/L)	89.76	43.56	110.00	0.33*	0.52	0.09*
Zn	Particulate (mg/kg)	714.25	287.55	672.00	46.15*	86.60	4.13*

Thèse accessible à l'adresse : https://theses.insa-lyon.fr/publication/2025ISAL0011/these.pdf © [D. Gonçalves Portela], [2025], INSA Lyon, tous droits réservés

ANNEX 2

The 93 compounds analyzed at least once were: 6PPD; 6PPD-quinone (6PPD-Q); ABT; Amisulpride (ASP); Amoxicillin (AXL); Ampicilin; Atenolol (ANL); Azithromycin; Azoxystrobin; BAC-C12; BAC-C14; BAC-C16; Benzophenone; Benzotriazole (BZL); Benzoylecgonine (BZG); Bicalutamid; BT; Caffeine (CFN); Candesartan; Carbamazepine (CBP); Carbendazim; Cetrazine (CTZ); Citalopram; Clarithromycin (CTM); Clindamycin; Cybutryne; DDAC-C10; DEET; Diatrizoic acid; Diazinon; Diclofenac (DFC); Diflufenican' - AE-0; Diflufenican' - AE-B; Diflufenican' - AE-C; Diflufenician; Dimethoate; Diuron; Doxycycline; Eprosartan; Erythromycin (ETM); Fexofenadine; Fluopyram; Furosemide; Gabapentin (GBP); Gemfibrozil; Hydrochlorothiazide; Imidachloprid; Iohexol; Iomeprol (IOP); Iopamidol (IOD); Iopromide (IOI); Irbesartan (IBT); Isoroturon; Lamotrigine; Lidocaine (LDN); Losartan; MBT; Mefenamic acid; Methamphetamine; Metoprolol; Miconazole; MTBT; Mycophenolic acid (MCL acid); OHBT; Olmesartan; Oxazepam (OXP); Oxcarbazepine; Phenazone; Primicarb; Propiconazole; Propranolol (PPL); Propyphenazone; Pyraclostrobin; Ranitidine; Rosuvastatin; Roxitromycin; Setraline; Simvastatin; Sotalol (STL); Sulfadiazine; Sulfamethizole; Sulfamethoxazole (STX); Sulfapyridine; TDAC-C12; Tebuconazole (TCZ); Terbutryn; THC-COOH; Thiachloprid; Tramadol; Trimethoprim (TRP); Valsartan (VST); Venlafaxine (VLX).

However, not all compounds were quantified. Therefore, the list below includes only dissolved micropollutants above the limit of detection at least once on one of the two pilots. Table 0.1 indicates the two periods where micropollutants from the chemical class of pharmaceuticals, industrial chemicals and pesticides were collected. In the initial phase, from May to November 2023, there was a larger variety of analyzed micropollutants. The occurrences marked with ** indicate that the compound was not analyzed for all sampled trials of that period. If a compound was identified in one sample but not in the other, the < LOQ or < LOD is referred. The legends for the marks are below the Table 0.1.

Table 0.1 - Frequency of compound occurrences at the inlet and outlet of both filters.

Compound	May – Nov. 2023				Dec. 2023 –March 2024				Class
	CSOA		CSOB		CSOA		CSOB		
	n = 19	n = 19	n = 8	n = 8	n = 8	n = 7	n = 6	n = 6	
	Inlet	Outlet	Inlet	Outlet	Inlet	Outlet	Inlet	Outlet	
6PPD-Q	5	< LOQ	5	< LOQ	-	-	-	-	Industrial chemical
ABT	12	4	7	5	-	-	-	-	Industrial chemical
ASP	1*	1*	4**	4**	< LOQ	< LOQ	1*	< LOQ	Pharmaceutical
AXL	<LOD**	<LOD**	1**	2**	6	1*	3*	< LOQ	Pharmaceutical
ANL	1**	1**	4**	4**	8	3+3*	6	4	Pharmaceutical
BZL	2**	1**	4**	4**	8	6+1*	6	6	Industrial chemical
BZG	1**	1**	3**	3**	4*	< LOQ	< LOQ	< LOD	Pharmaceutical

Thèse accessible à l'adresse : https://theses.insa-lyon.fr/publication/2025ISAL0011/these.pdf © [D. Gonçalves Portela], [2025], INSA Lyon, tous droits réservés

BT	12	8	3	< LOQ	-	-	-	-	Industrial chemical
CFN	1**	2**	4**	4**	8**	6+1*	6	5+1*	Pharmaceutical
CBP	1**	1**	3**	3**	3	1+3*	2	2+1*	Pharmaceutical
CTZ	1**	1**	3**	< LOQ**	6*	3+2*	4	2+2*	Pharmaceutical
CTM	1*.**	1*.**	2**	< LOQ**	2	< LOQ	< LOQ	< LOQ	Pharmaceutical
DEET	4**	4**	4**	< LOQ**	8	6+1*	6	6	Pharmaceutical
DFC	1**	1**	3**	< LOQ**	7	4+1*	2+1*	3	Pharmaceutical
ETM	1*.**	1*.**	4**	< LOQ**	1	1*	< LOQ	< LOQ	Pharmaceutical
GBP	4**	3**	4**	4**	8	6+1*	6	6	Pharmaceutical
IOP	5**	3**	4**	4**	8	6+1*	6	6	Pharmaceutical
IOD	1**	2**	3**	4**	8	6+1*	6	6	Pharmaceutical
IOI	1**	1**	3**	1**	< LOD	< LOD	< LOD	< LOD	Pharmaceutical
IBT	4**	4**	4**	4**	-	-	-	-	Pharmaceutical
LDN	1**	3**	4**	4**	8	5+2*	6	6	Pharmaceutical
MBT	1*	1*	< LOQ	< LOQ	-	-	-	-	Industrial chemical
MTBT	1	1*	3	2	-	-	-	-	Industrial chemical
MCL acid	1**	< LOD**	2**	1**	5	1	1+3*	1	Pharmaceutical
OHBT	19	17	8	6	-	-	-	-	Industrial chemical
OXP	1**	2**	4**	4**	8	6+1*	5+1*	6	Pharmaceutical
PPL	1**	< LOQ**	< LOQ**	< LOQ**	< LOD	< LOD	< LOD	< LOD	Pharmaceutical
STL	1**	1**	4**	4**	4	3*	2	2+2*	Pharmaceutical
STX	1**	1*.**	2**	1*.**	< LOD	< LOD	< LOQ	< LOQ	Pharmaceutical
TCZ	1	1*	1	1	-	-	-	-	Pesticides
TRP	1**	< LOD**	2**	1**	< LOD	< LOD	< LOD	< LOD	Pharmaceutical
VST	< LOQ**	< LOQ**	1**	2**	5	2+1*	2+1*	2+1*	Pharmaceutical
VLX	1*	2	3	2	4	5+1*	2+1*	1	Pharmaceutical

*The compound was quantified at a level equal to or less than LOQ.
**The compound was analyzed in a total of 5 samples of CSOA and 4 samples of CSOB.
- The compound was not analyzed for this period.

Table 0-1 LOD and LOQ of all selected compounds

	May – Nov. 2023		Dec. 2023 –March 2024	
	LOD µg/L	LOQ µg/L	LOD µg/L	LOQ µg/L
6PPD-quinone	0.01	0.02	-	-
ABT	0.02	0.05	-	-
Atenolol	0.1	0.1	0.01	0.01
Benzotriazole	0.02	0.05	0.02	0.05
BT	0.02	0.1	-	-
DEET	0.01	0.02	0.01	0.01
Carbamazepine	0.01	0.01	0.02	0.05
Diclofenac	0.01	0.05	0.01	0.02
Gabapentin	0.01	0.02	0.01	0.01
Iomeprol	0.01	0.01	0.05	0.05
Irbesartan	0.01	0.01	-	-

Thèse accessible à l'adresse : https://theses.insa-lyon.fr/publication/2025ISAL0011/these.pdf © [D. Gonçalves Portela], [2025], INSA Lyon, tous droits réservés

OHBT	0.05	0.1	-	-
Sulfamethoxazole	0.01	0.01	0.01	0.02
Sotalol	0.1	0.1	0.01	0.02

Thèse accessible à l'adresse : https://theses.insa-lyon.fr/publication/2025ISAL0011/these.pdf © [D. Gonçalves Portela], [2025], INSA Lyon, tous droits réservés

ANNEX 3

Statics measurement of standard parameters at the inlet and outlet for each aeration strategy (AS). All the presented values are in mg/L. The values under LOQ were replaced by LOQ to obtain the results

Table 0.1 –Temperature in CSOA

AS	n	Mean (±SD)		Max	Min	Median
F10	7	22.71	(±1.46)	24.40	19.90	22.80
F10/40	3	11.57	(±0.38)	12.00	11.30	11.40
10/40	4	12.32	(±0.29)	12.70	12.00	12.28
75/15	14	19.72	(±2.87)	23.00	14.60	21.00
C	33	11.69	(±4.03)	20.00	5.00	11.90
Qair_var	5	6.74	(±0.83)	8.00	6.00	6.70

Table 0.2 –TSS in CSOA

	Inlet						Outlet					
AS	n	Mean (±SD)		Max	Min	Median	n	Mean	(±SD)	Max	Min	Median
F10	7	216.07	139.82	485.00	94.00	159.00	7	22.94	4.93	30.00	15.00	23.00
F10/40	3	134.33	14.05	149.00	121.00	133.00	3	10.77	2.14	12.00	8.30	12.00
10/40	4	201.75	27.48	237.00	170.00	200.00	4	11.20	1.60	12.00	8.80	12.00
75/15	14	178.69	88.52	312.00	63.00	155.00	14	7.41	3.72	16.00	3.50	6.60
C	31	89.34	65.21	338.00	30.00	65.00	31	7.20	5.23	25.00	<1.00	6.00
Qair_var	5	165.20	137.04	333.00	58.00	74.00	5	3.86	2.72	7.50	<1.00	2.70

Table 0.3 –COD in CSOA

	Inlet						Outlet					
AS	n	Mean (±SD)		Max	Min	Median	n	Mean	(±SD)	Max	Min	Median
F10	7	350.93	76.70	455.00	253.00	348.00	7	159.61	62.83	252.00	72.00	153.00
F10/40	3	136.33	37.17	179.00	111.00	119.00	3	33.00	7.81	38.00	24.00	37.00
10/40	4	217.75	39.08	251.00	171.00	224.50	4	31.50	3.11	35.00	28.00	31.50
75/15	15	246.83	74.98	416.00	159.00	238.00	15	33.13	6.79	49.00	23.00	32.00
C	33	137.67	94.72	509.00	38.00	117.00	33	21.03	16.46	85.00	<10.00	14.00
Qair_var	5	176.40	69.34	270.00	117.00	135.00	5	24.00	20.96	57.00	<10.00	<10.00

Thèse accessible à l'adresse : https://theses.insa-lyon.fr/publication/2025ISAL0011/these.pdf © [D. Gonçalves Portela], [2025], INSA Lyon, tous droits réservés

Table 0.4 -Dissolved COD in CSOA

	Inlet						Outlet					
AS	n	Mean (±SD)		Max	Min	Median	n	Mean	(±SD)	Max	Min	Median
F10	7	201.43	82.42	315.00	110.00	183.00	7	137.44	61.83	226.00	58.00	124.00
F10/40	3	38.67	21.39	62.00	20.00	34.00	3	24.00	4.00	28.00	20.00	24.00
10/40	4	34.00	7.30	42.00	26.00	34.00	4	22.00	6.16	31.00	17.00	20.00
75/15	13	115.08	23.83	155.00	81.00	114.00	13	24.00	9.50	37.00	<10.00	25.00
C	33	79.55	66.86	349.00	10.00	73.00	33	12.70	6.93	38.00	<10.00	<10.00
Qair_var	5	81.80	17.11	104.00	65.00	73.00	5	21.40	17.29	49.00	<10.00	<10.00

Table 0.5 -DBO_5 in CSOA

	Inlet						Outlet					
AS	n	Mean (±SD)		Max	Min	Median	n	Mean	(±SD)	Max	Min	Median
F10	1	NA	NA	112.00	112.00	112.00	1	NA	NA	82.00	82.00	82.00
F10/40	0	NA	NA	NA	NA	NA	3	NA	NA	NA	NA	NA
10/40	1	NA	NA	77.00	77.00	77.00	1	NA	NA	17.00	17.00	17.00
75/15	2	110.00	5.66	114.00	106.00	110.00	2	7.65	0.92	8.30	7.00	7.65
C	4	95.50	25.46	117.00	65.00	100.00	4	7.55	2.67	11.00	5.30	6.95
Qair_var	1	NA	NA	61.00	61.00	61.00	1	NA	NA	2.10	2.10	2.10

Table 0.6 -NO_2-N in CSOA

	Inlet						Outlet					
AS	n	Mean (±SD)		Max	Min	Median	n	Mean	(±SD)	Max	Min	Median
F10	7	0.13	0.10	0.28	<0.01	0.15	7	0.21	0.27	0.73	<0.01	0.06
F10/40	3	0.04	0.02	0.05	<0.01	0.04	3	0.54	0.17	0.74	0.44	0.45
10/40	4	0.03	0.01	0.04	<0.01	0.03	4	0.67	0.18	0.91	0.50	0.63
75/15	15	0.33	0.23	0.85	<0.01	0.30	15	0.75	0.54	2.07	0.15	0.50
C	33	0.18	0.12	0.48	<0.01	0.15	33	0.23	0.24	0.90	<0.01	0.13
Qair_var	5	0.16	0.08	0.27	0.09	0.12	5	0.24	0.14	0.40	0.10	0.22

Table 0.7 -NO_3-N in CSOA

	Inlet						Outlet					
AS	n	Mean (±SD)		Max	Min	Median	n	Mean	(±SD)	Max	Min	Median
F10	7	33.3	4.9	0.77	<0.23	<0.23		0.99	1.09	3.06	0.23	0.23
F10/40	3	<0.23	0.0	<0.23	<0.23	<0.23		2.21	0.60	2.62	1.53	2.49
10/40	4	0.5	0.5	1.2	<0.23	<0.23		7.03	2.85	11.20	5.19	5.86
75/15	15	1.66	2.17	7.7	<0.23	0.7		10.33	4.66	19.20	4.51	8.30

Thèse accessible à l'adresse : https://theses.insa-lyon.fr/publication/2025ISAL0011/these.pdf © [D. Gonçalves Portela], [2025], INSA Lyon, tous droits réservés

C	33	4.2	4.3	17.7	<0.23	2.53		8.27	4.43	23.20	2.52	7.39
Qair_var	5	2.7	2.1	3.75	<0.23	2.1		4.85	1.41	6.32	2.96	5.01

Table 0.8 -NH_4-N in CSOA

	Inlet						Outlet					
AS	n	Mean (±SD)		Max	Min	Median	n	Mean	(±SD)	Max	Min	Median
F10	7	9.48	5.14	17.00	5.26	8.11	7	8.21	6.16	16.70	1.50	5.57
F10/40	3	7.65	2.71	10.70	5.51	6.75	3	3.12	1.31	4.54	1.96	2.86
10/40	4	13.46	0.94	14.70	12.50	13.32	4	4.89	0.92	6.18	4.15	4.62
75/15	15	17.19	8.19	36.20	4.28	19.40	15	5.42	4.72	18.30	0.12	4.10
C	33	7.75	6.09	25.50	0.13	6.96	33	2.08	2.07	7.17	<0.01	1.35
Qair_var	5	11.51	2.78	15.10	7.64	10.90	5	7.06	3.17	11.50	4.29	5.14

Table 0.9 -PO_4-P in CSOA

	Inlet						Outlet					
AS	n	Mean (±SD)		Max	Min	Median	n	Mean	(±SD)	Max	Min	Median
F10	7	1.01	0.21	1.23	0.68	1.03	7	0.90	0.35	1.44	0.51	0.79
F10/40	3	0.50	0.18	0.70	0.36	0.45	3	0.47	0.05	0.52	0.42	0.46
10/40	4	0.97	0.29	1.29	0.64	0.97	4	0.89	0.24	1.22	0.68	0.84
75/15	12	0.84	0.17	1.13	0.48	0.85	12	0.91	0.25	1.38	0.47	0.88
C	33	0.28	0.18	0.60	0.05	0.23	33	0.39	0.23	0.99	0.09	0.37
Qair_var	5	0.44	0.18	0.72	0.30	0.35	5	0.34	0.26	0.70	0.10	0.22

Table 0.10 –TKN in CSOA

	Inlet						Outlet					
AS	n	Mean (±SD)		Max	Min	Median	n	Mean	(±SD)	Max	Min	Median
F10	1	NA	NA	15.60	15.60	15.60	1	NA	NA	10.00	10.00	10.00
F10/40	0	NA	NA	NA	NA	NA	0	NA	NA	NA	NA	NA
10/40	1	NA	NA	22.00	22.00	22.00	1	NA	NA	6.00	6.00	6.00
75/15	2	34.15	1.20	35.00	33.30	34.15	2	18.00	3.39	20.40	15.60	18.00
C	8	9.54	6.12	19.10	2.30	8.30	8	3.30	2.22	7.60	0.50	3.15
Qair_var	1	NA	NA	15.60	15.60	15.60	1	NA	NA	7.00	7.00	7.00

Table 0.11 –TN in CSOA

	Inlet					Outlet					
AS	n	Mean (±SD)	Max	Min	Median	n	Mean	(±SD)	Max	Min	Median

Thèse accessible à l'adresse : https://theses.insa-lyon.fr/publication/2025ISAL0011/these.pdf © [D. Gonçalves Portela], [2025], INSA Lyon, tous droits réservés

F10	2	12.50	0.71	13.00	12.00	12.50	2	10.80	1.13	11.60	10.00	10.80
F10/40	0	NA	NA	NA	NA	NA	0	NA	NA	NA	NA	NA
10/40	1	NA	NA	18.40	18.40	18.40	1	NA	NA	16.00	16.00	16.00
75/15	1	NA	NA	31.50	31.50	31.50	1	NA	NA	7.50	7.50	7.50
C	4	10.93	7.69	22.30	5.70	7.85	4	8.61	6.13	17.80	5.25	5.70
Qair_var	1	NA	NA	15.40	15.40	15.40	1	NA	NA	11.00	11.00	11.00

Table 0.12 –Temperature in CSOB

AS	n	Mean (±SD)		Max	Min	Median
75/15	16	15.50	2.99	20.40	10.70	14.85
C	7	7.50	1.77	10.00	5.00	7.60
Qair_var	9	9.01	3.00	13.50	5.50	8.00

Table 0.13 –TSS in CSOB

	Inlet						Outlet					
AS	n	Mean (±SD)		Max	Min	Median	n	Mean	(±SD)	Max	Min	Median
75/15	13	154.25	71.84	277.00	52.00	125.00	13	4.36	2.77	11.00	<1.00	4.00
C	7	138.86	68.33	244.00	43.00	135.00	7	1.86	1.12	3.60	<1.00	<1.00
Qair_var	12	62.50	33.25	151.00	31.00	55.00	12	2.85	4.16	15.00	<1.00	<1.00

Table 0.14 –COD in CSOB

	Inlet						Outlet					
AS	n	Mean (±SD)		Max	Min	Median	n	Mean	(±SD)	Max	Min	Median
75/15	16	184.94	62.45	294.00	93.00	180.50	16	20.13	9.39	32.00	10.00	21.00
C	7	118.14	39.50	166.00	73.00	106.00	7	<10.00	0.00	<10.00	<10.00	<10.00
Qair_var	12	121.17	59.74	280.00	54.00	121.50	12	<10.00	0.00	<10.00	<10.00	<10.00

Table 0.15 -Dissolved COD in CSOB

	Inlet						Outlet					
AS	n	Mean (±SD)		Max	Min	Median	n	Mean	(±SD)	Max	Min	Median
75/15	16	89.25	24.22	131.00	56.00	87.00	16	16.25	7.49	30.00	10.00	12.50
C	7	58.86	22.28	85.00	21.00	67.00	7	<10.00	0.00	<10.00	<10.00	<10.00
Qair_var	12	79.42	62.37	240.00	10.00	79.50	12	<10.00	0.00	<10.00	<10.00	<10.00

Table 0.16 - NO_2-N in CSOB

	Inlet	Outlet

Thèse accessible à l'adresse : https://theses.insa-lyon.fr/publication/2025ISAL0011/these.pdf © [D. Gonçalves Portela], [2025], INSA Lyon, tous droits réservés

AS	n	Mean (±SD)		Max	Min	Median	n	Mean	(±SD)	Max	Min	Median
75/15	16	0.29	0.25	0.89	0.02	0.27	16	0.67	0.76	2.70	0.02	0.41
C	7	0.11	0.07	0.20	0.02	0.10	7	0.28	0.38	1.09	0.02	0.09
Qair_var	12	0.17	0.10	0.41	0.07	0.16	12	0.14	0.19	0.58	<0.01	0.04

Table 0.17 – NO_3-N in CSOB

	Inlet						Outlet					
AS	n	Mean (±SD)		Max	Min	Median	n	Mean	(±SD)	Max	Min	Median
75/15	16	2.05	2.2	7.39	0.22	1.07	16	13.11	7.69	37.20	5.72	10.60
C	7	5.7	5.3	18.1	0.56	3.4	7	10.21	4.12	17.80	7.13	8.20
Qair_var	12	2.05	1.58	4.8	0.22	1.9	12	10.39	6.29	24.40	4.86	7.19

Table 0.18 – NH_4-N in CSOB

	Inlet						Outlet					
AS	n	Mean (±SD)		Max	Min	Median	n	Mean	(±SD)	Max	Min	Median
75/15	16	14.80	6.88	25.00	6.28	14.75	16	3.44	4.14	13.10	0.01	1.24
C	7	7.71	3.42	12.60	1.88	8.07	7	1.64	1.51	4.32	0.10	1.27
Qair_var	12	6.94	5.65	22.60	1.07	5.45	12	0.41	0.52	1.93	0.09	0.20

Table 0.19 – PO_4-P in CSOB

	Inlet						Outlet					
AS	n	Mean (±SD)		Max	Min	Median	n	Mean	(±SD)	Max	Min	Median
75/15	13	0.59	0.35	1.15	0.13	0.62	16	0.25	1.04	0.24	0.41	0.25
C	7	0.29	0.18	0.61	0.12	0.23	7	0.07	0.41	0.26	0.29	0.07
Qair_var	12	0.29	0.17	0.49	<0.02	0.35	12	0.18	0.83	0.31	0.37	0.18

Thèse accessible à l'adresse : https://theses.insa-lyon.fr/publication/2025ISAL0011/these.pdf © [D. Gonçalves Portela], [2025], INSA Lyon, tous droits réservés

ANNEX 4

Granular distribution of the top layer
CSOA

Sieve	D (mm)	mass (g)	%pass	%accum
13	0.8	1.23	0.00	0.00
12	1	2.33	0.23	0.23
11	1.25	41.46	0.43	0.65
9	2	101.64	7.61	8.26
8	2.5	278.43	18.65	26.91
7	3.15	99.97	51.08	77.99
6	4	20.02	18.34	96.33
5	5	0	3.67	100.00
		545.08	100.00	

d_{10}	2.04
d_{60}	2.92
CU	1.42

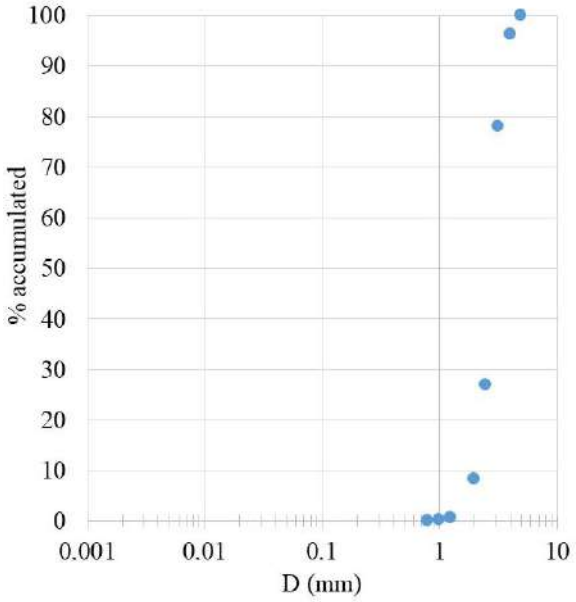

CSOB

Sieve	D (mm)	mass (g)	%pass	%accum
18	0.25	17.04		0.00
17	0.315	27.7	2.99	2.99
16	0.4	94.33	4.86	7.84
14	0.63	127.94	16.54	24.38
12	1	93.19	22.43	46.82
10	1.6	73.03	16.34	63.15
8	2.5	137.12	12.80	75.96
7	3.15	0	24.04	100.00
		570.35	100.00	

d_{10}	0.42
d_{60}	1.48
CU	3.45

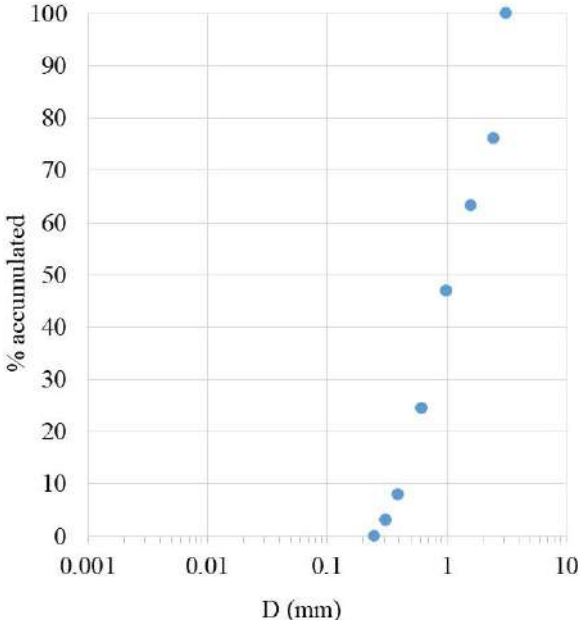

Thèse accessible à l'adresse : https://theses.insa-lyon.fr/publication/2025ISAL0011/these.pdf © [D. Gonçalves Portela], [2025], INSA Lyon, tous droits réservés

ANNEX 5

List of publications and communications

Publications:

• Portela, D., Tondera, K., Troesch, S., Molle, P., 2024. Impact of forced aeration on vertical flow treatment wetland performances for combined sewer overflow. Ecol. Eng. 208, 107359. https://doi.org/10.1016/j.ecoleng.2024.107359

International Conferences:

• Portela, D., Tondera, K., Troesch, S., Molle, P. 2022. Aerated Vertical Flow Treatment Wetlands Treating Combined Sewer Overflow and Stormwater to Improve Water Quality. IWA 17th International Conference on Wetland Systems for Water Pollution Control. Lyon, France. (Poster presentation)

• Tondera, K., Rizzo, A., Sarti, C., Portela, D., Molle, P. 2024. Treatment wetlands as Nature-based Solutions for combined sewer overflow treatment: an overview of applications and recent trend. 16th International Conference on Urban Drainage. Delft, Netherlands. (Oral presentation)

• Portela, D., Tondera, K., Troesch, S., Molle, P. 2023. Forced Aeration in a Vertical Flow Wetland to Treat Combined Sewer Overflow. 10th International Symposium On Wetland Pollutant Dynamics and Control - WETPOL. Bruges, Belgium. (Oral presentation)

• Portela, D., Tondera, K., Troesch, S., Molle, P. 2024. Portela, D., Tondera, K., Troesch, S., Molle, P. Nitrogen Removal in an aerated Vertical Flow Treatment Wetland for Combined Sewer Overflow. IWA 18th International Conference on Wetland Systems for Water Pollution Control. Martinique, France. (Oral presentation)

Thèse accessible à l'adresse : https://theses.insa-lyon.fr/publication/2025ISAL0011/these.pdf © [D. Gonçalves Portela], [2025], INSA Lyon, tous droits réservés

REFERENCES

Ahmed, W., Payyappat, S., Cassidy, M., Harrison, N., Besley, C., 2020. Sewage-associated marker genes illustrate the impact of wet weather overflows and dry weather leakage in urban estuarine waters of Sydney, Australia. Sci. Total Environ. 705, 135390. https://doi.org/10.1016/j.scitotenv.2019.135390

Alexander, M., 2000. Aging, Bioavailability, and Overestimation of Risk from Environmental Pollutants. Environ. Sci. Technol. 34, 4259–4265. https://doi.org/10.1021/es001069+

Andrés-Doménech, I., Hernández-Crespo, C., Martín, M., Andrés-Valeri, V.C., 2018. Characterization of wash-off from urban impervious surfaces and SuDS design criteria for source control under semi-arid conditions. Sci. Total Environ. 612, 1320–1328. https://doi.org/10.1016/j.scitotenv.2017.09.011

ANR, 2013. Système extensifs pour la Gestion et le Traitement des Eaux Urbaines de temps de Pluie. Extensive Systems for the Management and Treatment of Urban Stormwaters.

Asimakopoulos, A.G., Ajibola, A., Kannan, K., Thomaidis, N.S., 2013. Occurrence and removal efficiencies of benzotriazoles and benzothiazoles in a wastewater treatment plant in Greece. Sci. Total Environ. 452–453, 163–171. https://doi.org/10.1016/j.scitotenv.2013.02.041

ASTM Standard D2487, 2011. Practice for Classification of Soils for Engineering Purposes (Unified Soil Classification System). https://doi.org/10.1520/D2487-11

Auvinen, H., Gebhardt, W., Linnemann, V., Du Laing, G., Rousseau, D.P.L., 2017. Laboratory- and full-scale studies on the removal of pharmaceuticals in an aerated constructed wetland: effects of aeration and hydraulic retention time on the removal efficiency and assessment of the aquatic risk. Water Sci. Technol. 76, 1457–1465. https://doi.org/10.2166/wst.2017.328

Ávila, C., Salas, J.J., Martín, I., Aragón, C., García, J., 2013. Integrated treatment of combined sewer wastewater and stormwater in a hybrid constructed wetland system in southern Spain and its further reuse. Ecol. Eng. 50, 13–20. https://doi.org/10.1016/j.ecoleng.2012.08.009

Baum, P., Kuch, B., Dittmer, U., 2021. Adsorption of Metals to Particles in Urban Stormwater Runoff—Does Size Really Matter? Water 13, 309. https://doi.org/10.3390/w13030309

Becouze-Lareure, C., Dembélé, A., Coquery, M., Cren-Olivé, C., Bertrand-Krajewski, J.-L., 2019. Assessment of 34 dissolved and particulate organic and metallic micropollutants discharged at the outlet of two contrasted urban catchments. Sci. Total Environ. 651, 1810–1818. https://doi.org/10.1016/j.scitotenv.2018.10.042

Bertrand-Krajewski, J.-L., Chebbo, G., Saget, A., 1998. Distribution of pollutant mass vs volume in stormwater discharges and the first flush phenomenon. Water Res. 32, 2341–2356. https://doi.org/10.1016/S0043-1354(97)00420-X

Blecken, G.-T., Zinger, Y., Deletić, A., Fletcher, T.D., Viklander, M., 2009. Influence of intermittent wetting and drying conditions on heavy metal removal by stormwater biofilters. Water Res. 43, 4590–4598. https://doi.org/10.1016/j.watres.2009.07.008

Boog, J., Nivala, J., Aubron, T., Mothes, S., van Afferden, M., Müller, R.A., 2018. Resilience of carbon and nitrogen removal due to aeration interruption in aerated treatment wetlands. Sci. Total Environ. 621, 960–969. https://doi.org/10.1016/j.scitotenv.2017.10.131

Boog, J., Nivala, J., Aubron, T., Wallace, S., van Afferden, M., Müller, R.A., 2014. Hydraulic characterization and optimization of total nitrogen removal in an aerated vertical subsurface flow treatment wetland. Bioresour. Technol. 162, 166–174. https://doi.org/10.1016/j.biortech.2014.03.100

Thèse accessible à l'adresse : https://theses.insa-lyon.fr/publication/2025ISAL0011/these.pdf © [D. Gonçalves Portela], [2025], INSA Lyon, tous droits réservés

Botero-Coy, A.M., Martínez-Pachón, D., Boix, C., Rincón, R.J., Castillo, N., Arias-Marín, L.P., Manrique-Losada, L., Torres-Palma, R., Moncayo-Lasso, A., Hernández, F., 2018. 'An investigation into the occurrence and removal of pharmaceuticals in Colombian wastewater.' Sci. Total Environ. 642, 842–853. https://doi.org/10.1016/j.scitotenv.2018.06.088

Botturi, A., Ozbayram, E.G., Tondera, K., Gilbert, N.I., Rouault, P., Caradot, N., Gutierrez, O., Daneshgar, S., Frison, N., Akyol, Ç., Foglia, A., Eusebi, A.L., Fatone, F., 2021. Combined sewer overflows: A critical review on best practice and innovative solutions to mitigate impacts on environment and human health. Crit. Rev. Environ. Sci. Technol. 51, 1585–1618. https://doi.org/10.1080/10643389.2020.1757957

Bozovic, R., Cedo Maksimovic, Mijic, A., Smith, K., Suter, I., Reeuwijk, M.V., 2017. Blue Green Solutions. A Systems Approach to Sustainable, Resilient and Cost-Efficient Urban Development. https://doi.org/10.13140/RG.2.2.30628.07046

Brix, H., 1997. Do macrophytes play a role in constructed treatment wetlands? Water Sci. Technol. 35. https://doi.org/10.1016/S0273-1223(97)00047-4

Bruch, I., Fritsche, J., Bänninger, D., Alewell, U., Sendelov, M., Hürlimann, H., Hasselbach, R., Alewell, C., 2011. Improving the treatment efficiency of constructed wetlands with zeolite-containing filter sands. Bioresour. Technol. 102, 937–941. https://doi.org/10.1016/j.biortech.2010.09.041

Brunsch, A.F., Ter Laak, T.L., Christoffels, E., Rijnaarts, H.H.M., Langenhoff, A.A.M., 2018. Retention soil filter as post-treatment step to remove micropollutants from sewage treatment plant effluent. Sci. Total Environ. 637–638, 1098–1107. https://doi.org/10.1016/j.scitotenv.2018.05.063

Brunsch, A.F., Zubieta Florez, P., Langenhoff, A.A.M., Ter Laak, T.L., Rijnaarts, H.H.M., 2020. Retention soil filters for the treatment of sewage treatment plant effluent and combined sewer overflow. Sci. Total Environ. 699, 134426. https://doi.org/10.1016/j.scitotenv.2019.134426

Butterworth, E., Dotro, G., Jones, M., Richards, A., Onunkwo, P., Narroway, Y., Jefferson, B., 2013. Effect of artificial aeration on tertiary nitrification in a full-scale subsurface horizontal flow constructed wetland. Ecol. Eng. 54, 236–244. https://doi.org/10.1016/j.ecoleng.2013.01.034

Carletti, G., Fatone, F., Bolzonella, D., Cecchi, F., 2008. Occurrence and fate of heavy metals in large wastewater treatment plants treating municipal and industrial wastewaters. Water Sci. Technol. 57, 1329–1336. https://doi.org/10.2166/wst.2008.230

Characklis, G.W., Dilts, M.J., Simmons, O.D., Likirdopulos, C.A., Krometis, L.-A.H., Sobsey, M.D., 2005. Microbial partitioning to settleable particles in stormwater. Water Res. 39, 1773–1782. https://doi.org/10.1016/j.watres.2005.03.004

Cheng, L., AghaKouchak, A., 2015. Nonstationary Precipitation Intensity-Duration-Frequency Curves for Infrastructure Design in a Changing Climate. Sci. Rep. 4, 7093. https://doi.org/10.1038/srep07093

Choubert, J.M., Martin Ruel, S., Esperanza, M., Budzinski, H., Miège, C., Lagarrigue, C., Coquery, M., 2011. Limiting the emissions of micro-pollutants: what efficiency can we expect from wastewater treatment plants? Water Sci. Technol. 63, 57–65. https://doi.org/10.2166/wst.2011.009

Choubert, J.-M., Martin Ruel, S., Miege, C., Coquery, M., 2017. Rethinking micropollutant removal assessment methods for wastewater treatment plants – how to get more robust data? Water Sci. Technol. 75, 2964–2972. https://doi.org/10.2166/wst.2017.181

Choubert, J.-M., Pomiès, M., Martin Ruel, S., Coquery, M., 2011. Influent concentrations and removal performances of metals through municipal wastewater treatment processes. Water Sci. Technol. 63, 1967–1973. https://doi.org/10.2166/wst.2011.126

Thèse accessible à l'adresse : https://theses.insa-lyon.fr/publication/2025ISAL0011/these.pdf © [D. Gonçalves Portela], [2025], INSA Lyon, tous droits réservés

Collins, K.A., Lawrence, T.J., Stander, E.K., Jontos, R.J., Kaushal, Newcomer, T.A., Grimm, N.B., Ekberg, M.L.C., 2010. Opportunities and challenges for managing nitrogen in urban stormwater: A review and synthesis. Ecol. Eng. 36, 1507–1519. https://doi.org/doi:10.1016/j.ecoleng.2010.03.015

Cooper, P., 1999. A review of the design and performance of vertical-flow and hybrid reed bed treatment systems. Water Sci. Technol. 40. https://doi.org/10.1016/S0273-1223(99)00414-X

Cross, K., Tondera, K., Rizzo, A., Andrews, L., Pucher, B., Istenič, D., Karres, N., McDonald, R. (Eds.), 2021. Nature-Based Solutions for Wastewater Treatment: A Series of Factsheets and Case Studies. IWA Publishing. https://doi.org/10.2166/9781789062267

Davie, T., 2010. Fundamentals of hydrology, 2. ed., repr. (twice). ed, Routledge fundamentals of physical geography series. Routledge, London.

Del Río, H., Suárez, J., Puertas, J., Ures, P., 2013. PPCPs wet weather mobilization in a combined sewer in NW Spain. Sci. Total Environ. 449, 189–198. https://doi.org/10.1016/j.scitotenv.2013.01.049

Dittmer, U., 2006. Processes of retention and accumulation of carbon and nitrogen compounds in retention soil filters for combined sewer overflow. Technischen Universität Kaiserslautern, Kaiserslautern.

Dittmer, U., Meyer, D., Tondera, K., Lambert, B., Fuchs, S., 2016. Treatment Of CSO In Retention Soil Filters - Lessons Learned From 25 Years Of Research And Practice. Presented at the NOVATECH, Lyon, France.

Dong, H., Qiang, Z., Li, T., Jin, H., Chen, W., 2012. Effect of artificial aeration on the performance of vertical-flow constructed wetland treating heavily polluted river water. J. Environ. Sci. 24, 596–601. https://doi.org/10.1016/S1001-0742(11)60804-8

Dotro, G., Langergraber, G., Molle, P., Nivala, J., Puigagut, J., Stein, O., von Sperling, M., 2017. Biological Wastewater Treatment Series: Treatment Wetlands. IWA.

Dou, T., Troesch, S., Petitjean, A., Gábor, P.T., Esser, D., 2017. Wastewater and Rainwater Management in Urban Areas: A Role for Constructed Wetlands. Procedia Environ. Sci. 37, 535–541. https://doi.org/10.1016/j.proenv.2017.03.036

Dunqiu, W., Shaoyuan, B., Mingyu, W., Qinglin, X., Yinian, Z., Hua, Z., 2012. Effect of Artificial Aeration, Temperature, and Structure on Nutrient Removal in Constructed Floating Islands. Water Environ. Res. 84, 405–410. https://doi.org/10.2175/106143012X13347678384684

DWA-A178, 2019. Retentionsbodenfilteranlagen. Retention soil filter sites. German Association for Water, Wastewater and Waste. Hennef.

Ellis, J.B., Marsalek, J., Chocat, B., 2005. Urban Water Quality, in: Anderson, M.G., McDonnell, J.J. (Eds.), Encyclopedia of Hydrological Sciences. Wiley. https://doi.org/10.1002/0470848944.hsa099

European Commission 2022/0345(COD), 2022. Proposal for a Directive of the European Parliament and of the Council concerning urban wastewater treatment (recast) COM/2022/541.

European Union 91/271/EEC, 1991. Council Directive 91/271/EEC of 21 May 1991 concerning urban waste-water treatment.

European Union 2006/7/EC, 2006. DIRECTIVE 2006/7/EC OF THE EUROPEAN PARLIAMENT AND OF THE COUNCIL of 15 February 2006 concerning the management of bathing water quality and repealing Directive 76/160/EEC.

European Union 2008/105/EC, 2015. Directive 2006/123/EC of the European Parliament and of the Council of 12 December 2006.

Thèse accessible à l'adresse : https://theses.insa-lyon.fr/publication/2025ISAL0011/these.pdf © [D. Gonçalves Portela], [2025], INSA Lyon, tous droits réservés

European Union 2013/39, 2013. Directive 2013/39/EU of the European Parliament and of the Council of 12 August 2013 amending Directives 2000/60/EC and 2008/105/EC as regards priority substances in the field of water policy.

European Union 2020/741, 2020. REGULATION (EU) 2020/741 OF THE EUROPEAN PARLIAMENT AND OF THE COUNCIL of 25 May 2020 on minimum requirements for water reuse (Text with EEA relevance).

Fachini, A., Vasconcelos, M.T.S.D., 2006. Effects of zeolites on cultures of marine micro-algae: A brief review. Environ. Sci. Pollut. Res. 13, 414–417. https://doi.org/10.1065/espr2006.01.293

Fournel, J., 2012. Systemes Extensifs De Gestion Et De Traitement Des Eaux Urbaines De Temps De Pluie. Universite Montpellier II, France.

Frechen, F.-B., Schier, W., Felmeden, J., 2006. The Plant-Covered Retention Soil Filter (RSF): The Mechanical and Biological Combined Sewer Overflow (CSO) Treatment Plant. Eng. Life Sci. 6, 74–79. https://doi.org/10.1002/elsc.200620109

Freeman, A.I., Surridge, B.W.J., Matthews, M., Stewart, M., Haygarth, P.M., 2018. New approaches to enhance pollutant removal in artificially aerated wastewater treatment systems. Sci. Total Environ. 627, 1182–1194. https://doi.org/10.1016/j.scitotenv.2018.01.261

García, J., Rousseau, D.P.L., Morató, J., Lesage, E., Matamoros, V., Bayona, J.M., 2010. Contaminant Removal Processes in Subsurface-Flow Constructed Wetlands: A Review. Crit. Rev. Environ. Sci. Technol. 40, 561–661. https://doi.org/10.1080/10643380802471076

Garcia-Rodríguez, A., Matamoros, V., Fontàs, C., Salvadó, V., 2014. The ability of biologically based wastewater treatment systems to remove emerging organic contaminants—a review. Environ. Sci. Pollut. Res. 21, 11708–11728. https://doi.org/10.1007/s11356-013-2448-5

Gasperi, J., Laborie, B., Rocher, V., 2012a. Treatment of combined sewer overflows by ballasted flocculation: Removal study of a large broad spectrum of pollutants. Chem. Eng. J. 211–212, 293–301. https://doi.org/10.1016/j.cej.2012.09.025

Gasperi, J., Sebastian, C., Ruban, V., Delamain, M., Percot, S., Wiest, L., Mirande, C., Caupos, E., Demare, D., Kessoo, M.D.K., Saad, M., Schwartz, J.J., Dubois, P., Fratta, C., Wolff, H., Moilleron, R., Chebbo, G., Cren, C., Millet, M., Barraud, S., Gromaire, M.C., 2014. Micropollutants in urban stormwater: occurrence, concentrations, and atmospheric contributions for a wide range of contaminants in three French catchments. Environ. Sci. Pollut. Res. 21, 5267–5281. https://doi.org/10.1007/s11356-013-2396-0

Gasperi, J., Zgheib, S., Cladière, M., Rocher, V., Moilleron, R., Chebbo, G., 2012b. Priority pollutants in urban stormwater: Part 2 – Case of combined sewers. Water Res. 46, 6693–6703. https://doi.org/10.1016/j.watres.2011.09.041

Gilmore, K.R., Husovitz, K.J., Holst, T., Love, N.G., 1999. Influence of organic and ammonia loading on nitrifier activity and nitrification performance for a two-stage biological aerated filter system. Water Sci. Technol. 39. https://doi.org/10.1016/S0273-1223(99)00172-9

Gioia, A., Lioi, B., Totaro, V., Molfetta, M.G., Apollonio, C., Bisantino, T., Iacobellis, V., 2021. Estimation of Peak Discharges under Different Rainfall Depth–Duration–Frequency Formulations. Hydrology 8, 150. https://doi.org/10.3390/hydrology8040150

Gogien, F., Dechesne, M., Martinerie, R., Lipeme Kouyi, G., 2023. Assessing the impact of climate change on Combined Sewer Overflows based on small time step future rainfall timeseries and long-term continuous sewer network modelling. Water Res. 230, 119504. https://doi.org/10.1016/j.watres.2022.119504

Thèse accessible à l'adresse : https://theses.insa-lyon.fr/publication/2025ISAL0011/these.pdf © [D. Gonçalves Portela], [2025], INSA Lyon, tous droits réservés

Gooré Bi, E., Monette, F., Gasperi, J., 2015. Analysis of the influence of rainfall variables on urban effluents concentrations and fluxes in wet weather. J. Hydrol. 523, 320–332. https://doi.org/10.1016/j.jhydrol.2015.01.017

Hai, F.I., Li, X., Price, W.E., Nghiem, L.D., 2011. Removal of carbamazepine and sulfamethoxazole by MBR under anoxic and aerobic conditions. Bioresour. Technol. 102, 10386–10390. https://doi.org/10.1016/j.biortech.2011.09.019

Headley, T., Nivala, J., Kassa, K., Olsson, L., Wallace, S., Brix, H., van Afferden, M., Müller, R., 2013. Escherichia coli removal and internal dynamics in subsurface flow ecotechnologies: Effects of design and plants. Ecol. Eng. 61, 564–574. https://doi.org/10.1016/j.ecoleng.2013.07.062

Headley, T.R., Kadlec, R.H., 2007. Conducting hydraulic tracer studies of constructed wetlands: a practical guide. Ecohydrol. Hydrobiol. 7, 269–282. https://doi.org/10.1016/S1642-3593(07)70110-6

Heberer, T., 2002. Occurrence, fate, and removal of pharmaceutical residues in the aquatic environment: a review of recent research data. Toxicol. Lett. 131, 5–17. https://doi.org/10.1016/S0378-4274(02)00041-3

Ilyas, H., Masih, I., 2017. The performance of the intensified constructed wetlands for organic matter and nitrogen removal: A review. J. Environ. Manage. 198, 372–383. https://doi.org/10.1016/j.jenvman.2017.04.098

Ilyas, H., Masih, I., Van Hullebusch, E.D., 2021. Prediction of the removal efficiency of emerging organic contaminants based on design and operational parameters of constructed wetlands. J. Environ. Chem. Eng. 9, 104592. https://doi.org/10.1016/j.jece.2020.104592

Ilyas, H., Masih, I., Van Hullebusch, E.D., 2020. Pharmaceuticals' removal by constructed wetlands: a critical evaluation and meta-analysis on performance, risk reduction, and role of physicochemical properties on removal mechanisms. J. Water Health 18, 253–291. https://doi.org/10.2166/wh.2020.213

IPCC, 2023. Climate Change 2023: Synthesis Report. Contribution of Working Groups I, II and III to the Sixth Assessment Report of the Intergovernmental Panel on Climate Change [Core Writing Team, H. Lee and J. Romero (eds.)]. IPCC, Geneva, Switzerland. Intergovernmental Panel on Climate Change (IPCC). https://doi.org/10.59327/IPCC/AR6-9789291691647

Jamieson, T.S., Stratton, G.W., Gordon, R., Madani, A., 2003. The use of aeration to enhance ammonia nitrogen removal in constructed wetlands. Can. Biosyst. Eng. 45, 9–14.

Janzen, N., Banzhaf, S., Scheytt, T., Bester, K., 2009. Vertical flow soil filter for the elimination of micro pollutants from storm and waste water. Chemosphere 77, 1358–1365. https://doi.org/10.1016/j.chemosphere.2009.09.024

Jensen, D.M.R., Sandoval, S., Aubin, J.-B., Bertrand-Krajewski, J.-L., Xuyong, L., Mikkelsen, P.S., Vezzaro, L., 2022. Classifying pollutant flush signals in stormwater using functional data analysis on TSS MV curves. Water Res. 217, 118394. https://doi.org/10.1016/j.watres.2022.118394

John, Y., Langergraber, G., Adyel, T.M., Emery David, V., 2020. Aeration intensity simulation in a saturated vertical up-flow constructed wetland. Sci. Total Environ. 708, 134793. https://doi.org/10.1016/j.scitotenv.2019.134793

Kadlec, R., Wallace, S., 2008. Treatment Wetlands, 2nd ed. Taylor & Francis Group.

Kahl, S., Nivala, J., Van Afferden, M., Müller, R.A., Reemtsma, T., 2017. Effect of design and operational conditions on the performance of subsurface flow treatment wetlands: Emerging organic contaminants as indicators. Water Res. 125, 490–500. https://doi.org/10.1016/j.watres.2017.09.004

Thèse accessible à l'adresse : https://theses.insa-lyon.fr/publication/2025ISAL0011/these.pdf © [D. Gonçalves Portela], [2025], INSA Lyon, tous droits réservés

Khan, H.I.U.H., Groot, C.K., Schepers, O., Van Oirschot, D., Martens, M., Ronsse, F., Rousseau, D.P.L., 2022. Effect of controlled aeration on COD and nitrogen removal in aerated constructed wetlands used for effluent polishing. J. Environ. Chem. Eng. 10, 108043. https://doi.org/10.1016/j.jece.2022.108043

Kisielius, V., Äystö, L., Lehtinen, T., Kharel, S., Stapf, M., Zhiteneva, V., Perkola, N., Bester, K., 2024. Pharmaceutical emissions on the example of the Baltic Sea catchment: comparing measurements with multi-tier predictive models. J. Hazard. Mater. 476, 134998. https://doi.org/10.1016/j.jhazmat.2024.134998

König, A., Weidauer, C., Seiwert, B., Reemtsma, T., Unger, T., Jekel, M., 2016. Reductive transformation of carbamazepine by abiotic and biotic processes. Water Res. 101, 272–280. https://doi.org/10.1016/j.watres.2016.05.084

Kovalova, L., Siegrist, H., von Gunten, U., Eugster, J., Hagenbuch, M., Wittmer, A., Moser, R., McArdell, C.S., 2013. Elimination of Micropollutants during Post-Treatment of Hospital Wastewater with Powdered Activated Carbon, Ozone, and UV. Environ. Sci. Technol. 47, 7899–7908. https://doi.org/10.1021/es400708w

Kowalska, K., Felis, E., Sochacki, A., Bajkacz, S., 2019. Removal and transformation pathways of benzothiazole and benzotriazole in membrane bioreactors treating synthetic municipal wastewater. Chemosphere 227, 162–171. https://doi.org/10.1016/j.chemosphere.2019.04.037

Kugaprasatham, S., Nagaoka, H., Ohgaki, S., 1992. Effect of turbulence on nitrifying biofilms at non-limiting substrate conditions. Water Res. 26, 1629–1638. https://doi.org/10.1016/0043-1354(92)90162-W

Laber, J., 2000. Constructed wetland system for storm water treatment. J. Environ. Sci. Health Part A 35, 1279–1288. https://doi.org/10.1080/10934520009377036

Lamprea, K., Ruban, V., 2011. Pollutant concentrations and fluxes in both stormwater and wastewater at the outlet of two urban watersheds in Nantes (France). Urban Water J. 8, 219–231. https://doi.org/10.1080/1573062X.2011.596211

Langergraber, G., Dotro, G., Nivala, J., Rizzo, A., Stein, O.R. (Eds.), 2020. Practical information on design of specific wetland types and typical pitfalls, in: Wetland Technology: Practical Information on the Design and Application of Treatment Wetlands. IWA Publishing, pp. 83–125. https://doi.org/10.2166/9781789060171_0083

Langergraber, G., Dotro, G., Nivala, J., Stein, O.R., Rizzo, A. (Eds.), 2019. Wetland technology: practical information on the design and application of treatment wetlands, Scientific and technical report series. IWA Publishing, London.

Launay, M.A., Dittmer, U., Steinmetz, H., 2016. Organic micropollutants discharged by combined sewer overflows – Characterisation of pollutant sources and stormwater-related processes. Water Res. 104, 82–92. https://doi.org/10.1016/j.watres.2016.07.068

Lee, J., Bang, K.W., 2000. Characterization of urban stormwater runoff. Water Res. 34, 1773–1780. https://doi.org/10.1016/S0043-1354(99)00325-5

Lei, Y., Rijnaarts, H., Langenhoff, A., 2022. Mesocosm constructed wetlands to remove micropollutants from wastewater treatment plant effluent: Effect of matrices and pre-treatments. Chemosphere 305, 135306. https://doi.org/10.1016/j.chemosphere.2022.135306

Li, Y.L., Deletic, A., Alcazar, L., Bratieres, K., Fletcher, T.D., McCarthy, D.T., 2012. Removal of Clostridium perfringens, Escherichia coli and F-RNA coliphages by stormwater biofilters. Ecol. Eng. 49, 137–145. https://doi.org/10.1016/j.ecoleng.2012.08.007

Lough, G.C., Schauer, J.J., Park, J.-S., Deminter, J.T., Weinstein, J.P., 2005. Emissions of Metals Associated with Motor Vehicle Roadways. Environ. Sci. Technol. 39, 826–836.

Madoux-Humery, A.-S., Dorner, S., Sauvé, S., Aboulfadl, K., Galarneau, M., Servais, P., Prévost, M., 2013. Temporal variability of combined sewer overflow contaminants:

Thèse accessible à l'adresse : https://theses.insa-lyon.fr/publication/2025ISAL0011/these.pdf © [D. Gonçalves Portela], [2025], INSA Lyon, tous droits réservés

Evaluation of wastewater micropollutants as tracers of fecal contamination. Water Res. 47, 4370–4382. https://doi.org/10.1016/j.watres.2013.04.030

Madoux-Humery, A.-S., Dorner, S.M., Sauvé, S., Aboulfadl, K., Galarneau, M., Servais, P., Prévost, M., 2015. Temporal analysis of E. coli, TSS and wastewater micropollutant loads from combined sewer overflows: implications for management. Environ. Sci. Process. Impacts 17, 965–974. https://doi.org/10.1039/C5EM00093A

Mailler, R., Gasperi, J., Coquet, Y., Buleté, A., Vulliet, E., Deshayes, S., Zedek, S., Mirande-Bret, C., Eudes, V., Bressy, A., Caupos, E., Moilleron, R., Chebbo, G., Rocher, V., 2016. Removal of a wide range of emerging pollutants from wastewater treatment plant discharges by micro-grain activated carbon in fluidized bed as tertiary treatment at large pilot scale. Sci. Total Environ. 542, 983–996. https://doi.org/10.1016/j.scitotenv.2015.10.153

Malaviya, P., Singh, A., 2012. Constructed Wetlands for Management of Urban Stormwater Runoff. Crit. Rev. Environ. Sci. Technol. 42, 2153–2214. https://doi.org/10.1080/10643389.2011.574107

Maltais-Landry, G., Maranger, R., Brisson, J., Chazarenc, F., 2009. Nitrogen transformations and retention in planted and artificially aerated constructed wetlands. Water Res. 43, 535–545. https://doi.org/10.1016/j.watres.2008.10.040

Manini, E., Baldrighi, E., Ricci, F., Grilli, F., Giovannelli, D., Intoccia, M., Casabianca, S., Capellacci, S., Marinchel, N., Penna, P., Moro, F., Campanelli, A., Cordone, A., Correggia, M., Bastoni, D., Bolognini, L., Marini, M., Penna, A., 2022. Assessment of Spatio-Temporal Variability of Faecal Pollution along Coastal Waters during and after Rainfall Events. Water 14, 502. https://doi.org/10.3390/w14030502

Margot, J., Kienle, C., Magnet, A., Weil, M., Rossi, L., De Alencastro, L.F., Abegglen, C., Thonney, D., Chèvre, N., Schärer, M., Barry, D.A., 2013. Treatment of micropollutants in municipal wastewater: Ozone or powdered activated carbon? Sci. Total Environ. 461–462, 480–498. https://doi.org/10.1016/j.scitotenv.2013.05.034

Margot, J., Magnet, A., Thonney, A., Chèvre, D., De Alencastro, F., Rossi, L., 2011. Treatment of micropollutants inwastewater. Final report on Vidy (Lausannes) WWTP pilot tests. FOEN, Switzerland.

Masi, F., Rizzo, A., Bresciani, R., Conte, G., 2017. Constructed wetlands for combined sewer overflow treatment: Ecosystem services at Gorla Maggiore, Italy. Ecol. Eng. 98, 427–438. https://doi.org/10.1016/j.ecoleng.2016.03.043

Masi, F., Sarti, C., Cincinelli, A., Bresciani, R., Martinuzzi, N., Bernasconi, M., Rizzo, A., 2023. Constructed wetlands for the treatment of combined sewer overflow upstream of centralized wastewater treatment plants. Ecol. Eng. 193. https://doi.org/doi.org/10.1016/j.ecoleng.2023.107008

Matamoros, V., Arias, C., Brix, H., Bayona, J.M., 2007. Removal of Pharmaceuticals and Personal Care Products (PPCPs) from Urban Wastewater in a Pilot Vertical Flow Constructed Wetland and a Sand Filter. Environ. Sci. Technol. 41, 8171–8177. https://doi.org/10.1021/es071594+

Matamoros, V., Nguyen, L.X., Arias, C.A., Salvadó, V., Brix, H., 2012. Evaluation of aquatic plants for removing polar microcontaminants: A microcosm experiment. Chemosphere 88, 1257–1264. https://doi.org/10.1016/j.chemosphere.2012.04.004

Matamoros, V., Rodríguez, Y., Albaigés, J., 2016. A comparative assessment of intensive and extensive wastewater treatment technologies for removing emerging contaminants in small communities. Water Res. 88, 777–785. https://doi.org/10.1016/j.watres.2015.10.058

Thèse accessible à l'adresse : https://theses.insa-lyon.fr/publication/2025ISAL0011/these.pdf © [D. Gonçalves Portela], [2025], INSA Lyon, tous droits réservés

McBride, G.B., Tanner, C.C., 1999. Modelling biofilm nitrogen transformations in constructed wetland mesocosms with fluctuating water levels. Ecol. Eng. 14, 93–106. https://doi.org/10.1016/S0925-8574(99)00022-1

McDowell-Boyer, L.M., Hunt, J.R., Sitar, N., 1986. Particle transport through porous media. Water Resour. Res. 22, 1901–1921. https://doi.org/10.1029/WR022i013p01901

Metcalf, E., Abu-Orf, M., Bowden, G., Burton, F., Pfrang, W., Stensel, H., Tchobanoglous, G., Tsuchihashi, R., 2014. Wastewater engineering: treatment and resource recovery. New York: McGraw.

Meyer, D., Molle, P., Esser, D., Troesch, S., Dittmer, U., Masi, F., 2013. Constructed Wetlands for Combined Sewer Overflow Treatment—Comparison of German, French and Italian Approaches. Water 5, 12. https://doi.org/doi:10.3390/w5010001

Miyazaki, C.K., Morvannou, A., Higelin, E., Nivala, J., Molle, P., 2023. Aeration strategies and total nitrogen removal in a hybrid aerated treatment wetland. Blue-Green Syst. 5, 321–335. https://doi.org/10.2166/bgs.2023.045

Molle, P., Fournel, J., Meyer, D., Troesch, S., Clement, F., E. Brelot, L. Bacot, S. Guillermard, C. de Brito, J. Y. Toussaint, 2013. Système extensif pour la gestion et le traitement des eaux urbaines de temps de pluie.

Molle, P., Liénard, A., Boutin, C., Merlin, G., Iwema, A., 2005. How to treat raw sewage with constructed wetlands: an overview of the French systems. Water Sci. Technol. 51, 11–21. https://doi.org/10.2166/wst.2005.0277

Montoya-Coronado, V.A., Bret, P., Molle, P., Castebrunet, H., Tedoldi, D., Lipeme Kouyi, G., 2022. Stratégies de déconnexion des eaux pluviales à l'échelle d'un bassin versant pour réduire les déversements: C. Tech. Sci. Méthodes 27–37. https://doi.org/10.36904/tsm/202204027

Montoya-Coronado, V.A., Tedoldi, D., Lenormand, E., Castebrunet, H., Molle, P., Lipeme Kouyi, G., 2024. Combined sewer overflow mitigation through SUDS - A review on modelling practices, scenario elaboration, and related performances. J. Environ. Manage. 362, 121073. https://doi.org/10.1016/j.jenvman.2024.121073

Morvannou, A., Choubert, J.-M., Vanclooster, M., Molle, P., 2014. Modeling nitrogen removal in a vertical flow constructed wetland treating directly domestic wastewater. Ecol. Eng. 70, 379–386. https://doi.org/10.1016/j.ecoleng.2014.06.034

Morvannou, A., Troesch, S., Esser, D., Forquet, N., Petitjean, A., Molle, P., 2017. Using one filter stage of unsaturated/saturated vertical flow filters for nitrogen removal and footprint reduction of constructed wetlands. Water Sci. Technol. 76, 124–133. https://doi.org/10.2166/wst.2017.115

Murphy, C., Rajabzadeh, A.R., Weber, K.P., Nivala, J., Wallace, S.D., Cooper, D.J., 2016. Nitrification cessation and recovery in an aerated saturated vertical subsurface flow treatment wetland: Field studies and microscale biofilm modeling. Bioresour. Technol. 209, 125–132. https://doi.org/10.1016/j.biortech.2016.02.065

Mutzner, L., Furrer, V., Castebrunet, H., Dittmer, U., Fuchs, S., Gernjak, W., Gromaire, M.-C., Matzinger, A., Mikkelsen, P.S., Selbig, W.R., Vezzaro, L., 2022. A decade of monitoring micropollutants in urban wet-weather flows: What did we learn? Water Res. 223, 118968. https://doi.org/10.1016/j.watres.2022.118968

Nickel, J.P., Fuchs, S., 2019. Micropollutant emissions from combined sewer overflows. Water Sci. Technol. 80, 2179–2190. https://doi.org/10.2166/wst.2020.035

Nivala, J., Kahl, S., Boog, J., Van Afferden, M., Reemtsma, T., Müller, R.A., 2019. Dynamics of emerging organic contaminant removal in conventional and intensified subsurface flow treatment wetlands. Sci. Total Environ. 649, 1144–1156. https://doi.org/10.1016/j.scitotenv.2018.08.339

Thèse accessible à l'adresse : https://theses.insa-lyon.fr/publication/2025ISAL0011/these.pdf © [D. Gonçalves Portela], [2025], INSA Lyon, tous droits réservés

Nivala, J., Murphy, C., Freeman, A., 2020. Recent Advances in the Application, Design, and Operations & Maintenance of Aerated Treatment Wetlands. Water 12, 1188. https://doi.org/10.3390/w12041188
Nivala, J., Wallace, S., Headley, T., Kassa, K., Brix, H., Van Afferden, M., Müller, R., 2013. Oxygen transfer and consumption in subsurface flow treatment wetlands. Ecol. Eng. 61, 544–554. https://doi.org/10.1016/j.ecoleng.2012.08.028
Nivala, J., Wallace, S., Van Afferden, M., Müller, R.A., 2022. Evapotranspiration dynamics in aerated and non-aerated subsurface flow treatment wetlands. Sci. Total Environ. 843, 156605. https://doi.org/10.1016/j.scitotenv.2022.156605
Noyer, M., Reoyo-Prats, B., Aubert, D., Bernard, M., Verneau, O., Palacios, C., 2020. Particle-attached riverine bacteriome shifts in a pollutant-resistant and pathogenic community during a Mediterranean extreme storm event. Sci. Total Environ. 732, 139047. https://doi.org/10.1016/j.scitotenv.2020.139047
Oral, H.V., Carvalho, P., Gajewska, M., Ursino, N., Masi, F., Hullebusch, E.D. van, Kazak, J.K., Exposito, A., Cipolletta, G., Andersen, T.R., Finger, D.C., Simperler, L., Regelsberger, M., Rous, V., Radinja, M., Buttiglieri, G., Krzeminski, P., Rizzo, A., Dehghanian, K., Nikolova, M., Zimmermann, M., 2020. A review of nature-based solutions for urban water management in European circular cities: a critical assessment based on case studies and literature. Blue-Green Syst. 2, 112–136. https://doi.org/10.2166/bgs.2020.932
Pálfy, T.G., Gerodolle, M., Gourdon, R., Meyer, D., Troesch, S., Molle, P., 2017a. Performance assessment of a vertical flow constructed wetland treating unsettled combined sewer overflow. Water Sci. Technol. 75, 2586–2597. https://doi.org/10.2166/wst.2017.126
Pálfy, T.G., Gourdon, R., Meyer, D., Troesch, S., Molle, P., 2017b. Model-based optimization of constructed wetlands treating combined sewer overflow. Ecol. Eng. 101, 261–267. https://doi.org/10.1016/j.ecoleng.2017.01.020
Pálfy, T.G., Gourdon, R., Meyer, D., Troesch, S., Olivier, L., Molle, P., 2017c. Filling hydraulics and nitrogen dynamics in constructed wetlands treating combined sewer overflows. Ecol. Eng. 101, 137–144. https://doi.org/10.1016/j.ecoleng.2017.01.008
Palli, L., Giordano Rosadoni, Francesco Mori, Omar Milighetti, Claudio Lubello, 2021. Presence and behavior of metals in public sewage: long-term modelling with EPA SWMM. Urban Water J. 18, 53–60. https://doi.org/10.1080/1573062X.2020.1857799
Passerat, J., Ouattara, N.K., Mouchel, J.-M., Vincent Rocher, Servais, P., 2011. Impact of an intense combined sewer overflow event on the microbiological water quality of the Seine River. Water Res. 45, 893–903. https://doi.org/10.1016/j.watres.2010.09.024
Perera, T., McGree, J., Egodawatta, P., Jinadasa, K.B.S.N., Goonetilleke, A., 2019. Taxonomy of influential factors for predicting pollutant first flush in urban stormwater runoff. Water Res. 166, 115075. https://doi.org/10.1016/j.watres.2019.115075
Perry, W.B., Ahmadian, R., Munday, M., Jones, O., Ormerod, S.J., Durance, I., 2024. Addressing the challenges of combined sewer overflows. Environ. Pollut. 343, 123225. https://doi.org/10.1016/j.envpol.2023.123225
Phillips, P.J., Chalmers, A.T., Gray, J.L., Kolpin, D.W., Foreman, W.T., Wall, G.R., 2012. Combined Sewer Overflows: An Environmental Source of Hormones and Wastewater Micropollutants. Environ. Sci. Technol. 46, 5336–5343. https://doi.org/10.1021/es3001294
Platzer, C., 1999. Design recommendations for subsurface flow constructed wetlands for nitrification and denitrification. Water Sci. Technol. 40, 257–263.
Reddy, C.M., Quinn, J.G., 1997. Environmental Chemistry of Benzothiazoles Derived from Rubber. Environ. Sci. Technol. 31, 2847–2853. https://doi.org/10.1021/es970078o

Thèse accessible à l'adresse : https://theses.insa-lyon.fr/publication/2025ISAL0011/these.pdf © [D. Gonçalves Portela], [2025], INSA Lyon, tous droits réservés

Redmond, E.D., Just, C.L., Parkin, G.F., 2014. Nitrogen Removal from Wastewater by an Aerated Subsurface-Flow Constructed Wetland in Cold Climates. Water Environ. Res. 86, 305–313. https://doi.org/10.2175/106143013X13736496908591

Reed, S.C., Crites, R.W., Middlebrooks, E.J., 1995. Natural systems for waste management and treatment, 2. ed. ed, McGraw-Hill books of interest. McGraw-Hill, New York, NY.

Reemtsma, Thorsten., Fiehn, Oliver., Kalnowski, Guenter., Jekel, Martin., 1995. Microbial Transformations and Biological Effects of Fungicide-Derived Benzothiazoles Determined in Industrial Wastewater. Environ. Sci. Technol. 29, 478–485. https://doi.org/10.1021/es00002a025

Rizzo, A., Bresciani, R., Masi, F., Boano, F., Revelli, R., Ridolfi, L., 2018. Flood reduction as an ecosystem service of constructed wetlands for combined sewer overflow. J. Hydrol. 560, 150–159. https://doi.org/10.1016/j.jhydrol.2018.03.020

Rizzo, A., Tondera, K., Pálfy, T.G., Dittmer, U., Meyer, D., Schreiber, C., Zacharias, N., Ruppelt, J.P., Esser, D., Molle, P., Troesch, S., Masi, F., 2020. Constructed wetlands for combined sewer overflow treatment: A state-of-the-art review. Sci. Total Environ. 727, 138618. https://doi.org/10.1016/j.scitotenv.2020.138618

Rodgers, T.F.M., Wang, Y., Humes, C., Jeronimo, M., Johannessen, C., Spraakman, S., Giang, A., Scholes, R.C., 2023. Bioretention Cells Provide a 10-Fold Reduction in 6PPD-Quinone Mass Loadings to Receiving Waters: Evidence from a Field Experiment and Modeling. Environ. Sci. Technol. Lett. 10, 582–588. https://doi.org/10.1021/acs.estlett.3c00203

Rogers, H.R., 1996. Sources, behaviour and fate of organic contaminants during sewage treatment and in sewage sludges. Sci. Total Environ. 185, 3–26. https://doi.org/10.1016/0048-9697(96)05039-5

Ruppelt, J.P., Pinnekamp, J., Tondera, K., 2020. Elimination of micropollutants in four test-scale constructed wetlands treating combined sewer overflow: Influence of filtration layer height and feeding regime. Water Res. 169, 115214. https://doi.org/10.1016/j.watres.2019.115214

Ruppelt, J.P., Tondera, K., Schreiber, C., Kistemann, T., Pinnekamp, J., 2018. Reduction of bacteria and somatic coliphages in constructed wetlands for the treatment of combined sewer overflow (retention soil filters). Int. J. Hyg. Environ. Health 221, 727–733. https://doi.org/10.1016/j.ijheh.2018.04.011

Ruppelt, J.P., Tondera, K., Vorenhout, M., Van der Weken, L., Pinnekamp, J., 2019. Redox potential as a method to evaluate the performance of retention soil filters treating combined sewer overflows. Sci. Total Environ. 650, 1628–1639. https://doi.org/10.1016/j.scitotenv.2018.09.043

Ryu, J., Oh, J., Snyder, S.A., Yoon, Y., 2014. Determination of micropollutants in combined sewer overflows and their removal in a wastewater treatment plant (Seoul, South Korea). Environ. Monit. Assess. 186, 3239–3251. https://doi.org/10.1007/s10661-013-3613-5

Saeed, T., 2012. A review on nitrogen and organics removal mechanisms in subsurface flow constructed wetlands: Dependency on environmental parameters, operating conditions and supporting media. J. Environ. Manage.

Salerno, F., Gaetano, V., Gianni, T., 2018. Urbanization and climate change impacts on surface water quality: Enhancing the resilience by reducing impervious surfaces. Water Res. 144, 491–502. https://doi.org/10.1016/j.watres.2018.07.058

Samrani, A.G.E., Lartiges, B.S., Ghanbaja, J., Yvon, J., Kohler, A., 2004. Trace element carriers in combined sewer during dry and wet weather: an electron microscope investigation. Water Res.

Thèse accessible à l'adresse : https://theses.insa-lyon.fr/publication/2025ISAL0011/these.pdf © [D. Gonçalves Portela], [2025], INSA Lyon, tous droits réservés

Sanders, P.G., Xu, N., Dalka, T.M., Maricq, M.M., 2003. Airborne Brake Wear Debris: Size Distributions, Composition, and a Comparison of Dynamometer and Vehicle Tests. Environ. Sci. Technol. 37, 4060–4069.

Scheurer, M., Heß, S., Lüddeke, F., Sacher, F., Güde, H., Löffler, H., Gallert, C., 2015. Removal of micropollutants, facultative pathogenic and antibiotic resistant bacteria in a full-scale retention soil filter receiving combined sewer overflow. Environ. Sci. Process. Impacts 17, 186–196. https://doi.org/10.1039/C4EM00494A

Schmitt, N., Wanko, A., Laurent, J., Bois, P., Molle, P., Mosé, R., 2015. Constructed wetlands treating stormwater from separate sewer networks in a residential Strasbourg urban catchment area: Micropollutant removal and fate. J. Environ. Chem. Eng. 3, 2816–2824. https://doi.org/10.1016/j.jece.2015.10.008

Seidl, M., Servais, P., Mouchel, J.M., 1998. Organic matter transport and degradation in the river Seine (France) after a combined sewer overflow. Water Res. 32, 3569–3580. https://doi.org/10.1016/S0043-1354(98)00169-9

Seiwert, B., Nihemaiti, M., Troussier, M., Weyrauch, S., Reemtsma, T., 2022. Abiotic oxidative transformation of 6-PPD and 6-PPD quinone from tires and occurrence of their products in snow from urban roads and in municipal wastewater. Water Res. 212, 118122. https://doi.org/10.1016/j.watres.2022.118122

Séranne, L., Prost-Boucle, S., Clément, R., Nivala, J., Gillot, S., Molle, P., 2021. Influence of airflow, material type, and dripline density on gas transfer and bubble pathways in aerated vertical flow treatment wetlands. University of Natural Resources and Life Sciences, Vienna.

Shirdashtzadeh, M., Chua, L.H.C., Brau, L., 2022. Microbial Communities and Nitrogen Transformation in Constructed Wetlands Treating Stormwater Runoff. Front. Water 3, 751830. https://doi.org/10.3389/frwa.2021.751830

Shoushtarian, F., Negahban-Azar, M., 2020. Worldwide Regulations and Guidelines for Agricultural Water Reuse: A Critical Review. Water 12, 971. https://doi.org/10.3390/w12040971

Shutes, R.B.E., Revitt, D.M., Mungur, A.S., Scholes, L.N.L., 1997. The design of wetland systems for the treatment of urban run off. Water Sci. Technol. 35. https://doi.org/10.1016/S0273-1223(97)00048-6

Silva Thomsen, L.B., Carvalho, P.N., Dos Passos, J.S., Anastasakis, K., Bester, K., Biller, P., 2020. Hydrothermal liquefaction of sewage sludge; energy considerations and fate of micropollutants during pilot scale processing. Water Res. 183, 116101. https://doi.org/10.1016/j.watres.2020.116101

Soriano, L., Rubió, J., 2019. Impacts of Combined Sewer Overflows on surface water bodies. The case study of the Ebro River in Zaragoza city. J. Clean. Prod. 226, 1–5. https://doi.org/10.1016/j.jclepro.2019.04.033

Sorme, L., Lagerkvist, R., 2002. Sources of heavy metals in urban wastewater in Stockholm. Sci. Total Environ. 298, 131–145. https://doi.org/10.1016/S0048-9697(02)00197-3

Sperling, M. von, Verbyla, M.E., Oliveira, S.M.A.C., 2020. Assessment of Treatment Plant Performance and Water Quality Data: A Guide for Students, Researchers and Practitioners, First edition. ed. IWA Publishing, London. https://doi.org/10.2166/9781780409320

Stefanakis, A., 2019. The Role of Constructed Wetlands as Green Infrastructure for Sustainable Urban Water Management. Sustainability 11, 6981. https://doi.org/10.3390/su11246981

Stefanakis, A.I., Bardiau, M., Trajano, D., Couceiro, F., Williams, J.B., Taylor, H., 2019. Presence of bacteria and bacteriophages in full-scale trickling filters and an aerated

Thèse accessible à l'adresse : https://theses.insa-lyon.fr/publication/2025ISAL0011/these.pdf © [D. Gonçalves Portela], [2025], INSA Lyon, tous droits réservés

constructed wetland. Sci. Total Environ. 659, 1135–1145. https://doi.org/10.1016/j.scitotenv.2018.12.415
Sternbeck, J., Sjödin, Å., Andréasson, K., 2002. Metal emissions from road traffic and the influence of resuspension—results from two tunnel studies. Atmos. Environ. 36, 4735–4744. https://doi.org/10.1016/S1352-2310(02)00561-7
Stott, R., Sukias, J.P.S., McKergow, L.A., Davies-Colley, R.J., Tanner, C.C., 2023. Net export of E. coli from a constructed wetland treating agricultural drainage. Ecol. Eng. 194, 107023. https://doi.org/10.1016/j.ecoleng.2023.107023
Stott, R., Tondera, K., Blecken, G.-T., Schreiber, C., 2018. Chapter 4 Microbial Loads and Removal Efficiency Under Varying Flows, in: Ecotechnologies for the Treatment of Variable Stormwater and Wastewater Flows. pp. 54–74.
Sui, Q., Huang, J., Deng, S., Yu, G., Fan, Q., 2010. Occurrence and removal of pharmaceuticals, caffeine and DEET in wastewater treatment plants of Beijing, China. Water Res. 44, 417–426. https://doi.org/10.1016/j.watres.2009.07.010
Tadić, Đ., Sauvêtre, A., Cerqueira, F., Lestremau, F., Ait-Mouheb, N., Chiron, S., 2024. Partially saturated vertical surface flow constructed wetland for emerging contaminants and antibiotic resistance genes removal from wastewater: The effect of bioaugmentation with Trichoderma. J. Environ. Chem. Eng. 12, 112128. https://doi.org/10.1016/j.jece.2024.112128
Tang, X., Huang, S., Scholz, M., Li, J., 2009. Nutrient Removal in Pilot-Scale Constructed Wetlands Treating Eutrophic River Water: Assessment of Plants, Intermittent Artificial Aeration and Polyhedron Hollow Polypropylene Balls. Water. Air. Soil Pollut. 197, 61–73. https://doi.org/10.1007/s11270-008-9791-z
Tanner, C.C., 1996. Plants for constructed wetland treatment systems — A comparison of the growth and nutrient uptake of eight emergent species. Ecol. Eng. 7, 59–83. https://doi.org/10.1016/0925-8574(95)00066-6
Tao, J., Mancl, K.M., Tuovinen, O.H., 2010. Attenuation of pollutants in sanitary sewer overflow: Comparative evaluation of treatment with fixed media bioreactors. Bioresour. Technol. 101, 1781–1786. https://doi.org/10.1016/j.biortech.2009.10.038
Tao, W., Bays, J., Meyer, D., Smardon, R., Levy, Z., 2014. Constructed Wetlands for Treatment of Combined Sewer Overflow in the US: A Review of Design Challenges and Application Status. Water 6, 3362–3385. https://doi.org/10.3390/w6113362
Tchobanoglous, G., Burton, F.L., Stensel, H.D., Metcalf & Eddy, Inc (Eds.), 2003. Wastewater engineering: treatment and reuse, 4. ed., internat. ed., [Nachdr.]. ed, McGraw-Hill series in civil and environmental engineering. McGraw-Hill, Boston, Mass.
Thorpe, A., Harrison, R.M., 2008. Sources and properties of non-exhaust particulate matter from road traffic: A review. Sci. TOTAL Environ.
Tondera, K., 2019. Evaluating the performance of constructed wetlands for the treatment of combined sewer overflows. Ecol. Eng. 137, 53–59. https://doi.org/10.1016/j.ecoleng.2017.10.009
Tondera, K., Blecken, G.-T., Chazarenc, F., Tanner, C.C. (Eds.), 2018. Ecotechnologies for the Treatment of Variable Stormwater and Wastewater Flows, SpringerBriefs in Water Science and Technology. Springer International Publishing, Cham. https://doi.org/10.1007/978-3-319-70013-7
Tondera, K., Koenen, S., Pinnekamp, J., 2013. Survey monitoring results on the reduction of micropollutants, bacteria, bacteriophages and TSS in retention soil filters. Water Sci. Technol. 68, 1004–1012. https://doi.org/10.2166/wst.2013.340
Tondera, K., Rizzo, A., Molle, P., 2021. Treatment wetlands for combined sewer overflow, in: Nature-Based Solutions for Wastewater Treatment. IWA Publishing, p. 344.

Thèse accessible à l'adresse : https://theses.insa-lyon.fr/publication/2025ISAL0011/these.pdf © [D. Gonçalves Portela], [2025], INSA Lyon, tous droits réservés

Tondera, K., Ruppelt, J.P., Pinnekamp, J., Kistemann, T., Schreiber, C., 2019. Reduction of micropollutants and bacteria in a constructed wetland for combined sewer overflow treatment after 7 and 10 years of operation. Sci. Total Environ. 651, 917–927. https://doi.org/10.1016/j.scitotenv.2018.09.174

Trognon, J., Albasi, C., Choubert, J.-M., 2024. A critical review on the pathways of carbamazepine transformation products in oxidative wastewater treatment processes. Sci. Total Environ. 912, 169040. https://doi.org/10.1016/j.scitotenv.2023.169040

Uggetti, E., Hughes-Riley, T., Morris, R.H., Newton, M.I., Trabi, C.L., Hawes, P., Puigagut, J., García, J., 2016. Intermittent aeration to improve wastewater treatment efficiency in pilot-scale constructed wetland. Sci. Total Environ. 559, 212–217. https://doi.org/10.1016/j.scitotenv.2016.03.195

Uhl, M., Dittmer, U., 2005. Constructed wetlands for CSO treatment: an overview of practice and research in Germany. Water Sci. Technol. 51, 23–30.

Van Leerdam, J.A., Hogenboom, A.C., Van Der Kooi, M.M.E., De Voogt, P., 2009. Determination of polar 1H-benzotriazoles and benzothiazoles in water by solid-phase extraction and liquid chromatography LTQ FT Orbitrap mass spectrometry. Int. J. Mass Spectrom. 282, 99–107. https://doi.org/10.1016/j.ijms.2009.02.018

Vera-Puerto, I., Campal, J., Martínez, S., Cortés-Rico, L., Coy, H., Tan, S., Arias, C.A., Baquero-Rodríguez, G., Rosso, D., 2022. Effects of Environmental Conditions and Bed Configuration on Oxygen Transfer Efficiency in Aerated Constructed Wetlands. Water 14, 3284. https://doi.org/10.3390/w14203284

Villaverde, S., 2000. Nitrifying biofilm acclimation to free ammonia in submerged biofilters. Start-up influence. Water Res. 34, 602–610. https://doi.org/10.1016/S0043-1354(99)00175-X

Vymazal, J., 2007. Removal of nutrients in various types of constructed wetlands. Sci. Total Environ. 380, 48–65. https://doi.org/10.1016/j.scitotenv.2006.09.014

Vymazal, J., 1999. Removal of BOD5 in constructed wetlands with horizontal sub-surface flow: Czech experience. Water Sci. Technol. 40, 133–138. https://doi.org/doi.org/10.1016/S0273-1223(99)00456-4

Waldhoff, A., 2008. Hygienisierung von Mischwasser in Retentionsbodenfiltern (RBF). Sanitation of Combined Sewage in Retention Soil Filters (Disserattion). Kassel.

Wallace, S., Nivala, J., Meyers, T., 2008. Statistical Analysis of Treatment Performance in Aerated and Nonaerated Subsurface Flow Constructed Wetlands, in: Vymazal, J. (Ed.), Wastewater Treatment, Plant Dynamics and Management in Constructed and Natural Wetlands. Springer Netherlands, Dordrecht, pp. 171–180. https://doi.org/10.1007/978-1-4020-8235-1_15

Wallace, S., Oirschot, D., Stefanakis, A., 2020. Aerated Wetlands, in: Wetland Technology: Practical Information on the Design and Application of Treatment Wetlands. IWA Publishing, pp. 105–107.

Wießner, A., Kappelmeyer, U., Kuschk, P., Kästner, M., 2005. Influence of the redox condition dynamics on the removal efficiency of a laboratory-scale constructed wetland. Water Res. 39, 248–256. https://doi.org/10.1016/j.watres.2004.08.032

Woods Ballard, B., Wilson, S., Udale-Clarke, H., Illman, S., Scott, T., Ashley, R., Kellagher, R., 2016. The SuDs Manual. CIRIA, London.

Woźniak, R., Dittmer, U., Welker, A., 2007. Interaction of oxygen concentration and retention of pollutants in vertical flow constructed wetlands for CSO treatment. Water Sci. Technol. 56, 31–38. https://doi.org/10.2166/wst.2007.502

Wynn, T.M., Liehr, S.K., 2001. Development of a constructed subsurface-flow wetland simulation model. Ecol. Eng. 16, 519–536. https://doi.org/10.1016/S0925-8574(00)00115-4

Thèse accessible à l'adresse : https://theses.insa-lyon.fr/publication/2025ISAL0011/these.pdf © [D. Gonçalves Portela], [2025], INSA Lyon, tous droits réservés

Yavuz Corapcioglu, M., Haridas, A., 1984. Transport and fate of microorganisms in porous media: A theoretical investigation. J. Hydrol. 72, 149–169. https://doi.org/10.1016/0022-1694(84)90189-6

Yin, H., Lu, Y., Xu, Z., Li, H., Schwegler, B.R., 2017. Characteristics of the overflow pollution of storm drains with inappropriate sewage entry. Environ. Sci. Pollut. Res. 24, 4902–4915. https://doi.org/10.1007/s11356-016-8145-4

Zacharias, N., Essert, S.M., Brunsch, A.F., Christoffels, E., Kistemann, T., Schreiber, C., 2020. Performance of retention soil filters for the reduction of hygienically-relevant microorganisms in combined sewage overflow and treated wastewater. Water Sci. Technol. 81, 535–543. https://doi.org/10.2166/wst.2020.132

Zhang, D., Gersberg, R.M., Ng, W.J., Tan, S.K., 2014. Removal of pharmaceuticals and personal care products in aquatic plant-based systems: A review. Environ. Pollut. 184, 620–639. https://doi.org/10.1016/j.envpol.2013.09.009

Zhang, Linshan, Zhang, Lifu, Zhang, D., Cen, Y., Wang, S., Zhang, Y., Gao, L., 2023. Analysis of Seasonal Water Characteristics and Water Quality Responses to the Land Use/Land Cover Pattern: A Case Study in Tianjin, China. Water 15, 867. https://doi.org/10.3390/w15050867

Zheng, X., Zhuang, L.-L., Zhang, J., Li, X., Zhao, Q., Song, X., Dong, C., Liao, J., 2020. Advanced oxygenation efficiency and purification of wastewater using a constant partially unsaturated scheme in column experiments simulating vertical subsurface flow constructed wetlands. Sci. Total Environ. 703, 135480. https://doi.org/10.1016/j.scitotenv.2019.135480

Thèse accessible à l'adresse : https://theses.insa-lyon.fr/publication/2025ISAL0011/these.pdf © [D. Gonçalves Portela], [2025], INSA Lyon, tous droits réservés

FOLIO ADMINISTRATIF

THESE DE L'INSA LYON, MEMBRE DE L'UNIVERSITE DE LYON

NOM : GONÇALVES PORTELA DATE de SOUTENANCE : 05/02/2025

Prénoms : Daniella

TITRE : Treatment of combined sewer overflow by vertical flow treatment wetland with new design to improve water quality

NATURE : Doctorat Numéro d'ordre : 2025ISAL0011

Ecole doctorale : Chimie

Spécialité : Génie des procédés

RESUME :
Combined sewer overflow (CSO) spills are significant sources of aquatic pollution and have been effectively treated using vertical flow constructed wetlands. However, the system's performance in removing dissolved pollutants and micropollutants can be influenced by rainfall characteristics. For this reason, two vertical flow constructed wetlands (CSOA and CSOB), featuring a new design with forced aeration and a saturated layer of approximately one meter, were tested over a period of one and a half years. The top layer in CSOA was gravel, while CSOB was sand and also a transition layer. Tracer tests were conducted to evaluate their hydrodynamics. Aeration strategies were tested in CSOA, and the optimal aeration strategy was subsequently applied to both filters for comparison. The effects of variable organic and hydraulic loads were also assessed. Global water quality parameters, micropollutants and samples of fecal indicators (FI) were measured at the inlet and outlet. In addition, redox potential, N form (of NH_4-N and NO_3-N) and oxygen concentrations were monitored online. The results of tracer tests showed that continuous aeration increased residence time and mixing within the filters. Under highly aerated conditions, dissolved pollutants such as dissolved COD and NH_4-N were effectively removed. The removal of NH_4-N occurs mainly through nitrification during the event (feeding and drainage). However, observations of oxygen consumption rates suggest that transformation of NH_4-N into NO_3-N during feeding are limited to a maximum inlet concentration of 10 mg/L. Consequently, the accumulation of ammonium in the saturated layer and subsequent oxidation during the dry period or subsequent events is dependent on the TKN inlet concentration. The findings of this thesis demonstrate that aerated CSO TWs are an effective method for removing particulate and dissolved pollutants. They also show that these systems can promote direct nitrification, although there are some limitations in terms of ammonium removal and the absence of denitrification. For micropollutants and fecal indicator a polishing treatment is necessary to improve water quality.

MOTS-CLÉS : Biofilter; pollution control; intensified system; high hydraulic load.

Laboratoire (s) de recherche : INRAE - REVERSAAL

Directeur de thèse: Pascal MOLLE

Président de jury : Lipeme Kouyi, Gislain

Composition du jury :
Dittmer, Ulrich Professor (PhD) University of Kaiserslautern-Landau
Gajewska, Magdalena Professor (PhD) Gdańsk University
Morvannou, Ania Chargée de recherche (PhD) Ecobird
Lipeme Kouyi, Gislain Professor (PhD) INSA - Lyon
Molle, Pascal Directeur de recherche (HDR) INRAE
Tondera, Katharina Professor (PhD) ENTPE

Thèse accessible à l'adresse : https://theses.insa-lyon.fr/publication/2025ISAL0011/these.pdf © [D. Gonçalves Portela], [2025], INSA Lyon, tous droits réservés